UNIVERSIDADE ESTADUAL PAULISTA
"Júlio de Mesquita Filho"

INSTITUTO DE BIOCIÊNCIAS DE BOTUCATU

"Sinalização parácrina mediada por proteínas e microvesículas entre células ósseas e seu microambiente"

Célio Junior da Costa Fernandes

Tese apresentada ao Instituto de Biociências, Campus de Botucatu, UNESP, par obtenção do título de Doutor pelo Programa de Pós-Graduação em Biotecnologia.

Willian Fernando Zambuzzi

BOTUCATU – SP
2021

FICHA CATALOGRÁFICA ELABORADA PELA SEÇÃO TÉC. AQUIS. TRATAMENTO DA INFORM.
DIVISÃO TÉCNICA DE BIBLIOTECA E DOCUMENTAÇÃO - CÂMPUS DE BOTUCATU - UNESP
BIBLIOTECÁRIA RESPONSÁVEL: ROSEMEIRE APARECIDA VICENTE-CRB 8/5651

Fernandes, Célio Júnior da Costa.
Sinalização parácrina mediada por proteínas e microvesículas entre células
Sinalização parácrina mediada por proteínas e microvesículas entre células ósseas e seu microambiente / Célio Júnior da Costa Fernandes. - Botucatu, 2021

Tese (doutorado) - Universidade Estadual Paulista "Júlio de Mesquita Filho", Instituto de Biociências de Botucatu
Orientador: Willian Fernando Zambuzzi Capes:
20801009

1. Biotecnologia. 2. Osteoblastos. 3. Vesículas extracelulares. 4. Angiogênese. 5. Cross-talk.

Palavras-chave: Cross-talk; Osteoblasto; Osteócito; Tecido endotelial; Vesículas extracelulares .

UNIVERSIDADE ESTADUAL PAULISTA
"Júlio de Mesquita Filho"

INSTITUTO DE BIOCIÊNCIAS DE BOTUCATU

"Sinalização parácrina mediada por proteínas e microvesículas entre células ósseas e seu microambiente"

Célio Junior da Costa Fernandes

Tese apresentada ao Instituto de Biociências, Campus de Botucatu, UNESP, par obtenção do título de Doutor pelo Programa de Pós-Graduação em Biotecnologia.

Willian Fernando Zambuzzi

BOTUCATU – SP
2021

Dedicatória:

Aos Orixás,

Pela fantástica oportunidade me dada de passar por esse mundo. Agradeço aos meus Orixás que me auxiliam na superação das dificuldades e na compreensão de que os obstáculos são apenas fortalecimentos para continuar.

Às minhas mães,

Eu que tive a grata fortuna de ter duas mães: Minha Avó Catarina e minha Mãe Ana, que sem seus esforços, unidos, não mediram amor; dedicação e apoio. Agradeço por me fornecerem os melhores princípios para me formar como uma pessoa melhor.

À minha Bisa Antônia,

Um exemplo de dedicação e perseverança que sempre impulsionava minha coragem em caçar meus sonhos.

Aos meus Pais,

Ambos levados por Deus: um que me deu a vida, Célio. Outro pelo apoio dedicado na minha formação, Pedro.

À minha irmã Giovana,

Por me apoiar e suportar.

Ao meu irmão Pedrinho,

Por ser um grande amigo, ouvinte e confidente. Obrigado pelas longas conversar, conselhos e risadas. Vivemos momentos que sem um a outro, tudo poderia ter sido mais difícil.

Aos meus tios: Sebastião, Orestes, Odair e Adriana,

No meu amadurecimento serviram, em todos os momentos, como fonte de apoio e inspiração.

Aos meus professores de primário, Ronaldo e Edimilson.

Agradecimentos:

À UNESP, que conheci em 2010 ao ingressar no Curso de Ciências Biológicas em Ilha Solteira.

Aos amigos de Ilha Solteira e à Família formada na República Methiolate (Tia Cida, Creu, Curió, Torto, Pança e Torresmo). Aos irmãos que a UNESP de Botucatu me deu: Augusto, Daniel, Paula, Mariana Romão, Beto, Guilherme, Edimar e Gerson.

À Prof. Maria Terezinha Serrão Peraçoli e ao Lab 3, por me acolherem e me iniciar no ambiente científico.

Ao corpo Docente da UNESP, Graduação e Pós Graduação, por todos ensinamentos e dedicação, além de conselhos que foram fundamentais na minha formação como pesquisador.

Ao LaBio, Laboratório de Bioensaios e Dinâmica Celular, por todo apoio, risadas e parceira: da Silva R.A., Feltran G.S., Gomes A.M., Pinto T.S., Ferreira M.R., Andrade A.F.C., Almeida G.S.

Ao meu Orientador Prof. Willian F. Zambuzzi por ter aberto as portas do laboratório e acreditado na minha envergadura de desenvolvimento. Não há palavras para lhe agradecer: "*lá vem o Marco, descendo o Morro da vó Salvelina*.". Qualquer palavras jamais traria minha enorme e eterna gratidão por essa Amizade.

Ao Prof. Maikel Peppelenbosh e todo o grupo de pesquisa da Erasmus MC. Amigos que guardarei com carinho por toda vida, e aprendizados que permitiram uma evolução importante.

Às minhas amigas Pamela Overlanda, Carla Souza, Isabella Picolli, Thaís Silva, Ana Flávia, Juliana Campos e Magda Hartemam, pela parceria e paciência.

À FAPESP por todo financiamento (2014/22689-3; 2016/08888-9; 2019/21807-6; BEPE 2018/10856-3).

No Meio do Caminho

Carlos Drummond de Andrade

No meio do caminho tinha uma pedra

Tinha uma pedra no meio do caminho

Tinha uma pedra

No meio do caminho tinha uma pedra

Nunca me esquecerei desse acontecimento

Na vida de minhas retinas tão fatigadas

Nunca me esquecerei que no meio do caminho

Tinha uma pedra

Tinha uma pedra no meio do caminho

No meio do caminho tinha uma pedra.

Pé de Jacarandá

Célio Junior da Costa Fernandes

Numa dessas ruas de cidade pequena
de interior
onde puxam os vocábulos
e vergam a ortografia;
numa dessas ruas
com nome de pessoas afamadas
locais, estadistas
e donos de roça.
Foi numa dessas ruas que se alojou
um pé de jacarandá
que serve limão e mel
que recorre à sombra dos prédios;
foi numa dessas esquinas
que fui um fora da lei
da ordem e desordem
de uma cidade crescida.

* Obrigado Botucatu.

SUMÁRIO:

Capítulo 1:

Introdução 21

Angiogênese 25

Shear-Stress 27

Vesículas Extracelulares 29

Capítulo 2:

Fibroblast-secreted trophic factors up-modulate osteocyte gene markers and contribute with ECM remodeling stimulus in osteoblast 34

Capítulo 3:

Vascular smooth muscle cells drive osteoblast-to-osteocyte transition via β-Catenin signaling through exosome communication 50

Capítulo 4:

Unstressed Vascular Smooth Muscle Cell (VSMC) guarantees the osteocyte function phenotype 81

Capítulo 5:

Shear-stress melhora a capacidade das células endoteliais em estimular o fenótipo osteogênico 107

Capítulo 6:

VSMCs obatined extracellular vesicles loading elucidation and osteogenic potential characterization using mesenchymal stem cells 1117

Capítulo 7:

Discussão 147

Capítulo 8:

Constatações 149

Capítulo 9:

Conclusão 150

Capítulo 10:

Atividades desenvolvidas no período 151

Capítulo 11:

Referências Bibliográficas 161

LISTA DE FIGURAS:

Capítulo 1

Figura 1: Esquema de ossificação intramembranosa. 23

Figura 2: Esquema de ossificação endocondral com crescimento longitudinal do tecido ósseo. 25

Figura 3: Diagrama esquemático mostrando a geração do *Shear-Stress* 26

Figura 4: As células endoteliais são expostas a duas grandes forças 27

Figura 5: Vias envolvidas na biogênese da vesícula extracelular 31

Figura 6: A composição dos exossomos. 32

Figura 7: Esquema apresentando transporte de Vesículas Extracelulares através dos vasos sanguíneos em *Cross-talk* com o tecido ósseo 33

Capítulo 2

Figure 1: Experimental design of the study. 41

Fig.2. Contribution of fibroblast with osteogenic phenotype. 42

Fig.3. Partial inflammatory landscape. 43

Fig. 4. Osteoclastogenesis-related genes. 44

Fig.5. Fibroblast-induced ECM remodeling during osteoblast differentiation. 45

Capítulo 3

Fig.1. Endothelial cells promote dynamic osteogenic gene marker reprogramming. 54

Fig.S1. Outline of the experimental procedures adopted in this study to evaluate the effect of endothelial cells on osteoblast performance. 55

Fig.S2. TGF-ß signaling-based gene reprogramming is trigged in response to VSMC- conditioned medium. 55

Fig.2. VSMC, but not endothelial cells, promotes osteoblast-osteocyte transition. 57

Fig.S3. The regulation of Akt and MAP-kinase modulated by endothelial cells during osteoblast differentiation. 57

Fig.S4. mRNA encoding osteocyte markers by endothelial cells. 58

Fig.S5. Validation of experimentally acquired osteocytes through Shh signaling and RANKL expression. 59

Fig. S6. Characterization of CD9 in endothelial cells. 60

Fig.S7. Characterization of CD63 in endothelial cells. 61
Fig.S8. Characterization of CD81 in endothelial cells. 61
Fig.S9. Characterization of extracellular vesicles by endothelial cells and osteocyte gene expression. 62
Fig.3. Detailed analysis of AoSMCs-related exosome. 63
Fig.4. Exosomes are reservoir of Catenin signaling related members and deliver osteocytes gene markers. 63
Fig.5. AoSMCs require p-ß-Catenin signaling. 65
Fig.S10. Paracrine effect of endothelial cells on the expression of adhesion-related genes. 66
Fig.S11. Biological functions obtained with bioinformatic tools. 67
Fig.S12. Notch signaling is modulated in osteoblast-to-osteocyte transition. 67
Fig.S13. Endothelial cells modulate the expression of genes involved with ECM remodeling during osteoblast-to-osteocyte transition. 68
Fig.6. Exosomes deliver ATP and modulate expression involved with bone mineralization. 69
Fig.S14. Relative expression of mineralization-related genes in HUVECs, HCAECs, and AoSMCs. 70
Fig.7. Schematic representation of the main findings of this study. 73

Capítulo 4

Figure 1: VSMCs promote osteoblastic phenotype in a TGFβ pathway manner. 83
Figure S1: Members of the SMAD family in response to VSMCs. 84
Figure 2: Paracrine action of VSMCs in the Osteoblast-Osteocyte transition. 85
Figure S2: Differentiation markers of osteocytes differentially expressed in AoSMC under *Shear-Stress* effect. 85
Figure S3: FGFR family, Shh signaling members and RankL genes reprogramming in response to VSMCs. 86
Figure 3: Characterization of the extracellular vesicles. 87
Figure 4: Exosomes were evaluated. 88
Figure 5: Exosomes cargo evaluation shows mRNA encoding osteocyte markers. 88
Fig.6. VSMCs-conditioned medium promotes reprogramming of Notch signaling in osteocyte-like cells. 89

Figure 7: β-Catenin pathway seems being a constituve signaling in osteocytes. 90
Figure S4: Complementary analysis of β-Catenin signaling. 91
Fig.8. Mineral metabolism in osteocyte-like cells. 92
Figure S5: NPP1 and TNAP mRNA in VSMCs and their released exossomes. 93
Fig.9. Remodeling of the organic fraction of the matrix was also investigated. 93
Figure S6: Osteoblast adhesion signaling. 94
Figure 11: Schematization of the representative findings found in this study. 94

Capítulo 5

Fig.1. Meio condicionado por HUVEC modula marcadores da diferenciação de osteoblastos. 109
Fig.2. Efeito do meio condicionado por células endoteliais em marcadores da regulação da matriz extracelular em osteoblastos. 110
Fig.3. HUVEC ativa a expressão da via TGF-β e BMP em osteoblastos. 111
Fig.4. Expressão de genes envolvidos no remodelamento da matriz extracelular. 112
Fig.5. Indução da expressão de HIF em osteoblastos. 113
Fig.6. Efeito do *cross-talk* de HUVEC e osteoblastos na expressão da via de Sonic Hedgehog. 114
Fig.7. Expressão da via de Notch em osteoblastos. 115

Capítulo 6

Figure 1: Characterization of HSP70 in primary cells. 125
Figure 2: Characterization of extracellular vesicles by Nanotracking Particles Analyze. 126
Figure 3. Characterization of CD9 in endothelial cells. 127
Figure 4. Characterization of CD63 in endothelial cells. 127
Figure 5. Characterization of CD81 in endothelial cells. 128
Figure 6. Phosphatase profile in exosomes released by endothelial cells. 128
Figure 7. Characterization of adhesion proteins in exosomes released by primary cells. 129
Figure 8. *Shear-Stress* modulates the content of MAP-Kinases within Endothelial cell released exosomes. 130

Figure 9. Cluster identification to represent results of protein content expression in endothelial cell exosomes. 131

Figure 10. Effect on phosphorylation process in undifferentiated mesenchymal cells caused by endothelial cell products. 132

Figure 12: Primary cells modulate mineral homeostasis genes in MSC in the first hours of treatment. 133

Figure 12. Endothelial cells modulate β-Catenin pathway protein expression in undifferentiated Mesenchymal cells. 134

Figure 13. Exosomes modulate expression levels of osteocyte markers. 135

Figure 14. Paracrine effect of exosomes on proliferation and differentiation proteins evaluated in mesenchymal cells. 135

Figure 15. Effect of conditioned medium on phosphate calcium homeostasis on mesenchymal cell differentiation. 137

Figure 16. Effect of Exosome from Endothelial cells on phosphate calcium homeostasis on mesenchymal cell differentiation. 138

Figure 17. Gene expression profile of β-Catenin pathway components in undifferentiated mesenchymal cells. 139

Figure 18. Gene expression profile of β-Catenin pathway components in undifferentiated mesenchymal cells treated with Exosome from Endothelial cells. 140

Figure 19. Osteocyte gene markers evaluated in Mesenchymal Cells treated with media conditioned by primary endothelial cells. 141

Figure 20. Osteocyte markers evaluated in exosome treated mesenchymal cells released by primary endothelial cells. 142

Figure 22. Effect of primary cell conditioned medium on the expression of mesenchymal cell DNMTs and TETs. 143

Figure 23. Effect of exosomes released by primary cells on the expression of mesenchymal cell DNMTs and TETs. 144

Figure 24. Cellular crosstalk between endothelial and mesenchymal cells in DNA acetylation gene expression. 145

Figure 25. Effect on HOTTAIR and Hoxa8 in challenged mesenchymal stem cells. 146

LISTA DE TABELAS:

Capítulo 2:

Table 1. Expression primers sequences and PCR cycle conditions 39 – 40

Capítulo 3:

Table 1. Expression primers sequences and PCR cycle conditions 73 – 77

Capítulo 4:

Table 1. Expression primers sequences and PCR cycle conditions 98 – 102

Capítulo 6:

Table 1. Expression primers sequences and PCR cycle conditions 121 – 123

LISTA DE ABREVIAÇÕES:

AKT	Protein Kinase B
ALP	Alkaline Phosphatase
AMP	Adenosine Monophosphate Deaminase
AoSMC	Aortic Smooth Muscle Cells
ARF	Activation-Resorption-Formation
ATP	Adenosine triphosphate
BBE	Bovine Brain Extract
BEPE	Bolsa de Estágio e Pesquisa no Exterior
BGLAP	Osteocalcin
BMP2	Bone Morphogenetic Protein 2
BMP7	Bone Morphogenetic Protein 7
BMP9	Bone Morphogenetic Protein 9
BMPr1	Bone Morphogenetic Receptor 1
BMPr2	Bone Morphogenetic Receptor 2
BSA	Bovine Serum Albumin
BSP	Bone Sialo Protein
Ca^{2+}	Cálcio
CD63	Tetraspanin 63
CD73	Ecto-5'-nucleotidase
CD81	Tetraspanin 81
CD9	Tetraspanin 9
CDK	Cyclin Dependent Kinase
cDNA	Complement Deoxyribonucleic Acid
CNPq	Conselho Nacional de Desenvolvimento Científico e Tecnológic
Cofilin	Cofilin
Col 1A1	Collagen Type I Alpha 1 Chain
DAPI	4',6-Diamidine-2'-phenylindole dihydrochloride
DKK1	Dickkopf WNT Signaling Pathway Inhibitor 1
Dlx5	Distal-less homeobox 5
DMEM	Dulbecco's Modified Eagle Medium
DMP1	Dentin Matrix Acidic Phosphoprotein
DNA	Deoxyribonucleic Acid

dNTP	Phosphate Deoxyribonuc eotides
EBM-2	Endothelial Cell Basal Medium-2
ECM	Extracellular Matrix
EGTA	Ethylene Glycol Tetraacetic Acid
ERK	Extracellular Signal-Regulated Kinase
EV	Extracelullar Vesicles
Exo	Exosome
FAK	Focal Adhesion Kinase
FAPESP	Fundação de Amparo à Pesquisa do Estado de São Paulo
FBS	Fetal Bovine Serum
Fetuin A1	Fetuin A1
FGF23	Fibroblast Growth Factor 23
FGFr1	Fibroblast Growth Factor Receptor 1
FGFr2	Fibroblast Growth Factor Receptor 2
FGFr3	Fibroblast Growth Factor Receptor 3
FGFr4	Fibroblast Growth Factor Receptor 4
GAPDH	Glyceraldehyde-3-Phosphate Dehydrogenase
GLI	GLI Family Zinc Finger 1
GP-38	Glycoprotein 38
GSk3	Glycogen Synthase Kinase 3
GTP	Guanosine Triphosphate
HCAEC	Human Umbilical Vein Endothelial Cells
hEGF	human Epidermal Growth Factor
hFGF-B	human Fibroblast Growth Factor B
HOEL	Humam Osteoblast
HUVEC	Human Coronary Artery Endothelial Cells
IBB	Instituto de Biociências de Botucatu
IL-10	Interleukin 10
IL-13	Interleukin 13
IL-16	Interleukin 16
IL-18	Interleukin 18
IL-33	Interleukin 33
Integrin-β3	Integrin Subunit Beta 1
Jag1	Jagged Canonical Notch Ligand 1

Jag2	Jagged Canonical Notch Ligand 2
JNK	C-Jun N-terminal Kinase
kDa	kilodalton
L-1β	Interleukin 1 Beta
LRP4	Low-Density Lipoprotein Receptor-Related Prot in 4
LRP5	Low-Density Lipoprotein Receptor-Related Protein 5
LRP6	Low-Density Lipoprotein Receptor-Related Protein 6
MAPK	Mitogen-Activated Protein Kinase
miR-17	micro RNA 17
miR-23a	micro RNA 23a
MMP2	Matrix Metalloproteinase 2
MMP9	Matrix Metalloproteinase 9
mRNA	messenger RNA
MSC	Mesenchymal Stem Cells
NaOH	Sodium Hydroxide
NO	Nitric Oxide
Notch1	Neurogenic locus notch homolog protein 1
Notch2	Neurogenic locus notch homolog protein 2
Notch3	Neurogenic locus notch homolog protein 3
Notch4	Neurogenic locus notch homolog protein 4
NPP1	Necrosis-inducing protein 1
NTA	Nanoparticle Tracking Analysis
O.M.	Osteogenic Medium
OPG	Osteopotegrin
OTC	Osteocalcin
OTP	Osteopontin
OTX	Osterix
p-Cofilin	Phospho Cofilin
p-ERK	Phospho Mitogen-Activated Protein Kinase 1
p-FAK	Phospho Focal Adhesion Kinase
p-Rac1/cdc42	Phospho Ras-Related C3 Botulinum Toxin Substrate 1
p-β-Catenin	Phospho Beta Catenin
P38	Mitogen-Activated Protein Kinase 14
PAGE	Polyacrylamide Gel Electrophoresis

PBS	Phosphate Buffer Solution
PCR	Polymerase Chain Reaction
Pi	Phosphate inorganic
PI3k	Phosphoinositide 3-kinase
PPi	Pyrophosphate inorganic
Ptch1	Patched 1
PVDF	Polyvinylidene Difluoride
qPCR	Quantitative polymerase chain reaction
Rac1/cdc42	Ras-Related C3 Botulinum Toxin Substrate 1
Rank-L	Receptor activator of nuclear factor kappa-B ligand
Reck	Reversion Inducing Cysteine Rich Protein With Kazal Motifs
RNA	Ribonucleic Acid
RP2	Retinitis Pigmentosa 2
Runx2	Runt Related Transcription Factor 2
SDS	Sodium dodecyl sulfate
SEM	Scanning Electron Microscopy
Ser	Serine
sFRP1	Secreted Frizzled Related Protein 1
sFRP2	Secreted Frizzled Related Protein 2
Shh	Sonic Hedgehog
SHP2	Protein Tyrosine Phosphatase Non-Receptor Type 11
SMAD2	Mothers Against Decapentaplegic Homolog 2
SMAD3	Mothers Against Decapentaplegic Homolog 3
SMAD4	Mothers Against Decapentaplegic Homolog 4
SMAD5	Mothers Against Decapentaplegic Homolog 5
SMAD6	Mothers Against Decapentaplegic Homolog 6
SMAD7	Mothers Against Decapentaplegic Homolog 7
SmBM	Smooth Muscle Cell Basal Medium
SMPD3	Sphingomyelin Phosphodiesterase 3
SOST	Sclerostin
Src	Proto-oncogene tyrosine-protein kinase
SUFU	Suppressor of Fused Homolog
TBS	Tris Buffered Saline
TGF-β	Transforming Growth Factor Beta 1

Thr	Threonine
TIMP1	Tissue Inhibitor of Metalloproteinases 1
TIMP2	Tissue Inhibitor of Metalloproteinases 2
TNAP	Tissue Non-specific Alkaline Phosphatase
Tyr	Tyrosine
UNESP	Universidade Estadual Paulista
Wnt	Wingless-Type MMTV Integration Site Family, Member 1
α-β-Catenin	Alpha Beta Catenin
β-Actin	Beta Actin
β-Catenin	Beta Catenin

RESUMO:

Compreender os mecanismos envolvidos na manutenção e homeostase óssea requer elucidar o comportamento de células em seu microambiente. O objetivo deste estudo foi investigar como células ósseas (MC3t3-E1, HOEL) ou mesenquimais são moduladas através da sinalização parácrina desencadeada por fibroblastos (3t3-NIH), células endoteliais de veias (HUVEC) e de aorta (HCAEC), além de células de músculo liso (AoSMC/VSMC). Para avaliar essa capacidade de modulação de células ósseas, fibroblastos, células endoteliais e de musculatura lisa foram mantidas em cultura por 72 horas com o intuito de condicionar o meio, o qual foi coletado e utilizado para tratar MC3T3 ou HOEL ou células mesenquimais, com o intuito de fazer uso de ferramentas de biologia celular e molecular para investigar alterações de expressão gênica e fenotípica. Nossos resultados mostram que 3T3-NIH é capaz de modular a expressão de marcadores de diferenciação osteoblasto-osteócito (DMP1. SOST, RankL e OPG). Além disso, vimos que AoSMC em duas condições distintas - Estatico e *Shear-Stress* - são capazes de promover uma transição osteoblasto-osteócito através de vesículas extracelulares (EVs), ativando a expressão de biomarcadores moleculares deste processo (miR23-a, DMP1, SOST, FGF23 e GP38) e, neste contexto, nossos dados também mostram que o meio condicionado por HUVEC modula marcadores de diferenciação de osteoblastos (Runx2, Osterix e ALP) e genes que são traduzidos em proteínas e que atuam na homeostase dos minerais da matriz óssea (NPP1 e TNAP). Considerando que as células AoSMC e HUVEC são capazes de modular a osteocitogênese e a osteoblastogênese, respectivamente, o meio condicionado por essas células foi coletado e as vesículas foram extraídas coletadas para melhor caracterização em termos de tamanho, concentração, biomarcadores de membrana, carga elétrica de membrana e conteúdo proteico, o que revelou que o perfil AoSMC não apresentou diferença em termos de condições experimentais (estática e *Shear-Stress*), também vimos que as células mesenquimais que recebem o tratamento com meio de cultura condicionado por AoSMC aumentou os marcadores de osteocitogênese, enquanto os EVs isolados do meio condicionado por HUVEC modularam positivamente esses mesmos marcadores (PHEX, MEPE, MMP-14, GP-38, DMP1). Esses dados permitem concluir que o tecido endotelial e os fibroblastos contribuem para a homeostase do osso e sua remodelação dinâmica é modulada pela transição osteoblastos-osteócitos por meio de fatores tróficos e vesículas extracelulares.

Palavras-chave: Tecido endotelial, Cross-talk, Vesículas extracelulares, Osteócitos.

ABSTRACT:

Understanding the mechanisms involved in bone maintenance and homeostasis requires elucidating the behavior of bone tissue in relation to communication with other adjacent tissues. The aim of this study was to investigate how bone cells (MC3t3-E1, HOEL) or mesenchymal cells are modulated through paracrine signaling triggered by fibroblasts (3t3-NIH), vein endothelial cells (HUVEC) and aortic endothelial cells (HCAEC), in addition to smooth muscle cells (AoSMC/VSMC). The cells of the tissues adjacent to the bone remained in culture for 72 hours to condition the medium, this same medium was collected and used to treat MC3t3 or HOEL or mesenchymal cells. Our results show that 3t3-NIH is capable of modulating the expression of osteoblast-osteocyte differentiation markers (DMP1. SOST, RankL and OPG). In addition, we saw that AoSMC in two different conditions: Static and Shear-Stress, are capable of promoting an osteoblast-osteocyte transition through extracellular vesicles (EVs), activating the expression of molecular biomarkers of this process (miR23-a, DMP1, SOST, FGF23 and GP38), in this context our data also show that the medium conditioned by HUVEC modulates osteoblast differentiation markers (Runx2, Osterix and ALP) and genes that are translated into proteins and that act in the homeostasis of bone matrix minerals (NPP1 and TNAP). Considering that AoSMC and HUVEC cells are capable of modulating osteocytogenesis and osteoblastogenesis, respectively, the medium conditioned by these cells was collected and the vesicles were extracted for treatment: 1. medium rich in vesicles and other trophic factors, and 2. treatment only with vesicles. EVs were characterized in terms of size, concentration, membrane biomarkers, membrane electrical charge and protein content, which revealed that the AoSMC profile showed no difference in terms of experimental conditions (static and Shear-Stress), we also saw that the mesenchymal cells receiving treatment with AoSMC-conditioned culture medium increased osteocytogenesis markers, while EVs isolated from HUVEC-conditioned medium positively modulated these same markers (PHEX, MEPE, MMP-14, GP-38, DMP1). These data allow us to conclude that the endothelial tissue and fibroblasts contribute to bone balance by modulating the osteoblast-osteocyte transition through trophic factors and extracellular vesicles.

Keywords: Endothelial tissue, Cross-talk, Extracellular vesicles, Osteocytes.

CAPÍTULO 1

INTRODUÇÃO

O tecido ósseo, apesar de sua aparência estática, é um tecido altamente complexo e dinâmico, sobretudo orquestrado pela sua vascularização tecidual, importante para homeostase das células que depositam, degradam e remodelam a matriz extracelular (van der Eerden et al., 2014). Trata-se de um processo complexo, que diminui com tempo de vida e acarreta em maior vulnerabilidade à fraturas e comprometimento da regeneração do tecido, e impactando a interação com biomateriais (Aspenberg, 2013; Bezerra et al., 2017).

Além disso, o osso é também uma importante reserva de minerais que está relacionado com inúmeras funções no organismo atuando em diferentes processos e órgãos como rins e coração, fortemente engajados em questões sistêmicas e fisiológicas (Hill Gallant and Spiegel, 2017; Lima et al., 2016; Salari et al., 2017; Wang et al., 2017; Zhou et al., 2017). Cada vez mais tem sido mostrado que o tecido ósseo desenvolve mecanismos importantes na fisiologia dos vertebrados, onde é mostrado, principalmente sua sincronia com células do tecido endotelial.

Durante sua morfogênese, inúmeros fatores comprometem a maquinaria de células mesenquimais estimulando-as a diferenciarem em osteoblastos e se comprometem com o tecido. Osteoblastos são células capazes de produzir e mineralizar a matriz extracelular. Assim, um conjunto sequencial de proteínas inicia uma cascata de sinalização celular, dentre as quais se destacam as vias de sinalização promovida pelas Proteínas Morfogenéticas Ósseas (BMPs) que se acoplam a receptores específicos desencadeando processos de transcrição e síntese de fatores específicos da diferenciação: Fosfatase Alcalina, Colágeno tipo 1, Osteonectina, Osteocalcina e Sialoproteina Óssea (Carreira et al., 2014; Ducy et al., 1996; Laurie et al., 2016; Lee et al., 1997).

Embriologicamente, a gênese do esqueleto obedece a mecanismos muito bem definidos, os quais são agrupados à 2 tipos distintos de ossificação: a ossificação Intramembranosa e a ossificação endocondral, as quais são melhores apresentadas a seguir:

1. Ossificação Intramembranosa: Nesse processo a formação do novo tecido não depende de precursor cartilaginoso e se dá pela diferenciação de células mesenquimais em osteoblastos (Palumbo et al., 2003; Percival and Richtsmeier, 2013; Yang et al., 2012). Histologicamente, define-se aspectos morfológicos muito bem definidos no osso, como é o caso da matriz do osteóide, matriz recém-sinstetizada e rica em proteínas; sua completa mineralização depende de mecanismos endócrinos, com envolvimento de hormônios e vitaminas (Jabalee et al., 2013). O constante crescimento do osso, com atividade de osteoblastos, leva a despolarização do crescimento aposto à atividade osteoblastica, e os osteoblastos executam mecanismos de deposição da matriz óssea de modo irregular, ficando os osteoblastos aprisionados na própria matriz que secretou. Esse mecanismo leva ao aprisionamento dos osteoblastos à MEC, fator decisivo para mudança fenotípica dessas células. Osteoblastos retidos na matriz mineralizada são agora chamados de osteócitos, células ainda pouco estudadas devido ao difícil acesso técnico, uma vez que residem no nosso cortical. Os osteócitos são células especializadas do osso e garantem a hemeostase de cálcio, além de sabidamente contribuir com osteoclastogênese, já que são as células que mais expressam RANKL.

Apesar de aprisionado na matriz extracelular, os Osteócitos compreendem cerca de 95% das células ósseas e podem regular a formação e degradação do tecido mineralizado, uma vez que expressa proteínas chaves desses processos. A expressão de Esclerostina (SOST) inibe a diferenciação e proliferação de Osteoblastos e é um marcador importante de Osteócitos, que também é uma das principais fontes de Rank-L e Osteopotegrina (OPG). Essas proteínas atuam competindo com um receptor de membrana (RANK), e modulam positiva ou negativamente o processo de maturação de Osteoclastos (Winkler et al., 2003).

Uma vez embebidos na matriz extracelular os Osteócitos passam a se comunicar com células adjacentes via dendritos formando uma forte rede através das lacunas ósseas, e a forma ou orientação das lacunas irão influenciar na passagem de sinais químicos gerados (Nicolella et al., 2006; Shah et al., 2016). Essa comunicação ocorre inclusive com tecido endotelial que promove a nutrição e pode carregar fatores produzidos por Osteócitos. Acredita-se que esse processo esteja ligado a grande sensibilidade que essas células possuem quanto a mecanismos de mecanotransdução transformando sinais mecânicos em sinais químicos e que recrutam Osteoblastos ou Osteoclastos de acordo com estimulo recebido (Bonewald, 2011; van Oers et al., 2015;

Uda et al., 2017). Estudos recentes revelam que esse comportamento modula a expressão de outras proteínas como Fibroblast Growth Factor 23 (FGF23), que controla a homeostase de minerais como Fosfato e que é abundantemente estocado nos ossos, e níveis de Cálcio (Kuczera et al., 2016; Sakurai et al., 2017). Do mesmo modo, Dentin Matrix Protein 1 (DMP1) possui característica expressiva de acordo com as variações de sinais (Bonewald, 2011). Ainda sem ter a função totalmente elucidada, estudos nos últimos 15 anos veem sendo realizados para compreender melhor como Osteócitos se comportam no tecido ósseo.

De uma maneira geral, Osteócitos podem ser considerados orquestradores do processo de remodelamento do tecido e a morte dessas células pode levar a diversas doenças desencadeadas pela fragilidade óssea (Prideaux et al., 2016). Nesse sentido, compreender o Crosstalk entre tecido Endotelial, Muscular e Ósseo nos parece ser de grande valia na busca por melhor elucidação de mecanismos que envolvam a regeneração a traumas do tecido ósseo.

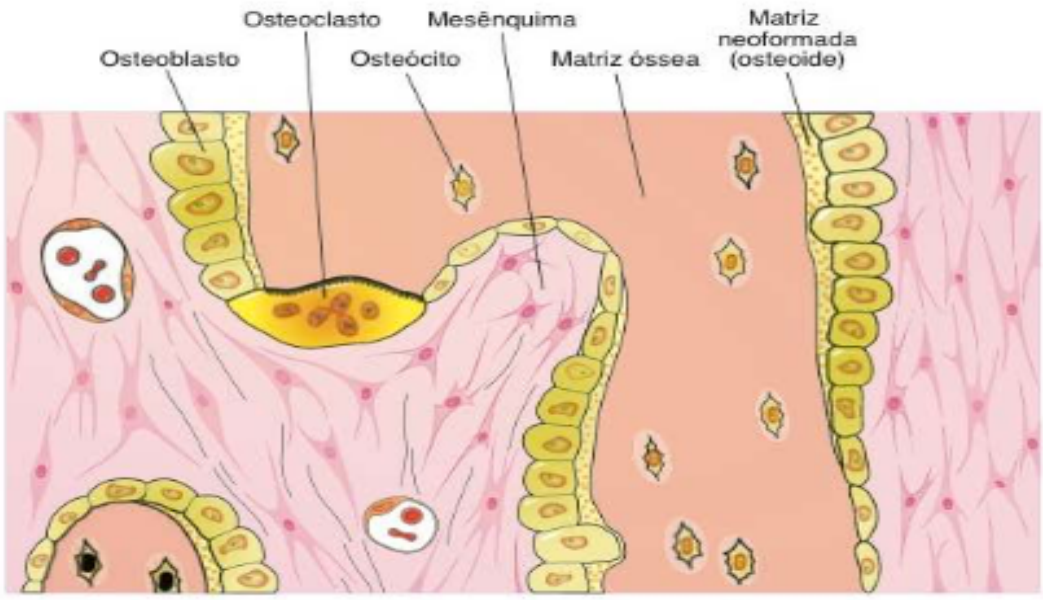

Figura 1: Esquema de ossificação intramembranosa. Osteoblastos diferenciados a partir de células mesenquimais promovem a sintese da matriz extracelular, que ao se aprisionarem na matriz se tornam osteócitos. Osteoclastos, multinucleares, fazem o papel antagônico degradando a matriz através da mecanismos físico-químicos e bioquímicos. **Fonte:** Histologia Básica, L.C. Junqueira e José Carneiro. - [12˚ Edição] - Rio de Janeiro: Guanabara koogan, 2013.

2. Ossificação endocondral: Diferente do processo intramembranoso, a ossificação endocondral depende de um molde cartilaginoso que permite e guia o crescimento longitudinal do tecido. Em eventos de cicatrização do tecido ósseo, é possível que os 2

eventos aconteçam, participando de modo combinado na regeneração do tecido. Alguns detalhes da ossificação endocondral seguem abaixo:

- Primeiramente, células progenitoras do pericôndrio se diferenciam em osteoblastos resultando no anel do periósteo; esse processo promove a formação de ossos longos através da ossificação do pericôndrio para as extremidades (Epífise Proximal e Epífise Distal), promovendo a calcificação da matriz e inibindo a produção de cartilagem (Yagami et al., 1999). Nesse momento, os vasos sanguíneos passam a invadir as lacunas deixadas pela mineralização e trazem nutrientes para manutenção do tecido e Condroclastos para reabsorver os debris cartilaginosos e aumentar o processo de vascularização do tecido ósseo. Esse processo irá formar a cavidade medular que abriga células específicas, algumas das quais com baixo índice de comprometimento tecidual, conferindo ao tecido sua plasticidade.

- A ossificação endocondral promove o crescimento longitudinal dos ossos que no final do desenvolvimento requer a substituição do tecido jovem por tecido ósseo lamelar duro (Ling et al., 2017; Zhao et al., 2015). Destaca-se ainda que esse crescimento ocorre com comprometimento da placa de crescimento, que diminui ao longo do tempo e idade.

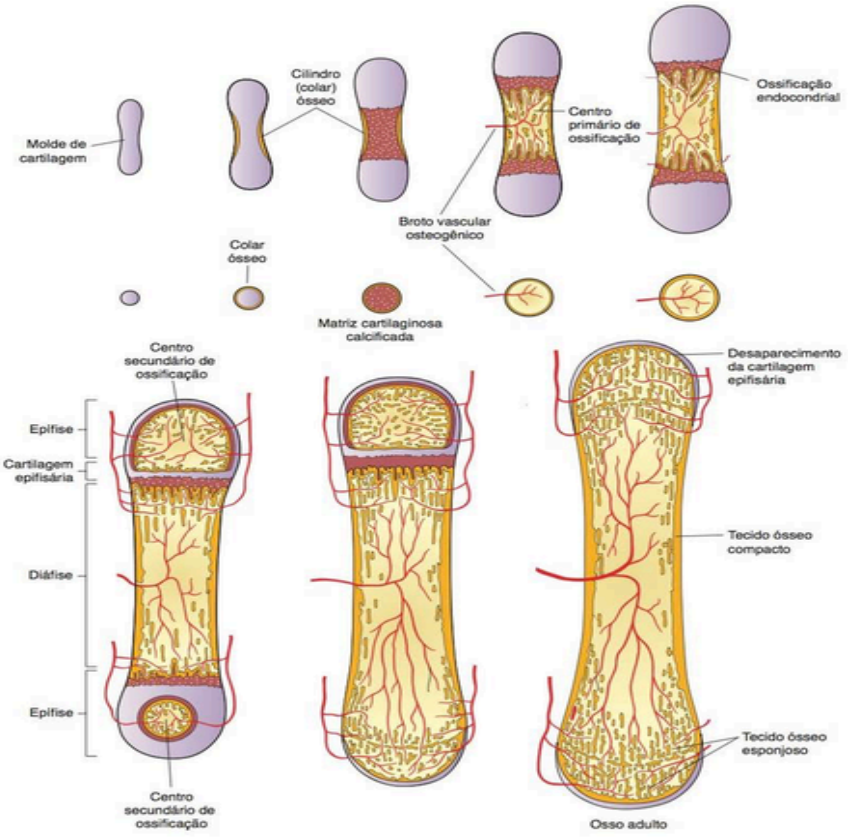

Figura 2: Esquema de ossificação endocondral com crescimento longitudinal do tecido ósseo a partir de um molde cartilaginoso. A partir de um molde de cartilagem forma-se o centro primário de ossificação com invasão de vasos na porção central do osso. Nas extremidades formam-se os centros secundários de ossificação que depois de vascularizado, irá promover a substituição completa de cartilagem por osso com auxílio de Condroclastos trazidos pela corrente sanguínea. **Fonte.** Histologia Básica, L.C. Junqueira e José Carneiro. - [12˚ Edição] - Rio de Janeiro: Guanabara koogan, 2013.

ANGIOGÊNESE

A angiogênese é de extrema importância na embriologia de vertebrados, participando ativamente na diferenciação celular, bem como na manutenção fisiológica dos tcidos. A formação dos vasos sanguíneos ocorre a partir de dois processos altamente refinados: O primeiro é a vasculogênese, onde angioblastos formam os vasos primitivos durante a embriogênese; o segundo processo é a angiogênese que ocorre a partir dos vasos neoformados, estabelecendo artérias, veias e capilares que irão promover a irrigação de todos os demais tecidos ao longo do desenvolvimento e crescimento do organismo (Plein et al., 2014; Rizov et al., 2017).

Durante a gênese dos vasos, as células ficam organizadas de maneira justapostas, com orientação a partir da direção do fluxo sanguíneo e com pouco material

extracelular, uma vez que ocorre a necessidade fisiológica de contração e relaxamento para passagem do sangue e transporte de fatores de manutenção dos tecidos, esse processo depende, inclusive, do tecido muscular liso que envolve o vaso lhe conferindo maior resistência a possíveis agressões ou alteração na pressão de bombeamento (Lacaud and Kouskoff, 2017; Matlung et al., 2009; Salsoso et al., 2017).

Assim, a vascularização é de fundamental importância, dependendo de moléculas específicas como hormônios, citosinas, e do Fator de Crescimento Vascular Endotelial (VEGF), que controla diversos processos celulares envolvidos com a formação de vasos através de dois receptores de Tirosina Quinase VEGF-r1 (FLT1) e VEGF-r2 (FLK2) influenciando na migração, proliferação e diferenciação de células mesenquimais em endoteliais (Eshkar-Oren et al., 2009; Fong et al., 1995; dela Paz et al., 2012; Shalaby et al., 1995).

A tensão exercida pela passagem do sangue na parede do vaso gera uma tensão que irá definir o fenótipo da célula de acordo com a pressão gerada, essa tensão hidrodinâmica é conhecida como *Shear-Stress* ou tensão de cisalhamento e mantém o *tônus* vascular, promove permeabilidade seletiva e interfere na adesão de leucócitos (Balaguru et al., 2016; Chien, 2008).

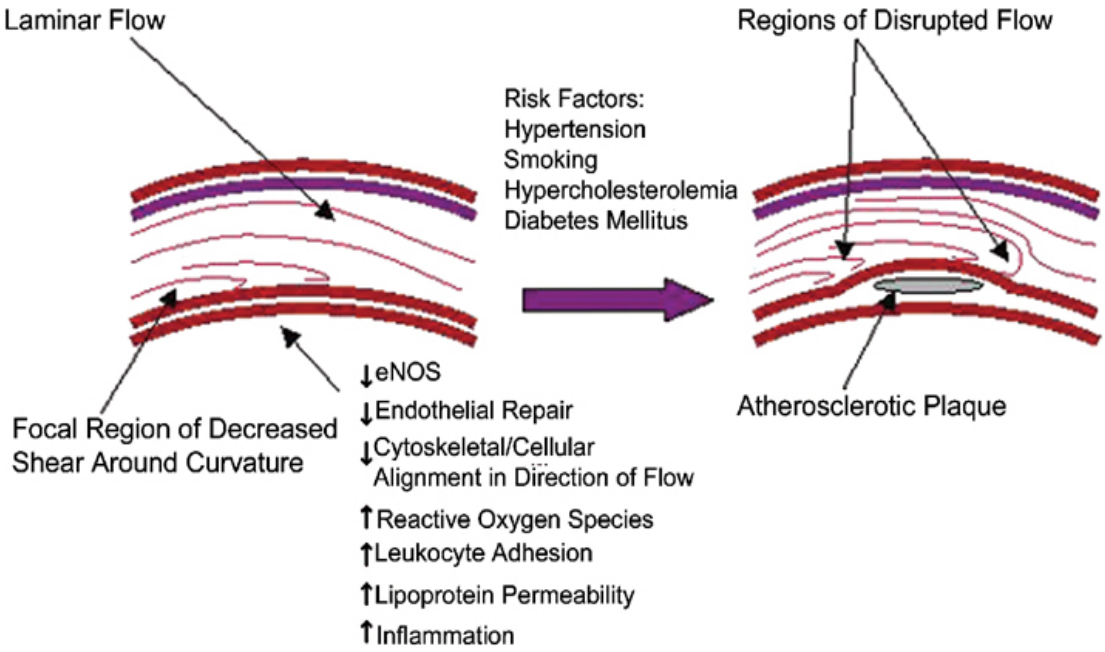

Figura 3: Diagrama esquemático mostrando a geração do *Shear-Stress* (paralelo a superfície das células endoteliais) pelo fluxo sanguíneo e a geração da tensão normal (perpendicular à superfície das células endoteliais) e o estiramento circunferencial devido a ação da pressão (Cunningham and Gotlieb, 2004). Note que, inclusive, algumas patologias instaladas como consequência a hábitos de vida do indivíduo podem interferir no fluxo sanguíneo e impactar o *shear-stress*.

Assim, o fluxo sanguíneo destaca-se como o mediador mais importante destas funções exercidas pelas células endoteliais, sobretudo respondendo a processos de mecanotransdução de sinais (Hahn and Schwartz, 2009). Desta forma, células endoteliais destacam-se como elemento chave na regulação da conversão de tensões mecânicas em respostas bioquímicas.

SHEAR-STRESS

O fluxo sanguíneo promove alterações na superfície endotelial, graças às variações de pressão decorrentes de atividades e/ou esforços, promovendo modulações fenotípicas nas células endoteliais (Bazmara et al., 2016; Califano and Reinhart-King, 2010). Assim, o desenvolvimento de fenótipos distintos pode estar associado a esta tensão (Passerini et al., 2004).

Sabendo que os vasos possuem uma camada de musculatura lisa envolvendo o tecido, é importante ressaltar que sua função é, também, promover o alongamento cíclico resultante da pressão exercida pela passagem do sangue, desse modo, a tensão de cisalhamento é absorvida e suportada pelas células endoteliais (Rodriguez-Nunez et al., 2016).

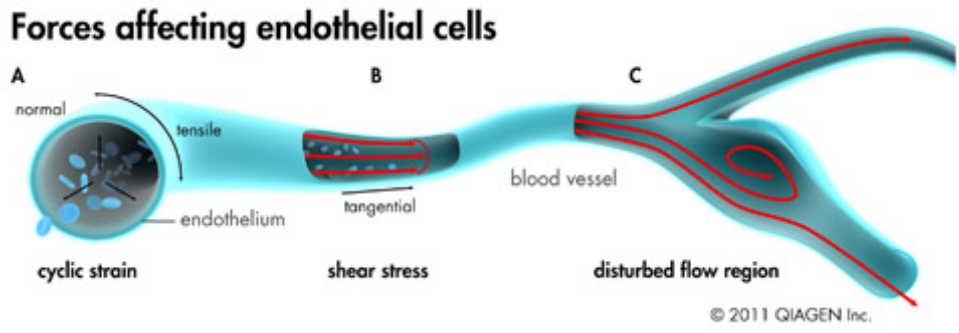

Figura 4: As células endoteliais são expostas a duas grandes forças: tensão cíclica **(A)** e *Shear-Stress* do fluido **(B)**. **(C)** Células Endoteliais em áreas de alta curvatura ou jusante das bifurcações (seio carotídeo, bifurcação coronária) são expostos a *shear stress* perturbado (oscilatório com baixo tempo médio de *Shear-Stress*). **Fonte: http://www.sabiosciences.com/pathwaymagazine/minireview/amm.php**

As mudanças fenotípicas supracitadas podem ser observadas em estudos de diferentes pesquisadores, que mostram que o modelo de *Shear-Stress* pode acarretar em baixa proliferação, como consequência a diminuição da taxa de síntese do DNA (Akimoto

et al., 2000; Lin et al., 2000; Sho et al., 2002; Xu et al., 2013). Esses processos regulatórios de taxa proliferativa e síntese de DNA está associado com um supressor tumoral p53 que induz $p21^{cip}$ que inibe Cdk, a tensão de cisalhamento aumenta essa associação de sinalização celular (Akimoto et al., 2000; Chien, 2008; Haga et al., 2003) e diminui a fosforilação da proteína Retinoblastoma (Rb). Essa proteína possui capacidade de se interagir ao DNA regulando o ciclo celular inibindo vários fatores de transcrição (Bartek et al., 1996; Lin et al., 2000; Nevins, 1998).

Em células de musculatura lisa, por sua vez, as demais forças hemodinâmicas afetam a proliferação e a migração tanto em experimentos *in vivo* quanto *in vitro*, porém os efeitos diretos da tensão de cisalhamento ainda não estão totalmente compreendidos (Haga et al., 2003). Desta forma, podemos destacar a importância das forças hemodinâmicas geradas principalmente pelo fluxo sanguíneo para a manutenção da homeostase da rede de vasos do sistema cardiovascular e em especial a tensão de cisalhamento a qual está intrinsecamente relacionada a remodelagem da parede do vaso sanguíneo, tanto em processos fisiológicos como também na patogênese de doenças cardiovasculares, como a aterosclerose e reestenose (Von Offenberg Sweeney et al., 2005; Urbich et al., 2002).

O tecido endotelial tem ganhado merecido destaque nos últimos anos, sobretudo ao que se refere seu alcance nos mais variados tecidos. Muitos pesquisadores de vanguarda têm apontado para esse tecido com real interesse em desvendar seu papel secundário ao transporte de nutrientes e gases. Sabe-se, neste sentido, que células endoteliais desempenham funções de extrema importância aos mecanismos de osteogênese, levando a uma ação acoplada entre células do endotélio e células do tecido ósseo. O grupo do Prof. Adam P. Kusumbe, especialista em tecido endotelial e microcirculação, tem buscado interpretar os mecanismos parácrinos desenvolvidos pelo endotélio, inquirindo compreender um papel do endotélio que até então não se discutia, sua capacidade em promover, fenotipicamente, células dos diferentes tecidos, favorecendo mecanismos de diferenciação e remodelamento tecidual. Alinhado a esta necessidade, nosso grupo tem centrado esforços em conhecer as moléculas parácrinas liberadas por células que mantêm o endotélio em sinalizar e modular fenotipicamente células ósseas e importantes resultados vêm sendo obtidos.

VESÍCULAS EXTRACELULARES

É sabido que durante o desenvolvimento de um organismo, o microambiente influencia diretamente sua fisiologia e bioquímica celular, podendo modular comportamentos específicos a respostas ambientais. Assim, o ambiente passa ser todo meio extracelular ou corpóreo. Desse modo, respostas internas são desencadeadas de acordo com o estímulo gerado (Hristov et al., 2004). O desenvolvimento depende, portanto, de um apurado ajuste entre o organismo e ambiente (Balaj et al., 2011; Clancy et al., 2015; Cocucci et al., 2009; Muralidharan-Chari et al., 2009). Da mesma forma ocorre com a comunicação celular, podendo sinalizar vários processos como morte, infecção por patógenos ou do desenvolvimento de câncer (Dolo et al., 1998; Koppler et al., 2006).

Uma das maneiras de comunicação que as células podem desencadear durante uma resposta fisiológica, é através de pequenas esferas, chamadas genericamente de Vesículas Extracelulares (EV's). Desse modo, o estudo de EV's, processo que ocorre em organismos procariontes, como Bactérias, e em organismos eucariontes (uni ou pluricelulares) vem para agregar ao entendimento do desenvolvimento e comunicação dos organismos com o meio em que estão inseridos. Essas partículas são formadas por dupla camada lipídica e são capazes de carregar moléculas em sua superfície ou em seu interior, como: Proteínas, Lipídeos, miRNA e mRNA. Estão presentes em todos os tipos de fluidos corporais como plasma, soro, urina e saliva (Admyre et al., 2007; Brody et al., 1983; Pisitkun et al., 2004). Portanto, um processo de comunicação que ocorre em todos os organismos, e que foi descrito ao longo dos anos por diferentes grupos de pesquisa, que encontraram essa relação comunicativa em indivíduos dos reinos Animalia - *Homo sapiens s.* (Anderson, 1969; CHARGAFF and WEST, 1946; Wolf, 1967), Protista - *Dictyostelium discordam* (Tatischeff et al., 1998; Tatischeff et al., 2008) e Plantae - *Helianthus annuus* (Regente et al., 2009).

Essas vesículas, descritas inicialmente na década de 1940, somente três décadas depois, com o uso da microscopia eletrônica puderam ser vistas e dimencionadas (Wolf, 1967). Apesar de ser um processo de comunicação que aparece em todos os organismos, a nomenclatura adotada para descrever EV's varia de acordo com as classes de organismos existentes, podendo ser encontrada na literatura como Vesículas extracelular (Bactérias) e Exossomos para organismos agrupado dentro do domínio Eukarya. Ainda em se tratando de nomenclatura de EV's, e mais especificamente para a espécie *Homo sapiens*, ocorre mais uma divisão a partir do tamanho das vesículas secretadas, e que

também pode variar de acordo com a célula que a libera, como por exemplo, derivadas de células dendriticas que são chamadas de Dexossomos (Kalra et al., 2016). São organizadas em três classes:

Exossomos (50nm a 100nm): Formado a partir da interação de uma molécula com proteínas de membrana que ativam um receptor específico e que através de proteínas específicas, como Caveolina e Clatrina, iniciam a formação de uma vesícula de fora para dentro que contem proteínas da membrana. Essa vesícula é denominada Endossomo. Dentro da célula, essa vesícula é preenchida por vesículas menores, forma-se um corpo Multivesicular. Quando essa vesícula maior sofre fusão com a membrana plasmática, libera essas vesículas menores para fora da célula, essas por sua vez, são os exossomos.

Microvesículas ou Ectossomos (100nm a 1000nm): Esse tipo de vesícula é formada a partir de uma pressão na membrana plasmática de dentro para fora, seguida de uma fissão da membrana (**Fig.5**), isso ocorre por rearranjo do citoesqueleto, por exemplo, e através de enzimas dependentes de cálcio (Ca^{2+}) desse modo o material imerso no citosol acaba dentro da vesícula formada e componentes originalmente na membrana plasmática passam a fazer parte da membrana da vesícula secretada (Schweitzer and D'Souza-Schorey, 2004).

Vesículas de apoptose (1µm a 5µm): A célula inicia uma cascata por ativação de ROCK, aumentando forças de contração e a membrana passa a eliminar vesículas (Biancone et al., 2012; Momen-Heravi et al., 2013).

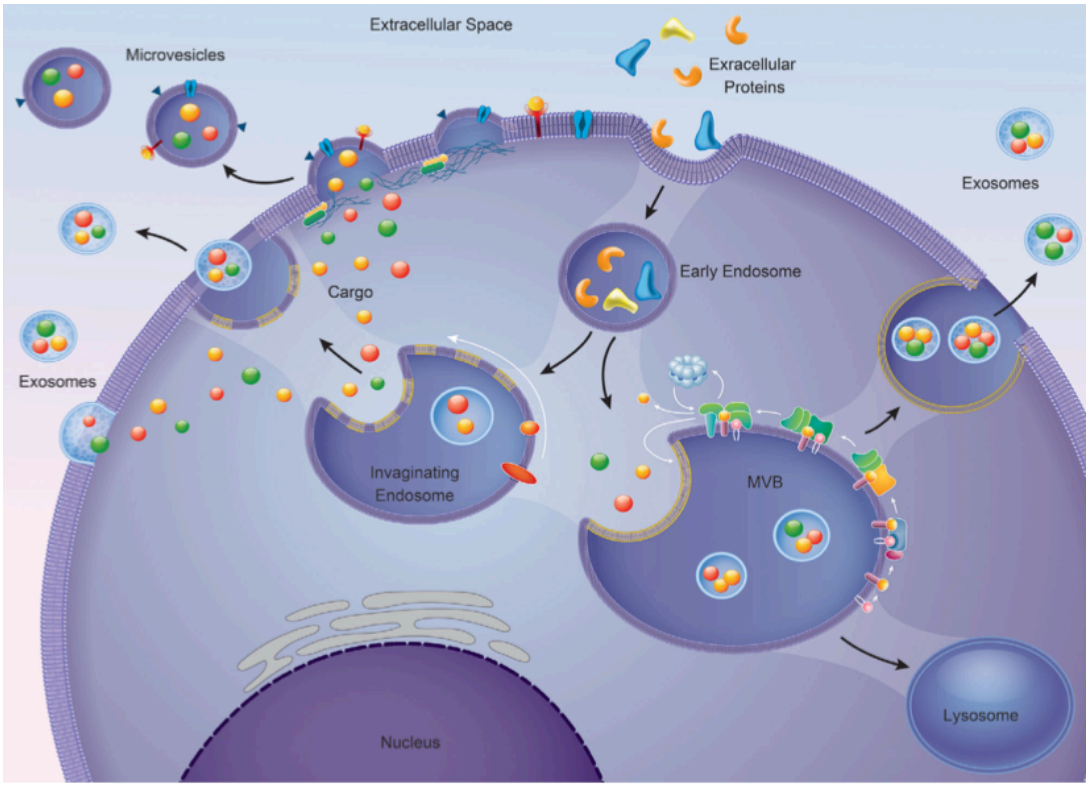

Figura 5: Vias envolvidas na biogênese da vesícula extracelular. Na via clássica, as proteínas extracelulares podem ser internalizadas para formar endossomos iniciais. A invaginação do endossomo inicial é responsável pela origem das vesículas intraluminais (ILV)/corpo multivesicular (MVB). O MVB pode se fundir diretamente à membrana plasmática liberando seu conteúdo, exossomos, ou se fundir com os lisossomos e ter seu conteúdo degradado. Outro mecanismo da biogênese dos exossomos é o brotamento direto da membrana plasmática. A biogênese da microvesícula ocorre pela geração de pequenas protrusões citoplasmáticas que fazem com que a membrana celular seja comprimida, dando origem às microvesículas. (Vechetti et al., 2021)

Ainda assim, a utilização de proteínas, da morfologia e da densidade dessas partículas não são suficientes para distinguir uma categoria da outra (Bobrie et al., 2011), mas o uso de ferramentas da Biologia Molecular pode trazer novas informações que possam caracterizar com maior exatidão essas diferentes classes de EV's (van der Pol et al., 2012). Para isso, alguns pesquisadores já trabalham no sequenciamento de RNA, codificantes ou não, que são carreados por EV's, esses resultados veem mostrando que cada célula secreta um perfil diferente de vesículas. É o que ocorre, por exemplo, nos diferentes tipos de tumores que um organismo pode estar alojando, cada tipo de célula mutável libera EV's com componentes específicos, permitindo a identificação de um perfil global de uma amostra de soro, através do sequenciamento, comparação, identificação do perfil de expressão e identificação do marcador específico (Cortez et al., 2011).

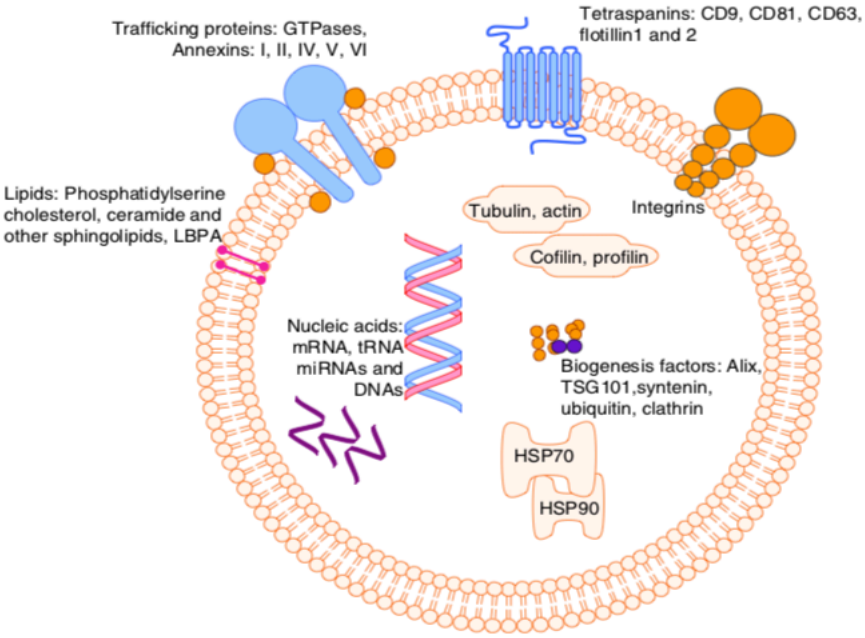

Figura 6: A composição dos exossomos. Os três componentes principais dos exossomos são lipídios, proteínas e ácidos nucleicos. Os lipídios são os principais componentes do esqueleto exossômico. Eles também estão envolvidos na biogênese do exossomos. Entre os lipídeos, os esteróis, os esfingolipídios e os fosfolípides são os dominantes responsáveis pela classificação de carga. Além dos lipídios, as proteínas também são enriquecidas na superfície exossômica. Considera-se que as tetraspaninas, Integrinas, GTPases e anexinas estão envolvidas na interação e tráfico de membranas após o reconhecimento das proteínas de superfície nos receptores. Existem também várias cargas de ácido nucleico, incluindo DNA, RNA e miRNA detectados nos exossomos que determinam a especificidade das funções exossômicas. **Fonte: Gao, M. et al.; 2018** (Gao et al., 2018).

Dentro do campo da Biologia, detectar e caracterizar EV's pode trazer respostas sobre diversas doenças e possíveis vias de interferência. Em torno do mundo, pesquisadores já utilizam esse canal de comunicação entre as células de diferentes tecidos para promover o carregamento de fármacos capaz de atingir um tecido alvo (Basso and Bonetto, 2016; Fruhbeis et al., 2013; Lawson et al., 2016). Obviamente, essas moléculas carregadas por EV's irão variar de acordo com a célula de origem e célula alvo, como supracitado, promovendo ação de coagulação, apoptose ou diferenciação celular, por exemplo. Participam, portanto de diferentes vias de respostas celulares (Colombo et al., 2014). O estudo de EV's pode trazer um novo horizonte para o desenvolvimento e busca de alternativas para tratamentos no campo biomédico, através da elucidação da biologia celular e de sua fisiologia.

Não obstante desse cenário, está o desenvolvimento do tecido ósseo, que durante sua formação depende de outros tecidos subjacentes e/ou distantes para que o processo ocorra de maneira harmoniosa **(Fig. 7)**. Assim, destacamos o processo de Osteogênese e Angiogênese, processos de formação de tecido ósseo e vasos, respectivamente. Que, em ambos os casos, as células de cada tecido produz EV's que atuam na formação do próprio tecido e de maneira parácrina no tecido vizinho (Anderson et al., 2005; Morel et al., 2004).

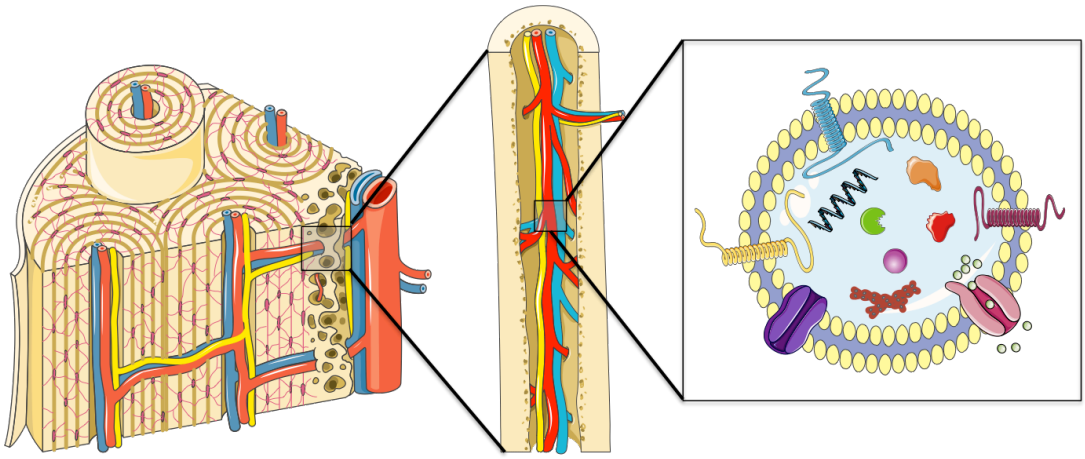

Figura 7: Esquema apresentando transporte de EVs através dos vasos sanguíneos em *crosstalk* com o tecido ósseo. Sabe-se que o tecido vascular é recoberto por uma túnica composta por tecido muscular liso, o que lhe confere habilidade contrativa, esses tecidos, podem interferir no processo de osteogênese de maneira parácrina, tal qual a hipótese central desse estudo. Fonte própria.

A compreensão da comunicação entre esses tecidos é de extrema relevância, uma vez que o tecido ósseo, apesar de sua aparência estática e estável, sofre alterações moleculares constantes e que podem ser geradas por fatores transportados via vasos uma vez que o tecido precisa ser nutrido. Na formação da porção endocondral do tecido ósseo, ocorre a invasão de vasos que irão nutrir o tecido para síntese de matriz mineralizada da cartilagem, esse processo permite o amadurecimento de células osteogênicas que iniciam a formação do tecido em questão sobre a cartilagem pré formada (Hasegawa et al., 2016; Ochi and Takeda, 2014).

Nos últimos anos, alguns grupos têm ganho destaque no estudo de inter-relações entre o tecido ósseo e os demais tecidos, e tem sido mostrado seu papel na regulação de funções celulares importantes, modificando seu metabolismo e fenótipo. Neste cenário, 2 grupos de pesquisa merecem destaque: o grupo liderado pelo Prof. Gerard Karsenty, EUA, quem tem evouido na compreensão da osteocalcina como molécula endócrina, e o grupo liderado pelo Prof. Ralf Adam, Alemanha, quem tem mostrado acoplamento entre

osteogênese à mecanismos parácrinos disparados por células endoteliais. No entanto, embora com avanço significativo neste contexto, pouco se sabe quais são os mecanismos que acoplam células ósseas e seu microambiente, sobretudo em resposta à fibroblastos e células do endotélio. Assim, o objetivo deste trabalho foi fazer uso de ferramentas de biologia celular e molecular para investigar mecanismos envolvidos com o comportamento de osteoblastos em resposta a fatores tróficos liberados por fibroblastos, células endoteliais e células musculares lisa, sobretudo buscando entender se tratar de mecanismos biológicos mediados por microvesículas.

CAPÍTULO 2

Biochimie. 2020 Jan;168:92-99. doi: 10.1016/j.biochi.2019.10.013.

Fibroblast-secreted trophic factors up-modulate osteocyte gene markers and contribute with ECM remodeling stimulus in osteoblast

Running title

Crosstalk between fibroblast and osteoblast

Célio Jr. da Costa Fernandes[1] & Willian Fernando Zambuzzi[1]*

[1]Lab. of Bioassays and Cell Dynamics, Department of Chemistry and Biochemistry, Institute of Biosciences, Universidade Estadual Paulista - UNESP, Botucatu, São Paulo, CEP 18618-970, Brazil;

Abbreviation list

ECM, Extracellular Matrix; MMP, Matrix Metalloproteinase; TIMPs, Tissue Inhibitors of Metalloproteinases; DMP1, Dentin Matrix Protein 1; SOST, Sclerostin; FGF23, Fibroblast Growth Factor 23; IL, Interleukin; OPG, Osteoprotegerin; RANKL, Receptor Activator of Nuclear factor-KappaB Ligand; qPCR, quantitative Polymerase Chain Reaction; ALP, Alkaline Phosphatase; TGFß1, Transforming Growth Factor Beta 1

*Corresponding author:

prof. Willian F. Zambuzzi - email: w.zambuzzi@unesp.br

ABSTRACT

Matrix Metalloproteinases (MMPs) play an important role in tissue remodeling and develop an important pre-requisite event to osteoblast differentiation. As osteogenesis is a multifactorial mechanism, we argued whether osteoblast-induced ECM remodeling might be modulated by trophic factors released by fibroblasts in a paracrine signaling manner. To address this issue, fibroblasts were cultured up to 72 hours when their conditioned medium was harvested and further used to challenge pre-osteoblasts (MC_3T_3-E1 cells) along 14 days *in vitro*. Preliminarily, we validated the potential effect of fibroblasts on contributing with osteogenic phenotype, which specifically requires significant expression of Dentin Matrix Protein 1 (DMP1; about 10-fold changes) and Sclerostin (SOST; about 7-fold changes). Additionally, fibroblast-conditioned medium induces osteogenic phenotype and promotes high level of both mRNA and MMP-9 activity, independently of upmodulation of RECK gene (about 13-fold changes); this mechanism seems being a constitutive pathway in those challenged osteoblasts. Considering inflammatory scenario, a couple of genes were addressed it being that both IL-13 (about 13-fold changes) and IL-33 (about 5-fold changes) were upregulated, as well as RANKL (about 8-fold changes) and OPG (about 3-fold changes). Although preliminarily, these data suggest a stimulus to finely controlling osteoclastogenesis, and this mechanism reinforces fibroblast role on bone remodeling and homeostasis. In conjunction, our results suggest an important crosstalk between fibroblasts and osteoblasts, where fibroblast-secreted trophic factors upmodulate osteocyte gene markers and contribute with ECM remodeling stimulus in osteoblast.

Key-words: Bone; Osteoblast; Fibroblast; Extracellular Matrix; Osteocyte; Crosstalk.

1. INTRODUCTION

Bone is a dynamic tissue undergoing continual adaption to maintain skeletal properties and further regulating its homeostasis [1]. Bone remodeling has been reported being to be important process for bone formation and places important behavior in response to mechanical loads [2,3]. In special, bone remodeling is also responsible for repairing injured tissue recruiting a multitude of synchronized cellular cues [4], mainly orchestrated by the balance of osteoblasts and osteoclasts activities [5]. In addition, it is known that immune cells and inflammatory cytokines mediate bone metabolism, indicating important cross-regulations between the immune and skeletal systems [6], where extracellular matrix (ECM) poses fundamental role on cellular anchorage and compromising influencing cell phenotype, governing the activity of osteoblasts, osteoclasts, osteocytes and fibroblasts [7–10].

In this way, the ECM-related components are decisive on triggering specific metabolic pathways, regulating bone homeostasis. To note, ECM remodeling requires efficient and regulated machinery, which composes including proteases and their specific inhibitors, such as matrix metalloproteinases (MMPs) and tissue inhibitors of metalloproteinases (TIMPs), respectively. It is very well known that MMPs process collagen fibers and gelatins A and B – in special, as their sub-products, as gelatin, are proteolytically processed by specific members of MMPs family, named MMP-2 and MMP-9, also known as gelatinases A and B, respectively, and they influence on events driving cell adhesion, migration and differentiation [7]. Altogether, these mechanisms undergoing driving ECM remodeling are involved with osteoblastogenesis and osteoclastogenesis. In fact, we have reported earlier there is a strict control of ECM remodeling stimulus during ascorbate-induced osteoblast differentiation *in vitro* [11]. As these processes are coupled, its disruption might be involved with etiology of bone diseases and it is necessary to understand whether osteoblast-induced ECM remodeling might be modulated by trophic factors released by fibroblasts. Importantly, as MMPs as drugable enzymes, we can suggest them within pharmacological protocols.

Certainly, the bone dynamism comes from a pleiotropic crosstalk involving paracrine-signaling requiring different cell lineages, as endothelial cells [12] and fibroblasts [13]. Looking for elucidating the mechanism for regenerating the ligament-to-bone interface, Wang et al (2007) focused on the role of heterotypic cellular interactions in the fibrocartilage tissue to propose a biomimetic co-culture model considering osteoblast–fibroblast interactions and the relevance of these communications in interface

formation and their findings suggest that osteoblast–fibroblast interactions may lead to cell trans-differentiation and eventual fibrocartilage formation. Although genetically close each other [14], studies reporting the interplay between osteoblasts and fibroblasts are very scarce. Although we have not considered cell-cell contact model, we have challenged cultures of osteoblasts with semiconfluent cultures of fibroblasts-conditioned medium and a positive crosstalk was related on guiding osteoblast differentiation. Moreover, although some achievement has been made on this matter, the bone and related tissues homeostasis seems being under a complex and dynamic mechanism involving heterotypic cellular interactions, and fibroblast has emerged as interesting member mainly as source of signaling trophic molecules able to modify surrounding cell phenotype.

The above-mentioned prompted us to better explore the behavior of pre-osteoblasts in response to a pool of released trophic factors by fibroblasts *in vitro*, considering a biological model previously proposed [13]. Here, our main focus was understanding whether the capacity of fibroblasts in modulating osteoblast performance and ECM remodeling, mainly because ECM is decisive substrates for maintaining survival signaling of adhering cells phenotypes, such as osteoblasts. Summarizing, our data shows there is a dynamic crosstalk between fibroblast and osteoblast, where fibroblast seems contributing on ECM remodeling stimulus during osteoblast differentiation. Moreover, the molecular picture under osteoblast responding to fibroblasts-secreted trophic factors reveals a strong stimulus to drive osteoblast-osteocyte transition, in a paracrine signaling manner.

2. MATERIALS AND METHODS

2.1. Chemicals and primers. All chemicals were analytical grade and purchased from Sigma Co. (St. Louis, MO, USA). The primers were obtained from Exxtend (Campinas, SP, Brazil).

2.2. Cells and culture. Pre-osteoblasts (MC_3T_3-E1, subclone 4) and Fibroblasts (NIH-$3T_3$-E1) were used in this study. The cells were maintained in incubator at 37ºC, 95% of humidity and 5% CO_2 in αMEM and DMEM medium respectively, both containing antibiotics (100 U/mL penicillin, 100 mg/mL streptomycin), Ribonucleosides and Deoxyribonucleotides, supplemented with 10% Fetal Bovine Serum (FBS) (Nutricell, Campinas, SP, Brazil). For the osteoblast differentiation assay, the pre-osteoblasts were

seeded on cell- culture dish plates with a density of $5x10^4$ cells cm^{-2} and maintained into incubator up to 14 days, when all the biological methodologies were performed. In parallel, fibroblasts were seeded at the same density of cells and after 3 days the medium was collected (named conditioned medium), filtered and used to challenge pre-osteoblasts. This culture medium was changed every 3 days to maintain the biological stimulus considered in this experimental design. Cultures treated with osteogenic medium [O.M.; ß-Glycerophosphate (10 mmol L^{-1}), Dexamethasone (0.03 g/mL), and ascorbate (50 µg/mL)] was considered the positive control [13].

2.3. Gene expression analysis. The quantitative polymerase chain reaction (qPCR) was performed using a PCR system in real time QuantStudio®3 to evaluate changes in transcription of a set of genes (**Table 1**). The total mRNA was harvested from cells using Ambion TRIzol Reagent (Fisher Scientific Inc, Walthan, MA, EUA) and thereafter the cDNA was synthesized using High Capacity cDNA Reverse Transcription Kit (Applied Biosystems, Foster City, CA). The reaction condition was as follow: 95°C for 3s; 55°C for 8s; 72°C for 20s. The changes were analyzed using the comparative CT method (ΔΔCt) normalizing the GAPDH expression.

Table 1. Expression primers sequences and PCR cycle conditions.

Gene	Primer	5'-3' Sequence
ALP	Forward	GAAGTCCGTGGGCATCGT
	Reverse	CAGTGCGGTTCCAGACATAG
OPG	Forward	CAGAGACTAATAGATCAAAGGCAGG
	Reverse	ATGAAGTCTCACCTGAGAAGAACC
RANKL	Forward	CGCTCTGTTCCTGTACTTTCGAGCG
	Reverse	TCGTGCTCCCTCCTTTCATCAGGTT
DMP-1	Forward	CCCAAAACAGGAAAGGATCA
	Reverse	ACCAGACTGCTTCTCCTCCA
SOST	Forward	CTTTGGCGTCATAGGGATGGT
	Reverse	CTTTGGCGTCATAGGGATGGT
FGF-23	Forward	CCACGGCAACATTTTTGGA
	Reverse	CTGGCGGAACTTGCAATTCT
MMP-2	Forward	AACTTTGAGAAGGATGGCAAGT
	Reverse	TGCCACCCATGGTAAACAA
MMP-9	Forward	TGTGCCCTGGAACTCACACGAC
	Reverse	ACGTCGTCCACCTGGTTCACCT
TIMP-1	Forward	ATCCTCTTGTTGCTATCACTG
	Reverse	GGTCTCGTTGATTTCTGGG
TIMP-2	Forward	GCAACAGGCGTTTTGCAATG
	Reverse	CGGAATCCACCTCCTTCTCG

RECK	Forward	CCTCAGTGAGCACAGTTCAGA
	Reverse	CCTGTGGCATCCACGAAACT
IL-1β	Forward	GACCTTCCAGGATGAGGACA
	Reverse	AGCTCATATGGGTCCGACAG
IL-6	Forward	AGTTGCCTTCTTGGGACTGA
	Reverse	CAGAATTGCCATTGCACAAC
IL-10	Forward	CCAAGCCCTTATCGGAAATGA
	Reverse	TTTTCACAGGGGAGAAATCG
IL-13	Forward	CAGTCCTGGCTCTTGCTTG
	Reverse	CCAGGTCCACACTCCATACC
IL-18	Forward	ACTTTGGCCGACTTCACTGT
	Reverse	GGGTTCACTGGCACTTTGAT
IL-33	Forward	CCTTCTCGCTGATTTCCAAG
	Reverse	CCGTTACGGATATGGTGGTC
GAPDH	Forward	AGGCCGGTGCTGAGTATGTC
	Reverse	TGCCTGCTTC ACCACCTTCT

2.4. Zymography. At 14 days of culture, the conditioned culture medium from osteoblasts were collected, centrifuged at 13,200 × g for 15 min at 4°C and the protein concentration determined by the Lowry method [15]. The gelatinolytic activity of the samples was evaluated by metalloproteinases resolving (MMP-2 and MMP-9) in 10% polyacrylamide gel containing 4% of gelatin. After the separation, the MMPs were renatured in Triton X-100 aqueous solution (2% m/v), incubated during 18h in proteolysis buffer (Tris-$CaCl_2$) at 37°C and gels were stained with dye solution of Comassie Blue R-250 0,05% for 3h [16]. To note, a molecular weight standard was run in separate lane in order to reference the high relative location of the MMPs activities into in the stained gels.

2.5. Alizarin red S staining. One mL of pre-osteoblasts (5x 10^4 cells/mL) was seeded in 24-well plates and at semi-confluence the cultures were treated with the fibroblast-conditioned medium until 14 days. The medium was changed every 3 days. The osteoblasts were equally fixed with phosphate-buffered 10% formalin for 30 min at room temperature, and thereafter washed with PBS and immediately incubated with 2% Alizarin-Red S dye for 45 min into a dark chamber [17]. Lastly, the stained cultures were newly washed with PBS to allow the images acquisition using an inverted microscope (Zeiss, Germany).

2.6. Statistics analyses. The results are represented as mean ± standard deviation (SD). They were verified analyzed utilizing One-Way ANOVA (non-parametric) with Tukey post-test in order to compare all pairs of groups, with $p<0,05$ considered significant

statistically and p<0,0001 considered highly significantly. The software utilized to perform the analyses was GraphPad Prism 6.

3. RESULTS

To better address the involvement of fibroblast during the osteoblasts differentiating differentiation, fibroblasts were cultured up to 72 hours, when the conditioned medium was harvested to further be used to challenge pre-osteoblasts until 14 days, as proposed elsewhere [13]. Thereafter, these challenged cultures of osteoblasts were forwarded to zymography and qPCR approaches in order to evaluate eventual ECM remodeling stimulus during differentiation mechanism (**Fig.1**).

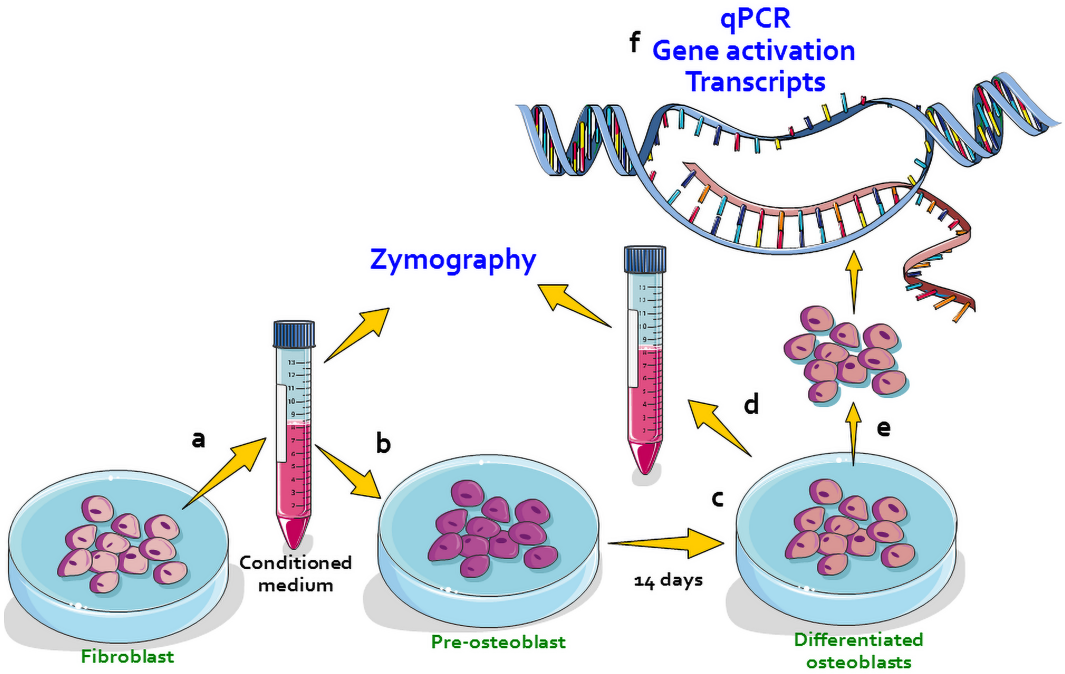

Figure 1: Experimental design of the study. a. Firstly, fibroblast cells (3T3) were cultured up to 72 hours, when the conditioned medium was harvested and after used to treat pre-osteoblast (MC3T3-E1, subclone 4) cultures up to 14 days in order to evaluate whether fibroblast contributes to osteoblast differentiation and performance (**b,c**). Differentiated osteoblasts were harvested and processed to identify the expression of genes related with inflammation, osteogenic gene markers and ECM remodeling (**e,f**). In addition, the conditioned medium at this period was collected and forwarded to evaluating MMP's activities by zymography (**d**). Illustrative images were obtained and adapted from the Creative Commons Attribution 3.0 Unported license.

3.1. Fibroblast-secreted factors promote osteocyte phenotype biomarkers expression in osteoblasts

Experimentally, the osteogenic potential was measured using positive control cultures, where the pre-osteoblasts were challenged with osteogenic medium [11]. In

fact, we show there is an important contribution of fibroblast-secreted factors on osteoblast performance, once as fibroblast conditioned medium stimulated up-increased expression of Alkaline Phosphatase (ALP) expression, reinforcing the positive influence on osteogenic phenotype (**Fig. 2b**). Curiously, our data show that fibroblast-released trophic factors promotes up-regulation of DMP1 (about 10-fold changes; **Fig. 2c**) and SOST (about 7-fold changes, **Fig. 2d**), both biomarkers of osteocyte phenotype, while FGF23 was down-modulated (**Fig. 2e**). Importantly, Alizarin Red S staining shows characteristics of mineralized matrix (**Fig. 2a**). Thus, our results seem to show an osteocytogenesis stimulus in the fibroblast/osteoblast interplay.

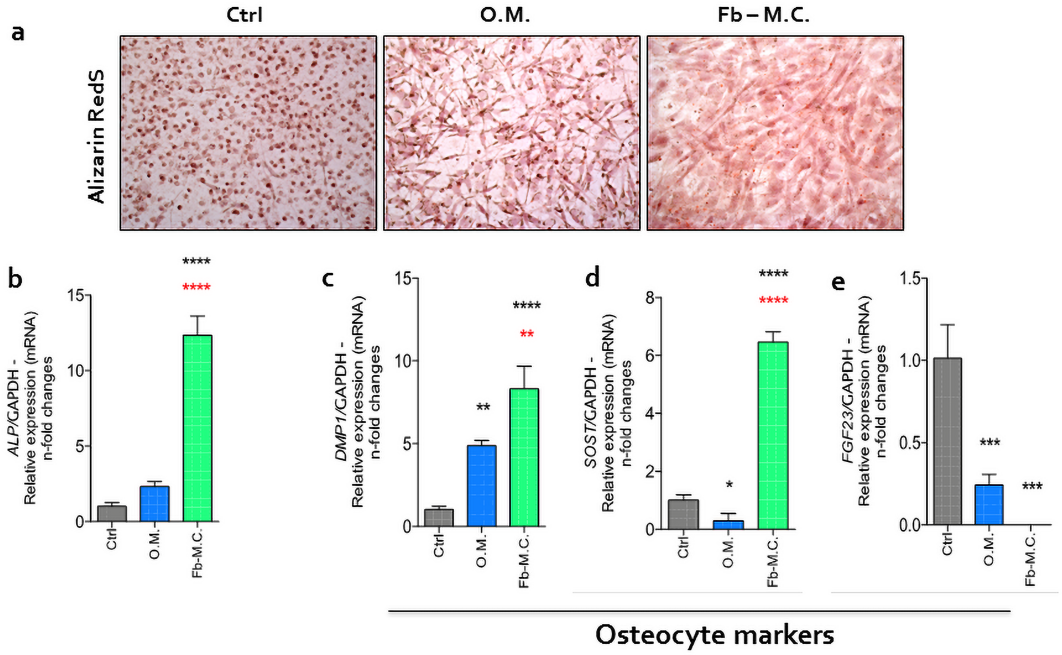

Fig.2. Contribution of fibroblast with osteogenic phenotype. Conditioned medium by fibroblasts contributed with the up-regulation of ALP (**b**) and mineralizing process of the matrix (**a**), reinforcing their potential in promoting osteogenic signals at day 14 *in vitro*. Later, we considered evaluating osteocyte-related biomarkers genes. Surprisingly, DMP1 (**c**) and SOST (**d**) genes were up-modulated, while FGF23, another gene related with osteocytes, was unchanged (**e**). Note: Crtl - control, culture of osteoblasts without any treatment; O.M. - positive control, culture of osteoblasts treated with osteogenic medium; Fb-M.C. - culture of osteoblasts treated with conditioned medium. Significances were considered when: *p<0.018, **p<0.0047, ***p<0.0004, ****p<0.0001, when compared to the control group, and **p<0.0058, ****p<0.0001, when compared to O.M.

3.2. Interleukins (ILs) and cytokines gene markers during fibroblast-induced osteoblast differentiation

Inflammation signaling have been reported being involved with osteoblast differentiation, participating actively on bone growth and repair [18–20]. Thus, we

evaluate a set of interleukins related with osteoblasts biology, looking to understand possible paracrine signaling. As expected [21], our data show that osteogenic medium (positive control) promotes up-regulations of IL-1ß (**Fig. 3a;**), IL-6 (**Fig. 3b;**) [22], IL-18 (**Fig. 3d;**) [23], and IL-33 (**Fig. 3e;**) [24,25]. Conversely, except to IL-13 and IL-33 (**Fig. 3c,e**), fibroblast-conditioned medium does not modulate IL-1ß, IL-6 and IL-18 in osteoblast (**Fig. 3**). Complimentarily, fibroblast-conditioned medium promotes up-regulation of IL-13 and IL-33 in osteoblast (**Fig. 3c,e**), and they seems develop necessary fibroblast-related signal transduction in osteogenic phenotype. To note, IL-13 mRNA shows a profile of about 13-fold changes higher compared with the control, while cultures of osteoblast responding to osteogenic medium do not present any changes (**Fig. 3c**).

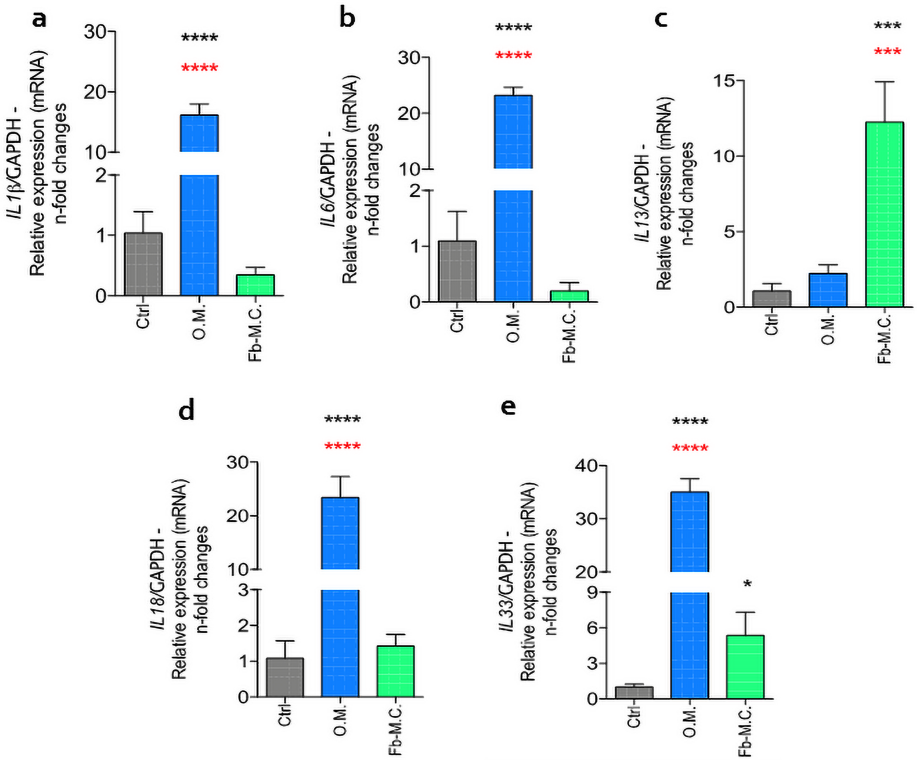

Fig.3. Partial inflammatory landscape. Considering our previously described model, osteoblasts were challenged by conditioned medium from fibroblasts up to 14 days, when the cells were lyzed and processed to evaluate inflammatory-related genes expressions with qPCR. While O.M. promoted an up-regulation of IL-1β (**a**), IL-6 (**b**), IL-18 (**d**), and IL-33 (**e**), fibroblast-released factors provoked up-regulation of Il-13 (**c**), and IL-33 (**e**). Significances were considered when: *p<0.015, ***p<0.0003, ****p<0.0001, when compared to the control group, and ***p<0.0003, ****p<0.0001, when compared to O.M.

Mostly, inflammation processes have been also reported with bone resorption with upmodulation of osteoclastogenesis. Thus, we were encouraged to investigate whether fibroblasts were able to modulate the expression of both RANKL and OPG in

challenged osteoblasts. Surprisingly, our data shows significant increase of both genes, being RANKL (about 8-fold changes; **Fig. 4a**) and OPG (about 3-fold changes; **Fig. 4b**). We have better addressed the effects of fibroblast on potential osteoclastogenesis signaling by considering the ratio of both genes (RANKL/OPG) and this analysis shows a positive effect of fibroblasts on driving osteoclastogenesis, since RANKL positively governs this process.

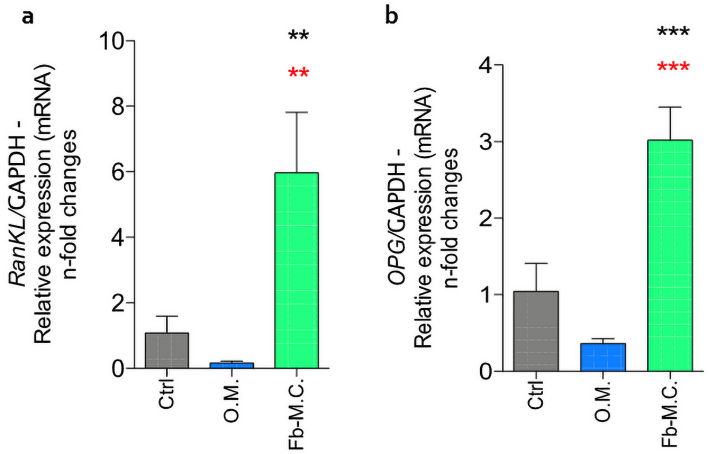

Fig. 4. Osteoclastogenesis-related genes. Both RANKL (**a**) and OPG (**b**) genes were increased in response to fibroblast-induced paracrine signaling. Partially, as osteocytes are major source of RANKL, these findings corroborate with the osteocyte phenotype of those challenged osteoblasts. Significances were considered when: **p<0.0057, ***p<0.0003, when compared to the control group, and **p<0.0057, ***p<0.0003, when compared to O.M.

3.3. Fibroblast contributes to ECM remodeling stimulus in osteoblast

Since both inflammation processes and mineralization mostly require a dynamic ECM remodeling, we decided investigating whether fibroblast was able to trigger ECM remodeling stimulus in osteoblasts. To investigate, we have evaluated transcripts and activities of matrix metalloproteinases (MMPs)-2 and -9, as well as the transcripts of TIMPs -1 and -2, and RECK (all of three are related with MMP activity regulation). Markedly, our data shows that fibroblast-conditioned medium promotes a significant up-regulation of MMP-9 (about 8-fold changes, **Fig. 5b**) and RECK (about 13-fold changes, **Fig. 5e**), while MMP2 (**Fig. 5a**), TIMP1 (**Fig. 5c**) and TIMP 2 (**Fig. 5d**) remained unchanged.

To validate the relevance of MMPs on this paracrine signaling, we harvested the conditioned medium from the unchallenged osteoblasts to allow evaluating the MMPs-2 and -9 activity by zymography technology (**Fig. 5f**) and taken these data into account our data shows significant induction of fibroblasts on MMP-9 activity during osteoblast differentiation (**Fig. 5g-k**). To date, in order to minimize potential bias and

misinterpretation of our data, we evaluated the fibroblast-conditioned medium as possible source of MMPs (control).

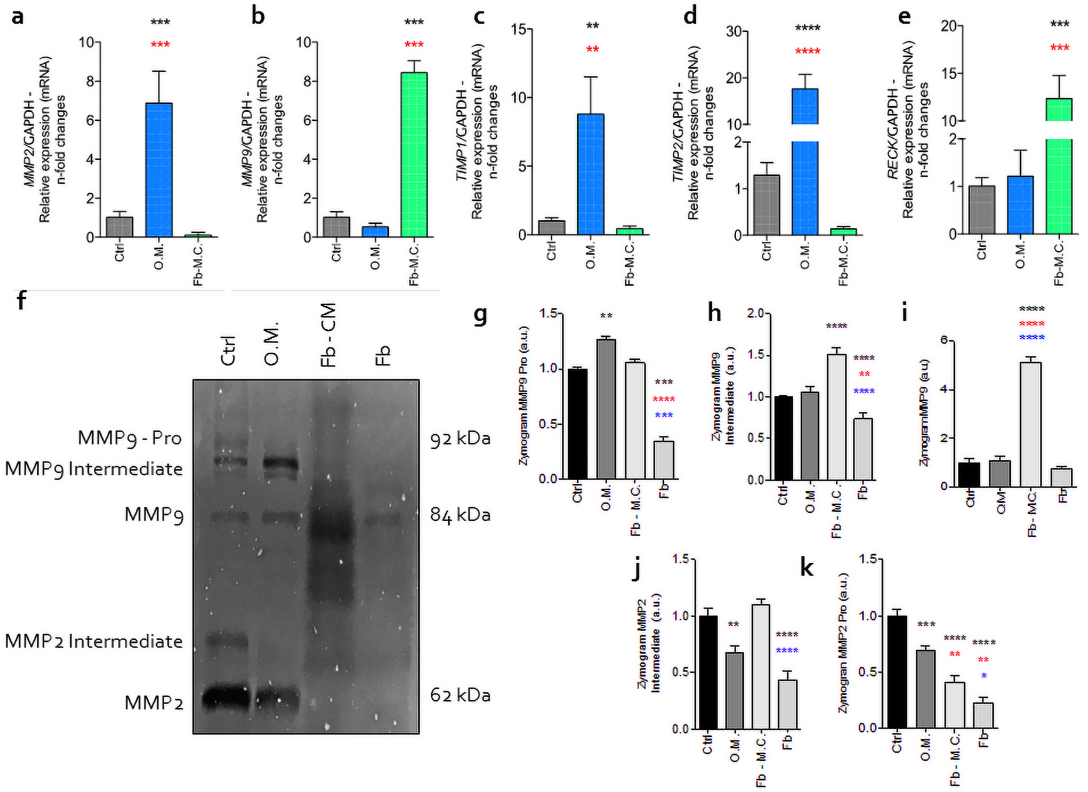

Fig.5. Fibroblast-induced ECM remodeling during osteoblast differentiation. In order to evaluate whether fibroblasts affect EM remodeling, we first evaluated the transcripts profile of ECM-related genes, such as MMP-2 (**a**); MMP-9 (**b**); TIMP-1 (**c**); TIMP-2 (**d**); and RECK (**e**). Among them, our results showed an-up-modulation of MMP-9 and RECK transcripts profiles, suggesting a synchrony between themselves. Complimentarily, MMP's activities were evaluated considering the gelatinolytic activity of MMPs- and -9 (**f-k**): there was an increase of MMP-9 activity in response to fibroblasts-released signals, while MMP-2 activity was decreased in the same condition. In order to avoid possible technical bias, we considered evaluating also the sole conditioned medium from fibroblasts (that used to treat the osteoblasts) as a potential source of MMP's activities. Significances were considered when: **p<0.0055, ***p<0.0003, ****p<0.0001, when compared to the control group; **p<0.0057, ***p<0.0003, ****p<0.0001 when compared to O.M.; and *p<0.014, ***p<0.0003, ****p<0.0001, when compared to Fb-MC.

4. DISCUSSION

Bone growth is a multifactorial mechanism undergoing responses to a multitude of signals secreted by several cell types. Over the last few years an advance on the comprehension of this mechanism was elegantly reported by Kusumbe et al (2014), who have demonstrated an important role of endothelium on osteogenesis [12,26], opening new avenue to understand the involvement of endothelial cells on osteoblast

differentiation. To better address this issue, we have focused on evaluating whether fibroblast is active on this process and considering a paracrine signaling, we have proposed earlier that fibroblast contributes to osteogenic phenotype by up-modulating ALP involvement [13] and this study opened new questions on the direction to understand whether this mechanism requires extracellular matrix remodeling, as it was shown elsewhere during osteoblast differentiation [11]. To address this issue, fibroblasts were cultured up to 72 hours, when the conditioned medium was harvested and further used to challenge pre-osteoblast up to 14 days as proposed by [13]. Thereafter, challenged osteoblasts were collected to evaluate the profile of ECM-related gene markers, as well as their conditioned medium for estimating the activity of matrix metalloproteinases (MMPs) secreted to the extracellular compartment. Despite intensive studies *in vitro*, in cell culture and in animal models, the normal physiological roles of these extracellular proteases have been elusive, mainly considering the crosstalk between fibroblast and osteoblasts.

On this sense, our data brings a panorama of ECM remodeling by evaluating MMPs-2 and -9 involvement, as well as their tissue inhibitors, TIMPs-1 and -2, and RECK. Important, our data reveals MMP-9 is significantly up-modulated at both transcriptional and activity levels in response to fibroblast-conditioned medium, while MMP-2 was decreased in this same experimental condition, maybe because of both MMPs act on the same substrates and are involved with the same mechanism in processing basement membrane degradation because of their ability to cleave collagen and gelatin [27].

Importantly, RECK was also increased (transcripts profile), suggesting as an immediate reflex to the higher MMP-9 activity, once RECK is a GPI-anchored protein modulating the activity of MMP-9 pericellularly [28,29]. Specifically in osteoblast, we have shown their importance on ECM remodeling considering ascorbate-induced osteoblast differentiation [11]. At this point, we suggest this stimulus of ECM remodeling modulation immediately in response to fibroblast-released factors as a pre-requisite to further mineralizing mechanism.

Thereafter, we were argued to evaluate the behavior of osteoblast biology-related gene markers, in addition those findings reported by da Costa Fernandes et al. (2017). Curiously, our data reveals a strong involvement of SOST and DMP-1 genes in osteoblasts responding to fibroblast-released factors. To note, both SOST and DMP-1 genes are involved with osteoblast/osteocyte transition. Taking into account the limitations of this study, our data supports a possible mechanism where fibroblast might

contributes to osteoblasts/osteocytes transition, at least in the beginning of this phenotype acquisition by significantly up-modulating SOST and DMP-1, knowingly osteocyte biomarkers [30,31].

Important on this scenario is the association of this molecular landscape with the involvement of interleukins and cytokines-related genes: conversely there is a significant requirement of IL-13 gene (about 12-fold changes) in fibroblast-challenged osteoblast, while osteogenic medium (positive control) requires the involvement of IL-1ß (about 15-fold changes) and IL-6 (about 20-fold changes). Mechanistically, IL-13 levels and MMP9 activity are substantially up-regulated in the presence of fibroblast-conditioned medium compared to control osteogenic medium and this open the hypothesis that IL-13 is a primary driver of MMP9-upregulation in the osteoblast-osteocyte transition in this model. However, this hypothesis was not fully addressed in this study and certainly a limitation was not performing a manipulation of IL-13 and further examine the effects on MMP9, as well as the osteoblast-osteocyte transition biomarkers. Similarly, validating the importance of MMP9 in driving osteoblast-osteocyte transition needs to be better addressed in the future. However, some lessons from literature show that IL-13 induces MMP-9 and TGFß1 expressions [32], and this coupling of signals is also involved with the migration of leukocytes [33]. Additionally, MMP-9 activity might contribute on TGFß1 signaling and trigger known pathways reported with osteoblast biology [34,35].

Until considering the inflammatory stimulus, challenged osteoblasts significantly up-express RANKL, a ligand involved with osteoclastogenesis [36]. Unsurprisingly, Nakasima et al (2011) have reported that osteocytes are the major source of RANKL in bone remodeling [37,38], reinforcing our hypothesis that fibroblasts contribute with the stimulus to osteoblast-osteocyte transition.

In conjunction, our results show an important crosstalk between fibroblasts and osteoblasts, at least considering a paracrine signaling, where fibroblast-secreted trophic factors upmodulate osteocyte gene markers and ECM remodeling in osteoblasts. Indeed, these findings need to be considered on the road to understanding the dynamic bone tissue homeostasis.

Acknowledgements

The authors are grateful to Fundação de Amparo à Pesquisa do Estado de São Paulo (FAPESP) for the financial support (grants: #2016/08888-9, 2014/22689-3).

5. REFERENCES

1. van der Eerden BCJ, Teti A, Zambuzzi WF. Bone, a dynamic and integrating tissue. Archives of biochemistry and biophysics. United States; 2014. p. 1–2.
2. Badilatti SD, Christen P, Parkinson I, Muller R. Load-adaptive bone remodeling simulations reveal osteoporotic microstructural and mechanical changes in whole human vertebrae. Journal of biomechanics. United States; 2016;49:3770–9.
3. Liu C, Carrera R, Flamini V, Kenny L, Cabahug-Zuckerman P, George BM, et al. Effects of mechanical loading on cortical defect repair using a novel mechanobiological model of bone healing. Bone. United States; 2018;108:145–55.
4. Chen C-H, Wang L, Serdar Tulu U, Arioka M, Moghim MM, Salmon B, et al. An osteopenic/osteoporotic phenotype delays alveolar bone repair. Bone. United States; 2018;112:212–9.
5. El-Jawhari JJ, Jones E, Giannoudis P V. The roles of immune cells in bone healing; what we know, do not know and future perspectives. Injury. Netherlands; 2016;47:2399–406.
6. Liu H, Li D, Zhang Y, Li M. Inflammation, mesenchymal stem cells and bone regeneration. Histochemistry and cell biology. Germany; 2018;149:393–404.
7. Paiva KBS, Granjeiro JM. Matrix Metalloproteinases in Bone Resorption, Remodeling, and Repair. Progress in molecular biology and translational science. Netherlands; 2017;148:203–303.
8. de Oliveira Demarchi ACC, Zambuzzi WF, Paiva KBS, da Silva-Valenzuela M das G, Nunes FD, de Cassia Savio Figueira R, et al. Development of secondary palate requires strict regulation of ECM remodeling: sequential distribution of RECK, MMP-2, MMP-3, and MMP-9. Cell and tissue research. Germany; 2010;340:61–9.
9. Paiva KBS, Zambuzzi WF, Accorsi-Mendonca T, Taga R, Nunes FD, Sogayar MC, et al. Rat forming incisor requires a rigorous ECM remodeling modulated by MMP/RECK balance. Journal of molecular histology. Netherlands; 2009;40:201–7.
10. Accorsi-Mendonca T, Paiva KB da S, Zambuzzi WF, Cestari TM, Lara VS, Sogayar MC, et al. Expression of matrix metalloproteinases-2 and -9 and RECK during alveolar bone regeneration in rat. Journal of molecular histology. Netherlands; 2008;39:201–8.
11. Zambuzzi WF, Yano CL, Cavagis ADM, Peppelenbosch MP, Granjeiro JM, Ferreira C V. Ascorbate-induced osteoblast differentiation recruits distinct MMP-inhibitors: RECK and TIMP-2. Molecular and cellular biochemistry. Netherlands; 2009;322:143–50.
12. Kusumbe AP, Ramasamy SK, Adams RH. Corrigendum: Coupling of angiogenesis and osteogenesis by a specific vessel subtype in bone. Nature [Internet]. Nature Publishing Group, a division of Macmillan Publishers Limited. All Rights Reserved.; 2014;513:574. Available from: http://dx.doi.org/10.1038/nature13720
13. da Costa Fernandes CJ, do Nascimento AS, da Silva RA, Zambuzzi WF. Fibroblast contributes for osteoblastic phenotype in a MAPK-ERK and sonic hedgehog signaling-independent manner. Molecular and cellular biochemistry. Netherlands; 2017;
14. Ducy P, Schinke T, Karsenty G. The osteoblast: a sophisticated fibroblast under central surveillance. Science (New York, N.Y.). United States; 2000;289:1501–4.
15. LOWRY OH, ROSEBROUGH NJ, FARR AL, RANDALL RJ. Protein measurement with the Folin phenol reagent. The Journal of biological chemistry. United States; 1951;193:265–75.
16. Lefebvre V, Peeters-Joris C, Vaes G. Production of gelatin-degrading matrix metalloproteinases ('type IV collagenases') and inhibitors by articular chondrocytes during their dedifferentiation by serial subcultures and under stimulation by interleukin-1 and tumor necrosis factor alpha. Biochimica et biophysica acta. Netherlands; 1991;1094:8–18.
17. Kang HR, da Costa Fernandes CJ, da Silva RA, Constantino VRL, Koh IHJ, Zambuzzi WF. Mg-Al and Zn-Al Layered Double Hydroxides Promote Dynamic Expression of Marker Genes in Osteogenic Differentiation by Modulating Mitogen-Activated Protein Kinases. Advanced healthcare materials. Germany; 2018;7.
18. Loi F, Cordova LA, Pajarinen J, Lin T, Yao Z, Goodman SB. Inflammation, fracture and bone repair. Bone. United States; 2016;86:119–30.
19. Adamopoulos IE. Inflammation in bone physiology and pathology. Current opinion in rheumatology. United States; 2018;30:59–64.

20. Giannoudis P V, Hak D, Sanders D, Donohoe E, Tosounidis T, Bahney C. Inflammation, Bone Healing, and Anti-Inflammatory Drugs: An Update. Journal of orthopaedic trauma. United States; 2015;29 Suppl 1:S6-9.
21. Sartoretto S, Gemini-Piperni S, da Silva RA, Calasans MD, Rucci N, Pires Dos Santos TM, et al. Apoptosis-associated speck-like protein containing a caspase-1 recruitment domain (ASC) contributes to osteoblast differentiation and osteogenesis. Journal of cellular physiology. United States; 2019;234:4140–53.
22. Peruzzi B, Cappariello A, Del Fattore A, Rucci N, De Benedetti F, Teti A. c-Src and IL-6 inhibit osteoblast differentiation and integrate IGFBP5 signalling. Nature communications. England; 2012;3:630.
23. Zhong X, Wang H, Huang S. Endothelin-1 induces interleukin-18 expression in human osteoblasts. Archives of oral biology. England; 2014;59:289–96.
24. Veeriah V, Zanniti A, Paone R, Chatterjee S, Rucci N, Teti A, et al. Interleukin-1beta, lipocalin 2 and nitric oxide synthase 2 are mechano-responsive mediators of mouse and human endothelial cell-osteoblast crosstalk. Scientific reports. England; 2016;6:29880.
25. Schulze J, Bickert T, Beil FT, Zaiss MM, Albers J, Wintges K, et al. Interleukin-33 is expressed in differentiated osteoblasts and blocks osteoclast formation from bone marrow precursor cells. Journal of bone and mineral research : the official journal of the American Society for Bone and Mineral Research. United States; 2011;26:704–17.
26. Ramasamy SK, Kusumbe AP, Wang L, Adams RH. Endothelial Notch activity promotes angiogenesis and osteogenesis in bone. Nature. England; 2014;507:376–80.
27. Page-McCaw A, Ewald AJ, Werb Z. Matrix metalloproteinases and the regulation of tissue remodelling. Nature reviews. Molecular cell biology. England; 2007;8:221–33.
28. Echizenya M, Kondo S, Takahashi R, Oh J, Kawashima S, Kitayama H, et al. The membrane-anchored MMP-regulator RECK is a target of myogenic regulatory factors. Oncogene. England; 2005;24:5850–7.
29. Oh J, Takahashi R, Kondo S, Mizoguchi A, Adachi E, Sasahara RM, et al. The membrane-anchored MMP inhibitor RECK is a key regulator of extracellular matrix integrity and angiogenesis. Cell. United States; 2001;107:789–800.
30. Rios HF, Ye L, Dusevich V, Eick D, Bonewald LF, Feng JQ. DMP1 is essential for osteocyte formation and function. Journal of musculoskeletal & neuronal interactions. Greece; 2005;5:325–7.
31. Kogawa M, Wijenayaka AR, Ormsby RT, Thomas GP, Anderson PH, Bonewald LF, et al. Sclerostin regulates release of bone mineral by osteocytes by induction of carbonic anhydrase 2. Journal of bone and mineral research : the official journal of the American Society for Bone and Mineral Research. United States; 2013;28:2436–48.
32. Yu Q, Stamenkovic I. Cell surface-localized matrix metalloproteinase-9 proteolytically activates TGF-beta and promotes tumor invasion and angiogenesis. Genes & development. United States; 2000;14:163–76.
33. Purwar R, Kraus M, Werfel T, Wittmann M. Modulation of keratinocyte-derived MMP-9 by IL-13: a possible role for the pathogenesis of epidermal inflammation. The Journal of investigative dermatology. United States; 2008;128:59–66.
34. Hinck AP, Mueller TD, Springer TA. Structural Biology and Evolution of the TGF-beta Family. Cold Spring Harbor perspectives in biology. United States; 2016;8.
35. Morikawa M, Derynck R, Miyazono K. TGF-beta and the TGF-beta Family: Context-Dependent Roles in Cell and Tissue Physiology. Cold Spring Harbor perspectives in biology. United States; 2016;8.
36. O'Brien CA, Nakashima T, Takayanagi H. Osteocyte control of osteoclastogenesis. Bone. United States; 2013;54:258–63.
37. Nakashima T, Hayashi M, Fukunaga T, Kurata K, Oh-Hora M, Feng JQ, et al. Evidence for osteocyte regulation of bone homeostasis through RANKL expression. Nature medicine. United States; 2011;17:1231–4.
38. Guerrini MM, Takayanagi H. The immune system, bone and RANKL. Archives of biochemistry and biophysics. United States; 2014;561:118–23.

CAPÍTULO 3

Em R1 na BONE (30 March, 2020)

Vascular smooth muscle cells drive osteoblast-to-osteocyte transition via β-Catenin signaling through exosome communication

Célio J.C. Fernandes[1,2], Rodrigo A. Silva[1], Gwenny M. Fuhler[2]; Maikel P. Peppelenbosch[2], Bram CJ van der Eerden[3]; Willian F. Zambuzzi[1,*]

[1]Bioassays and Cell Dynamics Lab, Dept. of Chemistry and Biochemistry, Bioscience
[2]Department of Gastroenterology and Hepatology and [3]Department of Internal Medicine, Erasmus MC, University Medical Center Rotterdam's Gravendijkwal 230, NL-3015 CE Rotterdam, The Netherlands;
*Correspondence to: w.zambuzzi@unesp.br

ABSTRACT

Blood vessel growth and osteogenesis in the skeletal system are coupled; however, fundamental aspects of vascular function in osteoblast-to-osteocyte transition have not been elucidated. Our study demonstrates that vascular smooth muscle cells (VSMCs), but not endothelial cells, are sufficient to drive osteoblast-to-osteocyte transition. We also found that VSMC-derived exosomes loaded with transcript encoding proteins are related to osteocyte phenotype and Wnt/ß-catenin signaling members. In contrast, endothelial cell-derived exosomes delivered stimuli to mature osteoblast differentiation, up-reprogramming TGF gene family and osteogenic transcriptional factors, Osterix and Runx2. Curiously, Shear-stress-unchallenged VSMCs triggered better performance, which released exosome that presented less membrane zeta potential. Another important issue was the high level of ATP inside the exosomes, facilitating mechanisms of mineralization, since ATP is a substrate for alkaline phosphatase. RNAseq and activity of gene encoding proteins related to intermittent mineralization, as well as sonic hedgehog signaling which reprogramed genes and significantly increased RANKL level validated osteocyte function. Our findings identify a novel and hitherto unexpected role of vascular smooth muscle cells driving osteoblast-to-osteocyte transition and open a new avenue to better understand bone-related diseases.

INTRODUCTION

Bone needs to continuously remodel throughout life to maintain optimal mineral homeostasis and structural integrity. This remodeling process involves several sequential steps referred to as the activation-resorption-formation cycle [1] and culminates in a strict balance between osteoblasts and bone-resorbing osteoclasts to avoid bone loss. Despite their central role in bone remodeling and health, development of osteocytes has received remarkably little attention. Unlike osteoblast development, little is known about the molecular and transcriptional regulators able to drive osteoblast-to-osteocyte transition. This may be because osteocytes have long been seen as quiescent cells trapped within compact bone, and their role in bone homeostasis has been underestimated [2] In addition, these cells are difficult to study due to their limited accessibility *in vitro* and *in vivo*. While composing over 95% of all bone cells, not much is known about osteocyte function in bone homeostasis. It has been suggested that osteocytes serve as mechanosensory of the body and release anabolic signals, including nitric oxide (NO), prostaglandins, and other small molecules, such as adenosine triphosphate (ATP). ATP is speculated to be a decisive factor during the intermittent mineralizing process by serving as phosphate donor to alkaline phosphatase (ALP) activity. Furthermore, NO (a short-lived free radical) inhibits bone resorption and promotes bone formation, mainly in response to mechanical strain.[3,4] NO also promotes angiogenesis, and studies by Adams et al. highlighted the dynamic activity of endothelial cells on bone formation and homeostasis by establishing an intricate molecular framework coupling angiogenesis, angiocrine signals, and osteogenesis [5].

A number of studies have demonstrated that both of these bone formation processes are coupled to angiogenesis.[6] Blood vessel formation does not only require endothelial cells lining these blood vessels, but also depends on the underlying cell layer consisting of vascular smooth muscle cells (VSMC). Although an intimate link between osteoblasts and endothelial cells has been made, the relevance of vascular smooth muscle cells in this scenario is unclear. Hence, we investigated the effect of VSMCs and their products on osteoblast-to-osteocyte transition. Our data demonstrates that both endothelial cells and VSMCs release 120nm-sized exosomes, which alter osteoblast function. However, while endothelial derived exosomes carry most factors required for osteoblast differentiation, VSMC-derived exosomes regulate osteoblast-to-osteocyte transition through ß-Catenin signaling. This increased understanding of the complex

communication between bone cells and blood vessels is necessary for development of novel therapies for bone-related disorders.

RESULTS

Endothelium contributes to osteogenic stimulus

Human coronary aorta endothelial cells (HCAEC) and Aortic smooth muscle cells (AoSMCs) significantly stimulated osteogenesis, since TGF -β1 (**Fig.1a**), BMP2 (**Fig.1e**), and BMP9 mRNA (**Fig.1f**) were upregulated, along with BMPRI (**Fig.1b**). Both RUNX2 (**Fig.1g**) and ALPL mRNA (**Fig.1i**) were upregulated in response to HCAEC and AoSMCs, while Osterix mRNA was significantly upregulated in response to AoSMCs (**Fig.1h**). Involvement of TGFb1/BMP signaling was validated by the upregulated of SMAD 2, 3, 4, 6 and SMAD7 mRNA (**Fig.S2a-f**). Curiously, vein-obtained endothelial cells (HUVEC) seem to deliver a pool of molecules with low osteogenic stimulus since all the biomarkers evaluated here were not responsive to HUVEC-conditioned medium. At this point, we also investigated the role of human Aortic smooth muscle cells (AoSMCs), which appear to be very active in osteogenic phenotype of osteoblasts by upregulating of the expression of TGF β, Osterix, and Runx2 (**Fig.1**), as well as SMADs. Curiously, AoSMCs seem to develop more effectiveness by promoting osteogenic phenotype.

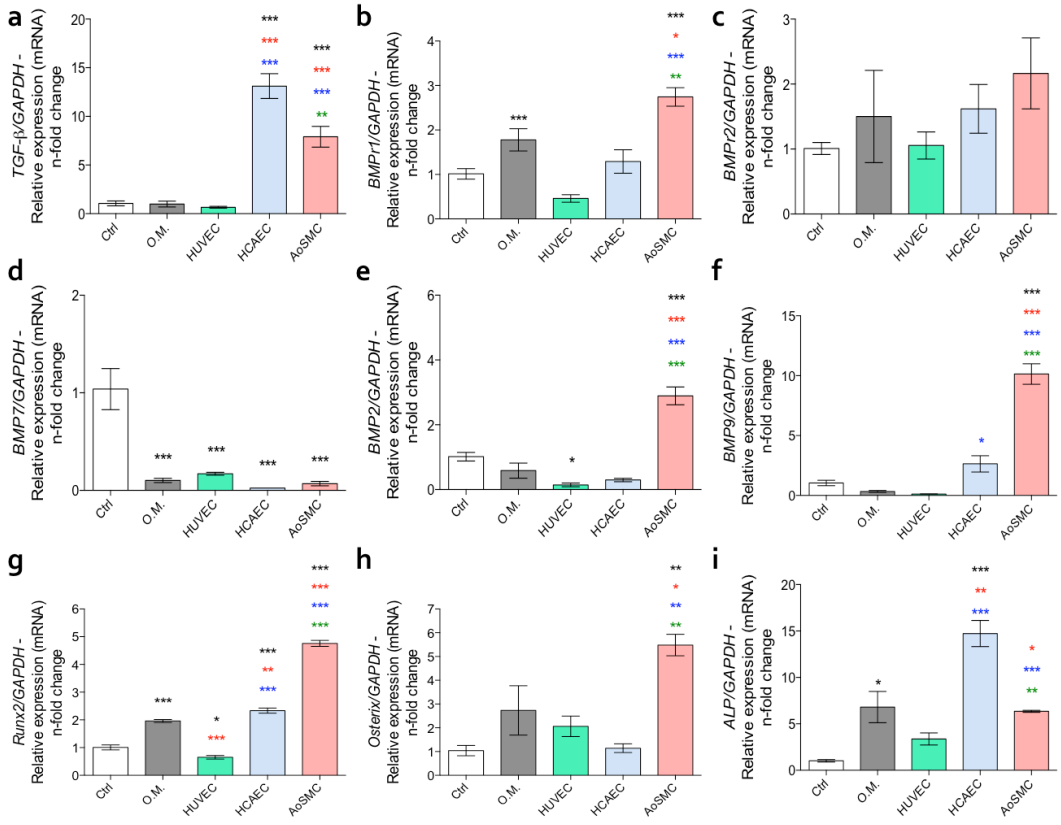

Fig.1. Endothelial cells promote dynamic osteogenic gene marker reprogramming. After 28 days of treatment with the different media conditioned by primary cells, osteoblasts were collected in TriZOL. After RNA extraction and cDNA synthesis, the osteoblast differentiation markers: (a) TGF-b, (b) BMPr1, (c) BMPr2, (d) BMP7, (e) BMP2, (f) BMP9, (g) Osterix, (h) Runx2, and (i) ALP, were expressed in different treatments, including the positive the osteogenic medium control group. The results were normalized by GAPDH expression. *p<0.05; **p<0.1906, ***p<0.0002: Statistically significant difference when compared to control. *p<0.05; **p<0.1906; ***p<0.0002: Statistical difference when compared with the Osteogenic medium. **p<0.1906; ***p<0.0002: Statistical difference when compared with the HUVEC-conditioned medium. **p<0.1906; ***p<0.0002: Statistical difference when compared with the HCAEC-conditioned medium.

Experimental design: To address the crosstalk of vascular cells with mature osteoblasts, primary endothelial and vascular smooth muscle cells were employed, and human osteoblasts were obtained from healthy donors subjected to orthopedic procedures (**Fig.1**). The culture medium conditioned by VSMCs and endothelial cell cultures were harvested and used to treat mature osteoblasts. In parallel, the conditioned medium was characterized, and our results revealed the presence of exosomes, which were properly characterized (**Fig.S1**). The conditioned medium was used further to challenge the human osteoblasts up to 28 days, when these cells were investigated by analyzing their

molecular basis and morphology (**Fig.S1**). We also compared these results with those triggered by endothelial cells obtained from artery or vein. Although endothelial cells communicate with bone cells[11–20], little is known about the signaling molecules that govern this crosstalk.

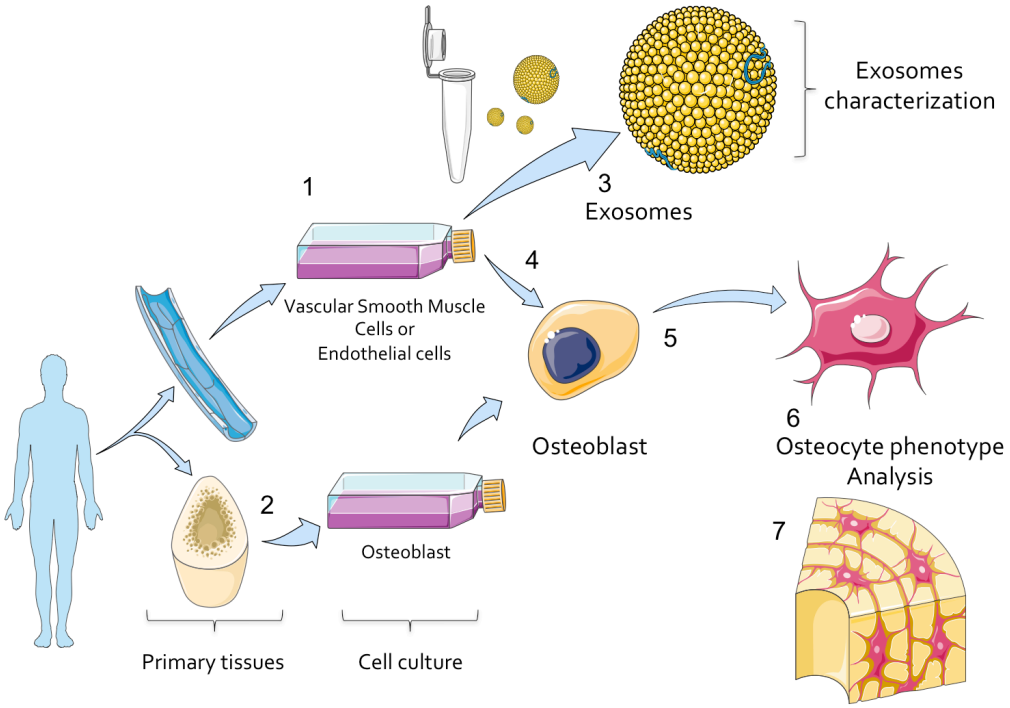

Fig.S1. Outline of the experimental procedures adopted in this study to evaluate the effect of endothelial cells on osteoblast performance. During the experimental procedures, we identified some dendrites in the cell body that appeared to be an osteocyte, and through specific methodologies, we validated this hypothesis.

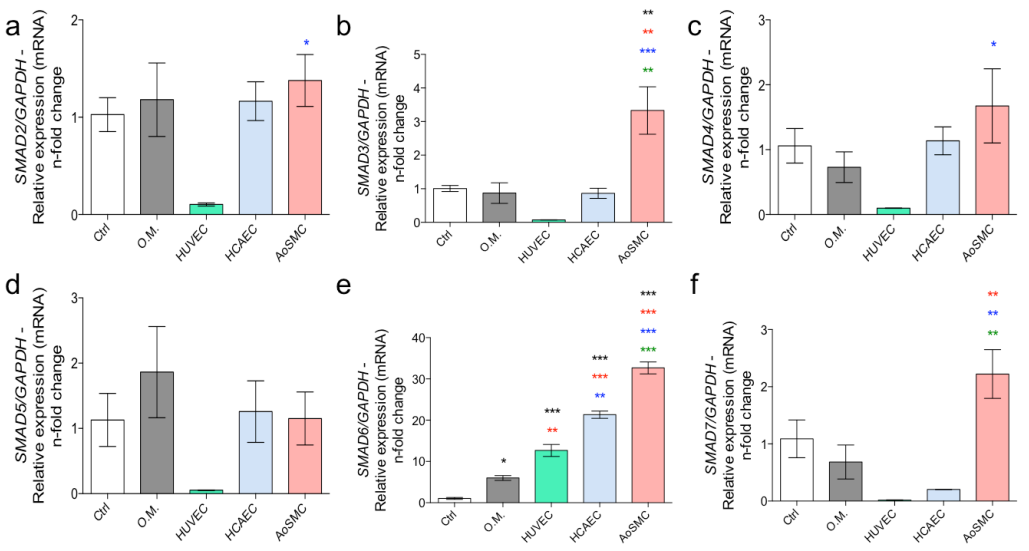

Fig.S2. TGF-ß signaling-based gene reprogramming is trigged in response to VSMC-conditioned medium. After 28 days of treatment with the different conditioned media

the Osteoblasts were collected in TriZOL for the following extraction of RNA and cDNA synthesis. Using real-time PCR technology, transcription factors acting on the TGF-ß pathway were evaluated: SMAD2, SMAD3, SMAD4, SMAD5, SMAD6, and SMAD7 (a-f). The results were normalized by the GAPDH expression values, which were considered the reference gene for this study. *p<0.05; ***p<0.0002: Statistically significant difference when compared to control. **p<0.1906; ***p<0.0002: Statistical difference when compared with the osteogenic medium. *p<0.05; **p<0.1906; ***p<0.0002: Statistical difference when compared with the HUVEC-conditioned medium. **p<0.1906; ***p<0.0002: Statistical difference when compared with the HCAEC-conditioned medium.

VSMCs, not endothelial cells, promote osteoblast-to-osteocyte transition.

Unexpectedly, the morphology of those osteoblast responding to trophic factors released by AoSMCs was very similar to osteocytes (**Fig.2a**). In fact, the number of osteocytes-like cells was significantly greater in response to AoSMCs than to endothelial cells (**Fig.2b**). Importantly, all the markers known to identify the osteocyte phenotype were significantly upregulated in osteoblasts responding to AoSMCs, including DMP1 (app. 15-fold change increase, **Fig.2c**), SOST (app 15-fold change increase, **Fig.2d**); FGF23 (app. 15-fold change increase; **Fig.2f**), and miR23a (app. 12-fold change increase; **Fig.2e**). In addition, the osteocyte-acquired phenotype in response to AoSMCs was viable since MAPK- and AKT-related genes are also significantly upregulated (**Fig.S3**). Next, we hypothesized that the increase of osteocyte biomarkers in osteoblast is facilitated by vesicle communication of AoSMCs. We first investigated whether AoSMCs were able to express those genes and found significant increase of DMP1 (**Fig.S4a**) and SOST mRNA (**Fig.S4b**) in AoSMCs, while HUVEC upregulated miR-23a (**Fig.S4c**) and FGF23 (**Fig.S4d**), which suggests the involvement of vesicles in driving the paracrine signaling between AoSMCs and osteoblasts. Finally, to further confirm the functionality of these osteocytes, we demonstrated the upregulation of Shh-related signaling and RANKL (**Fig.S5a-d**) as well as genes of the FGFR family (**Fig.S5e-h**).

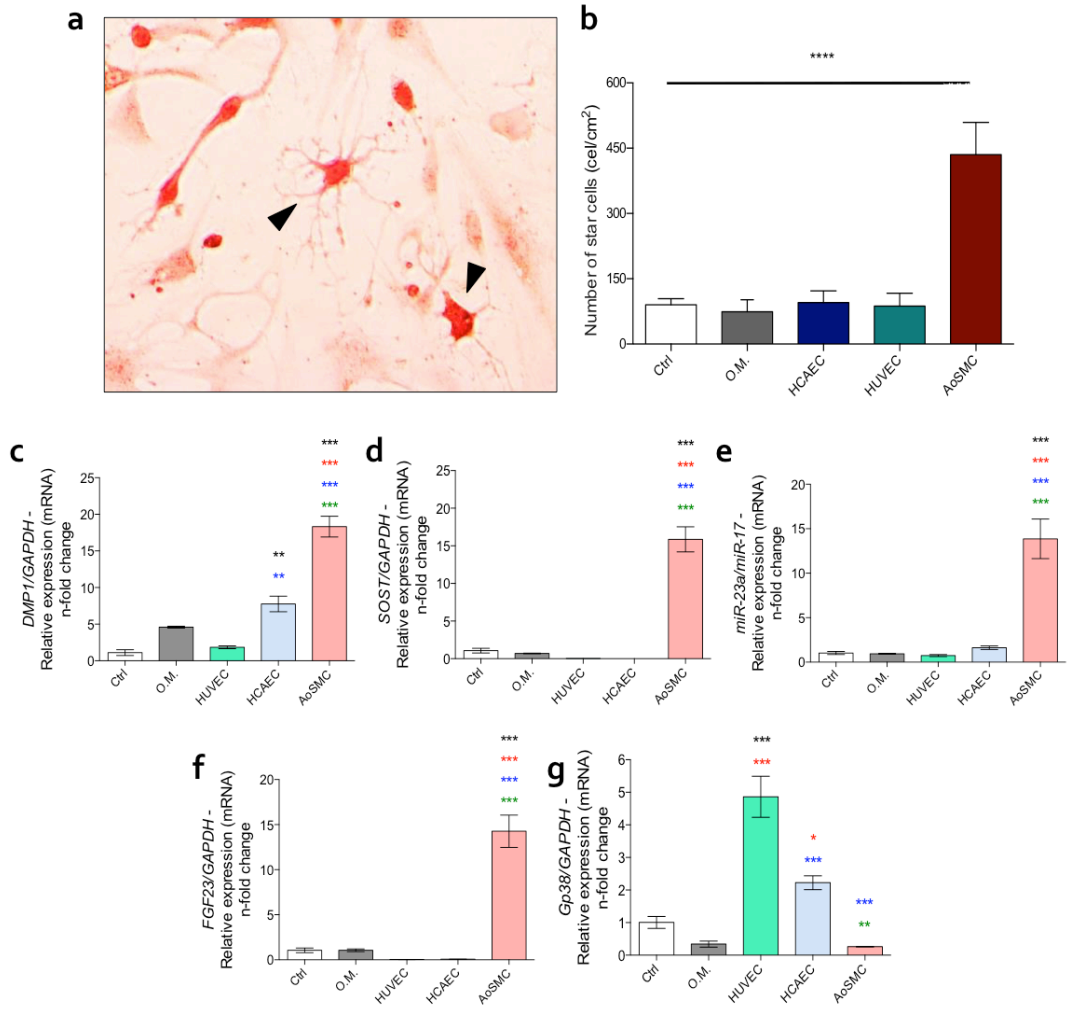

Fig.2. VSMC, but not endothelial cells, promotes osteoblast-osteocyte transition. After the treatment period, 28 days, osteoblasts were stained by Alizarin Red-S (a) and the number of osteocytes contacts individually (b). Osteocyte differentiation biomarkers were evaluated by PCR on osteoblasts that received the medium conditioned by endothelial cells: c) DMP1, d) SOST, e) miR-23a, f) FGF23, and g) Gp38. GAPDH was used as internal control of gene expression, and miR-17 was used for micro-RNA. **p<0.1906; ***p<0.0002, ****p<0.0001: Statistically significant difference when compared to control. *p<0.05; ***p<0.0002: Statistical difference when compared with the osteogenic medium. **p<0.1906; ***p<0.0002: Statistical difference when compared with the HUVEC-conditioned medium. **p<0.1906; ***p<0.0002: Statistical difference when compared with the HCAEC-conditioned medium.

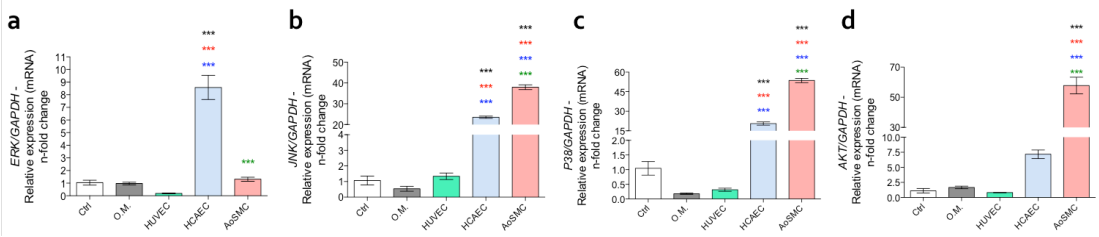

Fig.S3. The regulation of Akt and MAP-kinase modulated by endothelial cells during osteoblast differentiation. After 28 days of treatment with medium conditioned by

primary endothelial cells, osteoblasts were collected in TriZOL. After extraction of RNA and cDNA synthesis the expression, AKT and MAP-Kineses was evaluated by real time PCR: (a) ERK, (b) JNK, (c) P38, and (d) AKT. GAPDH was used as internal control of gene expression. ***p<0.0002: Statistically significant difference when compared to control. ***p<0.0002: Statistical difference when compared with the osteogenic medium. ***p<0.0002: Statistical difference when compared with the HUVEC-conditioned medium. ***p<0.0002: Statistical difference when compared with the HCAEC-conditioned medium.

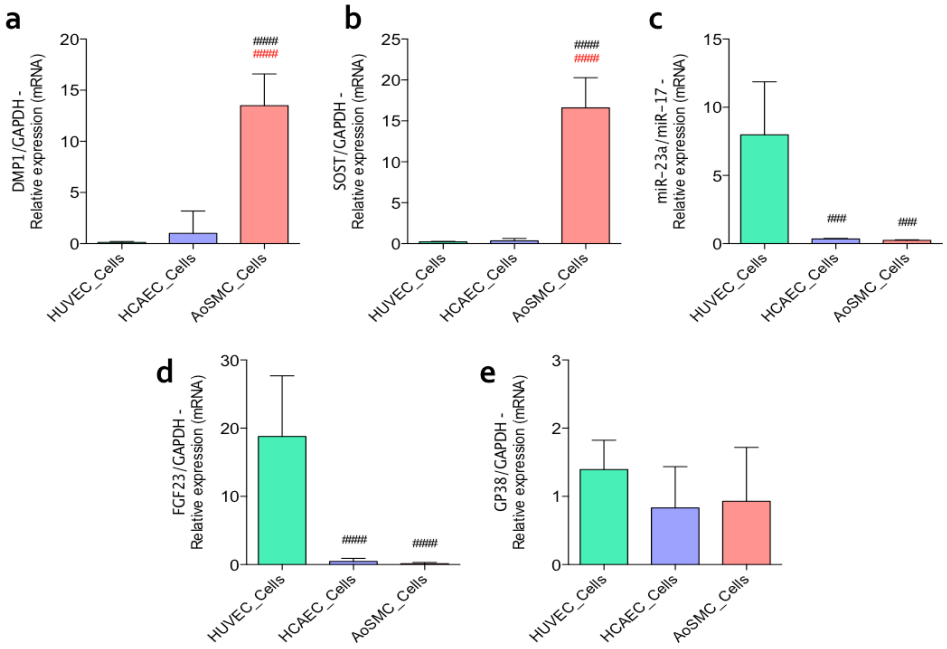

Fig.S4. mRNA encoding osteocyte markers by endothelial cells. After 3 days of culture, endothelial cells (HCAEC, HUVEC, and AoSMC) were collected in TriZOL for RNA extraction and subsequent cDNA synthesis. After these maturation markers of DMP1, SOST, miR-23a, FGF23, and Gp38 (a-e), osteocytes were investigated for expression levels by real-time PCR. GAPDH was used as internal control of gene expression, and miR-17 was used for micro-RNA. ####p<0.0001: Statistical difference when compared with the HUVEC cells; ####p<0.0001: Statistical difference when compared with the HCAEC cells.

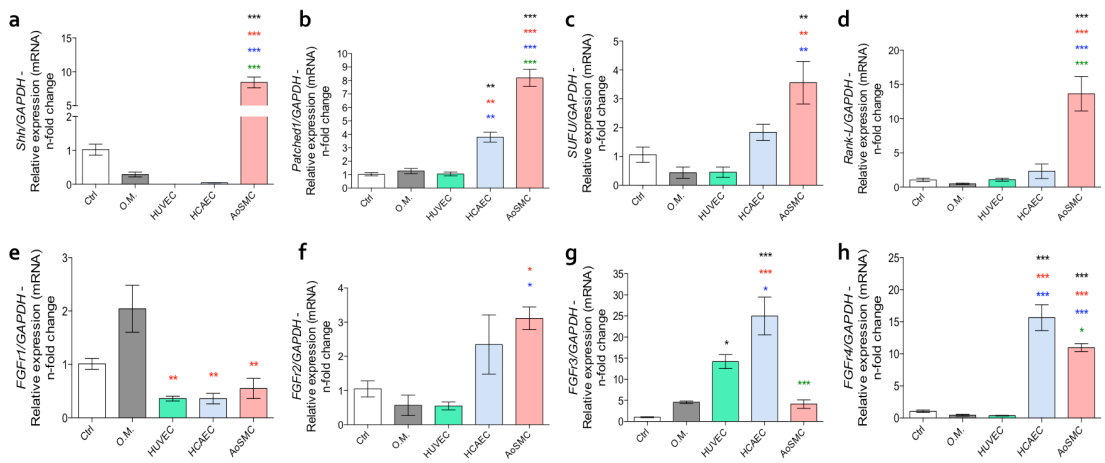

Fig.S5. Validation of experimentally acquired osteocytes through Shh signaling and RANKL expression. The RNA, extracted from osteoblasts after 28 days of treatment with the different media, was used for cDNA synthesis, and the gene expression evaluated by real-time PCR. mRNA encoding Shh signaling members and RANKL were investigated at this step. GAPDH was the reference gene. **p<0.1906; ***p<0.0002: Statistically significant difference when compared to control. *p<0.05; **p<0.1906; ***p<0.0002: Statistical difference when compared with the osteogenic medium. *p<0.05; **p<0.1906; ***p<0.0002: Statistical difference when compared with the HUVEC-conditioned medium. *p<0.05; ***p<0.0002: Statistical difference when compared with the HCAEC-conditioned medium.

VSMC releases exosomes containing osteocyte markers

We evaluated the capacity of endothelial and smooth muscle cells in expressing tetraspanin CD9, CD63, and CD81, biomarkers of exosome (**Fig.S6-S9**). **Fig.3** provides a complete report on this matter, reinforcing their capacity in producing exosomes. Scanning electron microscopy clearly illustrated vesicles budding on the surface of the endothelial and AoSMCs cells (**Fig.3a-f**). In detail, **Fig.3g** shows the exosome harvested from the conditioned medium by AoSMCs, which was later subjected to NTA to verify vesicle size and amount. We found a higher concentration of vesicles released by HCAEC cells (5.31×10^8 exosome/mL; **Fig.3j**). **Fig.3l** provides the zeta potential analysis, where the exosomes obtained from the AoSMCs at a static condition presented the smallest value < 10 mV. This variation should be considered with the capacity of the exosomes to interact with the biophysical properties of the plasma membrane in the target cells [7].Concluding the exosome characterization, we investigated whether they were able to express exosome-related biomarkers (**Fig.3m-p**).

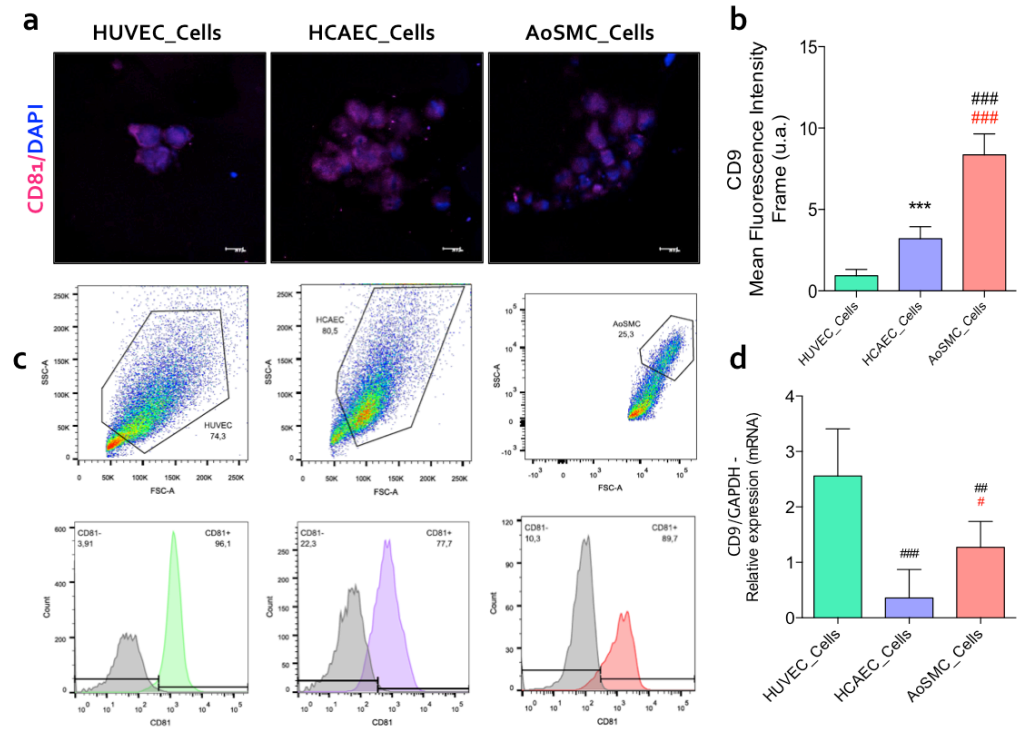

Fig. S6. Characterization of CD9 in endothelial cells. After 3 days of culture, the different cells were collected to evaluate the Tetraspanin-CD9. After the attachment stage, vesicle markers were evaluated in the cells using immunofluorescence and quantification of marked intensity levels (a–b). The same markers were evaluated by Flow Cytometry (c) and Real Time PCR (d). Expression assays were normalized with GAPDH reference gene. ###p<0.0002: Statistical difference when compared with the HUVEC cells. ###p<0.0002: Statistical difference when compared with the HCAEC cells.

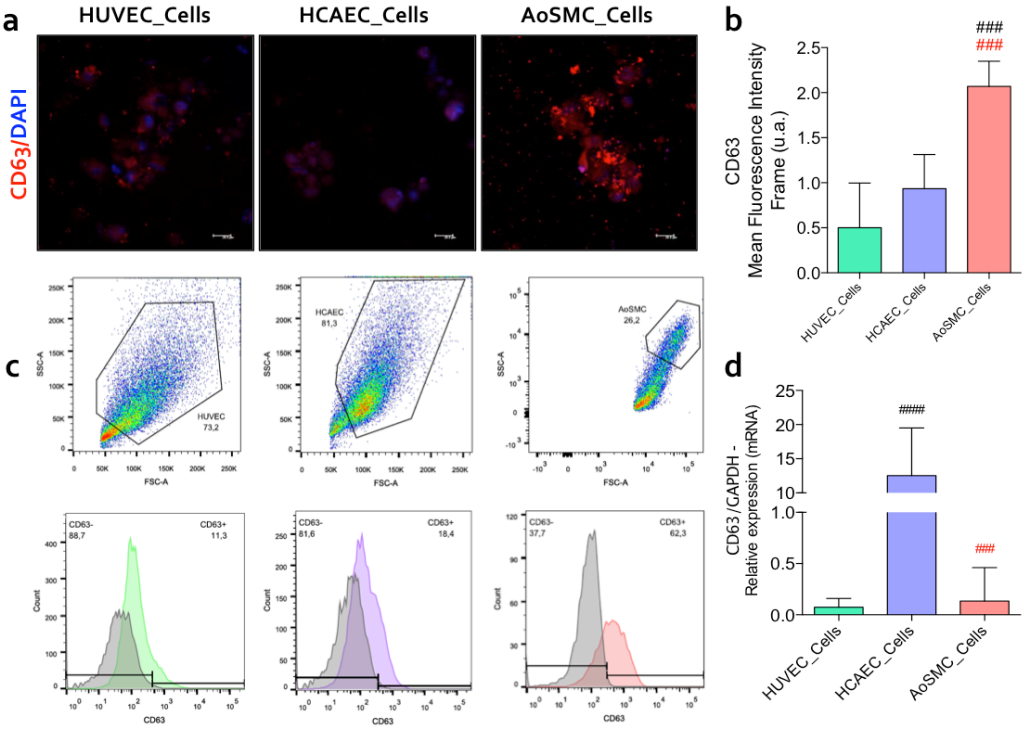

Fig.S7. Characterization of CD63 in endothelial cells. After 3 days of culture, the different cells were collected to evaluate the Tetraspanin-CD63. After the attachment stage, vesicle markers were evaluated in the cells using immunofluorescence and quantification of marked intensity levels (a–b). The same markers were evaluated by Flow Cytometry (c) and Real Time PCR (d). Expression assays were normalized with GAPDH reference gene. ###p<0.0002: Statistical difference when compared with the HUVEC cells. ###p<0.0002: Statistical difference when compared with the HCAEC cells.

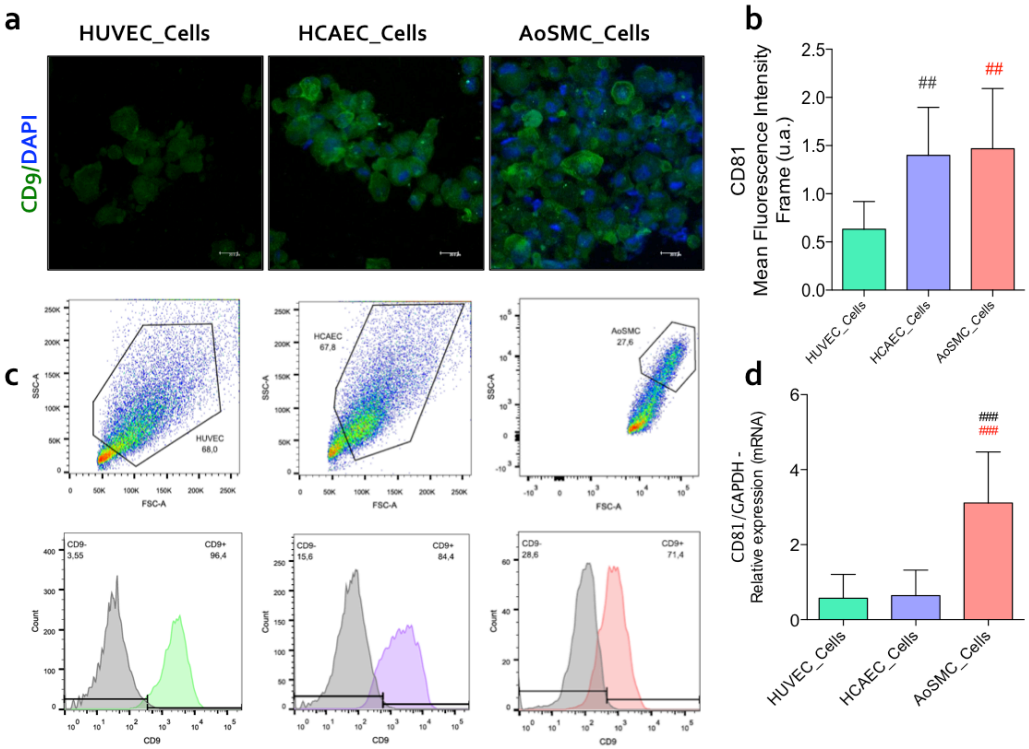

Fig.S8. Characterization of CD81 in endothelial cells. After 3 days of culture, the different cells were collected to evaluate the Tetraspanin-CD81. After the attachment stage, vesicle markers were evaluated in the cells using immunofluorescence and quantification of marked intensity levels (a–b). The same markers were evaluated by Flow Cytometry (c) and Real Time PCR (d). Expression assays were normalized with GAPDH reference gene. ##p<0.1906; ###p<0.0002: Statistical difference when compared with the HUVEC cells. #p<0.05; ##p<0.1906: Statistical difference when compared with the HCAEC cells.

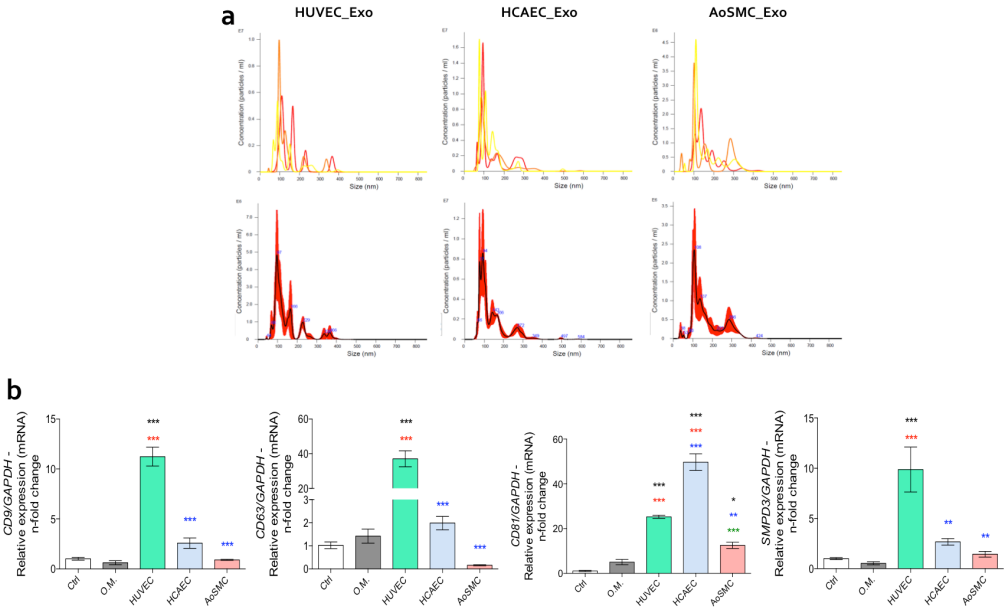

Fig.S9. Characterization of extracellular vesicles by endothelial cells and osteocyte gene expression. After conditioning the medium, the released extracellular vesicles were isolated and evaluated for size using NTA technology (a). Osteoblast cells were collected in TriZOL to evaluate vesicular biomarkers: (b) CD9, CD63, CD81, and SMPD3. Expression assays were normalized with GAPDH reference gene. *p<0.05; ***p<0.0002: Statistically significant difference when compared to control. ***p<0.0002: Statistical difference when compared with the osteogenic medium. **p<0.1906; ***p<0.0002: Statistical difference when compared with the HUVEC-conditioned medium. ***p<0.0002: Statistical difference when compared with the HCAEC-conditioned medium.

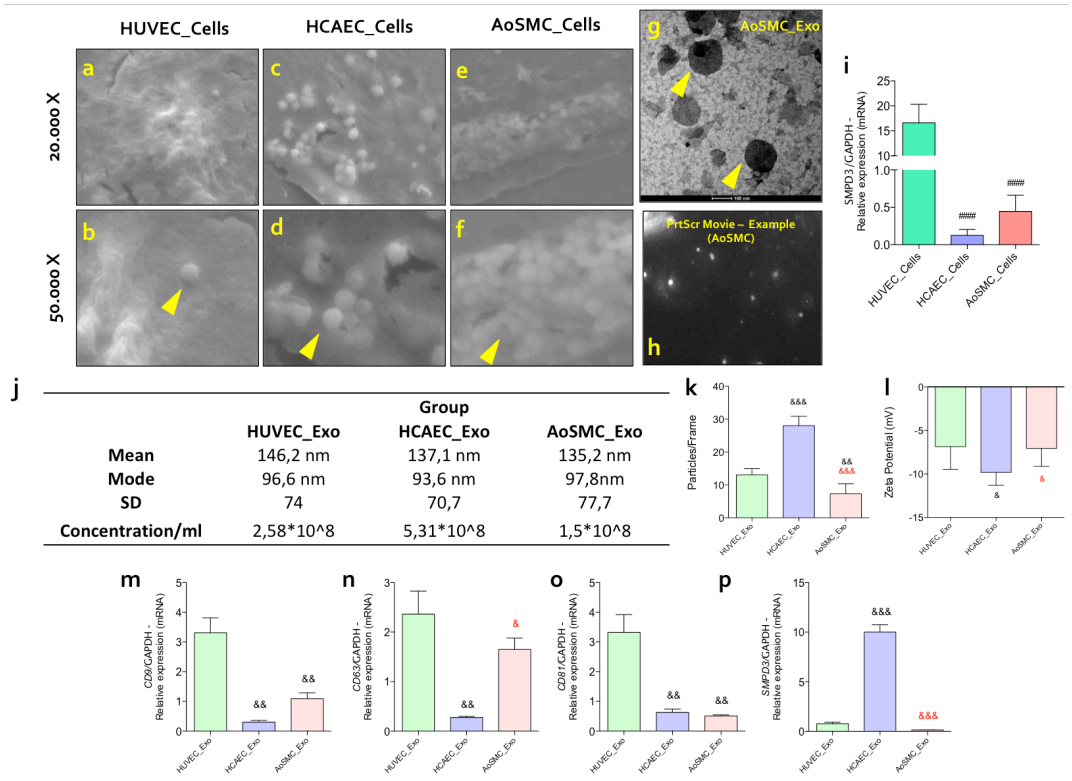

Fig.3. Detailed analysis of AoSMCs-related exosome. Smooth muscle cells were plated on petri dishes and, after 72 hours, evaluated for the exosome release profile. Cells were fixed and evaluated by transmission microscopy for possible vesicular process (a–f). After collecting the medium and isolating vesicles, transmission microscopy was used to verify the size of the particles released by smooth muscle cells (g), and nanoparticles tracking analysis (NTA) was used to verify the mean and concentration of vesicles in the different groups (h, j–k). To validate the capacity of incorporation by targets with use of the membrane charge, the exosomes were evaluated for load by zeta potential (l). Important biogenesis markers of vesicles were evaluated in exosomes after isolation, collection in TriZOL and cDNA synthesis: (m) CD9, (n) CD63, and (o) CD81. SMPD3 was evaluated in cells (i) and exosome (p). ####p<0.0001: Statistical difference when compared with the HUVEC cells. &p<0.05; &&p<0.1906; &&&p<0.0002: Statistical difference when compared with the HUVEC exosome. &p<0.05; &&p<0.1906: Statistical difference when compared with the HCAEC exosome.

After the effect of AoSMCs on mature osteoblasts demonstrated the relevance of exosome on this communication, we decide to investigate whether these exosomes might be loaded with mRNA related with osteocyte gene markers. Surprisingly, our data indicated the presence of FGF23 (**Fig.4a**; reaching 4-fold changes), SOST (**Fig.4b**; reaching 8-fold changes), miR23a (**Fig.4d**; reaching 15-fold changes), and GP38 (**Fig.4e**; reaching 3-fold changes). We also noticed transcripts encoding β-Catenin signaling proteins loaded in the exosomes, such as sFRP1, sFRP2, DKK, and β-Catenin, in which DKK (**Fig.4h**) and β-Catenin (**Fig.4i**) genes were up-modulated in exosome released by AoSMCs.

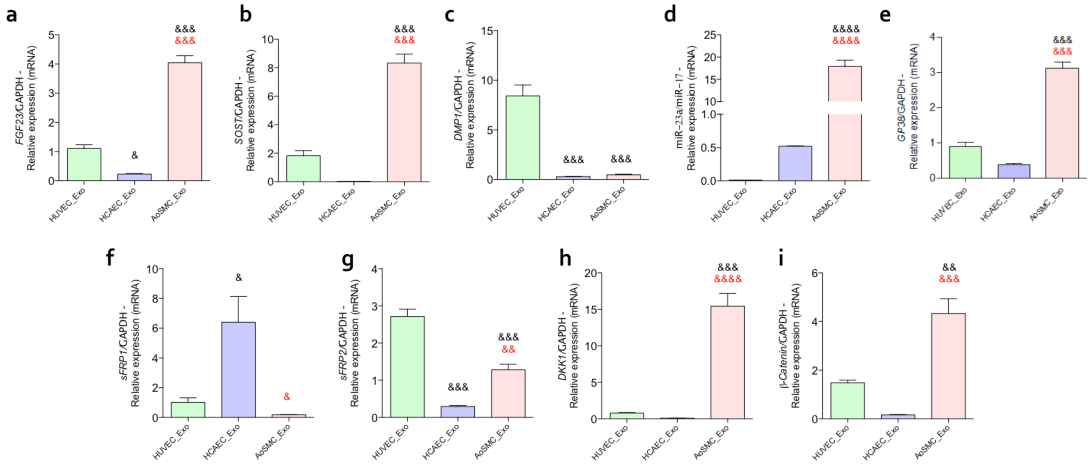

Fig.4. Exosomes are reservoir of Catenin signaling related members and deliver osteocytes gene markers. After harvesting the medium, the exosomes were properly isolated to allow extracting of total mRNA, and thereafter following for cDNA synthesis to evaluate a set of genes related with osteoblast to osteocyte transition: FGF23 (a), SOST (b), DMP1 (C), miR-23a (d), and Gp38 (e). Important genes of the ß-Catenin pathway were investigated for expression in vesicles released by endothelial cells (f-i).

GAPDH was used for internal control of gene expression, and miR-17 was used for micro-RNA. &p<0.05; &&p<0.1906; &&&p<0.0002; &&&&p<0.0001: Statistical difference when compared with the HUVEC exosome. &p<0.05; &&p<0.1906; &&&p<0.0002; &&&&p<0.0001: Statistical difference when compared with the HCAEC exosome.

VSMC promotes osteoblast-to-osteocyte transition through β-Catenin signaling.

A mode of the WNT/β-catenin signaling regulation occurred at the level of extracellular antagonists, secreting Frizzled-related Protein (sFRP; **Fig.5c**) and Dkk1 (**Fig.5d**) by AoSMCs. The capacity of AoSMCs to express β-catenin was confirmed by laser confocal microscopy (**Fig.5e**). Then, we showed that exosomes released by AoSMCs were loaded with both total and phosphorylated (S368) beta-catenin (**Fig.5f,g**). Our results clearly demonstrate that AoSMCs release sufficient signals to promote osteoblast-to-osteocyte transition via β-catenin, suggesting an intense regulation of these signals. The involved β-catenin signaling in those osteocytes obtained in response to AoSMCs was validate by quantitative RT-PCR technology (**Fig.5l–n**). Additionally, the crosstalk of endothelium with mature osteoblast was investigated with transcripts of WNT (**Fig.5l**), LRP5 (**Fig.5m**), and GSK3β (**Fig.5n**). Moreover, other points reinforce the importance of β-catenin in this scenario, such as the presence of WNT/β-catenin-related genes in the transcript pool of exosomes released by endothelial cells.

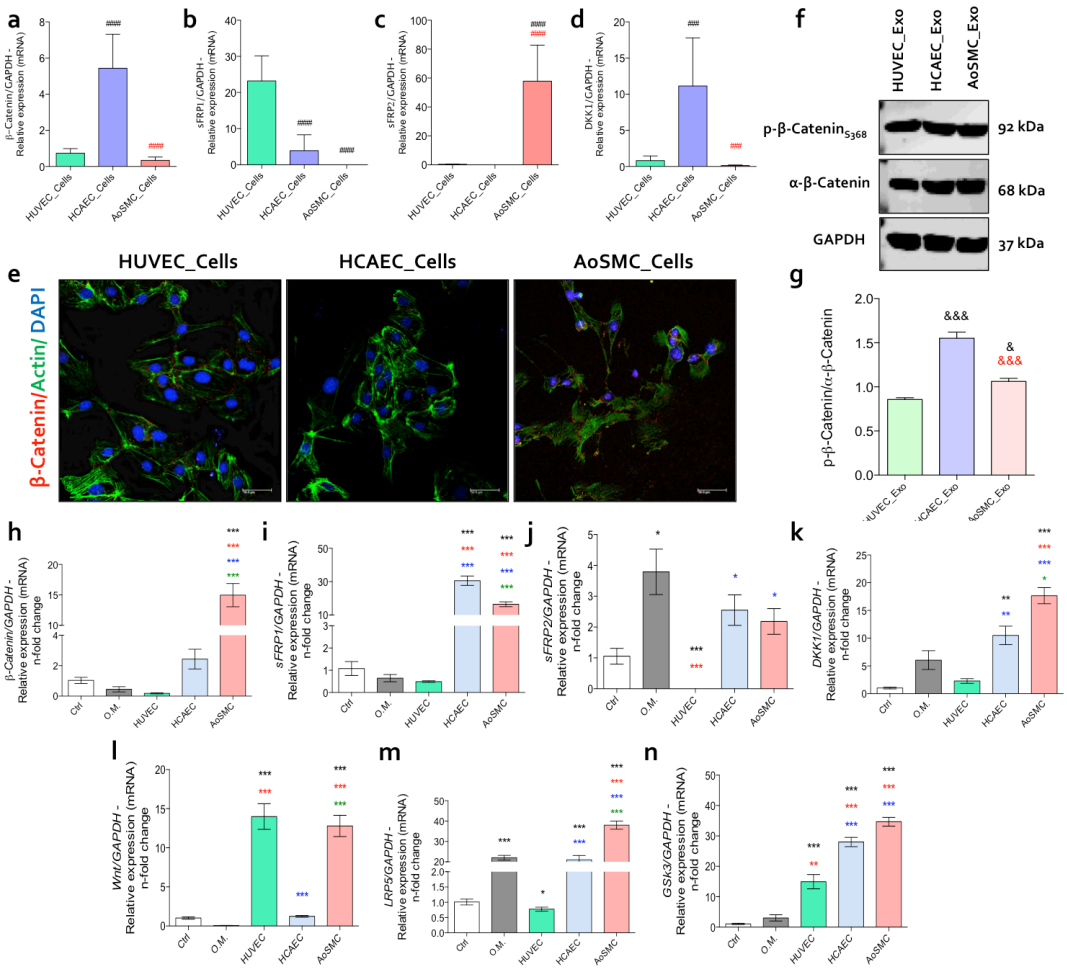

Fig.5. AoSMCs require p-ß-Catenin signaling. The cells were collected in TriZOL for RNA extraction and cDNA synthesis to evaluate ß-Catenin, sFRP1, sFRP2, and DKK1 gene expression (a–d), and the cells were Immunolabelled with ß -Catenin (e). Exosomes of these same cells were lysed, and the proteins p-ß-Catenin, α-ß-Catenin, and GAPDH were revealed by Western blotting (f–g). Following the same standard, the medium was collected and used to treat osteoblasts, which at the end of 28 days were collected in TriZOL to investigate expression levels of genes involved with ß-Catenin (h–n). The expression results were normalizing by GAPDH. ###p<0.0002; ####p<0.0001: Statistical difference when compared with the HUVEC cells. ###p<0.0002; ####p<0.0001: Statistical difference when compared with the HCAEC cells. &p<0.05; &&&p<0.0002: Statistical difference when compared with the HUVEC exosome. &&&p<0.0002: Statistical difference when compared with the HCAEC exosome. *p<0.05; **p<0.1906; ***p<0.0002: Statistically significant difference when compared to control. **p<0.1906; ***p<0.0002: Statistical difference when compared with the osteogenic medium. *p<0.05; **p<0.1906; ***p<0.0002: Statistical difference when compared with the HUVEC-conditioned medium. *p<0.05; ***p<0.0002: Statistical difference when compared with the HCAEC-conditioned medium.

We elucidated a strong influence of both endothelial and smooth muscle cells in osteocyte adhesion, by modulating the expression of β1-integrin, Src, FAK, and cofilin, a

protein related to cytoskeleton rearrangement, which is necessary during osteoblast-to-osteocyte transition (**Fig.S10**). Part of our results was validated in global data of transcriptome obtained from ArrayExpress (E-GE OD-61351; **Fig.S11**), while the NOTCH signaling related members also up-modulated osteocytes obtained in response to AoSMCs (**Fig.S12**). We suggest that these experimentally obtained osteocytes as functional cells by reporting the increase of ECM remodeling-related genes encoding Col1a1 (**Fig.S13a**), MMP2 (**Fig.S13b**), MMP9 (**Fig.S13c**), with AoSMCs stimulated an up-expression of MMP-related tissue inhibitors, such as TIMP1, TIMP2, and RECK. This indicates that these mechanisms are decisive in osteocytes, maybe to maintain the remodeling pericellularily (**Fig.S13d-f**).

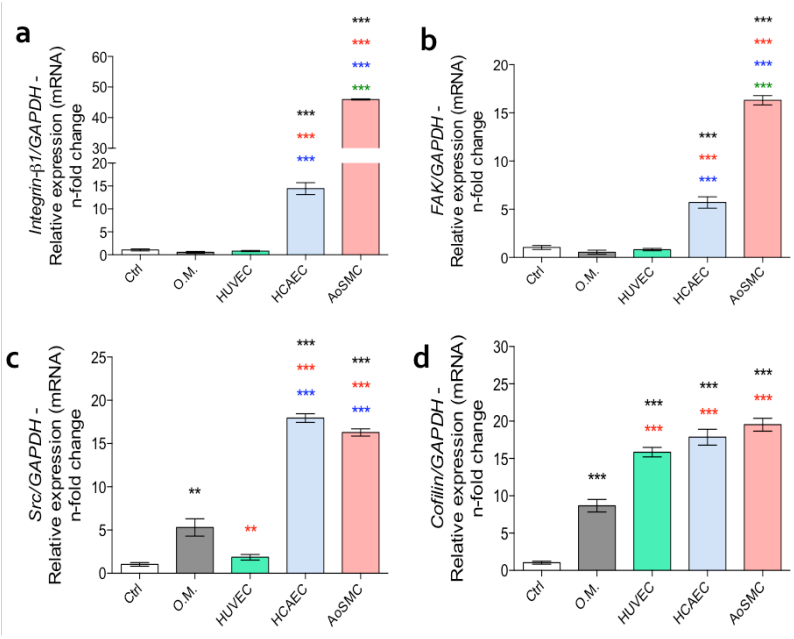

Fig.S10. Paracrine effect of endothelial cells on the expression of adhesion-related genes. After 28 days of treatment, with a change of medium every 3 days, osteoblasts were collected in TriZOL for RNA extraction, complementary DNA synthesis and evaluation of the gene expression of Integrin-β1 (a), FAK (b), Src (c), and Cofilin (d) by real-time PCR. The expression results were normalizing by GAPDH. **p<0.1906; ***p<0.0002: Statistically significant difference when compared to control. **p<0.1906; ***p<0.0002: Statistical difference when compared with the osteogenic medium. ***p<0.0002: Statistical difference when compared with the HUVEC-conditioned medium. ***p<0.0002: Statistical difference when compared with the HCAEC-conditioned medium.

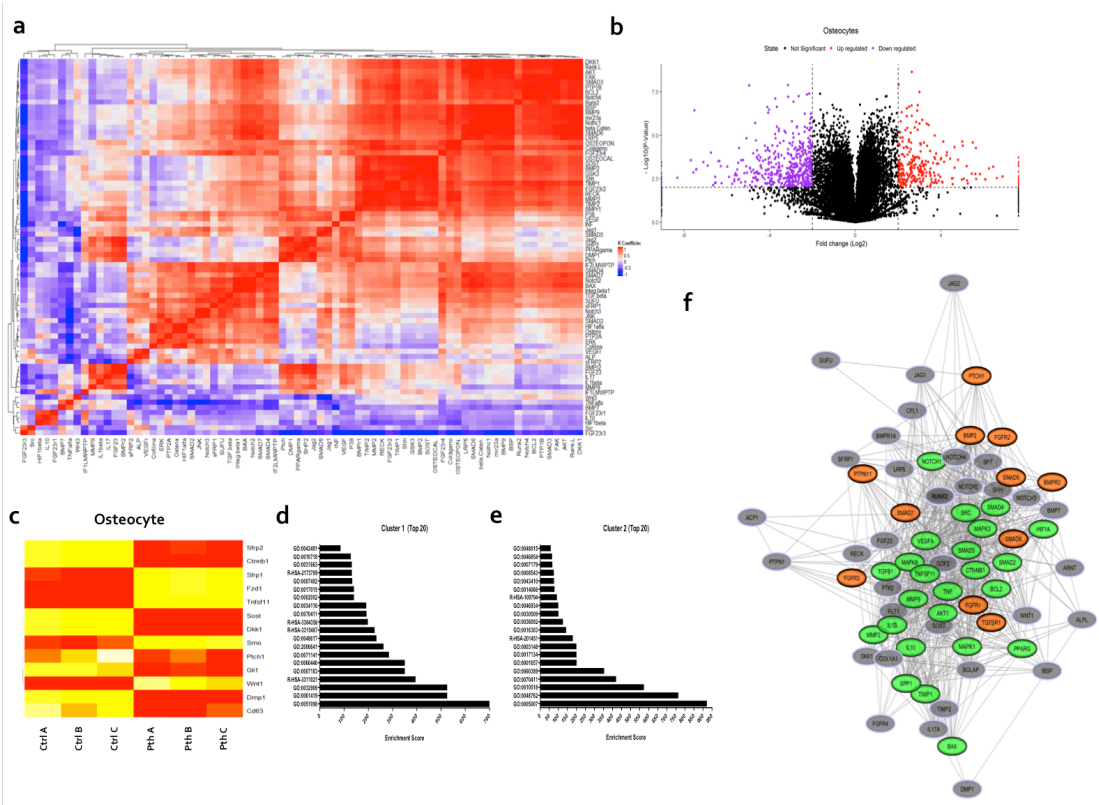

Fig.S11. Biological functions obtained with bioinformatic tools. Differential expression heatmap of E-GEOD-61351. Pearson's correlation (a). E-GE OD-61351, available at ArrayExpress, was chosen for this Analysis (b). E-GEOD-61351 dataset, which is based on GPL13112 platform [Illumina HiSeq 2000], contains 6 IDG-SW3 samples differentiated for 28 days, treated (n = 3) or not (n = 3) with PTH, both available at ArrayExpress, was chosen for this analysis (c). DAVID tools results for Cluster (d-e) and Protein-Protein interactome of proteins analyzed on this poster and MCODE reveals two clusters (f).

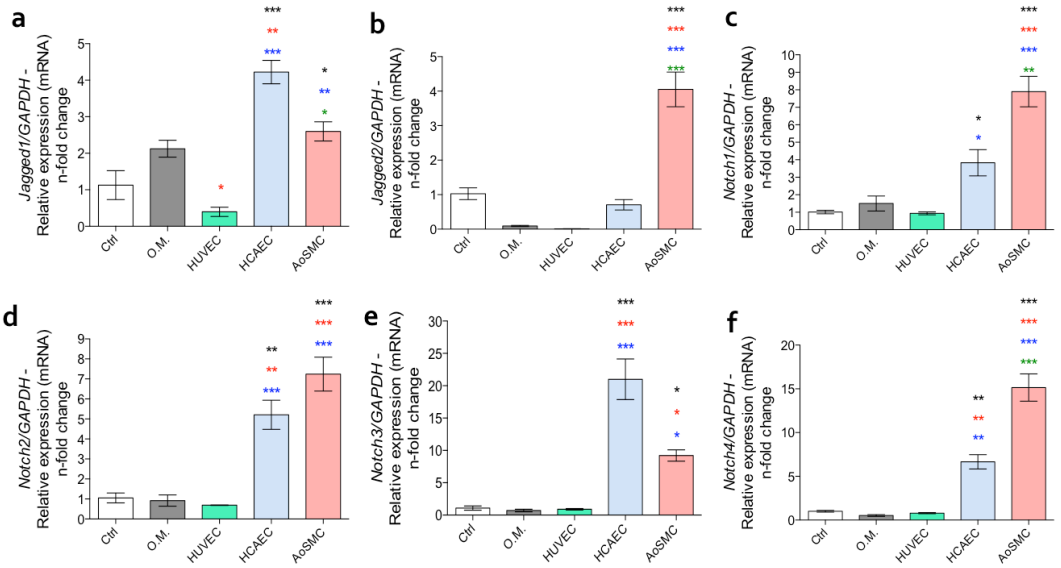

Fig.S12. Notch signaling is modulated in osteoblast-to-osteocyte transition. After 28 days of treatment with medium conditioned by endothelial cells (the medium was changed every 3 days to maintain the treatment properties), osteoblasts were collected in

TriZOL for RNA extraction and cDNA synthesis and then used in real-time PCR to investigate genes involved with the Notch pathway: a) Jagged1, b) Jagged2, c) Notch1, d) Notch2, e) Notch3, and f) Notch4. The expression results were normalizing by GAPDH. *p<0.05; **p<0.1906; ***p<0.0002: Statistically significant difference when compared to control. *p<0.05; **p<0.1906; ***p<0.0002: Statistical difference when compared with the osteogenic medium. *p<0.05; **p<0.1906; ***p<0.0002: Statistical difference when compared with the HUVEC-conditioned medium. *p<0.05; **p<0.1906; ***p<0.0002: Statistical difference when compared with the HCAEC conditioned medium.

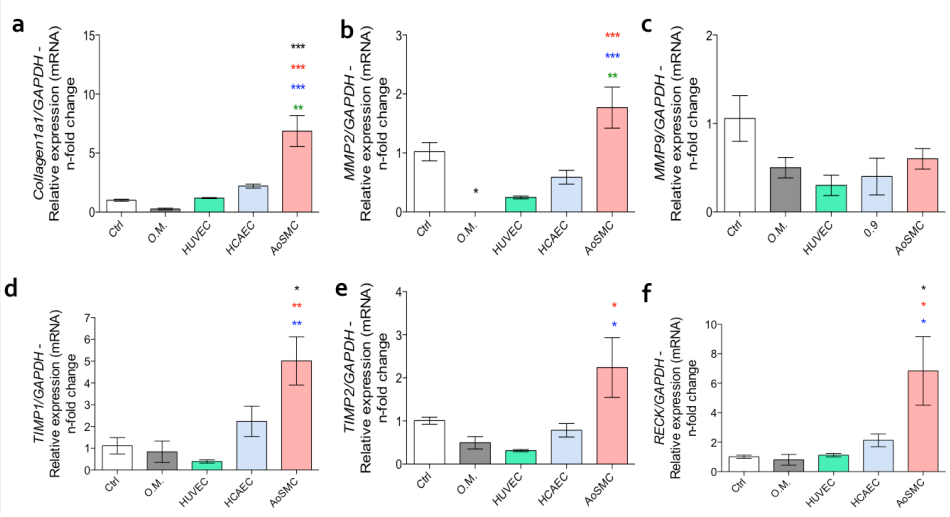

Fig.S13. Endothelial cells modulate the expression of genes involved with ECM remodeling during osteoblast-to-osteocyte transition. After conditioning with muscle cells (AoSMC) and endothelial cells (HCAEC and HUVEC), the culture medium was collected to treat osteoblast. The cells were collected in TriZOL, and following RNA isolation and cDNA synthesis, the genes involved with ECM remodeling were evaluated by q-PCR: (a) Collagen1a1, (b) MMP2, (c) MMP9, (d) TIMP1, (e) TIMP2 and (f) RECK. The expression results were normalizing by GAPDH. *p<0.05; ***p<0.0002: Statistically significant difference when compared to control. *p<0.05; **p<0.1906; ***p<0.0002: Statistical difference when compared with the osteogenic medium. *p<0.05; **p<0.1906; ***p<0.0002: Statistical difference when compared with the HUVEC-conditioned medium. **p<0.1906: Statistical difference when compared with the HCAEC-conditioned medium.

Finally, we investigated some mechanisms related with mineralizing phenotype of osteocyte biology (**Fig.6a**). First, we demonstrated the capacity of exosome released by endothelial and smooth muscle cells in delivering ATP (**Fig.6b**). Among them, HCAEC and AoSMCs were able to significantly increase their content in response to the mechanotransduction process (**Fig.6b**). The genes related with mineralizing process, NPP1, TNAP, and Fetuin A, were also investigated (**Fig.6f-h**; extended results in **Fig.S14**). Together, our results confirm the strong influence of blood vessels in promoting mineralizing phenotype of terminally differentiated osteocyte.

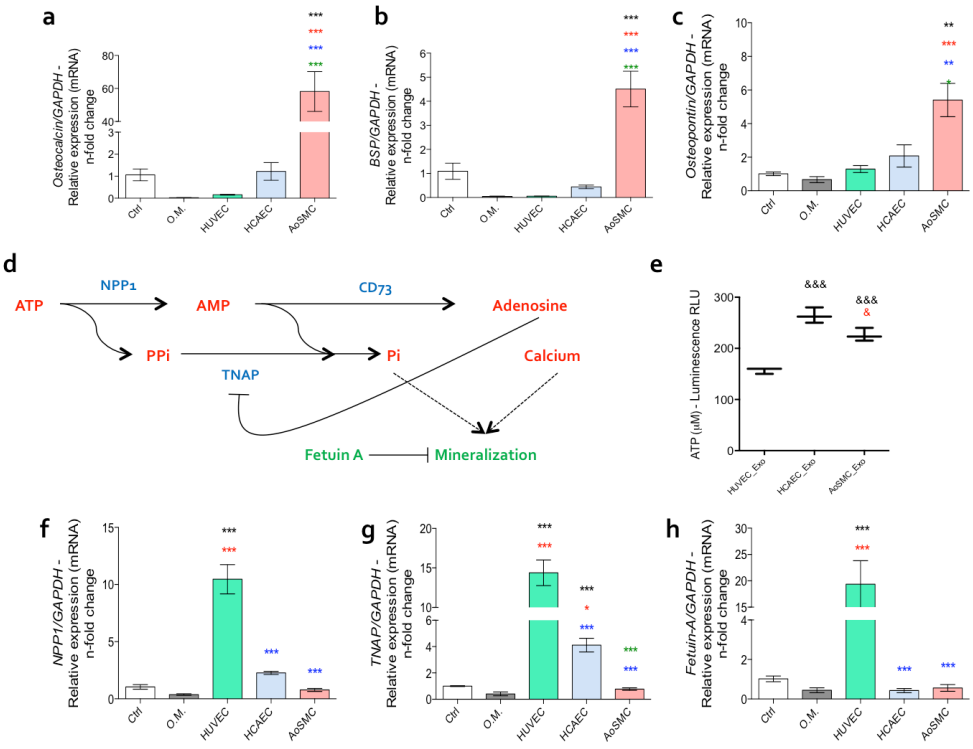

Fig.6. Exosomes deliver ATP and modulate expression involved with bone mineralization. At the end of the treatment period, osteoblasts were collected and evaluated for expression of genes important for tissue mineralization: (a) osteocalcin, (b) bone sialo protein (BSP), and (c) osteopontin. Scheme representing release of inorganic phosphate (Pi) for mineralization (d). After conditioning with muscle cells (AoSMC) and endothelial cells (HCAEC and HUVEC), the culture medium was collected for isolation of exosomes. These samples were evaluated for concentration of ATP that can be loaded (e) using a specific Kit (see Materials and methods). Osteoblasts that received the different conditioned medium were evaluated for the expression levels of marker genes from the synthesis of inorganic phosphate, NPP1, and TNAP (f-g) and for an important inhibitor of the mineralization process: Fetuin-A1 (h). For normalization effect, the expression results were considered from the expression values of the reference gene: GAPDH. &p<0.05: Statistical difference when compared with the HUVEC exosome. &&&p<0.0002: Statistical difference when compared with the HCAEC exosome. **p<0.1906; ***p<0.0002: Statistically significant difference when compared to control. *p<0.05; ***p<0.0002: Statistical difference when compared with the osteogenic medium. **p<0.1906; ***p<0.0002: Statistical difference when compared with the HUVEC-conditioned medium; *p<0.05; **p<0.1906: Statistical difference when compared with the HCAEC-conditioned medium.

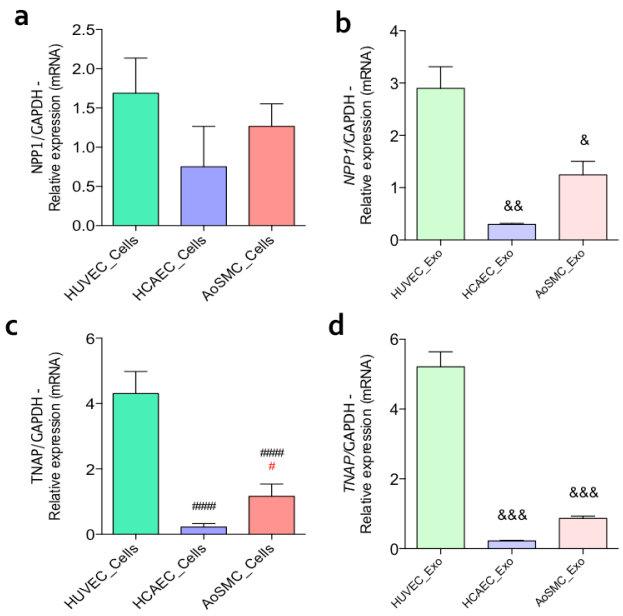

Fig.S14. Relative expression of mineralization-related genes in HUVECs, HCAECs, and AoSMCs. The cells were collected in TriZOL, and the NPP1 and TNAP (a, c) genes were evaluated by gene expression. After the same period, the medium was collected for isolation of exosomes and subsequent extraction of RNA, which was used to express the same markers as the phosphate (b, d) synthesis pathway. The results were normalized by the GAPDH expression values, which were considered the reference gene for this study. ####p<0.0001: Statistical difference when compared with the HUVEC cells. #p<0.05: Statistical difference when compared with the HCAEC cells. &p<0.05; &&p<0.1906; &&&p<0.0002: Statistical difference when compared with the HUVEC exosome.

DISCUSSION

In addition to their already known role in circulating blood throughout the entire body, researchers increasing seek to understand how vascular cells might contribute to bone homeostasis and physiological mechanism to maintain health. Although fabulous progress has been made, especially in the studies of R. Adams[5,6,8–15], information remains scarce about the repertoire of circulating molecules that deliver signals to drive already known bone cell phenotype. Studies on the crosstalk between vasculature and bone cells is supported by the fact that bone is highly vascularized[16], and blood vessels are found in most regions of the skeletal systems, except growth plate and articular cartilage. Likewise, bone formation and fracture healing are controlled by blood vessels [17].

Although the coupling of bone cells and vascular cells are clear, limited evidence is available that supports the relevance of vascular smooth muscle cells in this panorama. To evaluate the effect of endothelial and smooth muscle cells on mature osteoblasts,

medium conditioned by vascular cells was collected and used to further challenge human primary mature osteoblasts. Our data demonstrated a very active crosstalk between them, reinforcing previous studies. Moreover, we identified a novel mechanism promoted by vascular smooth muscle cells in driving osteoblast-to-osteocyte transition by releasing exosome to deliver the morphogenetic signals.

First, the mature osteoblasts responding to the signals from VSMCs presented morphology and molecular machinery of terminally differentiated osteocytes. We confirmed this achievement by evaluating SOST, DMP1, miR23a, all specific biomarkers of osteocyte phenotype. We also mirrored the experimental design using endothelial cells in order to understand whether they exert differential stimulus to the surrounding cell/tissue. Considering some technical limitation of this study, we can speculate a synchrony between endothelial and smooth muscle cells (mural cells) in promoting osteogenesis, where endothelial cell stimulates genes necessaries to maintain the osteogenic phenotype, such as TGF-beta family members, corroborating with previous findings that revealed the influence of endothelial cells and signaling on osteogenesis and bone *de novo* deposition. We suggest that this mechanism has considerable relevance as a pre-requisite to osteocytogenesis, orchestrated by AoSMCs. Overall, this study provides novel aspects covering bone remodeling, as osteocytes are the main resource of RANKL in the body; in turn, RANKL is a cytokine responsible for triggering signals to drive osteoclastoegenesis.[18–20]

Over the last century scientists have proven that osteocytes are derived from osteoblasts; however, the precise mechanism by which osteoblast becomes buried in bone matrix remains elusive, although osteocytes compose 90–95% of all the bone cells in adulthood. Osteocytes connect with each other or with other cells such as osteoblasts, monocytes, macrophages, and terminally obtained osteoclasts, through of cytoplasmic processes passing through bone canaliculli (100–300 nm).[21,22] The diameter of those canaliculli anatomically supports crosstalk with resident cells in bone using microvesicles released by other cells. In fact, our findings show that the osteocytogenic promoted effect is conducted by exosome, with median of approximately 120 nm. Mechanistically, AoSMC releases exosome loaded with decisive molecules to orchestrate the osteoblast-to-osteocyte transition, and this mechanism seems to be necessary and sufficient, through β-Catenin signaling. This finding corroborates with a line of evidence showing that WNT/β-Catenin pathway is an evolutionary conserved signaling cell that regulates differentiation and organogenesis.[23] WNT/β-Catenin pathway has been related with

fundamentals aspects in bone biology. Considering the canonical and noncanonical signaling of WNT/β-Catenin pathway, a critical molecule is β-Catenin. Mechanistically, at least 3 receptors (LRP4, 5, and 6) and multiple activators are known as WNTs, in addition to, several inhibitors, such as SOST (sclerostin), DKK1, and sFRPs.[24–28] Our study reinforces this complexity, highlighting this repertoire in the obtained osteocyte in response to VSMCs. Taken osteocyte biology into account, β-Catenin is essential for: (1) Maintenance of the cell viability[29]; (2) communication between osteocytes (potentially regulating connexin[30]; (3) bone integrity (regulating RANKL/OPG ratio)[31]; (4) response to anabolic loading[32]; and (5) involved with mechanotransduction. Duan & Bonewald (2016) considered all of these aspects, which reinforce the importance of β-Catenin on maintenance of cell embedded into mineralized matrix, such as osteocytes.

Remarkably, a number of reports have addressed the relationship between blood flow and bone loss/formation and further associated these findings with osteoporosis and osteopetrosis. Likewise, ageing is not only associated with bone loss but also with reduced blood flow in the skeletal system. In this condition, Ramasamy et al. (2016) evidenced the involvement of Notch pathway genes and some formations were strongly reduced by treatment that disturbed normal blood flow in aged animals.[9]

Despite many open questions and caveats, our findings clearly indicate that VSMCs-released exosome is sufficient to promote osteoblast-to-osteocyte transition through β-Catenin signaling, as suggested in the **Fig.7**. As osteocytes harbors bone remodeling in an intermittent manner, the function of VSMCs might be useful for the development of strategies to prevent endothelial disturbance in human disease.

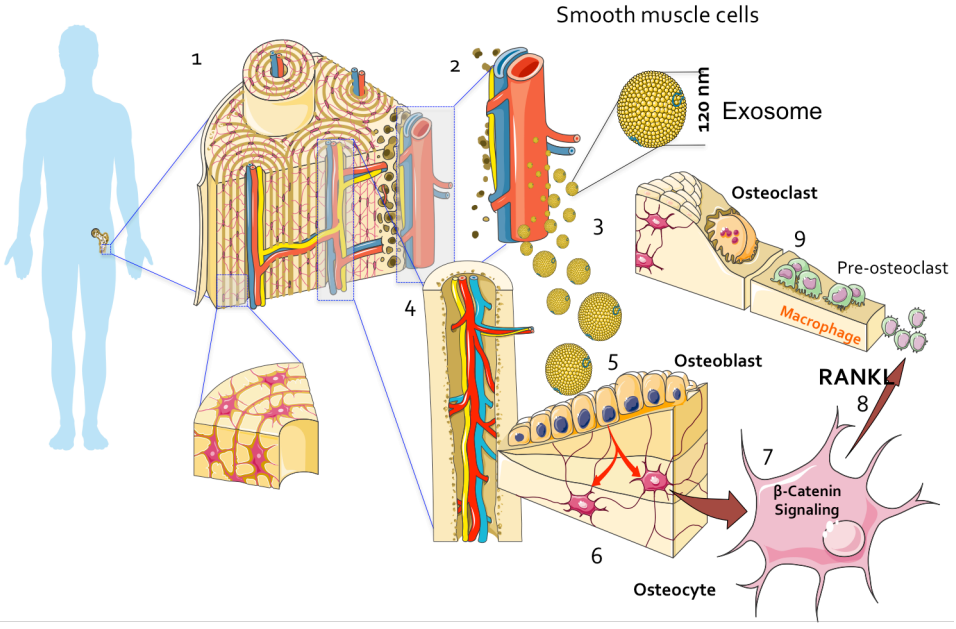

Fig.7. Schematic representation of the main findings of this study. This schematization provides a view overview of the main data obtained in this study. Briefly, osteoblast cells obtained from healthy donors were grown *in vitro* and challenged with conditioned medium by HUVECs, HCAEC, and AoSMCs, separately. We demonstrated that the crosstalk between AoSMCs cells and osteoblasts was carried by exosomes, leading osteoblast to differentiate into osteocytes.

METHODS

Cell culture. All cells were maintained at conventional conditions, exactly as reommended by the manufacturers. We used human osteoblasts (HOEL) derived from bone of healthy donors undergoing joint work at the School of Dentistry of Bauru, FOB-USP and maintained in our cell bank. As a positive control, we used the classical methodology in the differentiation literature, where β-Glycerophosphate (10 mM) + Dexamethasone (0.03 g/mL) + Ascorbic Acid (50 µg/mL), components were purchased together from Sigma-Aldrich and the in vitro Mineralization was analyzed by alizarin RedS Staining. The experimental design is schematized in **Fig.S1**.

Shear Stress and Collection of Conditioned Medium. The semi-confluent layers were subjected to shear stress (using orbital shaker) for 72 h in a humid atmosphere with 5% CO_2 at 37°C, as previously described. The rotation was determined using the maximum stress formula: $\tau max = a\sqrt{\rho\eta(2\pi f)}$, so that the rotation frequency is within the physiological arterial pressure (6-40 ~dynes/cm)[33].

Laser Confocal Microscopy. For confocal microscopy analysis, the cells were cultured in glass coverslips placed in the peripheral ring of the culture and subjected to shear stress, as we have reported previously[34–37].

Sample preparation for qPCR. To collect samples for qPCR technology, we have performed the TriZOL methodology, exactly as recommended by the manufacturer. Results were expressed as relative amounts of the transcripts with β-Actin as reference gene (housekeeping gene), using the comparative CT method (ΔΔCt)[38]. Primers and details are described in **Table 1**.

Table 1. Expression primers sequences and PCR cycle conditions.

Gene	Primer	5'-3' Sequence	Reaction' Condition
BMPr1	Forward	CATATTAGGCGTGTGCCAAAAA	95°C - 15s; 60°C - 30s; 72°C - 30s
	Reverse	GCTTGTGCTTGCTGTCGTTC	

BMPr2	Forward	ATTTGCAGCACAGACGGATATT	95°C - 15s; 60°C - 30s; 72°C - 30s
	Reverse	GACACTGAAAATCTGAGCCTTCT	
BMP2	Forward	CCCAGCGTGAAAGAGGAGAC	95°C - 15s; 60°C - 30s; 72°C - 30s
	Reverse	CCATGGTCGACCTTTAGGAG	
BMP7	Forward	ACTGTGAGGGGGAGTGTGC	95°C - 15s; 60°C - 30s; 72°C - 30s
	Reverse	CGAAGTAGAGGACGGAGATGG	
SMAD2	Forward	GCCGCCAGTTGTGAAGAGAC	95°C - 15s; 60°C - 30s; 72°C - 30s
	Reverse	TGGAGACGACCATCAAGAGACC	
SMAD3	Forward	GCTGACACGGAGACACATCG	95°C - 15s; 60°C - 30s; 72°C - 30s
	Reverse	AGCCTCAAAGCCCTGGTTG	
SMAD4	Forward	CTTTGAGGGACAGCCATCGT	95°C - 15s; 60°C - 30s; 72°C - 30s
	Reverse	GCCACAGAAATGTTGGGAAA	
SMAD5	Forward	GTAAAACGACGGCCAGTTTTCATGGTGAATACTA AGACTGGTTT	95°C - 15s; 60°C - 30s; 72°C - 30s
	Reverse	TTCAATGTAAGCTCACAGTATCTGTACTC	
SMAD6	Forward	TACTCTCGGCTGTCTCCTC	95°C - 15s; 60°C - 30s; 72°C - 30s
	Reverse	GAGTTGGTAGCCTCCGTTTC	
SMAD7	Forward	GCTGAAACAGGGGGAACGA	95°C - 15s; 60°C - 30s; 72°C - 30s
	Reverse	AGTATGCCACCACGCACCA	
TGFβ1	Forward	CAACGAAATCTATGACAAGTTCAAGCAG	95°C - 15s; 60°C - 30s; 72°C - 30s
	Reverse	CTTCTCGGAGCTCTGATGTG	
RUNX2	Forward	CCGTCCATCCACTCTACCAC	95°C - 15s; 60°C - 30s; 72°C - 30s
	Reverse	ATGAAATGCTTGGGAACTGC	
OSTERIX	Forward	CCAGGCAACACTCCTACTCC	95°C - 15s; 60°C - 30s; 72°C - 30s
	Reverse	GCCTTGCCATACACCTTGC	
RANKL	Forward	AGGGACTCCATCCAAGAAGG	95°C - 15s; 60°C - 30s; 72°C - 30s
	Reverse	GCAGTTTCTGTTCTATTATTCAGGTG	
SOST	Forward	GCGTTCAAGAATGATGCCACG	95°C - 15s; 60°C - 30s; 72°C - 30s
	Reverse	GCTGTACTCGGACACGTCTTTGG	
DMP1	Forward	CAGTGAGGATGAGGCAGACA	95°C - 15s; 60°C - 30s; 72°C - 30s
	Reverse	TCGATCGCTCCTGGTACTCT	
FGF23	Forward	TGAGCGTCCTCAGAGCCTAT	95°C - 15s; 60°C - 30s; 72°C - 30s
	Reverse	TTGTGGATCTGCAGGTGGTA	
FGFr1	Forward	CTGGGTAGCAACGTGGAGTT	95°C - 15s; 60°C - 30s; 72°C - 30s
	Reverse	ACCATGCAGGAGATGAGGAA	
FGFr2	Forward	GGAAAAGAACGGCAGTAAAT	95°C - 15s; 60°C - 30s; 72°C - 30s
	Reverse	GTAGTCTGGGGAAGCTGTAAA	
FGFr3	Forward	GGGCTTCTTCCTGTTCATCC	95°C - 15s; 60°C - 30s; 72°C - 30s
	Reverse	AGGGACACCTGTCGCTTGA	
FGFr4	Forward	AGATGCTCAAAGACAACGCCT	95°C - 15s; 60°C - 30s; 72°C - 30s
	Reverse	CGCACTTCCACGATCACGTA	
PTCH	Forward	GGGTCCTCGCTTACAAACTC	95°C - 15s; 60°C - 30s;

	Reverse	ATGATGCCATCTGCGTCTAC	72°C - 30s
SUFU	Forward	GAGGGCGAAGTAATTTGTGG	95°C - 15s; 60°C - 30s; 72°C - 30s
	Reverse	AGCCCTCCTTCTGAGTGCTT	
SHH	Forward	CACCGAGCAGTGGATATGTG	95°C - 15s; 60°C - 30s; 72°C - 30s
	Reverse	AGTGGCCAGGAGTGAAACTG	
miR-23a	Forward	CCGGCTGGGGTTCCTG	95°C - 15s; 60°C - 30s; 72°C - 30s
	Reverse	GGTCGGTTGGAAATCCCTGGC	
miR-17	Forward	TCAGAATAATGTCAAAGTGCTTACAGTGCAGG	95°C - 15s; 60°C - 30s; 72°C - 30s
	Reverse	GTCACCATAATGCTACAAGTGCCTTCACTC	
LRP5	Forward	AAGGGTGCTGTGTACTGGAC	95°C - 15s; 60°C - 30s; 72°C - 30s
	Reverse	AGAAGAGAACTTACGGGAC	
β-Catenin	Forward	GCGTGGACAATGGCTACTCAAG	95°C - 15s; 60°C - 30s; 72°C - 30s
	Reverse	GTCATTGCATACTGCCCGTCAA	
GSK3	Forward	GACTAAGGTCTTCCGACCCC	95°C - 15s; 60°C - 30s; 72°C - 30s
	Reverse	TTAGCATCTGACGCTGCTGT	
DKK1	Forward	CCTTGGATGGGTATTCCAGA	95°C - 15s; 60°C - 30s; 72°C - 30s
	Reverse	CCTGAGGCACAGTCTGATGA	
sFRP1	Forward	CGGCCAGCGAGTACGACTACGTGAGC	95°C - 15s; 60°C - 30s; 72°C - 30s
	Reverse	GCATCTCGGGCCAGATAGAAGCCGAAG	
sFRP2	Forward	CTCGCTGCTGCTGCTCTTC	95°C - 15s; 60°C - 30s; 72°C - 30s
	Reverse	GGCTTCACATACCTTTGGAG	
CD9	Forward	TTTAAAAGTGCAGCCGGAGA	95°C - 15s; 60°C - 30s; 72°C - 30s
	Reverse	GCGCCGATGATGTGGAATTT	
CD63	Forward	TGATGCCGTGGAAAGCAGAT	95°C - 15s; 60°C - 30s; 72°C - 30s
	Reverse	AGTCAAGCGTCTCGTGGAAG	
CD81	Forward	GCGGTGGAAGGAGGAATGAA	95°C - 15s; 60°C - 30s; 72°C - 30s
	Reverse	AGCCCCCTGGATTATGGTCT	
Fetuin A1	Forward	GAATTCCCCGCTCATCCTGTTCT	95°C - 15s; 60°C - 30s; 72°C - 30s
	Reverse	CGTGGAAATCGCAGTCTCCT	
TNAP	Forward	TTTATAAGGCGGCGGGGGTG	95°C - 15s; 60°C - 30s; 72°C - 30s
	Reverse	AGCCCAGAGATGCAATCGAC	
NPP1	Forward	TTTGCCGATTGAGGATTTTC	95°C - 15s; 60°C - 30s; 72°C - 30s
	Reverse	CCACTGACGACATTGACACC	
SMPD3	Forward	GCCTATCACTGTTACCCCAAC	95°C - 15s; 60°C - 30s; 72°C - 30s
	Reverse	GACGATTCTTTGGTCCTGAGG	
GP38	Forward	GGGAACGATGTGGAAGGTGT	95°C - 15s; 60°C - 30s; 72°C - 30s
	Reverse	GCTCTTTAGGGCGAGTACCT	
Notch1	Forward	GGAAGTGTGAAGCGGCCAATG	95°C - 15s; 60°C - 30s; 72°C - 30s
	Reverse	ATAGTCTGCCACGCCTCTGC	
Notch2	Forward	TGTCGAGATGGCTATGAACCCTG	95°C - 15s; 60°C - 30s; 72°C - 30s

	Reverse	GCAGCGGTTCTTCTCACAGG	
Nocth3	Forward	TGTCTGCCAGAGTTCAGTGGTG	95°C - 15s; 60°C - 30s; 72°C - 30s
	Reverse	AGGAGCAGAGGAAGCGTCCATC	
Notch4	Forward	TTGTCCTCCCTCCTTCTGTTCC	95°C - 15s; 60°C - 30s; 72°C - 30s
	Reverse	AGAAGTCCCGAAGCTGGCAC	
Jag1	Forward	TGCCTCTGTGAGACCAACTG	95°C - 15s; 60°C - 30s; 72°C - 30s
	Reverse	GTTGGGTCCTGAATACCCCT	
Jag2	Forward	GTGGCAAGAACTGCTCCGTG	95°C - 15s; 60°C - 30s; 72°C - 30s
	Reverse	TGCCTCTGTGAGACCAACTG	
BMP9	Forward	AGAACGTGAAGGTGGATTTCC	95°C - 15s; 60°C - 30s; 72°C - 30s
	Reverse	CGCACAATGTTGG ACGCTG	
Integrin β1	Forward	GCCGCGCGGAAAAGATGAA	95°C - 15s; 60°C - 30s; 72°C - 30s
	Reverse	TGCTGTTCCTTTGCTACGGT	
Src	Forward	CAACACAGAGGGAGACTGGT	95°C - 15s; 60°C - 30s; 72°C - 30s
	Reverse	AGCTTCTTCATGACCTGGGC	
FAK	Forward	TCAGCTCAGCACAATCCTGG	95°C - 15s; 60°C - 30s; 72°C - 30s
	Reverse	CTGAAGCTTGACACCCTCGT	
Cofilin	Forward	TGTGCGGCTCCTACTAAACG	95°C - 15s; 60°C - 30s; 72°C - 30s
	Reverse	TCCTTGACCTCCTCGTAGCA	
AKT	Forward	CAGCGCGGCCCGAAGGAC	95°C - 15s; 60°C - 30s; 72°C - 30s
	Reverse	GACGCTACAGCGCTCCTCTC	
ERK	Forward	AACAGGCTCTGGCCCACCCAT	95°C - 15s; 60°C - 30s; 72°C - 30s
	Reverse	GCAGCGCCTCCCTTGCTAGA	
JNK	Forward	AAAGGTGGTGTTTTGTTCCCAGGT	95°C - 15s; 60°C - 30s; 72°C - 30s
	Reverse	TGATGATGGATGCTGAGAGCCATTG	
p38	Forward	GAGAACTGCGGTTACTTA	95 °C - 3 s; 60 °C - 8 s; 72 °C - 20 s
	Reverse	ATGGGTCACCAGATACACAT	
ALP	Forward	CGGGCACCATGAAGGAAA	95°C - 15s; 60°C - 30s; 72°C - 30s
	Reverse	GGCCAGACCAAAGATAGAGTT	
BSP	Forward	GTTGCGTCTTGGAAGTGAGA	95°C - 15s; 60°C - 30s; 72°C - 30s
	Reverse	CAGCTGGCTGATCACTCAAA	
Osteopontin	Forward	AGCAAGAAGCCCTGCCTGA	95°C - 15s; 60°C - 30s; 72°C - 30s
	Reverse	TCCTACTTACACCTGGACAGGATT	
Osteocalcin	Forward	ATGAGAGCCCTCACACTCCTC	95°C - 15s; 60°C - 30s; 72°C - 30s
	Reverse	GCCGTAGAAGCGCCGATAGGC	
MMP2	Forward	AGCTCCCGGAAAAGATTGATG	95°C - 15s; 60°C - 30s; 72°C - 30s
	Reverse	CAGGGTGCTGGCTGAGTAGAT	
MMP9	Forward	CACGCACGACGTCTTCCA	95°C - 15s; 60°C - 30s;

	Reverse	AAGCGGTCCTGGCAGAAAT	72°C - 30s
TIMP1	Forward	CCGCAGCGAGGAGTTTCTC	95°C - 15s; 60°C - 30s; 72°C - 30s
	Reverse	GAGCTAAGCTCAGGCTGTTCCA	
TIMP2	Forward	CGACATTTATGGCAACCCTATCA	95°C - 15s; 60°C - 30s; 72°C - 30s
	Reverse	GGGCCGTGTAGATAAACTCTATATCC	
RECK	Forward	TGCAAGCAGGCATCTTCAAA	95°C - 15s; 60°C - 30s; 72°C - 30s
	Reverse	ACCGAGCCCATTTCATTTCTG	
Collagen 1A1	Forward	AACCAAGGCTGCAACCTGGA	95°C - 15s; 60°C - 30s; 72°C - 30s
	Reverse	GGCTGAGTAGGGTACACGCAGG	
Wnt	Forward	CCTTGCGCTCCCTGGATAAA	95°C - 15s; 60°C - 30s; 72°C - 30s
	Reverse	TGTTGGGTTCATGGCAGGTT	
GAPDH	Forward	GACTCATGACCACAGTCCATGC	95°C - 15s; 60°C - 30s; 72°C - 30s
	Reverse	AGAGGCAGGGATGATGTTCTG	

Isolation of exosomes and characterization. For analysis and exosomes, the culture medium was supplemented with extracellular vesicles from Free Fetal Serum, and extraction was performed in ultracentrifugation of 30,000 g for 18h[39–41]. Cells remained for 72 h with EV-free, Static, or *Shear-Stress* free medium, after which the medium was removed and used to isolate exosomes with the Total Cell Isolation Kit (Invitrogen - Thermo Fisher Scientific, Vilnius, Lithuania) according to the manufacturer's instructions. The exosomes were analyzed in Tecnai Spirit Electronic Transmission Microscope. NanoSight NS300 (Amesbury, UK) was used to determine the size and concentration of exosomes that perform nanoparticle tracing analysis based on light scattering and Brownian motion properties of the samples, and the Malvern Zetasizer Nano ZS instrument was used to measure zeta potential. Exosome markers analysis (anti-CD9, anti-CD63, and anti-CD81) was performed using *FACS.* To measure ATP, the exosomes were boiled at 45 °C for 2 min and dosing was performed according to the instructions of the CellTiter-Glo® Luminescent Cell Viability Assay Technical Bulletin Kit (Promega, Madison, WI, USA). To further analysis protein involvement, we have performed western blotting methodology.

Bioinformatic tools. E-GEOD-61351 and E-GEOD-57764, both available at ArrayExpress, were chosen for this analysis. E-GEOD-61351 dataset, which is based on GPL13112 platform (Illumina HiSeq 2000 [Mus musculus]), contains 6 IDG-SW3 samples differentiated for 28 days, treated (n = 3) or not (n = 3) with PTH. E-GEOD-57764 dataset, based on Agilent-G4851A SurePrint G3 Human GE 8x60K Microarray, which contains

samples from human primary airway smooth muscle cultured for 24 h in three conditions, Control (n = 4), FCS (n = 4) and FCS + Dex (n=4). The processed data were downloaded, and GEO2R [https://www.ncbi.nlm.nih.gov/geo/geo2r/] was used to calculate the differential expression of targets. P value<0.01 and |log2FC|>2 were considered as differentially expressed. R was used to draw heatmap graphs with the base package, and TCGAbiolinks package was used to draw a Volcano plot.

Statistical analysis. The results were represented as the mean ± standard deviation (SD). They were verified using One-Way ANOVA (non-parametric) with Tukey's post-test to compare all pairs of groups. In this case, with p <0.05 considered statistically significant and p <0.0001 considered highly significant. The software used was GraphPad Prism 6. ImageJ Software was used for particle counting to determine the number of points in the area recorded in the photo. For the statistical analysis, the groups were standardized by the percentage of the control. To determine the number of stellate cells, the number of nuclei in the area recorded in the photo were counted, followed by statistical analysis.

REFERENCES

[1] K. Henriksen, A. V Neutzsky-Wulff, L.F. Bonewald, M.A. Karsdal, Local communication on and within bone controls bone remodeling., Bone. 44 (2009) 1026–1033. doi:10.1016/j.bone.2009.03.671.

[2] H.-C. Zeng, Y. Bae, B.C. Dawson, Y. Chen, T. Bertin, E. Munivez, P.M. Campeau, J. Tao, R. Chen, B.H. Lee, MicroRNA miR-23a cluster promotes osteocyte differentiation by regulating TGF-beta signalling in osteoblasts., Nature Communications. 8 (2017) 15000. doi:10.1038/ncomms15000.

[3] L.F. Bonewald, Mechanosensation and Transduction in Osteocytes., BoneKEy Osteovision. 3 (2006) 7–15. doi:10.1138/20060233.

[4] A.D. Bakker, K. Soejima, J. Klein-Nulend, E.H. Burger, The production of nitric oxide and prostaglandin E(2) by primary bone cells is shear stress dependent., Journal of Biomechanics. 34 (2001) 671–677.

[5] S.K. Ramasamy, A.P. Kusumbe, L. Wang, R.H. Adams, Endothelial Notch activity promotes angiogenesis and osteogenesis in bone., Nature. 507 (2014) 376–380. doi:10.1038/nature13146.

[6] K.K. Sivaraj, R.H. Adams, Blood vessel formation and function in bone., Development (Cambridge, England). 143 (2016) 2706–2715. doi:10.1242/dev.136861.

[7] E. Beit-Yannai, S. Tabak, W.D. Stamer, Physical exosome:exosome interactions., Journal of Cellular and Molecular Medicine. 22 (2018) 2001–2006. doi:10.1111/jcmm.13479.

[8] U.H. Langen, M.E. Pitulescu, J.M. Kim, R. Enriquez-Gasca, K.K. Sivaraj, A.P. Kusumbe, A. Singh, J. Di Russo, M.G. Bixel, B. Zhou, L. Sorokin, J.M. Vaquerizas, R.H. Adams, Cell-matrix signals specify bone endothelial cells during developmental osteogenesis., Nature Cell Biology. 19 (2017) 189–201. doi:10.1038/ncb3476.

[9] S.K. Ramasamy, A.P. Kusumbe, M. Schiller, D. Zeuschner, M.G. Bixel, C. Milia, J. Gamrekelashvili, A. Limbourg, A. Medvinsky, M.M. Santoro, F.P. Limbourg, R.H. Adams, Blood flow controls bone vascular function and osteogenesis., Nature Communications. 7 (2016) 13601. doi:10.1038/ncomms13601.

[10] S.K. Ramasamy, A.P. Kusumbe, T. Itkin, S. Gur-Cohen, T. Lapidot, R.H. Adams, Regulation of Hematopoiesis and Osteogenesis by Blood Vessel–Derived Signals, Annual Review of

Cell and Developmental Biology. 32 (2016) 649–675. doi:10.1146/annurev-cellbio-111315-124936.
[11] J. Gamrekelashvili, R. Giagnorio, J. Jussofie, O. Soehnlein, J. Duchene, C.G. Briseno, S.K. Ramasamy, K. Krishnasamy, A. Limbourg, T. Kapanadze, C. Ishifune, R. Hinkel, F. Radtke, L.J. Strobl, U. Zimber-Strobl, L.C. Napp, J. Bauersachs, H. Haller, K. Yasutomo, C. Kupatt, K.M. Murphy, R.H. Adams, C. Weber, F.P. Limbourg, Regulation of monocyte cell fate by blood vessels mediated by Notch signalling., Nature Communications. 7 (2016) 12597. doi:10.1038/ncomms12597.
[12] T. Itkin, S. Gur-Cohen, J.A. Spencer, A. Schajnovitz, S.K. Ramasamy, A.P. Kusumbe, G. Ledergor, Y. Jung, I. Milo, M.G. Poulos, A. Kalinkovich, A. Ludin, O. Kollet, G. Shakhar, J.M. Butler, S. Rafii, R.H. Adams, D.T. Scadden, C.P. Lin, T. Lapidot, Distinct bone marrow blood vessels differentially regulate haematopoiesis., Nature. 532 (2016) 323–328. doi:10.1038/nature17624.
[13] S.K. Ramasamy, A.P. Kusumbe, R.H. Adams, Regulation of tissue morphogenesis by endothelial cell-derived signals., Trends in Cell Biology. 25 (2015) 148–157. doi:10.1016/j.tcb.2014.11.007.
[14] C. Xu, S.S. Hasan, I. Schmidt, S.F. Rocha, M.E. Pitulescu, J. Bussmann, D. Meyen, E. Raz, R.H. Adams, A.F. Siekmann, Arteries are formed by vein-derived endothelial tip cells., Nature Communications. 5 (2014) 5758. doi:10.1038/ncomms6758.
[15] A.P. Kusumbe, S.K. Ramasamy, R.H. Adams, Corrigendum: Coupling of angiogenesis and osteogenesis by a specific vessel subtype in bone, Nature. 513 (2014) 574. doi:10.1038/nature13145.
[16] H. V CROCK, A REVISION OF THE ANATOMY OF THE ARTERIES SUPPLYING THE UPPER END OF THE HUMAN FEMUR., Journal of Anatomy. 99 (1965) 77–88.
[17] B. Beamer, C. Hettrich, J. Lane, Vascular endothelial growth factor: an essential component of angiogenesis and fracture healing., HSS Journal : The Musculoskeletal Journal of Hospital for Special Surgery. 6 (2010) 85–94. doi:10.1007/s11420-009-9129-4.
[18] J. Xiong, K. Cawley, M. Piemontese, Y. Fujiwara, H. Zhao, J.J. Goellner, C.A. O'Brien, Soluble RANKL contributes to osteoclast formation in adult mice but not ovariectomy-induced bone loss., Nature Communications. 9 (2018) 2909. doi:10.1038/s41467-018-05244-y.
[19] C. Greenhill, Shared variants for osteoporosis and T2DM., Nature Reviews. Endocrinology. 14 (2018) 627. doi:10.1038/s41574-018-0095-0.
[20] W.J. Boyle, W.S. Simonet, D.L. Lacey, Osteoclast differentiation and activation., Nature. 423 (2003) 337–342. doi:10.1038/nature01658.
[21] P. Zhang, M. Su, S.M. Tanaka, H. Yokota, Knee loading stimulates cortical bone formation in murine femurs., BMC Musculoskeletal Disorders. 7 (2006) 73. doi:10.1186/1471-2474-7-73.
[22] G.Y. Rochefort, S. Pallu, C.L. Benhamou, Osteocyte: the unrecognized side of bone tissue., Osteoporosis International : A Journal Established as Result of Cooperation between the European Foundation for Osteoporosis and the National Osteoporosis Foundation of the USA. 21 (2010) 1457–1469. doi:10.1007/s00198-010-1194-5.
[23] R. Teo, F. Mohrlen, G. Plickert, W.A. Muller, U. Frank, An evolutionary conserved role of Wnt signaling in stem cell fate decision., Developmental Biology. 289 (2006) 91–99. doi:10.1016/j.ydbio.2005.10.009.
[24] T.A. Burgers, B.O. Williams, Regulation of Wnt/beta-catenin signaling within and from osteocytes., Bone. 54 (2013) 244–249. doi:10.1016/j.bone.2013.02.022.
[25] E. Canalis, Wnt signalling in osteoporosis: mechanisms and novel therapeutic approaches., Nature Reviews. Endocrinology. 9 (2013) 575–583. doi:10.1038/nrendo.2013.154.
[26] M. Capulli, R. Paone, N. Rucci, Osteoblast and osteocyte: games without frontiers., Archives of Biochemistry and Biophysics. 561 (2014) 3–12. doi:10.1016/j.abb.2014.05.003.
[27] J. Chen, Y. Lan, J.-A. Baek, Y. Gao, R. Jiang, Wnt/beta-catenin signaling plays an essential role in activation of odontogenic mesenchyme during early tooth development., Developmental Biology. 334 (2009) 174–185. doi:10.1016/j.ydbio.2009.07.015.
[28] Y. Chen, H.C. Whetstone, A.C. Lin, P. Nadesan, Q. Wei, R. Poon, B.A. Alman, Beta-catenin signaling plays a disparate role in different phases of fracture repair: implications for therapy to improve bone healing., PLoS Medicine. 4 (2007) e249.

doi:10.1371/journal.pmed.0040249.
[29] Y. Kitase, L. Barragan, H. Qing, S. Kondoh, J.X. Jiang, M.L. Johnson, L.F. Bonewald, Mechanical induction of PGE2 in osteocytes blocks glucocorticoid-induced apoptosis through both the beta-catenin and PKA pathways., Journal of Bone and Mineral Research : The Official Journal of the American Society for Bone and Mineral Research. 25 (2010) 2657–2668. doi:10.1002/jbmr.168.
[30] X. Xia, N. Batra, Q. Shi, L.F. Bonewald, E. Sprague, J.X. Jiang, Prostaglandin promotion of osteocyte gap junction function through transcriptional regulation of connexin 43 by glycogen synthase kinase 3/beta-catenin signaling., Molecular and Cellular Biology. 30 (2010) 206–219. doi:10.1128/MCB.01844-08.
[31] I. Kramer, C. Halleux, H. Keller, M. Pegurri, J.H. Gooi, P.B. Weber, J.Q. Feng, L.F. Bonewald, M. Kneissel, Osteocyte Wnt/beta-catenin signaling is required for normal bone homeostasis., Molecular and Cellular Biology. 30 (2010) 3071–3085. doi:10.1128/MCB.01428-09.
[32] B. Javaheri, A.R. Stern, N. Lara, M. Dallas, H. Zhao, Y. Liu, L.F. Bonewald, M.L. Johnson, Deletion of a single beta-catenin allele in osteocytes abolishes the bone anabolic response to loading., Journal of Bone and Mineral Research : The Official Journal of the American Society for Bone and Mineral Research. 29 (2014) 705–715. doi:10.1002/jbmr.2064.
[33] N.G. dela Paz, T.E. Walshe, L.L. Leach, M. Saint-Geniez, P.A. D'Amore, Role of shear-stress-induced VEGF expression in endothelial cell survival., Journal of Cell Science. 125 (2012) 831–843. doi:10.1242/jcs.084301.
[34] A.M. Gomes, T.S. Pinto, C.J. da Costa Fernandes, R.A. da Silva, W.F. Zambuzzi, Wortmannin targeting phosphatidylinositol 3-kinase suppresses angiogenic factors in shear-stressed endothelial cells., Journal of Cellular Physiology. 235 (2020) 5256–5269. doi:10.1002/jcp.29412.
[35] R.A. da Silva, M.R. Ferreira, A.M. Gomes, W.F. Zambuzzi, LncRNA HOTAIR is a novel endothelial mechanosensitive gene, Journal of Cellular Physiology. 235 (2020) 4631–4642. doi:10.1002/jcp.29340.
[36] T.S. Pinto, C.J. da C. Fernandes, R.A. da Silva, A.M. Gomes, J.C.S. Vieira, P. de M. Padilha, W.F. Zambuzzi, c-Src kinase contributes on endothelial cells mechanotransduction in a heat shock protein 70-dependent turnover manner., Journal of Cellular Physiology. 234 (2019) 11287–11303. doi:10.1002/jcp.27787.
[37] R.A. da Silva, C.J. da C. Fernandes, G. da S. Feltran, A.M. Gomes, A.F. de Camargo Andrade, D.C. Andia, M.P. Peppelenbosch, W.F. Zambuzzi, Laminar shear stress-provoked cytoskeletal changes are mediated by epigenetic reprogramming of TIMP1 in human primary smooth muscle cells., Journal of Cellular Physiology. 234 (2019) 6382–6396. doi:10.1002/jcp.27374.
[38] K.J. Livak, T.D. Schmittgen, Analysis of Relative Gene Expression Data Using Real-Time Quantitative PCR and the 2−ΔΔCT Method, Methods. 25 (2001) 402–408. doi:10.1006/meth.2001.1262.
[39] P. Carpintero-Fernandez, J. Fafian-Labora, A. O'Loghlen, Technical Advances to Study Extracellular Vesicles., Frontiers in Molecular Biosciences. 4 (2017) 79. doi:10.3389/fmolb.2017.00079.
[40] F. Momen-Heravi, L. Balaj, S. Alian, P.-Y. Mantel, A.E. Halleck, A.J. Trachtenberg, C.E. Soria, S. Oquin, C.M. Bonebreak, E. Saracoglu, J. Skog, W.P. Kuo, Current methods for the isolation of extracellular vesicles., Biological Chemistry. 394 (2013) 1253–1262. doi:10.1515/hsz-2013-0141.
[41] A. Mehdiani, A. Maier, A. Pinto, M. Barth, P. Akhyari, A. Lichtenberg, An innovative method for exosome quantification and size measurement., Journal of Visualized Experiments : JoVE. (2015) 50974. doi:10.3791/50974.

CAPÍTULO 4

Unstressed Vascular Smooth Muscle Cell (VSMC) drives osteocyte function phenotype

Célio J.C. Fernandes[3,4], Rodrigo A. Silva[1,4], Gwenny M. Fuhler[2], Maikel P. Peppelenbosch[2], Willian F. Zambuzzi[1,5]

[3]Bioassays and Cell Dynamics Lab, Dept. of Chemistry and Biochemistry, Bioscience Institute, UNESP, Botucatu, 18603-100, Sao Paulo, Brazil;
[4]Department of Gastroenterology and Hepatology, Erasmus MC, University Medical Center Rotterdam's Gravendijkwal 230, NL-3015 CE Rotterdam, The Netherlands;
[5]Electron Microscopy Center, São Paulo State University (UNESP), Institute of Biosciences, campus Botucatu, Brazil, 18603-100.
[4]Department of Biology, Dental School, University of Taubaté, 12020-340, Taubaté, São Paulo, Brazil.

Correspondence and requests for materials should be addressed to W.F.Z. (email: w.zambuzzi@unesp.br)

INTRODUCTION

Osteoblastogenesis and blood vessels growth are so far biological events coupled and responsible to bone homeostasis[1,2] – endochondral ossification requires a well coordinated gradual replacement of cartilage by bone, where chondrocytes and bone differentiating cells cooperate with the capillary network mainly coordinated by the Vascular Endothelial Growth Factor (VEGF) signaling[3–5]. Additionally, this crosstalk between bone cells and vascular network has been discussed during bone fracture repair[6–9].

Osteoblasts come from mesenchymal stem cells and are in constant response to the microenviroment. They respond simultaneously to a bombarding of signaling molecules which are responsible to drive bone remodeling[10-17]. Importanty, the regency of this processes takes osteoblast to differentiate in secreting cells and late to be embedded into the mineralized matrix, originating osteocytes. The osteoblast-osteocyte transition requires already known involvement of signaling pathways and obeys a schedule of events, as follows: GP38 protein promotes osteoblast morphological changes, while Connexin43 gurantees intercellular connections and trigger survival signaling in osteocytes. Fibroblast growth factor 23 (FGF23)[10–14] and Dentin Matrix Protein 1 (DMP1) possesses the homeostasis of minerals. This is also relevant that osteocyte is the major source of RANKL in vertebrates[15–21]. To note, RANKL is related controlling osteoclastogenesis and further bone remodeling.

Althought with some progress on comprehending osteocyte biology, the knowledge about osteocyte phnotype is scarse maybe because their localization within bone compact tissue. We have shown that vascular smooth mucle cells (VSMCs) favor osteoblast-osteocyte transition by modulating β-Catenin signaling in osteoblasts (data unplished) and here, we investigate the effect of shear stress on VSMCs and further their effect on the transition osteoblasts to osteocytes, mainly considering the involvement of exosomes (120 nm diameter) in this crosstalk. A better understanding of this complex communication between bone and vascular cells will provide a guidance on the development of new therapies for bone-related disorders.

RESULTS

VSMCs modulate the expression of genes involved with osteoblastic differentiation

Firstly, we subjected or not VSMCs to shear stress to 72 hours and thereafter the conditioned medium was collected to after challenge osteoblasts. The data shows a

positive and significant modulation of TGFβ1 **(Fig.1a)**, BMPR2 **(Fig.1c)**, BMP7 **(Fig.1e)** and BMP9 **(Fig.1f)** genes in response to shear-stress-obtained medium. Importantly, TGFβ1 and BMP9 genes were also up-modulated in response to conditionated medium without shear-stress. Later, we have investigated both RUNX2 and OSTERIX, both transcript factors involved with osteoblast differentiation. Both factors were significantly expressed in the groups receiving AoSMC conditioned medium, independent of the experimental condition **(Fig.1g-h)**. In an attempt to better understand the mechanism involved in the activation of the TGFβ1/BMP pathway, we also evaluated the possible involvement of SMADs. Our findings show an increase in the expression of SMADs 3, 5, 6 and 7 which suggests a positive involvement of TGFβ1/BMP signaling in osteogenic pathway promoted in crosstalk with VSMCs **(Fig. S1a-f)**.

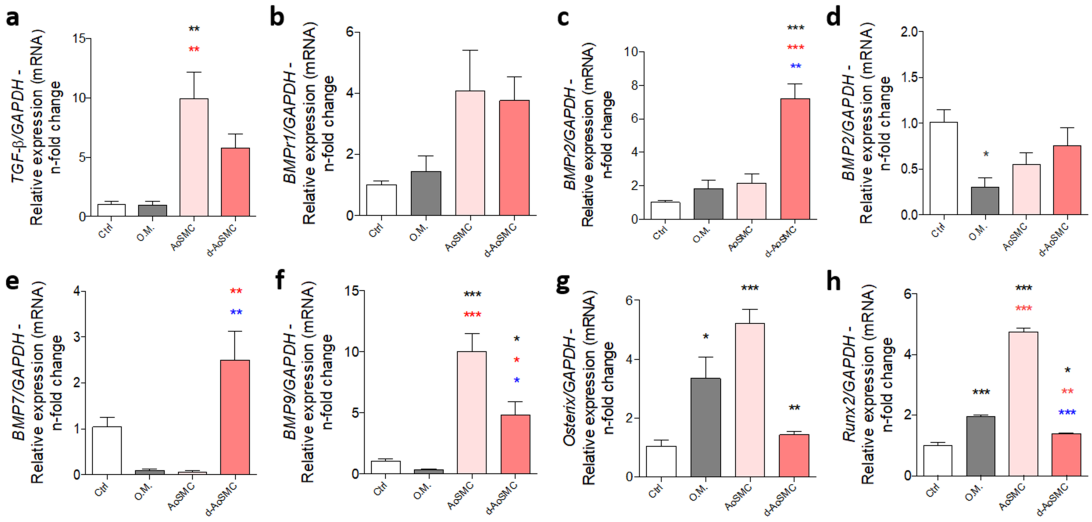

Figure 1: VSMCs promote osteoblastic phenotype in a TGFβ pathway manner. After 28 days of differentiation in response to VSMCs conditioned medium subjected (d-AoSMC) or not (AoSMC) to Shear Stress, mature osteoblasts were harvested in TriZOL for further extraction of mRNA. Genes involved with osteoblastic differentiation were evaluated, as follows: **a)** TGFβ, **b)** BMPr1, **c)** BMPr2, **d)** BMP7, **e)** BMP2, **f)** BMP9, **g)** Osterix and **h)** Runx2. In the different treatments, including the positive cultures subjected to classical osteogenic medium (O.M.). The data were normalized by GAPDH expression. *p<0.05; **p<0.1906, ***p<0.0002: Significant statistical difference when compared to control. *p<0.05; **p<0.1906; ***p<0.0002: Statistical difference when compared with the O.M. *p<0.05; **p<0.1906; ***p<0.0002: Statistical difference when compared Static and *Shear-Stress*.

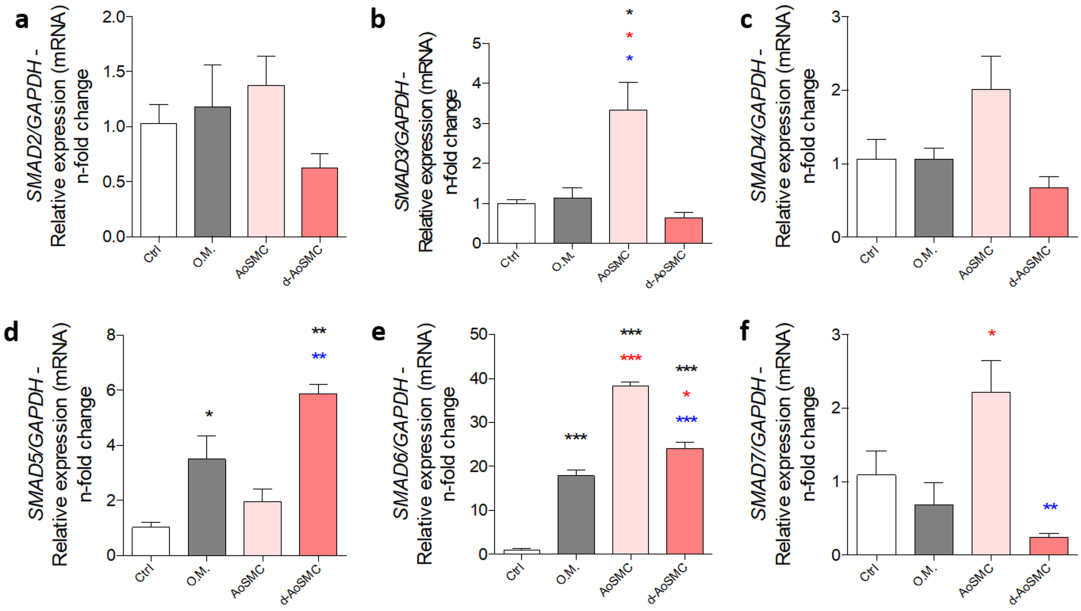

Figure S1: Members of the SMAD family in response to VSMCs. The biological model was newly applied in osteoblasts and the samples collected to investigated gene expression by using qRT-PCR technology. The SMAD2, 3, 4, 5, 6 and 7 genes were evaluated **(a-f)**. The data were normalized by the GADPH as housekeeping gene. *p<0.05; **p<0.1906, ***p<0.0002: Significant statistical difference when compared to control. *p<0.05; ***p<0.0002: Statistical difference when compared with the O.M. *p<0.05; **p<0.1906; ***p<0.0002: Statistical difference when compared Static and *Shear-Stress*.

Shear-stress distinguishes the VSMCs paracrine signaling related with osteoblast-osteocyte transition

Thereafter, osteoblasts were evaluated whether their morphology was changed. In fact, we have noticed that osteoblast presented cytoplasmatic projections just like osteocyte-related morphology **(Fig.2a)**. Both conditioned medium by VSMCs were able to provoke this osteocyte-like morphology in osteoblasts **(Fig.2b)**. Once shown the strong evidence of osteoblast-osteocyte transition in response to VSMCs paracrine signaling, we decided to better address osteocyte molecular biomarkers and, independently if subjected to shear stress or not, VSMCs showed strongly to stimulate osteocyte phenotype, as it was shown by evaluating mir-23a **(Fig 2c)**, DMP1, SOST, FGF23 and GP38 **(Fig.2d-g)**. Finally, we have investigated other functional biomarkers of osteocytes and the data comproved our hypothesis **(Fig.S3)**. Importantly, osteocytes are considered the major resource of RANKL within vertebrates, and our data show a significant gene expression in response to VSMCs without shear stress stimulus **(Fig.S3b)**.

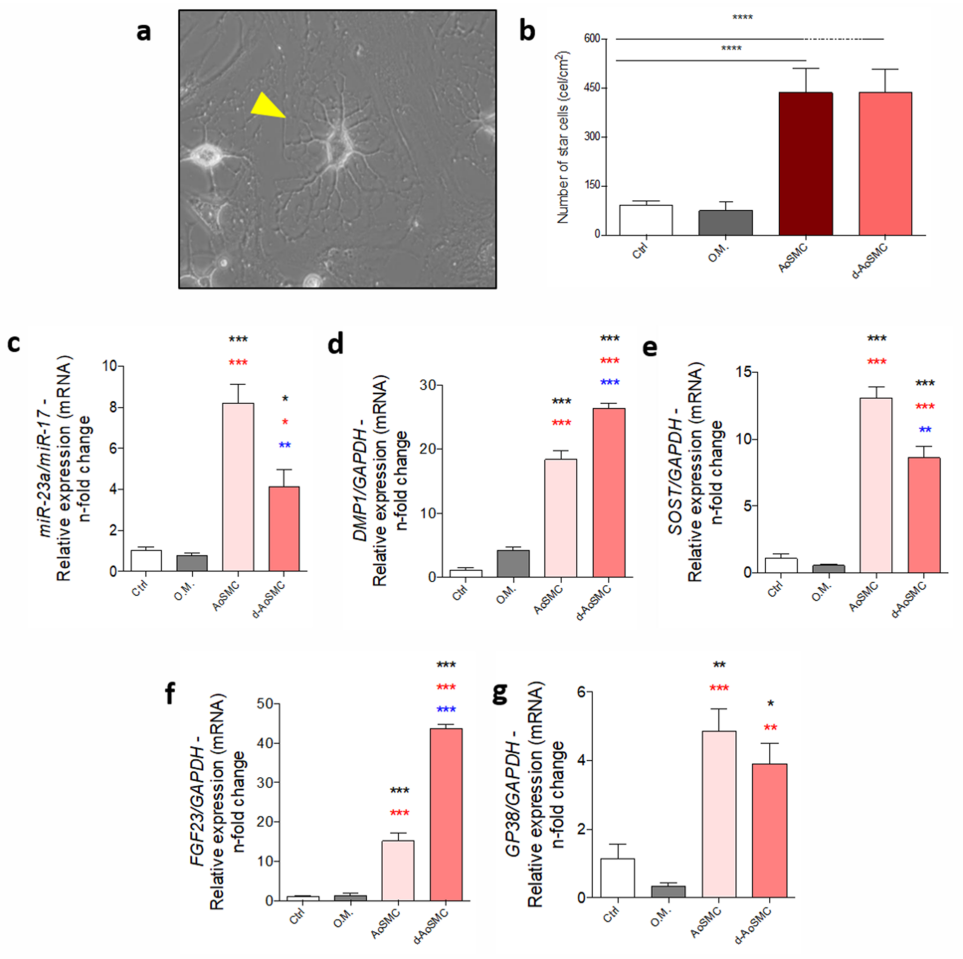

Figure 2: Paracrine action of VSMCs in the Osteoblast-Osteocyte transition. After 28 days of treatment, osteoblasts were evaluated for morphology **(a)** and counted the number of star cells **(b)**. RNA was extracted for the expression of miR-23a **(c)**, DMP1 **(d)**, SOST **(e)**, FGF23 **(f)** and GP38 **(g)**. The internal control of gene expression GAPDH was used and miR-17 was used for micro-RNA. *p<0.05; **p<0.1906, ***p<0.0002; ****p<0.0001: Significant statistical difference when compared to control. *p<0.05; ***p<0.0002: Statistical difference when compared with the Osteogenic Medium. **p<0.1906; ***p<0.0002: Statistical difference when compared Static and *Shear-Stress*.

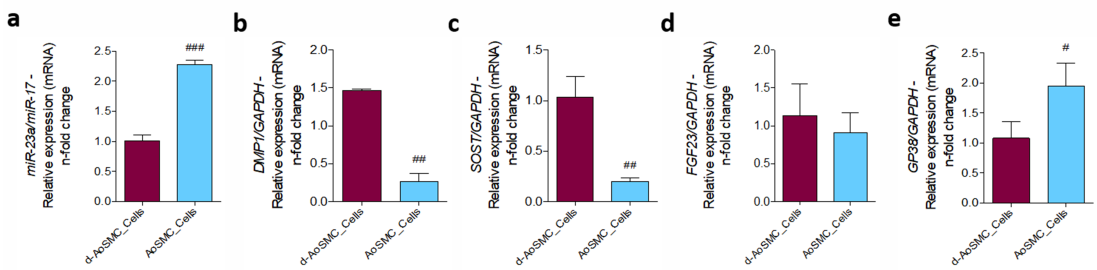

Figure S2: Differentiation markers of osteocytes differentially expressed in AoSMC under *Shear-Stress* effect. After 3 days in culture under experimental conditions, smooth muscle cells were collected in TriZOL and after extraction and cDNA synthesis, expression levels of miR-23a, DMP1, SOST, FGF23 and GP38 **(a-e)** were evaluated. The internal control of gene expression GAPDH was used and miR-17 was used for micro-RNA.

#p<0.05; ##p<0.1906, ###p<0.0002: Statistical difference when compared Static and *Shear-Stress* AoSMC.

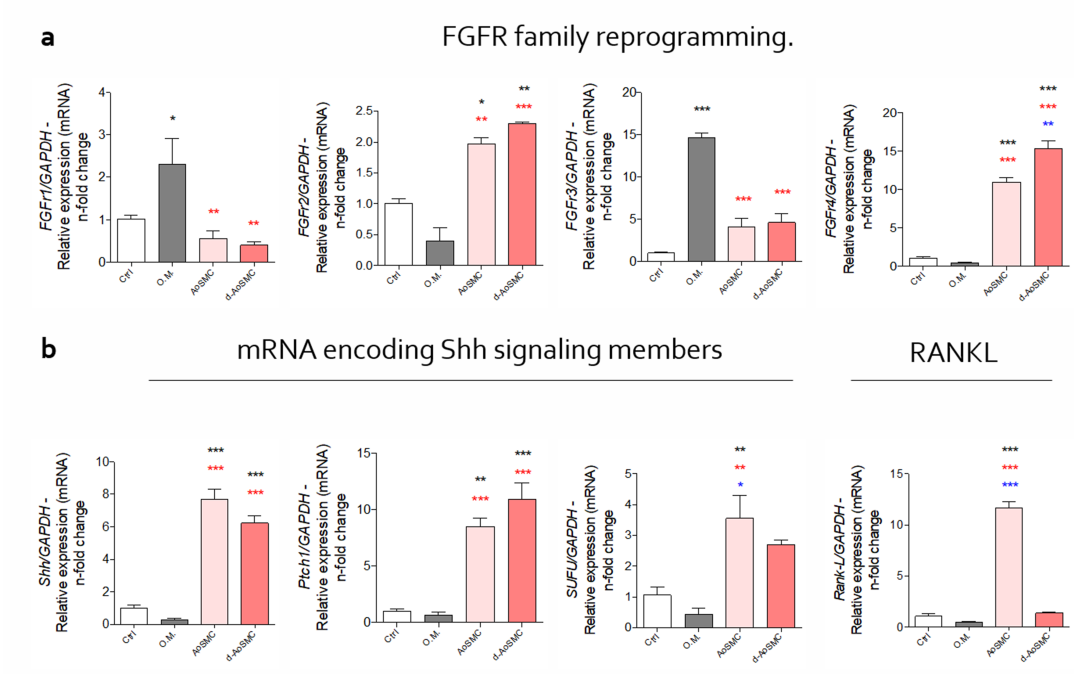

Figure S3: FGFR family, Shh signaling members and RankL genes reprogramming in response to VSMCs. During 28 days osteoblasts were subjected to the paracrine effects triggered by AoSMC in culture medium. After this period, Fibroblast Growth Factor 1-4 **(a)** family receptors, as well as Sonic Hedgehog (Shh, Ptchd and SUFU) and RankL **(b)** genes were investigated. The results were normalized by GAPDH expression. *p<0.05; **p<0.1906, ***p<0.0002: Significant statistical difference when compared to control. ***p<0.0002: Statistical difference when compared with the Osteogenic Medium. *p<0.05; **p<0.1906; ***p<0.0002: Statistical difference when compared Static and *Shear-Stress*.

The possible involvement of exosomes in the VSMCs-induced osteocyte acquisition

Our findings strongly suggest that VSMCs release molecules able to trigger signaling to promote osteoblast-osteocyte transition, however, very few is known about the cargo system to deliver this repertorie of signaling molecules. So, we have previously hypothesized the involvement of extracellular exosomes on this paracrine crosstalk between VSMCs and osteoblasts. In order to test this hypothesis, extracellular vesicles were properly isolated from the consitioned medium by VSMCs and characterized by using classical set of technologies. First, the data shows a significant involvement of tetraspanins (markers of EVs; CD9 and CD81) in both condition subjected VSMCs **(Fig. 3a-b)**, while CD63 was significantly up-expressed in VSMCs at static condition **(Fig. 3c)**, and this result was confirmed using fluorescence microscopy **(Fig. 3d)**. Additionally, Flow Cytometry technology also confirmed the presence of CD9, CD63 and CD81 in those

exosomes' surfaces **(Fig. 3e-f)**. Later, in order to measure the exosome size, Nano Tracking Analysis (NTA) was used, as well Transmission Microscopy. Altogether, the data shows that exossomos were about 140 nm diameter **(Fig. 4 a-f)**. Importantly, our findings also show that the concentration of exosomes in the Shear-Stress condition is higher when compared to the Static cultures, while the expression of SMPD3 (an important marker of vesicle biogenesis) corrobored with these findings **(Fig. 4g-h, j)**. Additionally, we evaluated the charge on the exosomes membrane, index considered to estimate their capacity to interact with the membrane of target cells **(Fig.4i)**.

Finally, we investigated exosomes cargo in order to evaluate osteocyte differentiation markers. The data shows that DMP1, SOST (app 100-fold changes increased) and FGF23 genes are superexpressed in the static VSMCs **(Fig. 5a-d)**. Again, exosomes markers were newly evaluated for expression profile of CD9, CD63, CD81 and SMPD3 **(Fig. 5 e-h)**.

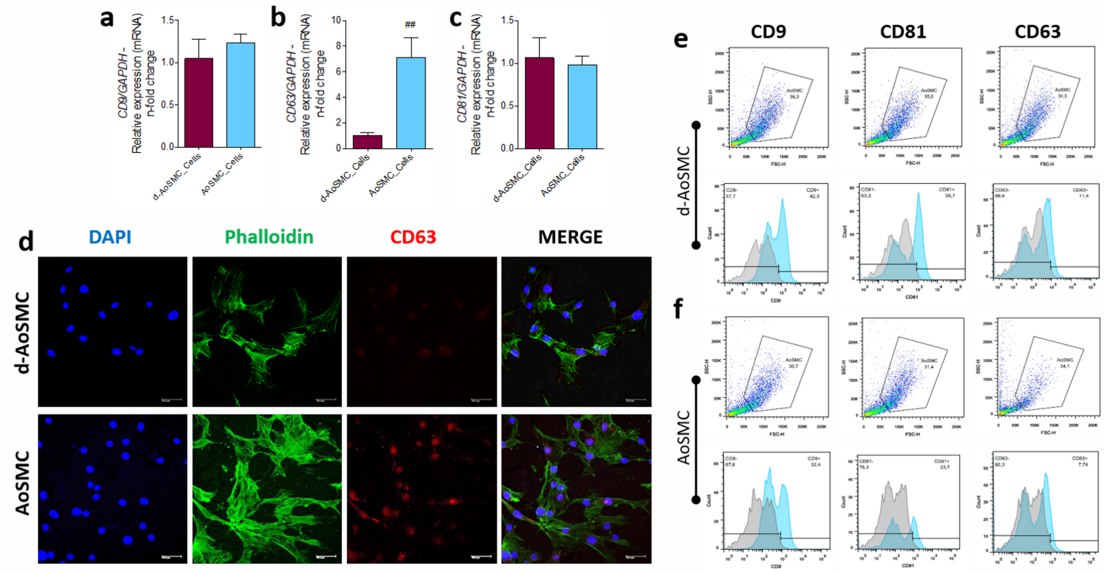

Figure 3: Characterization of the extracellular vesicles. After 3 days of culture the cells were collected in TriZOL to study the expression of Tetraspanins CD9, CD63 and CD81 **(a-c)**. Cells were plated on coverslips and labeled with CD63 specific Antibody and cells were photographed in fluorescence microscope **(d)**. After 3 days of conditioning the medium was collected for extraction of Exosomes, which were labeled with Antibodies for CD9, CD63 and CD81 and evaluated by Flow Cytometry **(e, f)**. The results to gene expression were normalized by GAPDH. ##p<0.1906: Statistical difference when compared Static and *Shear-Stress* AoSMC.

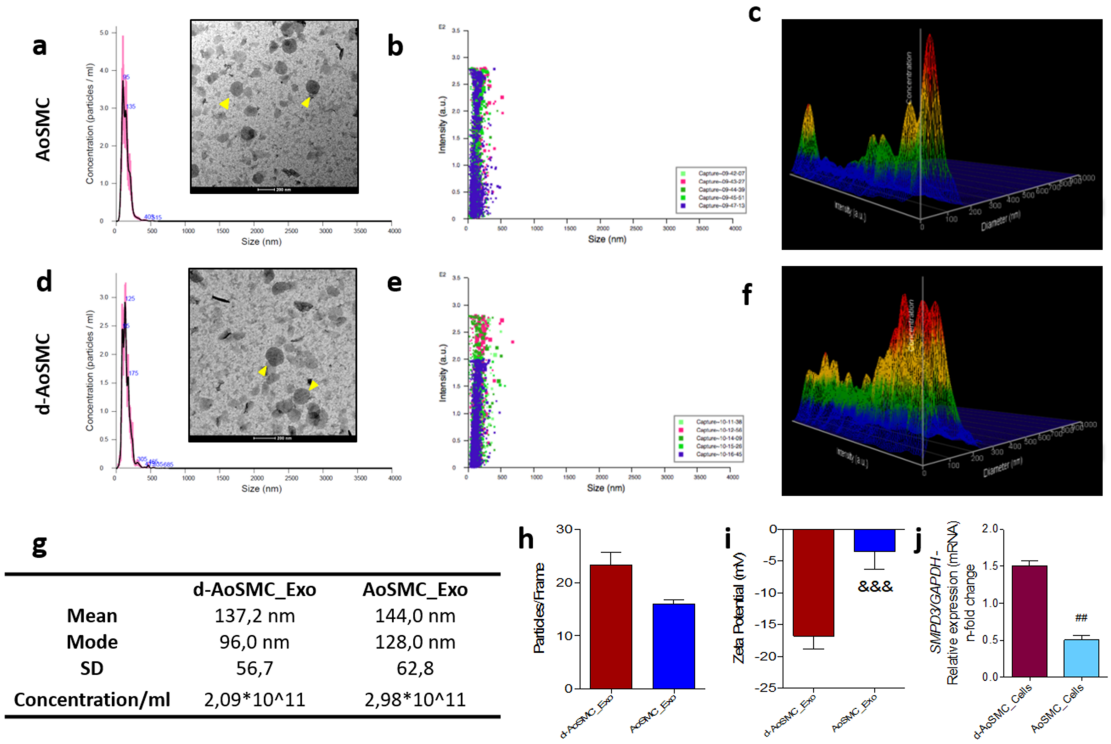

	d-AoSMC_Exo	AoSMC_Exo
Mean	137,2 nm	144,0 nm
Mode	96,0 nm	128,0 nm
SD	56,7	62,8
Concentration/ml	2,09*10^11	2,98*10^11

Figure 4: Exosomes were evaluated. AoSMC were plated in modified petri dish and subjected to the effect of *Shear-Stress*, as control cells were used without suffering mechanical tension. After 3 days under experimental conditions the medium was collected and used for extraction of exosomes. The particles were evaluated for size and concentration through NTA and Transmission Microscopy **(a-h),** in addition to being evaluated for mem- brane loading **(i)** by Zeta Potential. Cells were also collected to evaluate the gene expression of SMPD3 **(j)**. The results were normalized by GAPDH expression. &&&p<0.0002: Statistical difference when compared Static with the *Shear-Stress* Exosome. ##p<0.1906: Statistical difference when compared Static and *Shear-Stress* AoSMC.

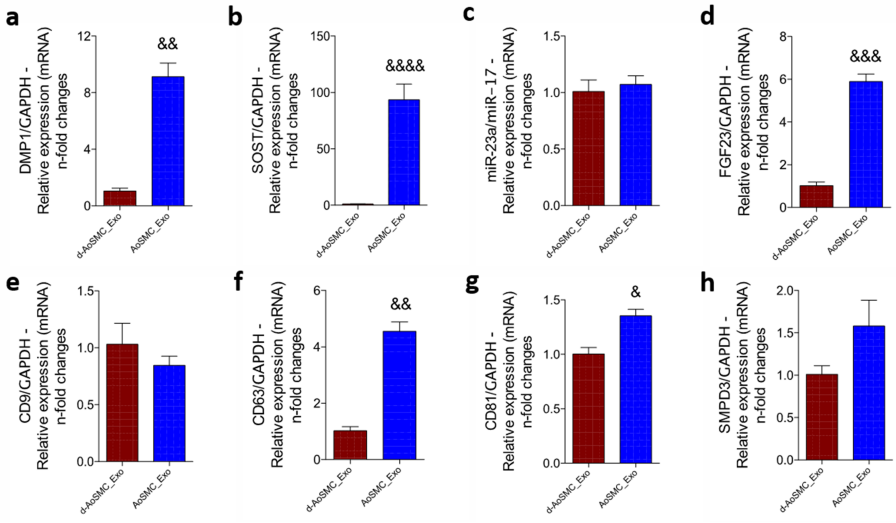

Figure 5: Exosomes cargo evaluation shows mRNA encoding osteocyte markers. After 3 days of culture, AoSMC were collected in TriZOL for RNA extraction and subsequent

cDNA synthesis. After these maturation markers of DMP1, SOST, miR-23a and FGF23 **(a-d)** osteocytes were investigated for expression levels by real-time PCR, além de marcadores específicos de Exossomos: CD9, CD63, CD81 e SMPD3 **(e-h)**. As internal control of gene expression GAPDH was used and miR-17 was used for micro-RNA. &p<0.05; &&p<0.1906, &&&p<0.0002; &&&&p<0.0001: Statistical difference when compared Static with the *Shear-Stress* Exosome.

Osteocyte-like cells showed dependency of both Notch and Wnt/β-Catenin siganling

Both signaling pathways were previously listed being important in mature osteoblasts and osteocytes. The **Fig. 6a-f** shows positive gene expression of Jagged 1 and 2, of the Notch1-4 family, while the **Fig. 7a** brings important panorama of β-Catenin involvement in osteocyte-like cells. Later, we also investigated the hypothesis that **e**xosomes were cellular structures able to carry these molecules, and the **Fig. 7b-c** shows low levels of phospho-β-Catenin (S368) and phospho-Connexin 43. Complimentarily, osteoblasts challenged with VSMCs conditioned medium show high levels of β-Catenin expression in both VSMCs conditions **(Fig. 7 d-g)**. A complete panorama of Notch and Wnt/β-Catenin siganling members is delivered at **(Fig. S4)**.

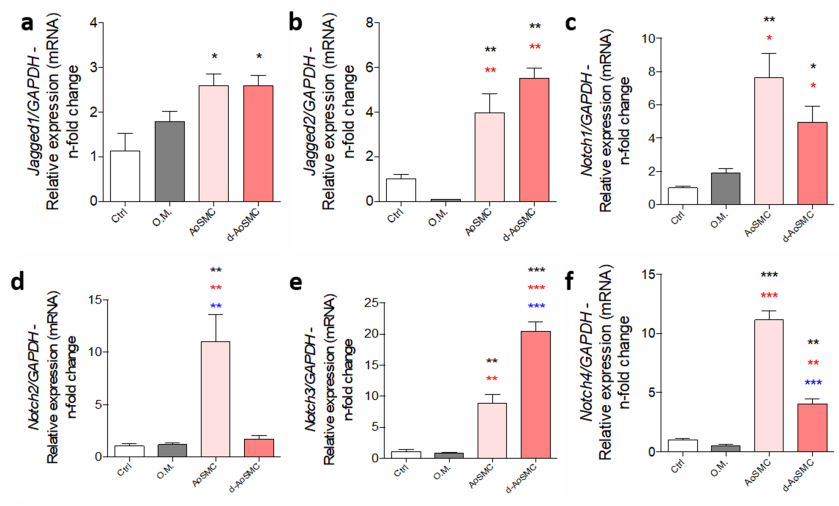

Fig.6. VSMCs-conditioned medium promotes reprogramming of Notch signaling in osteocyte-like cells. After 28 days of treatment with conditioned medium by endothelial cells (the medium was changed every 3 days to maintain the treatment properties), Osteoblasts were collected in TriZOL for RNA extraction and cDNA synthesis that was used in real-time PCR for investigate genes involved with the Notch pathway: **a)** Jagged1, **b)** Jagged2, **c)** Notch1, **d)** Notch2, **e-)** Notch3 and **f-)** Notch4. The expression results were normalizing by GAPDH, a housekeepig gene. *p<0.05; **p<0.1906, ***p<0.0002: Significant statistical difference when compared to control. *p<0.05; **p<0.1906, ***p<0.0002: Statistical difference when compared with the Osteogenic Medium. **p<0.1906; ***p<0.0002: Statistical difference when compared Static and *Shear-Stress*.

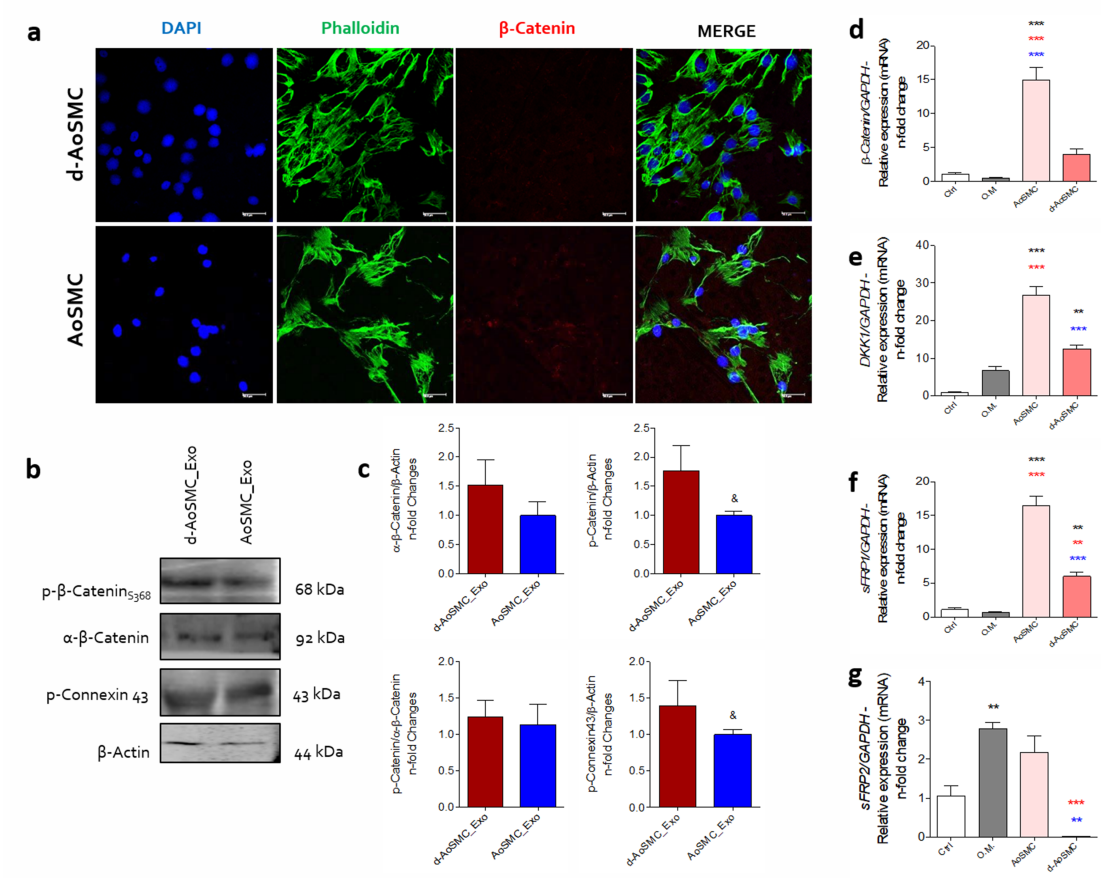

Figure 7: β-Catenin pathway seems being a constituve signaling in osteocytes. AoSMC were grown on coverslips and after 72 hrs under experimental conditions were fixed and labeled for β-Catenin **(a)**. The medium was collected and after extraction, exonsomes were lysed and p-β-Catenin, β-Catenin and p-Conx43 investigated for protein content by Western Blotting **(b-c)**. Osteoblasts, which received the conditioned medium for 28 days were collected in TriZOL to investigate the expression of β-Catenin **(d)**, DKK1 **(e)**, sFRP1 **(f)** and sFRP2 **(g)**. &p<0.05: Statistical difference when compared Static with the *Shear-Stress* Exosome. **p<0.1906, ***p<0.0002: Significant statistical difference when compared to control. **p<0.1906, ***p<0.0002: Statistical difference when compared with the Osteogenic Medium. **p<0.1906; ***p<0.0002: Statistical difference when compared Static and *Shear-Stress*.

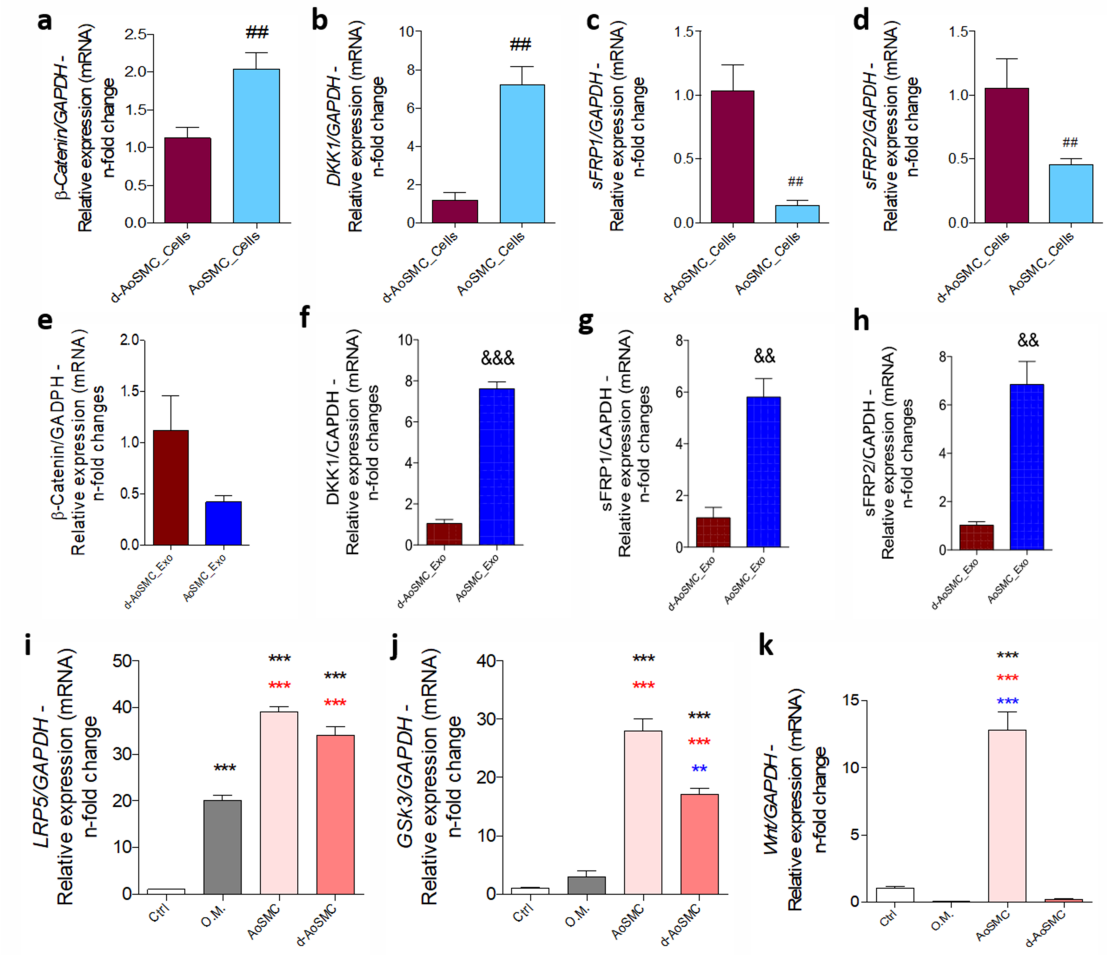

Figure S4: Complementary analysis of β-Catenin signaling. After the experimental periods AoSMC (Statico or *Shear-Stress*), Exosomes (Static or *Shear-Stress*) and osteoblasts were harvested in TriZOL to further evaluate the expression of genes involved in the B-Catenin pathway. B-Catenin, DKK1, sFRP1 and sFRP2 were evaluated in AoSMC **(a-d)** and Exossomos **(e-h)**. Osteoblasts were evaluated for: LRP5, GSK3 and Wnt **(i-k)**. The expression results were normalizing by GAPDH, a housekeeping gene. ##p<0.1906: Statistical difference when compared Static and *Shear-Stress* AoSMC. &&p<0.1906, &&&p<0.0002: Statistical difference when compared Static with the *Shear-Stress* Exosome. ***p<0.0002: Significant statistical difference when compared to control. ***p<0.0002: Statistical difference when compared with the Osteogenic Medium. **p<0.1906; ***p<0.0002: Statistical difference when compared Static and *Shear-Stress*.

Mineralizing osteocytes was also investigated

Extracellular matrix-related metabolism must be considered in functional osteocytes, mainly because the constitutive changes on osteoid matrix surrounding them. Since ATP is critical in the hydroxyapatite crystal growth, they were evaluated. Importantly, VSMCs-released exosomes carry high levels of ATP in both cultures, it being higher in shear-stressed VSMCs **(Fig. 8a)**. Therafter, genes related with mineral homeostasis were also investigated, Fetuin-A, NPP1 and TNAP genes **(Fig.8b-d; Fig.S5a-**

d). Additionally, classical ALP, BSP, Osteocalcin and Osteopontin genes were also positively regulated in osteocytes **(Fig.8e-h)**.

The remodeling of the organic fraction of the matrix was also investigated, we have shown high profile of collagen 1a1 and MMP2 genes **(Fig.9a-b)**. However, in spite of high levels of TIMP1, TIMP2 and RECK **(Fig.9d-f)**, we observed an increase in the activity of MMP2 **(Fig.9g-i)** as measured by zymography technology. This suggested ECM remodeling provokes cell morphology changes by rearranging cytoskeleton and it was investigated by evaluating genes related with cell adhesion Integrin-β3, FAK, Src and Cofilin, which they were highly expressed in those osteoblasts **(Fig. S6a-d)**.

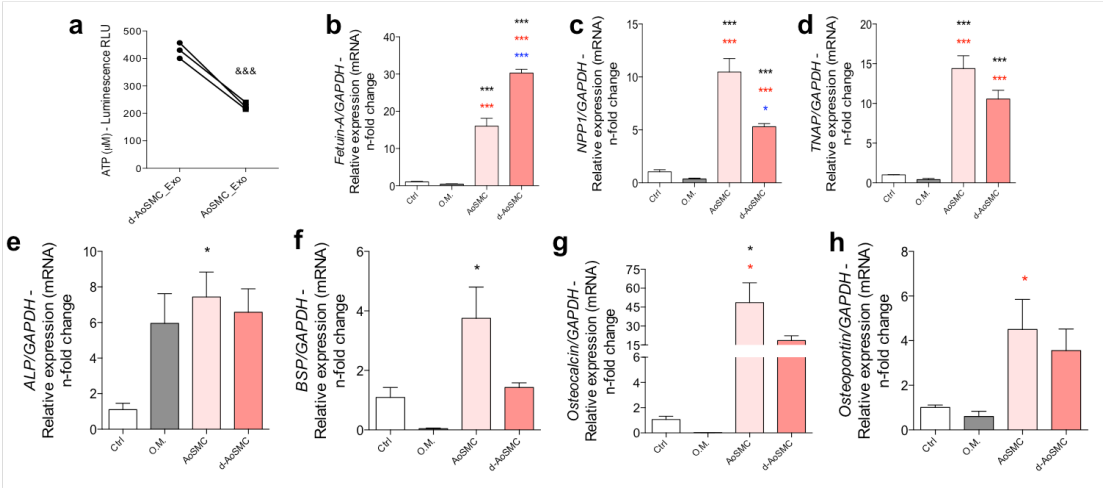

Fig.8. Mineral metabolism in osteocyte-like cells. After conditioning the culture medium was collected for isolation of Exosomes, these samples were evaluated for concentration of ATP that can be loaded **(a)**, the same medium was used to treat Osteoblast. After 28 days of treatment with media conditioned by primary endothelial cells, Osteoblasts were collected in TriZOL and after extraction of RNA and cDNA synthesis the expression Fetuin-A, NPP1, TNAP, ALP, BSP, Osteocalcin, Osteopontin **(b-h)**. The expression results were normalizing by GAPDH. &&&p<0.0002: Statistical difference when compared Static with the *Shear-Stress* Exosome. *p<0.05; **p<0.1906, ***p<0.0002: Significant statistical difference when compared to control. *p<0.05; **p<0.1906, ***p<0.0002: Statistical difference when compared with the Osteogenic Medium. *p<0.05; **p<0.1906; ***p<0.0002: Statistical difference when compared Static and *Shear-Stress*.

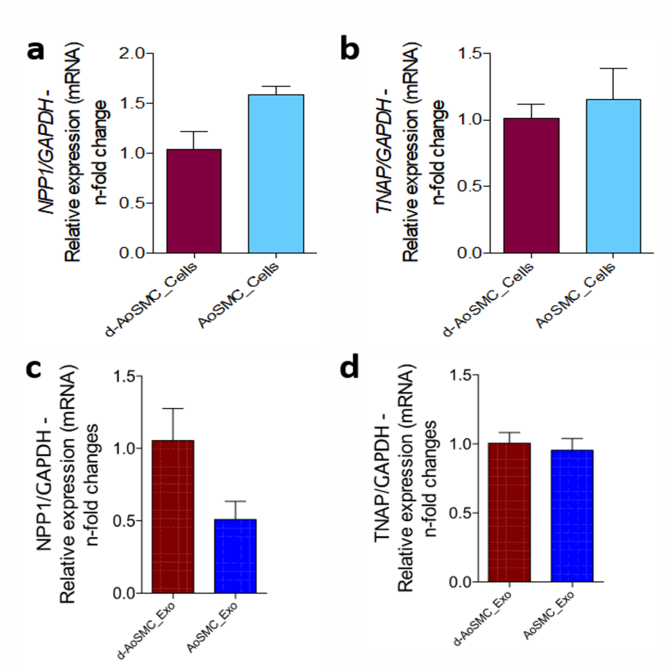

Figure S5: NPP1 and TNAP mRNA in VSMCs and their released exossomes. After 3 days under Experimental conditions the cells were collected in TriZOL, the medium was collected and Exossomos were isolated and submitted to RNA extraction with TriZOL. The expression of NPP1 and TNAP in cells and exosomes were evaluated **(a-d)**. The expression results were normalizing by GAPDH, a housekeeping gene.

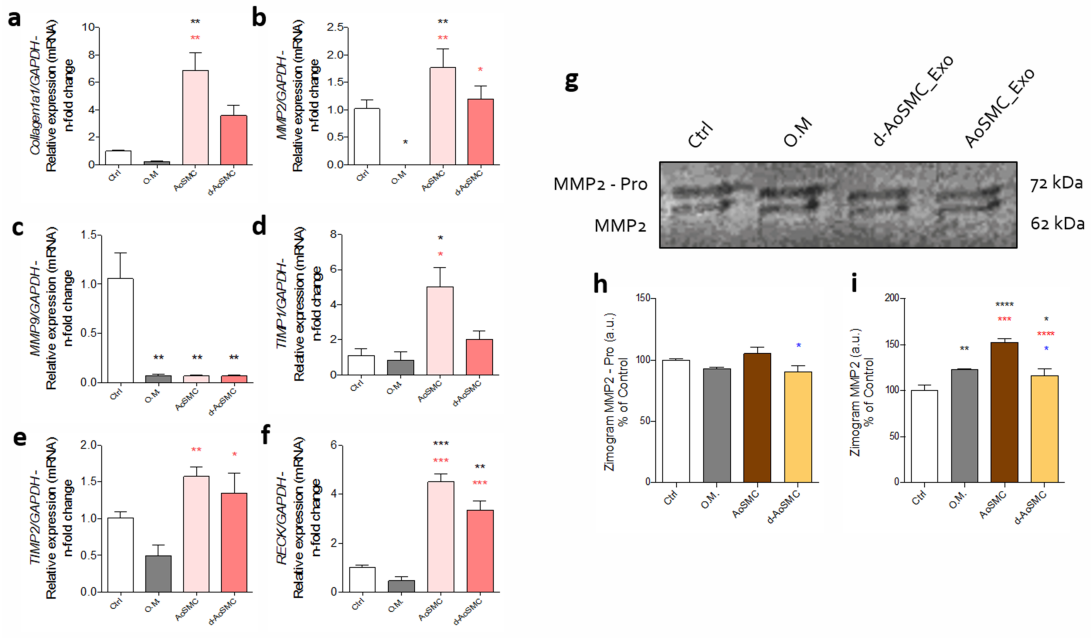

Fig.9. Remodeling of the organic fraction of the matrix was also investigated. The cells were harvested in TriZOL to provide mRNA isolation and further cDNA synthesis. The genes involved with ECM remodeling was evaluated by qPCR, as follows: **a)** Collagen1a1, **b)** MMP2, **c)** MMP9, **d)** TIMP1, **e)** TIMP2 and **f)** RECK. MMP's activities were evaluated by performing zymography technology **(g-h)**. The expression results were normalizing by GAPDH, a housekeeping gene. *p<0.05; **p<0.1906, ***p<0.0002:

Significant statistical difference when compared to control. *p<0.05; **p<0.1906, ***p<0.0002; ****p<0.0001: Statistical difference when compared with the Osteogenic Medium. *p<0.05: Statistical difference when compared Static and *Shear-Stress*.

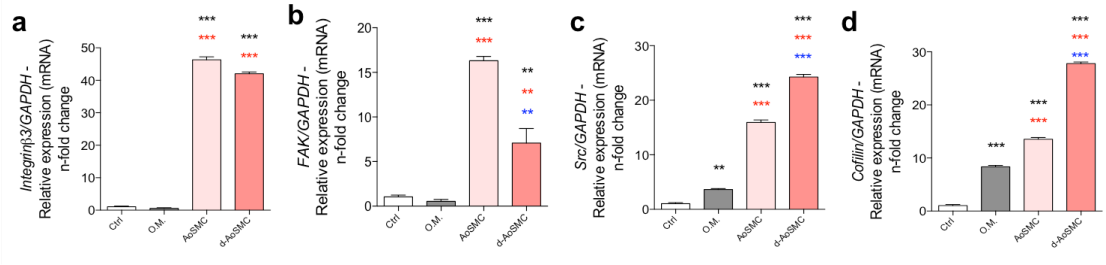

Figure S6: Osteoblast adhesion signaling. After 28 days of treatment with the different media conditioned by primary cells, osteoblasts were collected in TriZOL and after extraction of RNA and cDNA synthesis the expression of genes involved with the cell adhesion pathway was performed: **a-)** Integrin-β1, **b-)** Src and **c-)** FAK, besides a marker of cellular cytoskeleton remodeling: Cofilin **(d)**. For normalization effect, the expression results were considered from the expression values of the reference gene: GAPDH. **p<0.1906, ***p<0.0002: Significant statistical difference when compared to control. **p<0.1906, ***p<0.0002: Statistical difference when compared with the Osteogenic Medium. **p<0.1906; ***p<0.0002: Statistical difference when compared Static and *Shear-Stress*.

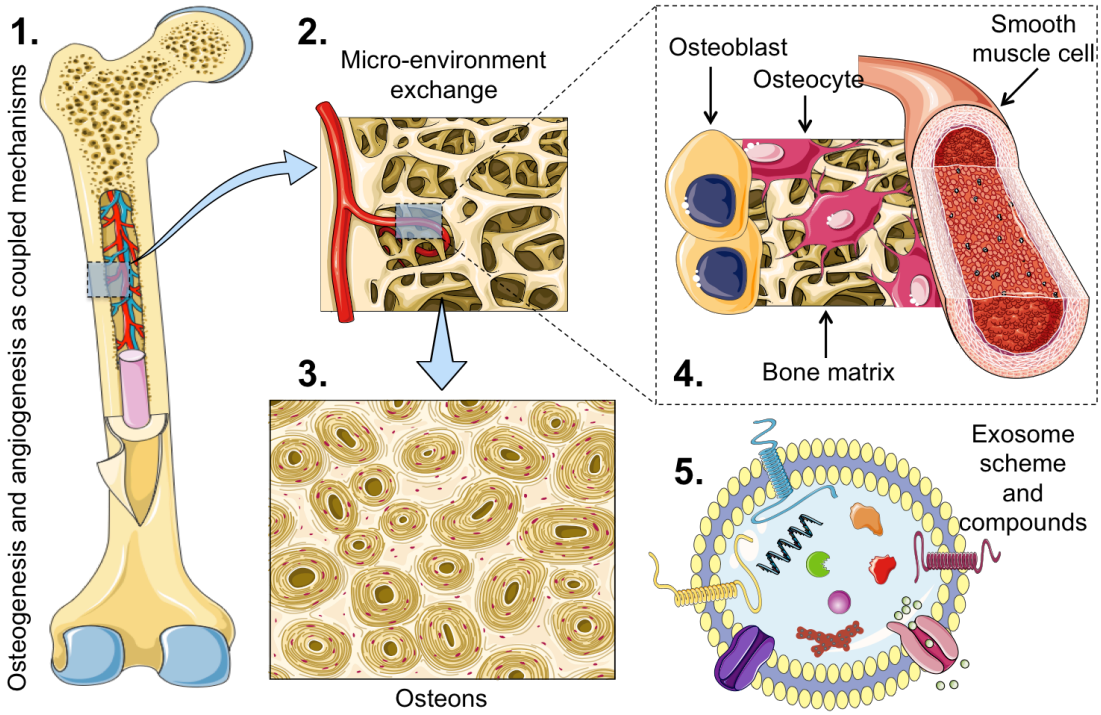

Figure 11: Schematization of the representative findings found in this study.

DISCUSSION

Understanding mechanisms involving the biology of bone remodeling through the paracrine action of the endothelial tissue will open new perspectives to comprehend the

biology of fractures healing and loss of bone tissue. Over the last years, it has been discussed about the importance of the network of vessels and capillaries in assist the bone health for guaranteining its homeostasis during the extracellular matrix remodeling [1,8,22,23]. Most recently, elegant studies have described this fine coupling between endothelial cells and bone cells triggers a set of molecular cascades able to drive osteoblast differentiation and osteogenesis. Although some progress has been made on identifying the effect of endothelial cells on bone health, very scarces are the findings reporting the relevance of Vascular Smooth Muscle Cells (VSMCs, or AoSMC) on this scenario. Here, we have gathered enough data to explain the importance of VSMCs on promoting osteocytogenesis, as well better investigating the relevance of the shear stress on this biological process. Additionally, this study is very interesting within bone biology field once osteocyte is not so far comprehended in full maybe because their position embedded into compact bone tissue and in vitro strategies bring new perspectives on elucidating still opened questions into bone biology area, considering osteocytes under spot.

In this study we have considered imput knowlwdge whether mechanosignaling in VSMCs were able to potencialize their effect on osteoblast-osteocyte transition and obtain gain on this comprehension within osteocytes biology. This is important to state that bone is under constant and dynamic forces which are already known to guarantee the dynamic bone remodeling and health, and osteocytes are known as important mechanosensors and play pivotal role in bone remodeling once because they are the main postnatal source of sclerostin and RANKL, two regulators of osteoblast and osteoclast function in vertebrates [24] and these findings open the discussion supporting the combat of osteoporosis with aerobic exercises [25].

Our data elucidate the relevance of shear-stress on modulating VSMCs paracrine signaling and their effect on already known osteocyte signaling. Firstly, we have reported there is no significances of shear-stressed VSMCs on obtaing osteocyte-like cells morphology, reinforcing that both condition where VSMCs were subjected promote osteoblast-osteocyte transition, since both conditions lead to the expression of classical osteocyte markers such as mir23a, Dmp1, Sost, GP38, and FGF23 genes. However, significant changes were shown in triggering osteocyte signaling and expressing bone remodeling pathways, such as the maintainence of TGF-ß signaling in the osteocyte responding to unshear-stressed VSMCs and this signaling cuminates with the constitutive

expression of Osterix, a gene required for the maturation of osteoblast in a stage preliminar to osteocyte transition [26].

The inactivation of Osterix in mice causes defects in the osteocyte maturation and function [26]. Here, the function of the acquired osteocytes obtained in response to paracrine signaling of VSMCs by investigating already described genes related with. Although both VSMCs released repertories promote the activation of SHH signaling in osteocytes, which could be involved with the star-shaped morphology of the cells as discussed previously [27], only static VSMC guarantess the significant over expression of RANKL (>10fold-changes higher) and we associated this difference with to the higher CD63 positive cells and consequently relasing a higher number of exosomes delivering molecular cargo to maintain the function of those osteocytes, as clarly shown in the Fig.5, and it seems being dependent of ß-catenin/Wnt signaling. Additionally, osteocyte functional is also shown by considering mineralizing function, both maintain high levels of biomarkers of mineralizing markers. Important, it seems that unshear-stressed VSMCs promote a higher expression of osteocalcin in obtained osteocytes which open the possibility of these cells contribute with well-described importance on energy metabolism.

Altogether, our data reinforces that VSMCs are able to contribute with osteoblast-osteocyte transition, where the static condition of VSMCs guarantees higher expression of osteocyte functions biomarkers.

METHODS

Antibodies: The following antibodies were purchased from: β-Catenin (6B3) Rabbit mAb #9582, Phospho-β-Catenin (Ser33/37/Thr41) Antibody #9561, Phospho-Connexin 43 (Ser368) Antibody #3511 (Cell Signalling, Danvers, MA, USA), β-Actin Antibody sc-47778 (Santa Cruz Biotechnology, Dallas, Texas, USA).

Cell culture: all cells were maintained at 37°C and at 5% CO_2 atmosphere and 95% humidity. Cells were daily evaluated for morphological variability, color of the culture medium, etc. **1.) Osteoblastic cells:** For differentiation we used human osteoblasts (HOEL) obtained through joint work with the School of Dentistry of Bauru, FOB-USP, and maintained in our cell bank. During growth, they were maintained and grown in Dulbecco's Modified Eagle Medium (DMEM, Low glucose) containing antibiotics (100 U/mL penicillin, 100 mg/mL streptomycin) and 10% Bovine Fetal Serum (SFB, Nutricell,

Campinas, SP) , Brazil). **2.) Endothelial Cells:** Endothelial cells, HCAEC and HUVEC, were maintained in Endothelial Cell Basal Medium-2 (EBM-2) medium supplemented with 0.5 mL of Epidermal Growth Factor (hEGF), 0.5 mL of Hydrocortisone, 0.5 mL of Gentamicin Sulfate Amphotericin B (GA-1000), 2.0 mL Bovine Brain Extract (BBE), 10 mL Fetal Bovine Serum (FBS), 0.5 mL Ascorbic Acid and antibiotics (100 U/mL penicillin, 100 mg/mL streptomycin). The cells, medium and the trophic factors were obtained together with LONZA; Muscle Cells: Already the smooth muscle cell of aortic origin was maintained in adequate medium - Smooth Muscle Cell Basal Medium (SmBM) supplemented with 0.5 mL Insulin, 1.0 mL Human Fibroblast Growth Factor B (hFGF-B), 0.5 mL Gentamicin Sulfate Amphotericin B (GA-1000), 25 mL Fetal Bovine Serum (FBS), 0.5 mL Epidermal Growth Factor (hEGF) and antibiotics (100 U/mL penicillin, 100 mg/mL streptomycin). Cells and factors were obtained along with LONZA.

***Shear-Stress* and Collection of Conditioned Medium:** The cells were cultured in appropriate medium until they reached semi-confluence (90%), in culture plates 100, prepared by sterilization under UV light for 15 minutes. Then the medium was replaced with DMEM medium supplemented with 1% antibiotic and 1% FBS. The semi-confluent layers were subjected to *Shear-Stress* (using orbital shaker) for 72 h under a humid atmosphere with 5% CO_2 at 37°C, as previously described by Rodríguez and González, de la Paz et al. The rotation was determined using the maximum stress formula: $\tau max = a\sqrt{\rho\eta(2\pi f)^3}$ so that the rotation frequency is within the physiological arterial pressure (6-40 dynes/cm), mimicking the mechanical forces encountered by blood flow[28–30]. At the end, conditioned medium was collected, centrifuged and stored for further analysis. As a control the medium used was conditioned by cells that were maintained static (no rotation) during the culture, under the same culture conditions.

Osteogenic induction: For induction of osteoblast differentiation, we treated Osteoblasts with conventional medium in the control group and Bovine Fetal Serum reduced to 1%. As a positive control, we used classical methodology in the differentiation literature, where β-Glycerophosphate (10 mM) + Dexamethasone (0.03 g/mL) + Ascorbic Acid (50 µg/mL), components purchased together with Sigma- Aldrich. Additional groups were tested, where Osteoblasts were treated with conditioned medium by Endothelial and Muscle Cells under Static and *Shear-Stress* conditions. The cells were kept in the

greenhouse for 28 days, the respective medium being exchanged every 3 days to maintain the biological properties of the study.

In Vitro Mineralization Analysis - Alizarin RedS: Cells were plated and maintained exactly as detailed above. After 28 days of treatment, in vitro mineralization was measured by the ability of calcium incorporation to the matrix synthesized by osteoblasts through Alizarina RedS labeling. The culture medium was gently sucked and washed with PBS. Then the PBS was sucked out and 0.5 ml of 10% Formalin was added for cell attachment. The plate was held in that solution for 30 minutes at room temperature. After this period Formalin was sucked and Alizarin solution added (1%) and the plate incubated in the dark for 45 minutes. After this time, the wells were washed with PBS, plate was photographed under an inverted microscope (Zeiss, Germany).

Matrix metalloproteinase activities: Osteoblast cultures were treated as detailed previously when the conditioned medium was collected. The gelatinolytic activities of the samples were evaluated by solving the sample from cell culture supernatants, and SDS-PAGE was performed on gels containing 0.1% gelatin and 10% polyacrylamide. Samples, pre-mixed with loading buffer (2% SDS and 0.1% bromophenol blue), were electrophoresed. After electrophoresis, the gels were washed in 2% Triton X-100 and immersed in 50 mM Tris-HCl buffer (pH 7.6), 200 mM NaCl and 10 mM CaCl 2 for 18 hours at 37˚C. (1:4:5 vol/vol/vol) and decolorized with acetic acid/methanol/water (1:2:7 vol.) were mixed with 0.5% Coomassie Blue G-250 in acetic acid[31].

Sample preparation for qPCR: For collection of samples for qPCR, after 28 days of treatment, 3 for Endothelial cells or Exosome isolation, the TriZOL (500 µL) was added. RNA samples were quantitated using plate reader (SYNERGY-HTX multi-mode reader, Biotek, USA). The cDNA synthesis using the High-Capacity cDNA Reverse Transcription Kit. Applied Biosystems (2.0 µL of 10 X RT Buffer, 0.8 µL 25 X dNTP Mix (100 mM), 2.0 µL 10 X RT Randon Primers, 1.0 µL MultiScribleTM Reverse Transcriptase, 4.2 µL Nuclease-Free H2O). After this process the material was collected and sample was stored in -80˚C freezer.

Table 1. Expression primers sequences and PCR cycle conditions.

Gene	Primer	5'-3' Sequence	Reactions Condicition

BMPr1	Forward	catattaggcgtgtgccaaaaa	95°C - 15s; 60°C - 30s; 72°C - 30s
	Reverse	gcttgtgcttgctgtcgttc	
BMPr2	Forward	atttgcagcacagacggatatt	95°C - 15s; 60°C - 30s; 72°C - 30s
	Reverse	gacactgaaaatctgagccttct	
BMP2	Forward	cccagcgtgaaagaggagac	95°C - 15s; 60°C - 30s; 72°C - 30s
	Reverse	ccatggtcgacctttaggag	
BMP7	Forward	actgtgaggggagtgtgc	95°C - 15s; 60°C - 30s; 72°C - 30s
	Reverse	cgaagtagaggacggagatgg	
SMAD2	Forward	gccgccagttgtgaagagac	95°C - 15s; 60°C - 30s; 72°C - 30s
	Reverse	tggagacgaccatcaagagacc	
SMAD3	Forward	gctgacacggagacacatcg	95°C - 15s; 60°C - 30s; 72°C - 30s
	Reverse	agcctcaaagccctggttg	
SMAD4	Forward	ctttgagggacagccatcgt	95°C - 15s; 60°C - 30s; 72°C - 30s
	Reverse	gccacagaaatgttgggaaa	
SMAD5	Forward	gtaaaacgacggccagttttcatggtgaatactaagactggttt	95°C - 15s; 60°C - 30s; 72°C - 30s
	Reverse	ttcaatgtaagctcacagtatctgtactc	
SMAD6	Forward	tactctcggctgtctcctc	95°C - 15s; 60°C - 30s; 72°C - 30s
	Reverse	gagttggtagcctccgtttc	
SMAD7	Forward	gctgaaacaggggaacga	95°C - 15s; 60°C - 30s; 72°C - 30s
	Reverse	agtatgccaccacgcacca	
TGFβ1	Forward	caacgaaatctatgacaagttcaagcag	95°C - 15s; 60°C - 30s; 72°C - 30s
	Reverse	cttctcggagctctgatgtg	
RUNX2	Forward	ccgtccatccactctaccac	95°C - 15s; 60°C - 30s; 72°C - 30s
	Reverse	atgaaatgcttgggaactgc	
OSTERIX	Forward	ccaggcaacactcctactcc	95°C - 15s; 60°C - 30s; 72°C - 30s
	Reverse	gccttgccatacaccttgc	
RANKL	Forward	agggactccatccaagaagg	95°C - 15s; 60°C - 30s; 72°C - 30s
	Reverse	gcagtttctgttctattattcaggtg	
SOST	Forward	gcgttcaagaatgatgccacg	95°C - 15s; 60°C - 30s; 72°C - 30s
	Reverse	gctgtactcggacacgtctttgg	
DMP1	Forward	cagtgaggatgaggcagaca	95°C - 15s; 60°C - 30s; 72°C - 30s
	Reverse	tcgatcgctcctggtactct	
FGF23	Forward	tgagcgtcctcagagcctat	95°C - 15s; 60°C - 30s; 72°C - 30s
	Reverse	ttgtggatctgcaggtggta	
FGFr1	Forward	ctgggtagcaacgtggagtt	95°C - 15s; 60°C - 30s; 72°C - 30s
	Reverse	accatgcaggagatgaggaa	
FGFr2	Forward	ggaaaagaacggcagtaaat	95°C - 15s; 60°C - 30s;

	Reverse	gtagtctggggaagctgtaaa	72°C - 30s
FGFr3	Forward	gggcttcttcctgttcatcc	95°C - 15s; 60°C - 30s; 72°C - 30s
	Reverse	agggacacctgtcgcttga	
FGFr4	Forward	agatgctcaaagacaacgcct	95°C - 15s; 60°C - 30s; 72°C - 30s
	Reverse	cgcacttccacgatcacgta	
PTCH	Forward	gggtcctcgcttacaaactc	95°C - 15s; 60°C - 30s; 72°C - 30s
	Reverse	atgatgccatctgcgtctac	
SUFU	Forward	gagggcgaagtaatttgtgg	95°C - 15s; 60°C - 30s; 72°C - 30s
	Reverse	agccctccttctgagtgctt	
SHH	Forward	caccgagcagtggatatgtg	95°C - 15s; 60°C - 30s; 72°C - 30s
	Reverse	agtggccaggagtgaaactg	
miR23a	Forward	ccggctggggttcctg	95°C - 15s; 60°C - 30s; 72°C - 30s
	Reverse	ggtcggttggaaatccctggc	
miR17	Forward	tcagaataatgtcaaagtgcttacagtgcagg	95°C - 15s; 60°C - 30s; 72°C - 30s
	Reverse	gtcaccataatgctacaagtgccttcactc	
LRP5	Forward	aagggtgctgtgtactggac	95°C - 15s; 60°C - 30s; 72°C - 30s
	Reverse	agaagagaacttacgggac	
β-Catenin	Forward	gcgtggacaatggctactcaag	95°C - 15s; 60°C - 30s; 72°C - 30s
	Reverse	gtcattgcatactgcccgtcaa	
GSK3	Forward	gactaaggtcttccgacccc	95°C - 15s; 60°C - 30s; 72°C - 30s
	Reverse	ttagcatctgacgctgctgt	
DKK1	Forward	ccttggatgggtattccaga	95°C - 15s; 60°C - 30s; 72°C - 30s
	Reverse	cctgaggcacagtctgatga	
sFRP1	Forward	cggccagcgagtacgactacgtgagc	95°C - 15s; 60°C - 30s; 72°C - 30s
	Reverse	gcatctcgggccagatagaagccgaag	
sFRP2	Forward	ctcgctgctgctgctcttc	95°C - 15s; 60°C - 30s; 72°C - 30s
	Reverse	ggcttcacatacctttggag	
CD9	Forward	tttaaaagtgcagccggaga	95°C - 15s; 60°C - 30s; 72°C - 30s
	Reverse	gcgccgatgatgtggaattt	
CD63	Forward	tgatgccgtggaaagcagat	95°C - 15s; 60°C - 30s; 72°C - 30s
	Reverse	agtcaagcgtctcgtggaag	
CD81	Forward	gcggtggaaggaggaatgaa	95°C - 15s; 60°C - 30s; 72°C - 30s
	Reverse	agccccctggattatggtct	
Fetuin A	Forward	gaattccccgctcatcctgttct	95°C - 15s; 60°C - 30s; 72°C - 30s
	Reverse	cgtggaaatcgcagtctcct	

TNAP	Forward	tttataaggcggcgggggtg	95°C - 15s; 60°C - 30s; 72°C - 30s
	Reverse	agcccagagatgcaatcgac	
NPP1	Forward	tttgccgattgaggattttc	95°C - 15s; 60°C - 30s; 72°C - 30s
	Reverse	ccactgacgacattgacacc	
SMPD3	Forward	gcctatcactgttaccccaac	95°C - 15s; 60°C - 30s; 72°C - 30s
	Reverse	gacgattctttggtcctgagg	
GP38	Forward	gggaacgatgtggaaggtgt	95°C - 15s; 60°C - 30s; 72°C - 30s
	Reverse	gctctttagggcgagtacct	
VEGF	Forward	tgcagattatgcggatcaaacc	95°C - 15s; 60°C - 30s; 72°C - 30s
	Reverse	tgcattcacatttgttgtgctgtag	
VEGFr	Forward	caggcccagtttctgccatt	95°C - 15s; 60°C - 30s; 72°C - 30s
	Reverse	ttccagctcagcgtggtcgta	
Notch1	Forward	ggaagtgtgaagcggccaatg	95°C - 15s; 60°C - 30s; 72°C - 30s
	Reverse	atagtctgccacgcctctgc	
Notch2	Forward	tgtcgagatggctatgaaccctg	95°C - 15s; 60°C - 30s; 72°C - 30s
	Reverse	gcagcggttcttctcacagg	
Nocth3	Forward	tgtctgccagagttcagtggtg	95°C - 15s; 60°C - 30s; 72°C - 30s
	Reverse	aggagcagaggaagcgtccatc	
Notch4	Forward	ttgtcctccctccttctgttcc	95°C - 15s; 60°C - 30s; 72°C - 30s
	Reverse	agaagtcccgaagctggcac	
Jag1	Forward	tgcctctgtgagaccaactg	95°C - 15s; 60°C - 30s; 72°C - 30s
	Reverse	gttgggtcctgaataccccct	
Jag2	Forward	gtggcaagaactgctccgtg	95°C - 15s; 60°C - 30s; 72°C - 30s
	Reverse	tgcctctgtgagaccaactg	
BMP9	Forward	agaacgtgaaggtggatttcc	95°C - 15s; 60°C - 30s; 72°C - 30s
	Reverse	cgcacaatgttgg acgctg	
HIF1α	Forward	cataaagtctgcaacatggaaggt	95°C - 15s; 60°C - 30s; 72°C - 30s
	Reverse	atttgatgggtgaggaatgggtt	
HIF1β	Forward	caagccccttgagaagtcag	95°C - 15s; 60°C - 30s; 72°C - 30s
	Reverse	gaggggctaggccactattc	
Integrin β1	Forward	gccgcgcggaaaagatgaa	95°C - 15s; 60°C - 30s; 72°C - 30s
	Reverse	tgctgttccttttgctacggt	
Src	Forward	caacacagagggagactggt	95°C - 15s; 60°C - 30s; 72°C - 30s
	Reverse	agcttcttcatgacctgggc	
FAK	Forward	tcagctcagcacaatcctgg	95°C - 15s; 60°C - 30s;

	Reverse	ctgaagcttgacaccctcgt	72°C - 30s
Cofilin	Forward	tgtgcggctcctactaaacg	95°C - 15s; 60°C - 30s;
	Reverse	tccttgacctcctcgtagca	72°C - 30s
AKT	Forward	cagcgcggcccgaaggac	95°C - 15s; 60°C - 30s;
	Reverse	gacgctacagcgctcctctc	72°C - 30s
ERK	Forward	aacaggctctggcccacccat	95°C - 15s; 60°C - 30s;
	Reverse	gcagcgcctcccttgctaga	72°C - 30s
JNK	Forward	aaaggtggtgttttgttcccaggt	95°C - 15s; 60°C - 30s;
	Reverse	tgatgatggatgctgagagccattg	72°C - 30s
p38	Forward	gagaactgcggttactta	95°C - 15s; 60°C - 30s;
	Reverse	atgggtcaccagatacacat	72°C - 30s
GAPDH	Forward	gactcatgaccacagtccatgc	95°C - 15s; 60°C - 30s;
	Reverse	agaggcagggatgatgttctg	72°C - 30s

Confocal microscopy: For confocal microscopy analysis, the cells were cultured in glass coverslips placed in the peripheral ring of the culture and subjected to Shear-Stress and Static. The cells were then washed with PBS, fixed in PBS-paraformaldehyde (4% v/v), permeabilized in PBS containing 0.2% Triton-X 100 and 1% BSA at 37°C for 1 h stained with the appropriate specific primary antibodies, at the concentration recommended by the manufacturer. Then, after washing with PBS to remove the primary antibody, for fluorescence analysis, cells were stained with anti-rabbit or mouse IgA Alexa Fluor 594 antibody for 1 h. For actin cytoskeletal rearrangement analyzes, the cells were incubated for 40 minutes at 4 mg/ml, Alexa Fluor 488-labeled phalloidin (Invitrogen/Molecular Probes, USA). Cells were washed and mounted on glass slides using Fluorosield with DAPI (Sigma) and then viewed on an inverted laser scanning confocal microscope (Leica TCS SP_5).

Scanning Electron Microscopy (SEM): Cells were plated on modified plates under coverslips and after 72 hours under static or *Shear-Stress* experimental conditions were fixed with 2.5% glutaraldehyde in 0.1 M phosphate buffer pH 7, 3 for 24 h. After the dehydration steps, they were sent to the critical point, assembled in the "stubs" and then metalized. SEM analyzes were performed on a Quanta 200-FEI Company scanning electron microscope at an acceleration voltage of 12.5 kV.

Isolation of exosomes: For analysis and exosomes the culture medium was supplemented with extracellular vesicles Free Fetal Serum, Extraction was performed in ultracentrifugation of 30,000 g for 18 hours [32]. Cells remained for 72 hours with EV-free, Static or *Shear-Stress*, after which the medium was withdrawn and used to isolate exosomes with the Total Cell Isolation Kit (Invitrogen - Thermo Fisher Scientific , Vilnius, Lithuania) according to the manufacturer's instructions.

Nanoparticle screening (NTA): NanoSight NS300 (Amesbury, UK) was used to determine the size and concentration of exosomes. After isolation of the EVs from the culture medium the exosomes were resuspended in PBS for analysis. In all analyzes the samples were diluted 1:1000 in PBS filtered in a 0.22 µm pore filter. Each experiment was performed at 25°C in triplicate with acquisition of five 1 minute videos. The values of concentration, mean size and particle distribution (D10, D50 and D90) were obtained in each of the experiments using the corresponding software (NanoSight software version 2.3).

Zeta potential A: The Malvern Zetasizer Nano ZS instrument was used to measure zeta potential. Exosomes were first diluted 100 times in PBS and pH was adjusted to neutral pH (7.4 - 7.7) with standard NaOH (0.1 N). Samples were then loaded into a pre-rinsed folded capillary cell, and measurements were taken at 25°C for all samples using an applied voltage of 150V of three measurements were made for each sample.

Transmission Electron Microscopy: For Transmission Microscopy analysis, the Exosomes were added to the forked coated nickel cadmium for 2 hours. After this period the grid was washed in PBS and the material was fixed in 2% paraformaldehyde for 15 minutes. Then the grades were washed again with PBS and treated with 2.5% glutaraldehyde fixative powder for 10 minutes. The material was washed in deionized water and contrasted with 2% uranyl acetate for 15 minutes. Finally, the sample was incubated with 0.13% methylcellulose and 0.4% uranyl acetate for 10 minutes. The excess liquid was removed and after drying the material was analyzed in Fei Company's Tecnai Spirit Electronic Transmission Microscope.

Analysis of exosome markers by flow cytometry: After isolation the exosomes were coupled to Latex Beads (ThermoFisher) overnight. The next day the samples were

centrifuged and washed with 1M Glycine. The exosomes were distributed in tubes for cytometry and incubated with BD Biosciences antibodies, with respective fluorochromes: anti-CD9, anti-CD63 and anti-CD81 for 30 minutes in the dark. After that time they were centrifuged at 400g for 5 minutes and the pellet resuspended in PBS. For the design of the standards, the control tubes were incubated with isotype antibodies specific for each fluorochrome in each test performed. Measurements, 10,000 events for each sample were required on a FACSCantoTM II flow cytometer (BD Biosciences) with FACSDIVA software (BD Biosciences). The results were analyzed in FLOWJO software, version vX.10x6 (FlowJo, LLC, Ashland, OR).

ATP Assay: For ATP dosing the Exosomes were boiled at 45°C for 2 minutes and dosing was performed according to the instructions of the CellTiter-Glo® Luminescent Cell Viability Assay Technical Bulletin Kit (Promega, Madison, Wisconsin, USA).

Western blotting performance: Isolated exosomes were lysed on ice for 2 h with Lysis Cocktail (Tris [tris (hydroxymethyl) aminomethane] -HCl [pH 7.4], 1% Tween 20, 0.25% sodium deoxycholate, 150 mM NaCl, 1 mM EGTA (ethylene glycol tetracetic acid), 1 mM O-Vanadate, 1 mM NaF and protease inhibitors [1 µg/mL aprotinin, 10 µg/mL leucine, and 1 mM 4- (2-amino -ethyl) -benzolsulfonyl-fluoro-hydrochloride]). After being lysed, the samples were sonicated (1 pulse per second; SONICS Vibra-Cell, USA). The protein extracts were clarified and the protein concentration determined by the Lowry method[33–35]. Protein extracts were resolved by SDS-PAGE (12%) and transferred to PVDF membranes (Bio-Rad, Hercules, CA, USA). Immediately, the membranes were blocked with bovine serum albumin (2.5%) in Tris buffered saline (TBS) -20 (0.05%) and incubated overnight at 4°C with appropriate primary antibody. After washing in TBS-Tween 20 (0.05%), the membranes were incubated with secondary antibodies conjugates for 1 hour. Subsequently, Enhancement Chemiluminescence (ECL, Pierce, USA) was used to detect the bands.

Statistical analysis: The results were represented as mean ± standard deviation (SD). They were verified using One-Way ANOVA (non-parametric) with Tukey's post test in order to compare all pairs of groups. In this case, with $p<0.05$ considered statistically significant and $p<0.0001$ considered highly significant. The software used was GraphPad

Prism 6. To determine the number of stellate cells, counting the number of nuclei in the area recorded in the photo was performed, followed by statistical analysis.

REFERENCES

1. Kusumbe, A. P., Ramasamy, S. K. & Adams, R. H. Corrigendum: Coupling of angiogenesis and osteogenesis by a specific vessel subtype in bone. *Nature* **513,** 574 (2014).
2. Kusumbe, A. P. & Adams, R. H. Osteoclast progenitors promote bone vascularization and osteogenesis. *Nature medicine* **20,** 1238–1240 (2014).
3. Romeo, S. G. *et al.* Endothelial proteolytic activity and interaction with non-resorbing osteoclasts mediate bone elongation. *Nature cell biology* **21,** 430–441 (2019).
4. Yang, Y.-Q. *et al.* The role of vascular endothelial growth factor in ossification. *International Journal of Oral Science* **4,** 64–68 (2012).
5. Beamer, B., Hettrich, C. & Lane, J. Vascular endothelial growth factor: an essential component of angiogenesis and fracture healing. *HSS journal : the musculoskeletal journal of Hospital for Special Surgery* **6,** 85–94 (2010).
6. Ramasamy, S. K., Kusumbe, A. P. & Adams, R. H. Regulation of tissue morphogenesis by endothelial cell-derived signals. *Trends in cell biology* **25,** 148–157 (2015).
7. Sivaraj, K. K. & Adams, R. H. Blood vessel formation and function in bone. *Development (Cambridge, England)* **143,** 2706–2715 (2016).
8. Ramasamy, S. K. *et al.* Blood flow controls bone vascular function and osteogenesis. *Nature communications* **7,** 13601 (2016).
9. Saran, U., Gemini Piperni, S. & Chatterjee, S. Role of angiogenesis in bone repair. *Archives of biochemistry and biophysics* **561,** 109–117 (2014).
10. Kuczera, P., Adamczak, M. & Wiecek, A. Fibroblast Growth Factor-23-A Potential Uremic Toxin. *Toxins* **8,** (2016).
11. Sakurai, A. *et al.* Chronological immunolocalization of sclerostin and FGF23 in the mouse metaphyseal trabecular and cortical bone. *Biomedical research (Tokyo, Japan)* **38,** 257–267 (2017).
12. Yamamoto, H. *et al.* Posttranslational processing of FGF23 in osteocytes during the osteoblast to osteocyte transition. *Bone* **84,** 120–130 (2016).
13. Mattinzoli, D. *et al.* FGF23-regulated production of Fetuin-A (AHSG) in osteocytes. *Bone* **83,** 35–47 (2016).
14. Bonewald, L. F. The amazing osteocyte. *Journal of bone and mineral research : the official journal of the American Society for Bone and Mineral Research* **26,** 229–238 (2011).
15. Xiong, J. *et al.* Matrix-embedded cells control osteoclast formation. *Nature medicine* **17,** 1235–1241 (2011).
16. Kramer, I. *et al.* Osteocyte Wnt/beta-catenin signaling is required for normal bone homeostasis. *Molecular and cellular biology* **30,** 3071–3085 (2010).
17. Dallas, S. L., Prideaux, M. & Bonewald, L. F. The osteocyte: an endocrine cell ... and more. *Endocrine reviews* **34,** 658–690 (2013).
18. van Oers, R. F. M., Wang, H. & Bacabac, R. G. Osteocyte shape and mechanical loading. *Current osteoporosis reports* **13,** 61–66 (2015).
19. Shah, K. M., Orton, P., Mani, N., Wilkinson, J. M. & Gartland, A. Osteocyte physiology and response to fluid shear stress are impaired following exposure to cobalt and chromium: Implications for bone health following joint replacement. *Journal of orthopaedic research : official publication of the Orthopaedic Research Society* (2016). doi:10.1002/jor.23449
20. Davenport, C. *et al.* RANKL promotes osteoblastic activity in vascular smooth muscle cells by upregulating endothelial BMP-2 release. *The international journal of biochemistry & cell biology* **77,** 171–180 (2016).
21. Bezerra, M. C., Carvalho, J. F., Prokopowitsch, A. S. & Pereira, R. M. R. RANK, RANKL and osteoprotegerin in arthritic bone loss. *Brazilian journal of medical and biological research = Revista brasileira de pesquisas medicas e biologicas* **38,** 161–170 (2005).
22. Langen, U. H. *et al.* Cell-matrix signals specify bone endothelial cells during developmental osteogenesis. *Nature cell biology* **19,** 189–201 (2017).
23. Ramasamy, S. K. *et al.* Regulation of Hematopoiesis and Osteogenesis by Blood Vessel-Derived

Signals. *Annual review of cell and developmental biology* **32,** 649–675 (2016).
24. Xiong, J. *et al.* Osteocytes, not Osteoblasts or Lining Cells, are the Main Source of the RANKL Required for Osteoclast Formation in Remodeling Bone. *PloS one* **10,** e0138189 (2015).
25. Pagnotti, G. M. *et al.* Combating osteoporosis and obesity with exercise: leveraging cell mechanosensitivity. *Nature reviews. Endocrinology* **15,** 339–355 (2019).
26. Zhou, X. *et al.* Multiple functions of Osterix are required for bone growth and homeostasis in postnatal mice. *Proceedings of the National Academy of Sciences of the United States of America* **107,** 12919–12924 (2010).
27. Marumoto, A. *et al.* Phosphoproteome analysis reveals a critical role for hedgehog signalling in osteoblast morphological transitions. *Bone* **103,** 55–63 (2017).
28. dela Paz, N. G., Walshe, T. E., Leach, L. L., Saint-Geniez, M. & D'Amore, P. A. Role of shear-stress-induced VEGF expression in endothelial cell survival. *Journal of cell science* **125,** 831–843 (2012).
29. da Silva, R. A. *et al.* The role of triiodothyronine hormone and mechanically-stressed endothelial cell paracrine signalling synergism in gene reprogramming during hBMSC-stimulated osteogenic phenotype in vitro. *Molecular and cellular endocrinology* **478,** 151–167 (2018).
30. da Silva, R. A. *et al.* Laminar shear stress-provoked cytoskeletal changes are mediated by epigenetic reprogramming of TIMP1 in human primary smooth muscle cells. *Journal of cellular physiology* **234,** 6382–6396 (2019).
31. Lefebvre, V., Peeters-Joris, C. & Vaes, G. Production of gelatin-degrading matrix metalloproteinases ('type IV collagenases') and inhibitors by articular chondrocytes during their dedifferentiation by serial subcultures and under stimulation by interleukin-1 and tumor necrosis factor alpha. *Biochimica et biophysica acta* **1094,** 8–18 (1991).
32. Mehdiani, A. *et al.* An innovative method for exosome quantification and size measurement. *Journal of visualized experiments : JoVE* 50974 (2015). doi:10.3791/50974
33. LOWRY, E. C., BLUMBERG, J. M., RHEA, R. L. & RANSON, J. P. Serum levels of orally administered penicillin. *United States Armed Forces medical journal* **2,** 265–270 (1951).
34. LOWRY, O. H., ROSEBROUGH, N. J., FARR, A. L. & RANDALL, R. J. Protein measurement with the Folin phenol reagent. *The Journal of biological chemistry* **193,** 265–275 (1951).
35. Hartree, E. F. Determination of protein: a modification of the Lowry method that gives a linear photometric response. *Analytical biochemistry* **48,** 422–427 (1972).

CAPÍTULO 5

Shear-stress melhora a capacidade das células endoteliais em estimular o fenótipo osteogênico

Manuscrito em preparação

MATERIAIS E MÉTODOS

Cultivo e Obtenção de células: todas as células foram mantidas à 37°C e à atmosfera de 5% de CO_2 e 95% de umidade. As células eram diariamente avaliadas quanto a variabilidade morfológica, cor do meio de cultivo, etc. Células Osteoblásticas: Para diferenciação utilizamos Osteoblastos humanos (HOEL) obtidas através de trabalhos conjuntos com a Faculdade de Odontologia de Bauru, FOB-USP, e mantidas em nosso banco de células. Durante o crescimento foram mantidas e cultivadas em meio Dulbecco's Modified Eagle Medium (DMEM, Low glucose) contendo antibióticos (100 U/mL penicilina, 100 mg/mL estreptomicina) e foi adicionado 10% Soro Fetal Bovino (SFB, Nutricell, Campinas, SP, Brasil). Células Endoteliais: As células endoteliais, HCAEC e HUVEC, foram mantidas em meio Endothelial Cell Basal Medium-2 (EBM-2) suplementado com 0,5 mL de Epidermal Growth Factor (hEGF), 0,5 mL de Hidrocortisone, 0,5 mL de Gentamicin Sulfate Amphotericin B (GA- 1000), 2,0 mL de Bovine Brain Extract (BBE), 10 mL de Fetal Bovine Serum (FBS), 0,5 mL de Ascorbic Acid e antibióticos (100 U/mL penicilina, 100 mg/mL estreptomicina). As células, meio e os fatores tróficos, foram obtidos junto a LONZA;

Tensão de Cisalhamento (Shear-stress) e coleta do meio condicionado: As células foram cultivadas em meio apropriado até atingirem a semi-confluência (90%), em placas de petri modificadas, preparadas através de esterilização sob luz UV durante 15 minutos. Em seguida o meio foi substituído por meio DMEM suplementado com 1% de antibiótico e 10% SFB. As camadas semi-confluentes foram submetidas à tensão cisalhamento (Shear-stress) (utilizando agitador orbital) durante 72 h (Rodríguez e González, 2014; de la Paz et al. 2012). A rotação foi determinada utilizando a formula de tensão máxima: $\tau max=a\sqrt{\rho\eta(2\pi f)3}$ para que a frequência de rotação fique dentro do valor da tensão

arterial fisiológica (6-40 ~ dynes/cm), mimetizando as forças mecânicas encontradas pelo fluxo sanguíneo (dela Paz et al. 2012). Ao término, o meio condicionado foi coletado, centrifugado e armazenado a -80°C para posterior analise. Como controle o meio utilizado foi o condicionado por células que foram mantidas estáticas (sem rotação) durante a cultura, nas mesmas condições de cultivo.

Indução Osteogênica: Como controle positivo fizemos uso de metodologia clássica na literatura de diferenciação, onde foi adicionado ß-Glicerofosfato (10 mM) + Dexametasona (0,03 g/mL) + Ácido Ascórbico (50 µg/mL) (Sigma-Aldrich). As células foram mantidas em estufa por 28 dias, sendo o meio respectivo a cada grupo trocado a cada 3 dias, para manter as propriedades biológicas do estudo.

Análise de diferenciação celular - Fosfatase Alcalina (ALP): As células foram plaqueadas em densidade de 8.104 células/mL em placas de 24 poços e, em semi-confluência, tratadas com os diferentes meios como já descrito anteriormente, respeitando os diferentes grupos avaliados. A diferenciação celular foi medida pela atividade da enzima Fosfatase Alcalina (ALP), aqui avaliada por um método de coloração. A solução foi preparada utilizando o kit Sigma-Aldrich (SIGMAFAST BCIP/NBT). Cabe destacar que esta metodologia foi praticada de acordo com as instruções do fabricante.

Zimografia: O meio de cultura condicionado foi centrifugado a 14000 rpm por 15 min e a concentração proteica determinada pelo método de Lowry (LOWRY et al. 1951). A atividade gelatinolítica das amostras foi avaliada pelo fracionamento das Metaloproteinases (MMP-2 e MMP-9) em gel de poliacrilamida 12% contendo 4% de gelatina. Após o fracionamento, as MMP's foram renaturadas em solução aquosa de Triton X-100 (2% m/v), incubados por 18 h em tampão de proteólise (Tris-$CaCl_2$) a 37°C e corados com solução corante de Coomassie Blue R- 250 0,05% por 3 h (Lefebvre et al. 1991).

Análise estatística: Os resultados foram representados como média ± desvio padrão (DP). Eles foram verificados utilizando One-Way ANOVA (não paramétrico) com pós teste de Tukey, para comparar todos os pares de grupos. Neste caso, com $p<0,05$ considerado estatisticamente significante e $p<0,0001$ considerado altamente significativo. O software utilizado foi GraphPad Prism 6. Para Contagem de partículas foi utilizado o Software

Image-J que determinou o número de pontos na área registrada em foto, e para a análise estatística os grupos foram padronizados pela porcentagem do controle. Para determinação do número de células estreladas, foi realizado contagem do número de núcleos na área registrada em foto, em seguida aplicada análise estatística.

RESULTADOS

Células endoteliais modulam a expressão de marcadores da diferenciação de Osteoblastos: Runx2 e Osterix genes

Após 72 horas em que as células endoteliais permaneceram em cultura condicionando o meio, estático ou Shear-Stress, este foi utilizado para tratar osteoblastos humanos por 28 dias. Ao final desse período investigamos o perfil de ativação de marcadores de diferenciação e componentes envolvidos com a homeostase de íons e mineralização da matriz extracelular. Nossos dados mostram que o uso do meio condicionado por HUVEC, independente da condição de cultura, promove ativação de transcritos envolvidos com o processo de adesão celular e que pode modular o rearranjo do citoesqueleto celular. Observamos significativo aumento de Integrina-b1, FAK, Src e Cofilina (**Fig.1e-h**). Além disso investigamos a expressão de Runx2 e Osterix (**Fig.1i-j**). Um outro importante marcador do processo de mineralização é a Fosfatase Alcalina (ALP), aqui investigada através da atividade enzimática (**Fig. 1a-d**) e expressão gênica (**Fig.1l**).

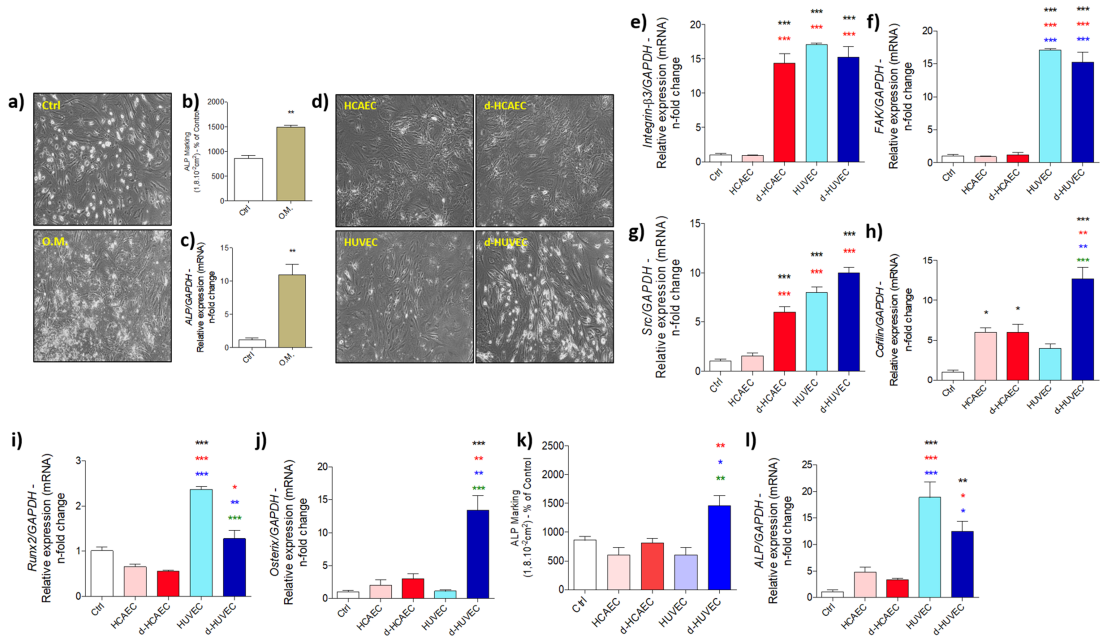

Figura 1. Meio condicionado por HUVEC modula marcadores da diferenciação de osteoblastos e mineralização da matrix. Após 72 horas sob o efeito do Shear-Stress ou em condição estático, o meio condicionado por células endoteliais (HUVEC e HCAEC) foi

coletado para tratar osteoblastos por 28 dias. Ao final, as células foram avaliadas quando ao perfil da atividade de Fosfatase Alcalina **(a-d, k)**. Além disso, as células foram coletadas em TriZOL para Extração de RNA e investigação da expressão de genes envolvidos com adesão celular: e) Integrina, **f)** FAK, **g)** Src e **h)** Cofilina. Outros marcadores envolvidos com o genótipo de diferenciação de osteoblastos foram avaliados: **i)** Runx2, **j)** Osterix e **l)** ALP. Como controle positivo do experimento, utilizamos o Meio Osteogênico (O.M.). Para normalização dos valores de expressão considerados o GAPDH como gene de referência. *p<0.0292 **p<0.0094; ***p<0.0010: Diferença estatística quando comparado ao grupo controle. *p<0.0292; **p<0.0094; ***p<0.0010: Diferença estatística quando comparado ao grupo HCAEC. *p<0.0292; **p<0.0094; ***p<0.0010: Diferença estatística quando comparado ao grupo d-HCAEC. **p<0.0094; ***p<0.0010: Diferença estatística quando comparada ao grupo HUVEC.

O processo de mineralização pode afetar a expressão de marcadores que controlam a homeostase de íons cálcio de fosfato, responsáveis por formar a porção mineralizada do tecido ósseo. Nesse sentido, avaliamos a expressão de osteocalcina, que esteve aumentada apenas no grupo HUVEC, enquanto os demais apresentavam valores menores de expressão quando comparado ao grupo controle (**Fig.2a**). Outros genes importantes foram considerados: BSP, NPP1 e TNAP que estavam aumentados nos grupos que receberam o meio condicionado por HUVEC (**Fig.2b-d**).

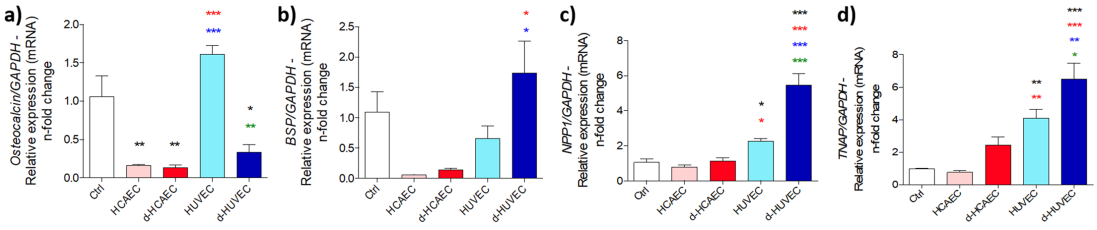

Figura 2. Efeito do meio condicionado por células endoteliais em marcadores da regulação da matriz extracelular em osteoblastos. Células endoteliais de artéria (HCAEC) e de veia (HUVEC) foram utilizadas para condicionar o meio de cultura em duas condições: Shear-Stress e Estático. Após 72 horas o meio foi coletado e utilizado para tratar osteoblastos. Ao final de 28 dias foi avaliada a expressão de Osteocalcina **(a),** Bone Sialoprotein – BSP **(b),** NPP1 **(c)** e TNAP **(d)**. GAPDH foi considerado gene endógeno para normalizar os valores de ΔΔCT. *p<0.0292 **p<0.0094; ***p<0.0010: Diferença estatística quando comparado ao grupo controle. *p<0.0292; **p<0.0094; ***p<0.0010: Diferença estatística quando comparado ao grupo HCAEC. *p<0.0292; **p<0.0094; ***p<0.0010: Diferença estatística quando comparado ao grupo d-HCAEC. *p<0.0292; **p<0.0094; ***p<0.0010: Diferença estatística quando comparada ao grupo HUVEC.

Em fase de diferenciação celular, osteoblastos ativam duas importantes vias de sinalização que modulam a translocação de fatores de transcrição para o núcleo. A expressão de TGF-b e BMP9 mostrou significativos níveis de expressão nos grupos HUVEC e d-HUVEC (**Fig. 3a-b**). Além disso os fatores de transcrição SMAD2, 3, 4, 5 e 7 aumentaram em grupos HUVEC, mas apresentaram comportamento antagônico nos grupos HCAEC (**Fig.3c-i**). Essas vias quando ativadas promovem a translocação de complexos SMAD2/3/4 e SMAD1/5/8/4 e que podem atuar modulando a expressão de Runx2 e Osterix.

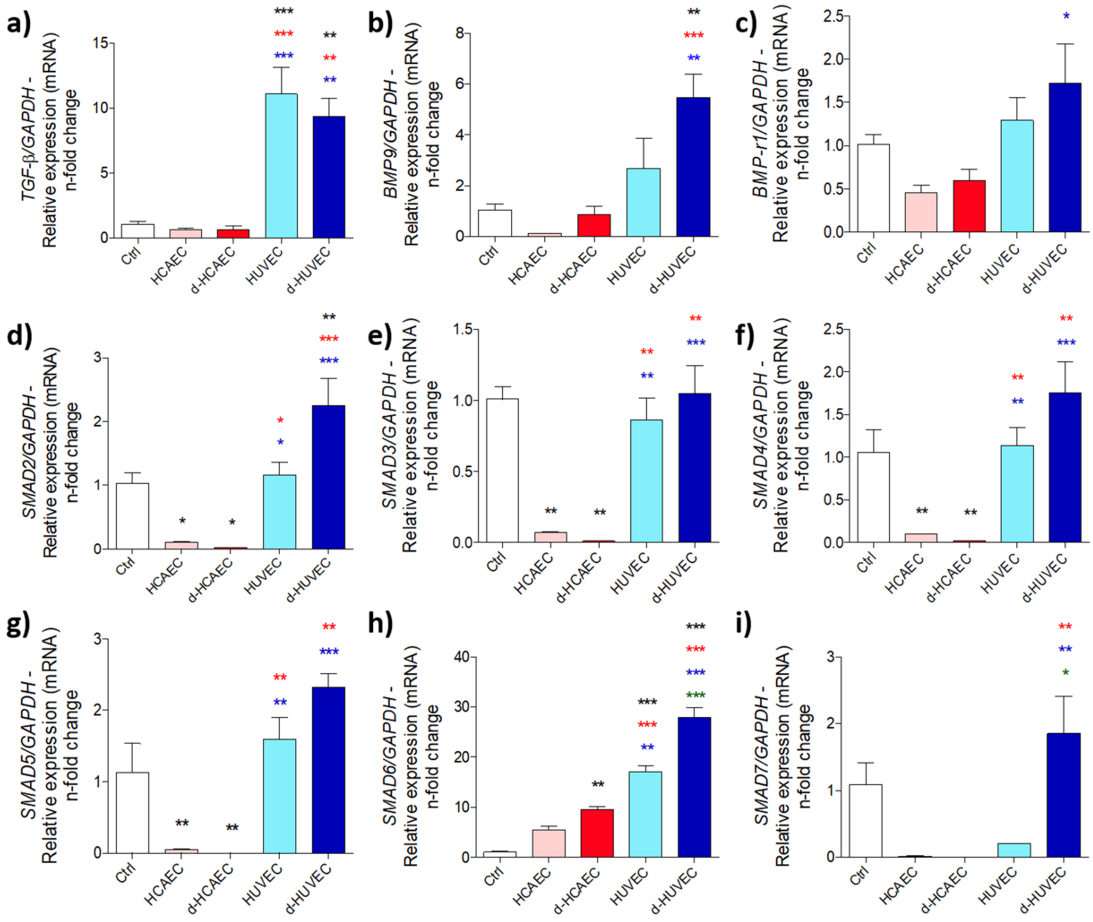

Fig.3. HUVEC ativa a expressão de genes envolvidos na via TGF-β em osteoblastos. Osteoblastos receberam o meio condicionado por HCAEC e HUVEC por 28 dias, ao final foram coletados para Extração de RNA, sintese de cDNA e análise de expressão gênica. Investigamos o perfil de expressão de TGF-β **(a)**, BMP9 **(b)**, receptor de BMP **(c)** e grupo de SMAD's que atuam como fatores de transcrição **(d-i)**. Os experimentos representam n = 3. Como marcador interno de expressão utilizamos GAPDH. *p<0.0292 **p<0.0094; ***p<0.0010: Diferença estatística quando comparado ao grupo controle. *p<0.0292; **p<0.0094; ***p<0.0010: Diferença estatística quando comparado ao grupo HCAEC. *p<0.0292; **p<0.0094; ***p<0.0010: Diferença estatística quando comparado ao grupo d-HCAEC. *p<0.0292; ***p<0.0010: Diferença estatística quando comparada ao grupo HUVEC.

Remodelamento da MEC de osteoblastos é modulado por células endoteliais

Para compreender o processo de remodelamento da ECM investigamos a expressão de alguns genes envolvidos no rearranjo da porção orgânica da matriz. Inicialmente, nossos dados mostram que o grupo HUVEC estimulou a expressão de Colágeno 1a1 nos osteoblastos (**Fig. 4a**). Além disso vimos diminuição na expressão gênica de Metaloproteinases de matriz (MMP2 e MMP9) (**Fig. 4b-c**), porem a atividade enzimática dessas proteases estavam ligeiramente aumentadas em todos os grupos que receberam meio condicionado por células endoteliais (**Fig. 4g-i**). Metaloproteinases são moduladas negativamente pelos inibidores teciduais (TIMPs) e RECK e, ao analisar esses genes nesse modelo biológico, vimos que TIMP1 e TIMP2 estavam moduladas negativamente no tratamento e RECK apresentou ligeiro aumento nos grupos HUVEC, mas sem significativa diferença quando comparado aos demais grupos.

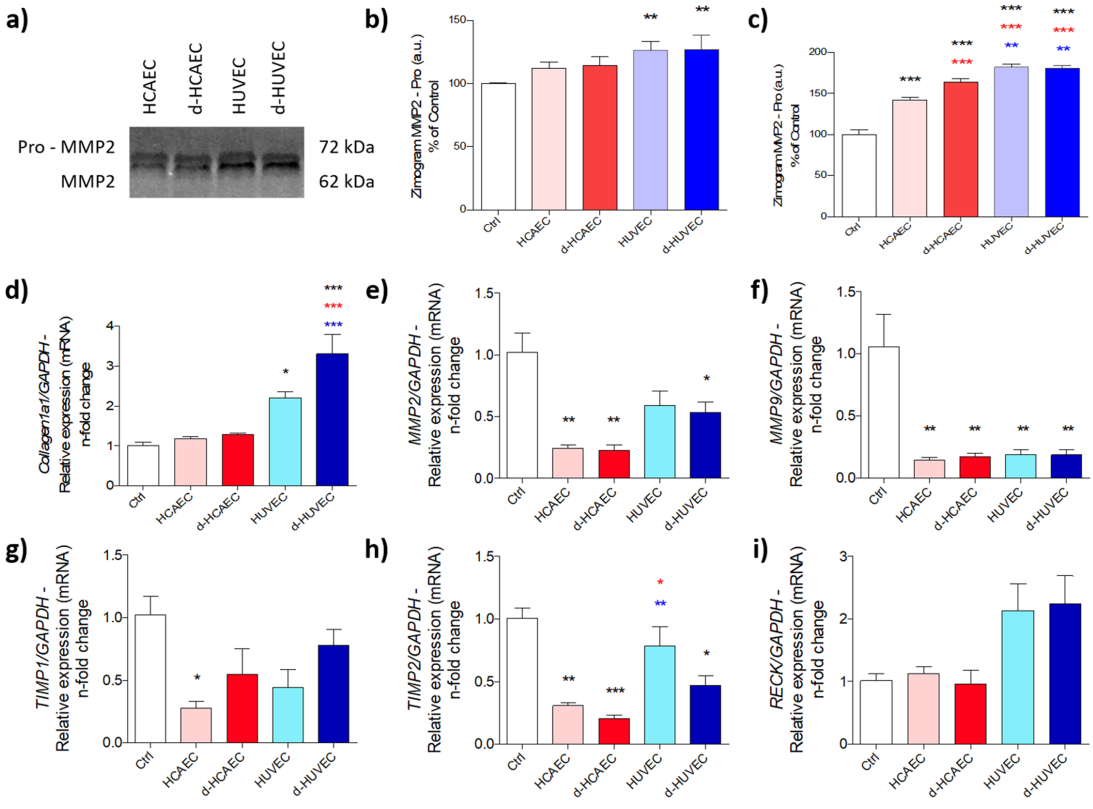

Figura 4. Expressão de genes envolvidos no remodelamento da matriz extracelular. Osteoblastos que receberam o meio condicionado por HUVEC e HCAEC foram coletados em TriZOL após 28 dias de tratamento. Foi avaliada a expressão de Colágeno 1a1, MMP2, MMP9, TIMP1, TIMP2 e RECK (a-f). Além disse, o meio foi coletado para investigar a atividade de Metaloproteinases potencialmente liberadas no meio de Osteoblastos (g-i). *p<0.0292 **p<0.0094; ***p<0.0010: Diferença estatística quando comparado ao grupo

controle. *p<0.0292; **p<0.0094; ***p<0.0010: Diferença estatística quando comparado ao grupo HCAEC. *p<0.0292; **p<0.0094; ***p<0.0010: Diferença estatística quando comparado ao grupo d-HCAEC. *p<0.0292; ***p<0.0010: Diferença estatística quando comparada ao grupo HUVEC.

Células endoteliais e osteoblastos: crosstalk necessário para homeostase do microambiente tecidual

Vários estudos mostram que no microambiente do osso existem vários tipos celulares em constante comunicação, e que esse processo permite a homeostase de formação e diferenciação de tecido. Nesse sentido, o crosstalk entre o tecido endotelial e o tecido ósseo é fundamental para que o osso desempenhe processos de remodelamento. Durante o acoplado processo de formação de vasos e tecido ósseo, células endoteliais levam ao tecido componentes como oxigênio e nutrientes, numa via de mão dupla osteoblastos promovem manutenção dos vasos a partir da liberação de Fator Indutor de Hipóxia (HIF) e Fator Endotelial de Crescimento Vascular (VEGF). Assim, decidimos também analisar o comportamento desses genes, onde dados mostram aumento desses marcadores em osteoblastos que receberam o meio condicionado por células endoteliais venosas (**Fig. 5**).

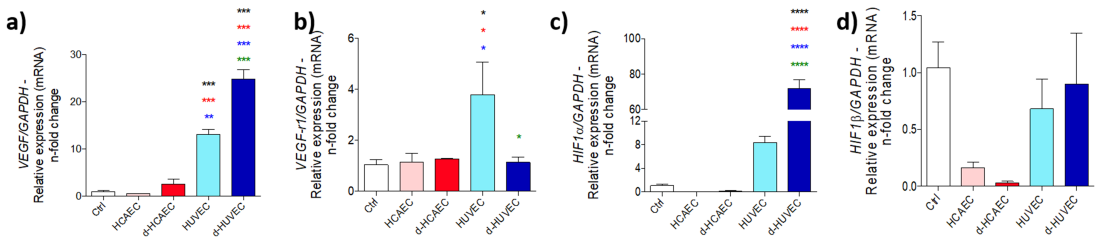

Fig.5. Indução da expressão de VEGF e HIF em osteoblastos desafiados por células endoteliais. Osteoblastos foram tratados por 28 dias com meio condicionado por células endoteliais, o meio foi trocado a cada 3 dias. A expressão gênica foi avaliada em PCR em tempo real e os valores de expressão avaliados por ΔΔCT. Investigamos os genes: a) VEGF, b) VEGF-r1, c) HIF-1α e d) HIF-1β. *p<0.0292 ***p<0.0010; ****p<0.0001: Diferença estatística quando comparado ao grupo controle. *p<0.0292; ***p<0.0010; ****p<0.0001: Diferença estatística quando comparado ao grupo HCAEC. *p<0.0292; **p<0.0094; ***p<0.0010; ****p<0.0001: Diferença estatística quando comparado ao grupo d-HCAEC. *p<0.0292; ***p<0.0010; ****p<0.0001: Diferença estatística quando comparada ao grupo HUVEC.

A super expressão de VEGF pelos osteoblastos fortemente sugerem um acoplamento necessário entre células edoteliais e osteoblastos, sendo que esta interação na direção da angiogênese do tecido ósseo tem sido pouco explorada, e certamente lança

a possibilidade de eventos co-estimuladores entre essas duas células no microambiente ósseo. Além disso, reforça eventos de angiogênese o aumento da expressão de HIF pelos osteoblastos. Em conjunto, esses eventos demonstram um importante repertório de interações celulares que devem ser explorados em condições patológicas, como na osteoporose, bem como em condições de reparo de injúrias que acometem o tecido ósseo, como traumas e ressecções de tumores.

Outra via que chama atenção no tecido ósseo é a via de de Sonic Hedgehog (Shh) [1–3], bastante discutida na ativação da transcrição de VEGF [4–7]. Assim, avaliamos também essa via no modelo proposto e nossos achados mostram que Shh (ligante) estavam diminuídas em todos os tratamentos quando comparados ao grupo controle (**Fig. 6a**), mas um resultado interessante foi o aumento da expressão de Ptchd1 e SUFU nos grupos HUVEC (**Fig. 6b-c**). Esses resultados demonstram que osteoblastos desafiados por meio condicionado pelas células endoteliais não são requeridos em manter expressão constitutiva de Shh, porém estas células mantém a via de Shh ativa, demonstrando aumento de seu receptor (PTCH1) e intermediário da via de sinalização com ativação de GLI (SUFU). Gli é um fator de transcrição que também contribui com a transcrição de VEGF [8, 9], sendo assim, um elo importante entre células ósseas e osteoblastos.

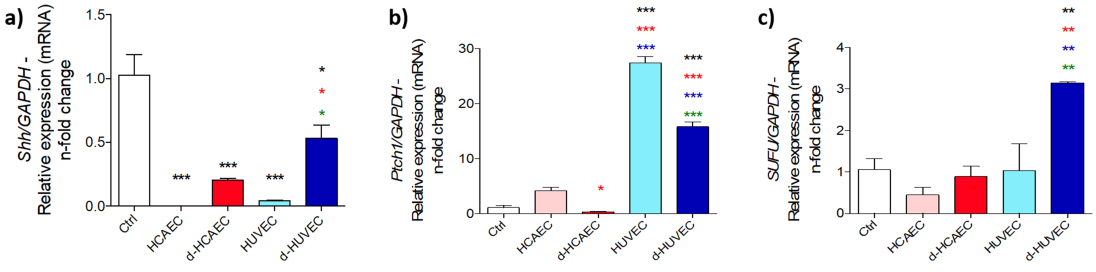

Fig.6. Efeito do *crosstalk* entre células endoteliais e osteoblastos na expressão da via de Sonic Hedgehog. Osteoblastos foram coletados em TriZOL para Extração de RNA, em seguida foi sintetizado o cDNA para Avaliação da expressão de Sonic Hedgehog (Shh), Patched (Ptch1) e SUFU (a-c). GAPDH foi considerado gene endógeno para normalizar os valores de ΔΔCT. *p<0.0292 **p<0.0094; ***p<0.0010: Diferença estatística quando comparado ao grupo controle. *p<0.0292; **p<0.0094; ***p<0.0010: Diferença estatística quando comparado ao grupo HCAEC. **p<0.0094; ***p<0.0010: Diferença estatística quando comparado ao grupo d-HCAEC. *p<0.0292; **p<0.0094; ***p<0.0010: Diferença estatística quando comparada ao grupo HUVEC.

Por fim, tem-se mostrado por trabalhos pioneiros na literatura de crosstalk entre células endoteliais e células ósseas a ativação da via de sinalização Notch [10–14].

Avaliamos esta via através da expressão de genes e detectamos que, de fato, estes genes estavam ativadas nas células que receberam o meio condicionado por HUVEC. Verificamos aumento da família de Notch 1, 2, 3 e 4 nas células que receberam o meio de HUVEC nas duas condições (estático e Shear-stress) (**Fig. 7a-f**). Destaca-se que estes resultados corroboram com estudos in vivo, onde esta interação foi relevada, creditando valor de validação ao modelo in vitro proposto aqui, no caminho de buscar o desenvolvimento de métodos alternativos ao uso de animais de experimentação.

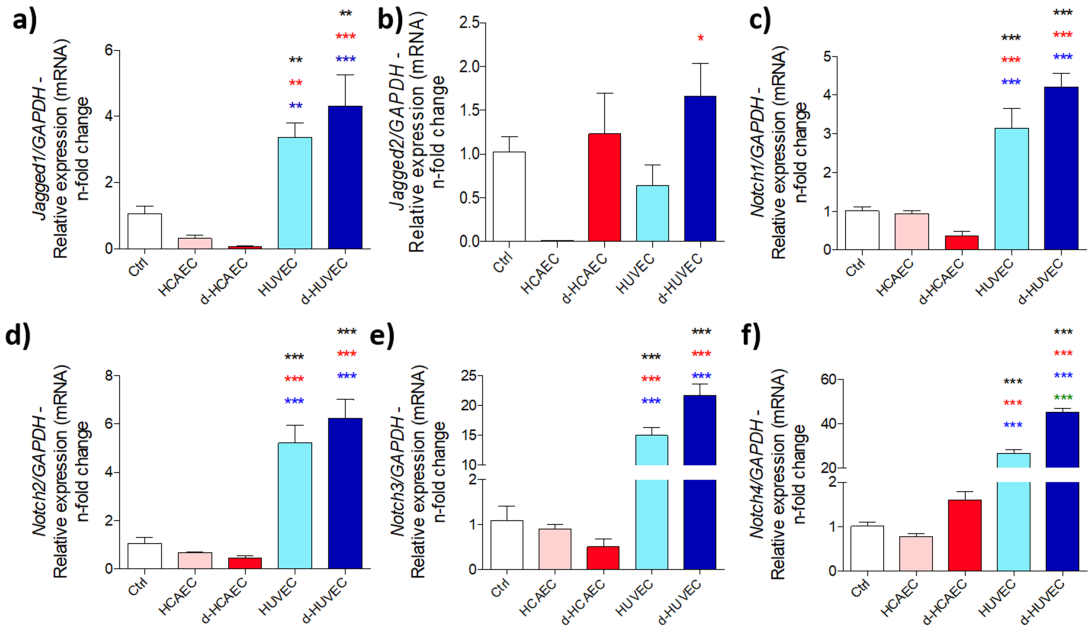

Fig.7. Expressão da via de Notch em osteoblastos desafiados com fatores tróficos liberados por células endoteliais. O meio condicionado foi utilizado para tratar osteoblastos, após 28 dias foi realizada coleta de RNA. Em equipamento de PCR em tempo real foi avaliada a expressão de Jagged, Jagged2, Notch1, Notch2, Notch3 e Notch4, (a-f). GAPDH foi considerado gene endógeno para normalizar os valores de ΔΔCT. **p<0.0094; ***p<0.0010: Diferença estatística quando comparado ao grupo controle. *p<0.0292; **p<0.0094; ***p<0.0010: Diferença estatística quando comparado ao grupo HCAEC. **p<0.0094; ***p<0.0010: Diferença estatística quando comparado ao grupo d-HCAEC. ***p<0.0010: Diferença estatística quando comparada ao grupo HUVEC.

REFERÊNCIAS

1. Kazmers NH, McKenzie JA, Shen TS, et al (2015) Hedgehog signaling mediates woven bone formation and vascularization during stress fracture healing. Bone 81:524–532. doi: 10.1016/j.bone.2015.09.002
2. Marumoto A, Milani R, da Silva RA, et al (2017) Phosphoproteome analysis reveals a critical role for hedgehog signalling in osteoblast morphological transitions. Bone 103:55–63. doi: 10.1016/j.bone.2017.06.012
3. Merchant JL, Ding L (2017) Hedgehog Signaling Links Chronic Inflammation to Gastric Cancer Precursor Lesions. Cellular and molecular gastroenterology and hepatology 3:201–210. doi: 10.1016/j.jcmgh.2017.01.004

4. Caradu C, Guy A, James C, et al (2018) Endogenous Sonic Hedgehog limits inflammation and angiogenesis in the ischemic skeletal muscle of mice. Cardiovascular research. doi: 10.1093/cvr/cvy017
5. Zhao Q, Shen X, Zhang W, et al (2012) Mice with increased angiogenesis and osteogenesis due to conditional activation of HIF pathway in osteoblasts are protected from ovariectomy induced bone loss. Bone 50:763–770. doi: 10.1016/j.bone.2011.12.003
6. Maes C, Carmeliet G, Schipani E (2012) Hypoxia-driven pathways in bone development, regeneration and disease. Nature reviews Rheumatology 8:358–366. doi: 10.1038/nrrheum.2012.36
7. Grosso A, Burger MG, Lunger A, et al (2017) It Takes Two to Tango: Coupling of Angiogenesis and Osteogenesis for Bone Regeneration. Frontiers in bioengineering and biotechnology 5:68. doi: 10.3389/fbioe.2017.00068
8. Sun Q, Bai J, Lv R (2016) Hedgehog/Gli1 signal pathway facilitates proliferation, invasion, and migration of cutaneous SCC through regulating VEGF. Tumour biology : the journal of the International Society for Oncodevelopmental Biology and Medicine. doi: 10.1007/s13277-016-5435-x
9. Zhang J, Fan J, Zeng X, et al (2021) Hedgehog signaling in gastrointestinal carcinogenesis and the gastrointestinal tumor microenvironment. Acta pharmaceutica Sinica B 11:609–620. doi: 10.1016/j.apsb.2020.10.022
10. le Noble F, le Noble J (2014) Bone biology: Vessels of rejuvenation. Nature 507:313–314. doi: 10.1038/nature13210
11. Ramasamy SK, Kusumbe AP, Schiller M, et al (2016) Blood flow controls bone vascular function and osteogenesis. Nature communications 7:13601. doi: 10.1038/ncomms13601
12. Chen S, Lee BH, Bae Y (2014) Notch signaling in skeletal stem cells. Calcified tissue international 94:68–77. doi: 10.1007/s00223-013-9773-z
13. Canalis E (2018) Notch in skeletal physiology and disease. Osteoporosis international : a journal established as result of cooperation between the European Foundation for Osteoporosis and the National Osteoporosis Foundation of the USA 29:2611–2621. doi: 10.1007/s00198-018-4694-3
14. Ramasamy SK, Kusumbe AP, Wang L, Adams RH (2014) Endothelial Notch activity promotes angiogenesis and osteogenesis in bone. Nature 507:376–380. doi: 10.1038/nature13146

CAPÍTULO 6

VSMCs-obatined EVs: cargo elucidation and effect on mesenchymal stem cells

Célio J.C. Fernandes, Gwenny M. Fuhler[2], Maikel P. Peppelenbosch[2], Bram van der Eerden[2]; Willian F. Zambuzzi[1]

Note: This part of the report brings partial data obtained during BEPE-FAPESP covering international training.

CONTEXTUALIZATION

Bone defects gaining prominence in the medical-dental area, mainly due to the increase in life expectancy of the population. Reconstructing the lost tissue is one of the great challenges for surgeons in the area, often requiring the application of a biomaterial that allows good functional tissue regeneration. In this area, previous osteosubstitutes are one of the most common and oldest forms of regenerative therapy. Despite their medical, social, and economic importance, there are few advances in terms of bioanalysis methodologies capable of ranking new therapies, although some advances have been made in the sense of knowing the biological events about the physiological mechanisms responsible for bone regeneration. In this sense, knowing the biological events that govern bone development represents an extremely significant step in the search for more effective therapies. We now know that bone development and regeneration is a complex event and that it requires sequentially intercellular signaling mechanisms, involving endothelium and bone cells 1,2. According to these authors, angiogenesis and osteogenesis are coupled physiological, but who are the signaling molecules involved in this scenario? What differential impact do the macro and microvasculature have on bone cells: osteoblasts? Are these preserved in bone defect regeneration mechanisms? These questions prompt the search for these biological markers.

BEPE PERIOD - BRAZIL AND THE NETHERLANDS

Prof. Peppelenbosch was the supervision of part of this set of data, which the workflow was initially proposed based on the data obtained in Brazil. Here, we have better addressed the loading of the EV's. Specifically, the possibility to stay abroad in an important center in EU, as Erasmus Medical Center is, was very important to better understand the crosstalk between cells, mainly better characterizing the those EV's released by Smooth muscle cells, which they are able to trigger osteogenic stimulus in osteoblastic cells. Indeed, the training period was also important to being in contact with different technologies, such as: **1.** Organoid Culture, **2.** Isolation and Characterization of extracellular vesicles of different body fluids (Blood, Urine and Pancreatic Juice) and **3.** CrisprCas-9 approach. In addition, this period was also important because Célio stayed in touch with another important professor in Holland working within bone field, Prof. Bram van der Eerden, who has proposed to validate our already obtained data in mesenchymal stem cells.

In fact, the biological model was newly performed in Holland and the main findings

confirmed on those cells, as it is presented also here. Of course, this purpose has promoted important gains to the student. This set of data has been better described to allow being submitted soon in a specialized journal.

MATERIAL AND METHODS

Antibodies: GeneTex: Anti-CD81 antibody [1D6] (GTX43505). Santa Cruz: GAPDH (SC51906); PTP1B (SC113259); β-Actin (SC77718). Cell Siganling: p-SHP1$_{Tyr536}$ #11318; p-Integrin-β3$_{Tyr773}$ #11060-1; FAK (#3285); p-Src$_{Tyr416}$ (#21135); Src (#21235); p-ERK$_{Thr202/Tyr204}$ (#43705); ERK (#46965); p-P38$_{Thr180/Tyr182}$ (#4511); p-JNK$_{Thr183/Tyr185}$ (#9255); p-STAT3$_{Ser727}$ (#9136); p-Rac1/cdc42$_{Ser71}$ (#2461); p-β-Catenin$_{Ser675}$ (#9567); p-STAT3$_{Tyr705}$ (#9145); p-JAK1$_{Tyr1034/1035}$ (3331). Abcam: Anti-TSG101 antibody [EPR7130(B)] (ab125011); Anti-Cofilin (phospho S3) antibody (ab12866); Anti-HOXA13 antibody (ab106503). SignalWay: PI3K (p85 alpha beta gamma) (ab-467/199/464). Thermo Fisher: p-FAK$_{Tyr397}$ (44625G). Antibodies: Anti-alkaline phosphatase (intestinal) Antibody (A36514)

Cell culture: all cells were maintained at 37°C and at 5% CO2 atmosphere and 95% humidity. Cells were daily evaluated for morphological variability, color of the culture medium, etc. ***Mesenchymal Stem Cells (MSC):*** For differentiation we used MSC, during growth, they were maintained and grown in Dulbecco's Modified Eagle Medium (DMEM) containing antibiotics (100 U/mL penicillin, 100 mg/mL streptomycin) and 10% Bovine Fetal Serum (SFB). ***Osteogenic induction:*** To induce osteoblast differentiation, medium (αMEM; Gibco BRL, Life Technologies) was supplemented with freshly added 10 mM β-glycerophosphate (Sigma-Aldrich) and 100 nM dexamethasone (Sigma-Aldrich) and replaced every 2 or 3 days. ***Endothelial Cells (HCAEC and HUVEC):*** Were maintained in Endothelial Cell Basal Medium-2 (EBM-2) medium supplemented with 0.5 mL of Epidermal Growth Factor (hEGF), 0.5 mL of Hydrocortisone, 0.5 mL of Gentamicin Sulfate Amphotericin B (GA-1000), 2.0 mL Bovine Brain Extract (BBE), 10 mL Fetal Bovine Serum (FBS), 0.5 mL Ascorbic Acid and antibiotics (100 U/mL penicillin, 100 mg/mL streptomycin). The cells, medium and the trophic factors were obtained together with LONZA. ***Smooth Muscle Cells:*** Already the smooth muscle cell of aortic origin was maintained in adequate medium - Smooth Muscle Cell Basal Medium (SmBM) supplemented with 0.5 mL Insulin, 1.0 mL Human Fibroblast Growth Factor B (hFGF-B), 0.5 mL Gentamicin Sulfate Amphotericin B (GA-1000), 25 mL Fetal Bovine Serum (FBS), 0.5 mL Epidermal Growth Factor (hEGF) and antibiotics (100 U/mL penicillin, 100 mg/mL

streptomycin). Cells and factors were obtained along with LONZA.

Shear-Stress and Collection of Conditioned Medium: The cells were cultured in appropriate medium until they reached semi-confluence (90%), in culture plates 100, prepared by sterilization under UV light for 15 minutes. Then the medium was replaced with DMEM medium supplemented with 1% antibiotic and 1% FBS. The semi-confluent layers were subjected to shear stress (using orbital shaker) for 72 h under a humid atmosphere with 5% CO2 at 37°C, as previously described Rodríguez and González, de la Paz et al. The rotation was determined using the maximum stress formula: τmax = a√ρη(2πf) 3 so that the rotation frequency is within the physiological arterial pressure (6-40~dynes/cm), mimicking the mechanical forces encountered by blood flow (dela Paz et al. 2012) At the end, conditioned medium was collected, centrifuged and stored for further analysis. As a control the medium used was conditioned by cells that were maintained static (no rotation) during the culture, under the same culture conditions.

Isolation of exosomes: For analysis and exosomes the culture medium was supplemented with extracellular vesicles Free Fetal Serum, Extraction was performed in ultracentrifugation of 30,000 g for 18 hours. Cells remained for 72 hours with EV-free, Static or *Shear-Stress* free medium, after which the medium was withdrawn and used to isolate exosomes with the Total Cell Isolation Kit (Invitrogen - Thermo Fisher Scientific, Vilnius, Lithuania) according to the manufacturer's instructions.

Nanoparticle screening (NTA): NanoSight NS300 (Amesbury, UK) was used to determine the size and concentration of exosomes that performs nanoparticle tracing analysis based on light scattering and Brownian motion properties of the samples. The NS300 uses a laser light source (405 nm) to illuminate nanometer particles (10-2000 nm) which are visualized as individual points. After isolation of the EVs from the culture medium the exosomes were resuspended in PBS for analysis. In all analyzes the samples were diluted 1:1000 in PBS filtered in a 0.22 μm pore filter. Each experiment was performed at 25°C in triplicate with acquisition of five 1-minute videos. The values of concentration, mean size and particle distribution (D10, D50 and D90) were obtained in each of the experiments using the corresponding software (NanoSight software version 2.3).

Analysis of exosome markers by flow cytometry: After isolation the exosomes were

coupled to Latex Beads (ThermoFisher) overnight. The next day the samples were centrifuged and washed with 1M Glycine. The exosomes were distributed in tubes for cytometry and incubated with BD Biosciences antibodies, with respective fluorochromes: anti-CD9, anti-CD63 and anti-CD81 for 30 minutes in the dark. After that time they were centrifuged at 400g for 5 minutes and the pellet resuspended in PBS. For the design of the standards, the control tubes were incubated with isotype antibodies specific for each fluorochrome in each test performed. Measurements, 10,000 events for each sample were required on a FACSCantoTM II flow cytometer (BD Biosciences) with FACSDIVA software (BD Biosciences). The results were analyzed in FLOWJO software, version vX.10x6 (FlowJo, LLC, Ashland, OR).

Sample preparation for qPCR: For collection of samples for qPCR, after 28 days of treatment or 3 for Endothelial and Muscle cells or Exosome isolation, the TriZOL (500 µL) was added. Then the procedure of centrifugation, addition of Chloroform and a new centrifugation, was started phases of DNA, RNA and proteins in everything. RNA samples were quantitated using plate reader (NanoDrop™ 2000/c Spectrophotometers, Thermo Fisher Scientific, USA). The next step was cDNA synthesis using the Tanaka Kit. After this process the material was collected and each sample was stored in -80˚C freezer.

Table 1. Expression primers sequences and PCR cycle conditions.

Gene	Primer	5'-3' Sequence	Reactions Condition
NPP1	Forward	TTTGCCGATTGAGGATTTTC	95°C - 15s; 60°C - 30s; 72°C - 30s
	Reverse	CCACTGACGACATTGACACC	
TNAP	Forward	TTTATAAGGCGGCGGGGGTG	95°C - 15s; 60°C - 30s; 72°C - 30s
	Reverse	AGCCCAGAGATGCAATCGAC	
ALP	Forward	CGGGCACCATGAAGGAAA	95°C - 15s; 60°C - 30s; 72°C - 30s
	Reverse	GGCCAGACCAAAGATAGAGTT	
Fetuin A1	Forward	GAATTCCCCGCTCATCCTGTTCT	95°C - 15s; 60°C - 30s; 72°C - 30s
	Reverse	CGTGGAAATCGCAGTCTCCT	
DKK1	Forward	CCTTGGATGGGTATTCCAGA	95°C - 15s; 60°C - 30s; 72°C - 30s
	Reverse	CCTGAGGCACAGTCTGATGA	
sFRP2	Forward	CTCGCTGCTGCTGCTCTTC	95°C - 15s; 60°C - 30s; 72°C - 30s
	Reverse	GGCTTCACATACCTTTGGAG	
b-Catenin	Forward	GCGTGGACAATGGCTACTCAAG	95°C - 15s; 60°C - 30s; 72°C - 30s
	Reverse	GTCATTGCATACTGCCCGTCAA	

SOST	Forward	GCGTTCAAGAATGATGCCACG	95°C - 15s; 60°C - 30s; 72°C - 30s
	Reverse	GCTGTACTCGGACACGTCTTTGG	
FGF23	Forward	TGAGCGTCCTCAGAGCCTAT	95°C - 15s; 60°C - 30s; 72°C - 30s
	Reverse	TTGTGGATCTGCAGGTGGTA	
DMP1	Forward	TAGGCTAGCTGGTGGCTTCT	95°C - 15s; 60°C - 30s; 72°C - 30s
	Reverse	AACTCGGAGCCGTCTCCAT	
Ki-67	Forward	AAGCCCTCCAGCTCCTAGTC	95°C - 15s; 60°C - 30s; 72°C - 30s
	Reverse	TCCCGAAGCACCACTTCTTCT	
Osteocalcin	Forward	ATGAGAGCCCTCACACTCCTC	95°C - 15s; 60°C - 30s; 72°C - 30s
	Reverse	GCCGTAGAAGCGCCGATAGGC	
Runx2	Forward	CCGTCCATCCACTCTACCAC	95°C - 15s; 60°C - 30s; 72°C - 30s
	Reverse	ATGAAATGCTTGGGAACTGC	
GP-38	Forward	GGGAACGATGTGGAAGGTGT	95°C - 15s; 60°C - 30s; 72°C - 30s
	Reverse	GCTCTTTAGGGCGAGTACCT	
MEPE	Forward	AAACTCCTGGGGGAAGAAAA	95°C - 15s; 60°C - 30s; 72°C - 30s
	Reverse	AATACGATGGGTGCTTTTGC	
PHEX	Forward	AAGAGGACCCTGGGAGAAAA	95°C - 15s; 60°C - 30s; 72°C - 30s
	Reverse	GGCAGCTTCTGGTCTGTAGG	
MMP14	Forward	CACTGCCTACGAGAGGAAGG	95°C - 15s; 60°C - 30s; 72°C - 30s
	Reverse	TTGGGGTACTCGCTATCCAC	
Connexin43	Forward	ATGAGCAGTCTGCCTTTCGT	95°C - 15s; 60°C - 30s; 72°C - 30s
	Reverse	TCTGCTTCAAGTGCATGTCC	
DNMT1	Forward	GAGCCACAGATGCTGACAAA	95°C - 15s; 60°C - 30s; 72°C - 30s
	Reverse	GACACAGGTGACCGTGCTTA	
DNMT3A	Forward	AAGGAGGAGCGGCCAGAG	95°C - 15s; 60°C - 30s; 72°C - 30s
	Reverse	GGATGGGGACTTGGAGATCA	
TET1	Forward	CTGTTGGCACCGTTAAGCAC	95°C - 15s; 60°C - 30s; 72°C - 30s
	Reverse	CATACAGGCCTTTCCTGGCA	
TET2	Forward	GGACATGATCCAGGAAGAGC	95°C - 15s; 60°C - 30s; 72°C - 30s
	Reverse	CCCTCAACATGGTTGGTTCT	
TET3	Forward	CCCACAAGGACCAGCATAAC	95°C - 15s; 60°C - 30s; 72°C - 30s
	Reverse	CCATCTTGTACAGGGGGAGA	
HDAC1	Forward	TCACCGAATCCGCATGACTCATAA	95°C - 15s; 60°C - 30s; 72°C - 30s
	Reverse	CTGGACGGATGGAGCGCAAGA	
HDAC2	Forward	GGAGGAGGCTACACAATCCG	95°C - 15s; 60°C - 30s; 72°C - 30s
	Reverse	TCTGGAGTGTTCTGGTTTGTCA	
HDAC5	Forward	AGCACCGAGGTAAAGCTGAG	95°C - 15s; 60°C - 30s;

	Reverse	GAACTCTGGTCCAAAGAAGCG	72°C - 30s
Sirt1	Forward	GAGATAACCTTCTGTTCGGTGATGAA	95°C - 15s; 60°C - 30s; 72°C - 30s
	Reverse	CGGCAATCAAATCTTTAAGAATTGTTCG	
HOTTAIR	Forward	CCTATCCCTACTCGGCCCAAGT	95°C - 15s; 60°C - 30s; 72°C - 30s
	Reverse	CAGGACGCTGTTCTTGTTGA	
HoxD8	Forward	TCTTCCTCTTCGTCTACCAGG	95°C - 15s; 60°C - 30s; 72°C - 30s
	Reverse	TAATATTGGCGAGGACCCAG	
GAPDH	Forward	GACTCATGACCACAGTCCATGC	95°C - 15s; 60°C - 30s; 72°C - 30s
	Reverse	AGAGGCAGGGATGATGTTCTG	
RP2	Forward	GGTCCTGTTATTGCCTTGGA	95°C - 15s; 60°C - 30s; 72°C - 30s
	Reverse	AAGTCCTGGTTCCACATTGC	
18S	Forward	CGGACAGGATTGACAGATTGATAGC	95°C - 15s; 60°C - 30s; 72°C - 30s
	Reverse	TGCCAGAGTCTCGTTCGTTATCG	

Confocal microscopy: For confocal microscopy analysis, the cells were cultured in glass coverslips placed in the peripheral ring of the culture and subjected to shear stress. The cells were then washed with PBS, fixed in PBS-paraformaldehyde (4% v/v) for 1 h, permeabilized in PBS containing 0.2% Triton-X 100 and 1% BSA at 37°C for 1 h stained with the appropriate specific primary antibodies (HSP70), at the concentration recommended by the manufacturer. Then, after washing with PBS to remove the primary antibody, for fluorescence analysis, cells were stained with anti-rabbit or mouse IgA Alexa Fluor 594 antibody for 1 h. Cells were washed and mounted on glass slides using Fluorosield with DAPI (Sigma) and then viewed on an inverted laser scanning confocal microscope (Leica TCS SP5).

Western blotting performance: MSC or Exosomes were collected and lysed in Laemilli buffer. The protein extracts were clarified and the protein concentration determined by the Lowry method. Protein extracts were resolved by SDS-PAGE (12%) and transferred to PVDF membranes (Bio-Rad, Hercules, CA, USA). Immediately, the membranes were blocked with bovine serum albumin (2.5%) in Tris buffered saline (TBS) -20 (0.05%) and incubated overnight at 4°C with appropriate primary antibody. Dilutions of 1:1000 overnight. After washing in TBS-Tween 20 (0.05%), the membranes were incubated with secondary antibodies conjugates in dilutions of 1:5000 for 1 hour. Subsequently, Enhancement Chemiluminescence (ECL, Pierce, USA) was used to detect the bands.

Xylenol Orange: For determination of the mineralization process was added to the Xylenol Orange culture medium according to the manufacturer's instructions (Sigma – Aldrich).

Agarose Gel: After running in real-time PCR, amplifiers were collected and added to green buffer for agarose gel running (2%).

CIMminer: Proteins revealed by Western Blotting were analyzed for band intensity and values normalized by the reference gene, GAPDH. The results were used in an online tool that produces Clustered Image Maps.

Statistical analysis: The results were represented as mean ± standard deviation (SD). They were verified using One-Way ANOVA (non-parametric) with Tukey's post test in order to compare all pairs of groups. In this case, with $p < 0.05$ considered statistically significant and $p < 0.0001$ considered highly significant. The software used was GraphPad Prism 6.

RESULTS AND PARTIAL DISCUSSION

Exosome Characterization:

Firstly, we have already presented the potential involvement of vascular smooth muscle cells to promote osteocyte acquisition phenotype from osteoblasts. Since the conditioned medium by AoSMCs contain several metabolites, we hypothesized that this Osteoblast - Osteocyte transition processing would be by Extracellular Vesicles, which when characterized showed being Exosomes (50 - 200 nm). Since these cells are able to release EVs, the next step was to investigate whether these exossomes would be carrying at the level of protein and mRNA.

Initially, during characterization, we show that primary cells (HCAEC, HUVEC and AoSMC) respond differently to the *Shear-Stress* mechanism in regard the releasing of exosomes. We investigated an important protein that participates in exosomal biogenesis: HSP70. Immunofluorescence shows that *Shear-Stress* environment increases their content in smooth muscle cells, while the same experimental condition decreased this protein in endothelial cells **(Fig. 1)**. To validate these data, we used the Nano Tracking Analyze (NTA) technique and conversely, we have observed that *Shear-Stress*

promotes increased release of exosome by AoSMC, while the same process promotes the decrease in endothelial cells **(Fig. 2b-e)**.

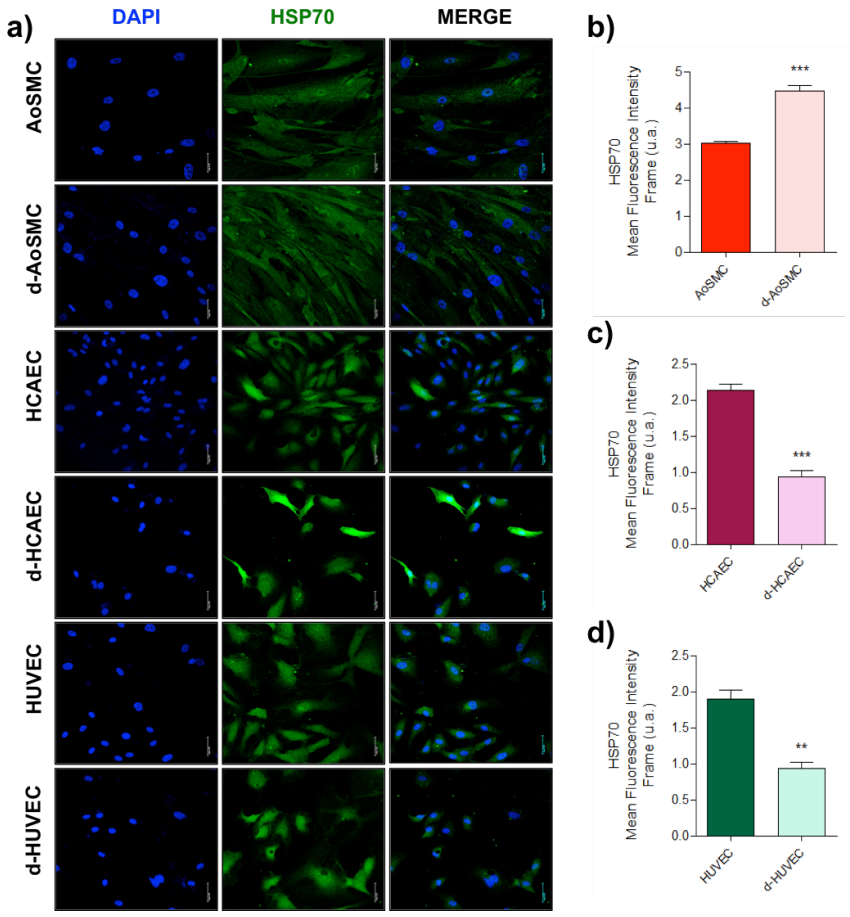

Figure 1: Characterization of HSP70 in primary cells. After 3 days in culture, under the effect of *Shear-Stress* or Static, the cells were fixed and stained with primary antibody to HSP70 **(a)**. Labeling was quantified on each cell under different conditions **(b-d)**. **p<0.1906; ***p<0.0002: Significant statistical difference when compared Static and *Shear-Stress*.

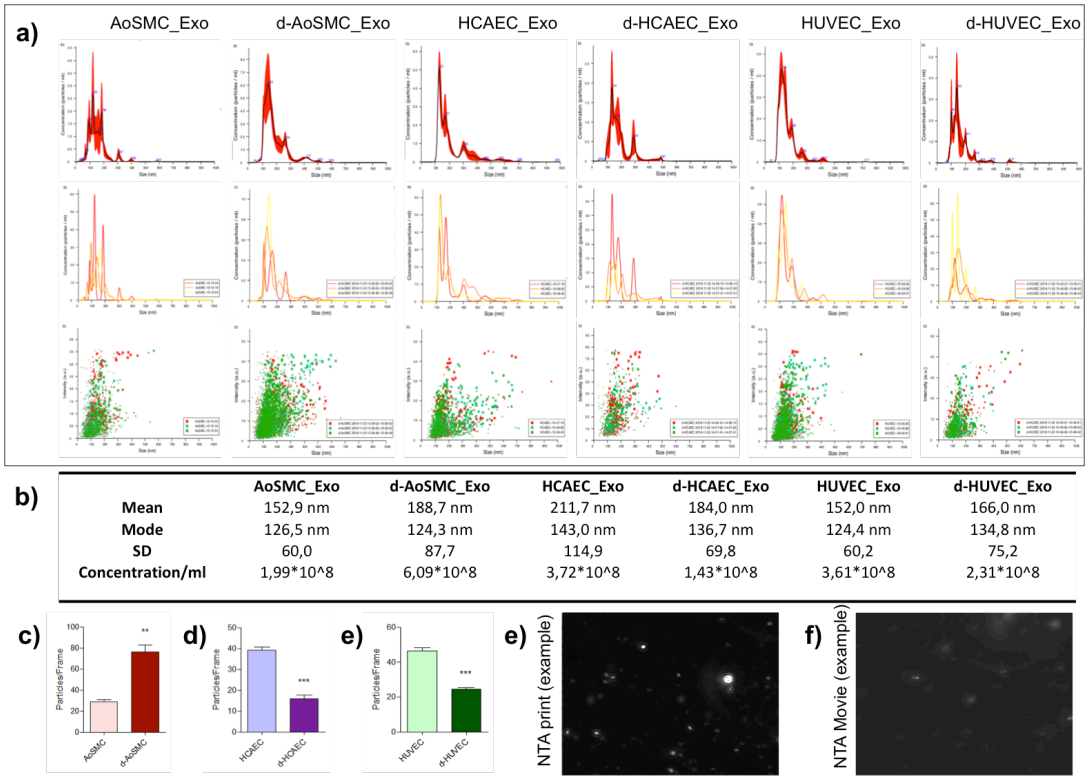

	AoSMC_Exo	d-AoSMC_Exo	HCAEC_Exo	d-HCAEC_Exo	HUVEC_Exo	d-HUVEC_Exo
Mean	152,9 nm	188,7 nm	211,7 nm	184,0 nm	152,0 nm	166,0 nm
Mode	126,5 nm	124,3 nm	143,0 nm	136,7 nm	124,4 nm	134,8 nm
SD	60,0	87,7	114,9	69,8	60,2	75,2
Concentration/ml	1,99*10^8	6,09*10^8	3,72*10^8	1,43*10^8	3,61*10^8	2,31*10^8

Figure 2: Characterization of extracellular vesicles by Nanotracking Particles Analyze. Isolated exosomes of primary cells were characterized by size **(a, b)** and concentration **(c - e)**. **p<0.1906; ***p<0.0002: Significant statistical difference when compared Static and *Shear-Stress*.

Another important technique used to validate the EVs was Flow Cytometry (FACS). We observed the presence of exosome-specific membrane biomarkers: Tetraspanins - CD9, CD63 and CD81 **(Fig. 3 - 5)** which was also evaluated by Western Blotting **(Fig. 5b-e)**.

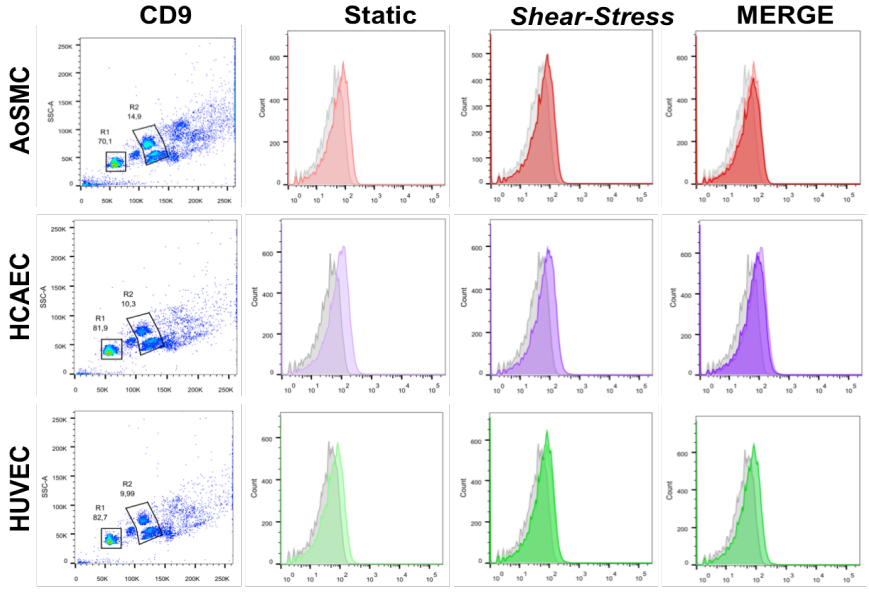

Figure 3. Characterization of CD9 in endothelial cells. After 3 days of culture the different cells were collected to evaluate the Tetraspanin-CD9. After the stage of attachment vesicle markers were evaluated in the cells using Flow Cytometry.

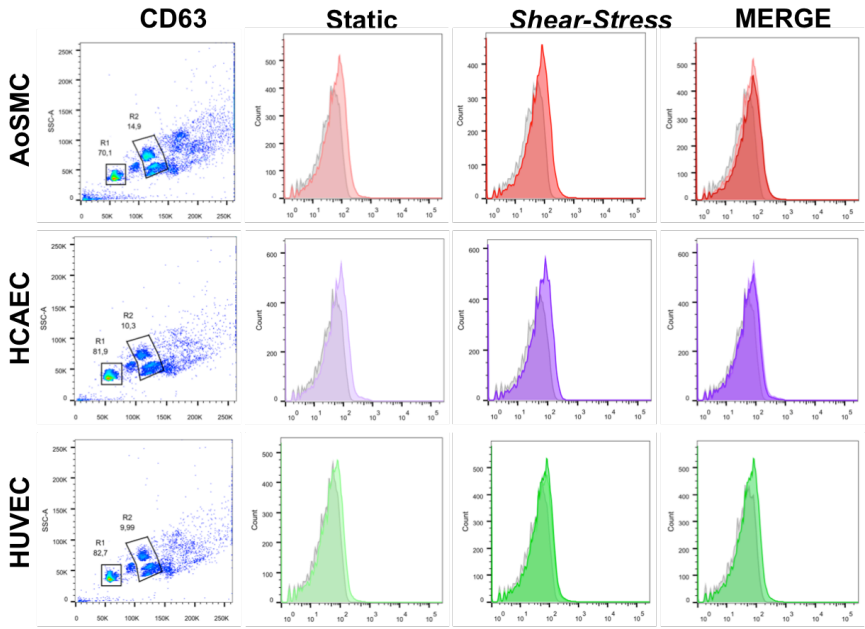

Figure 4. Characterization of CD63 in endothelial cells. After 3 days of culture the different cells were collected to evaluate the Tetraspanin-CD63. After the stage of attachment vesicle markers were evaluated in the cells using Flow Cytometry.

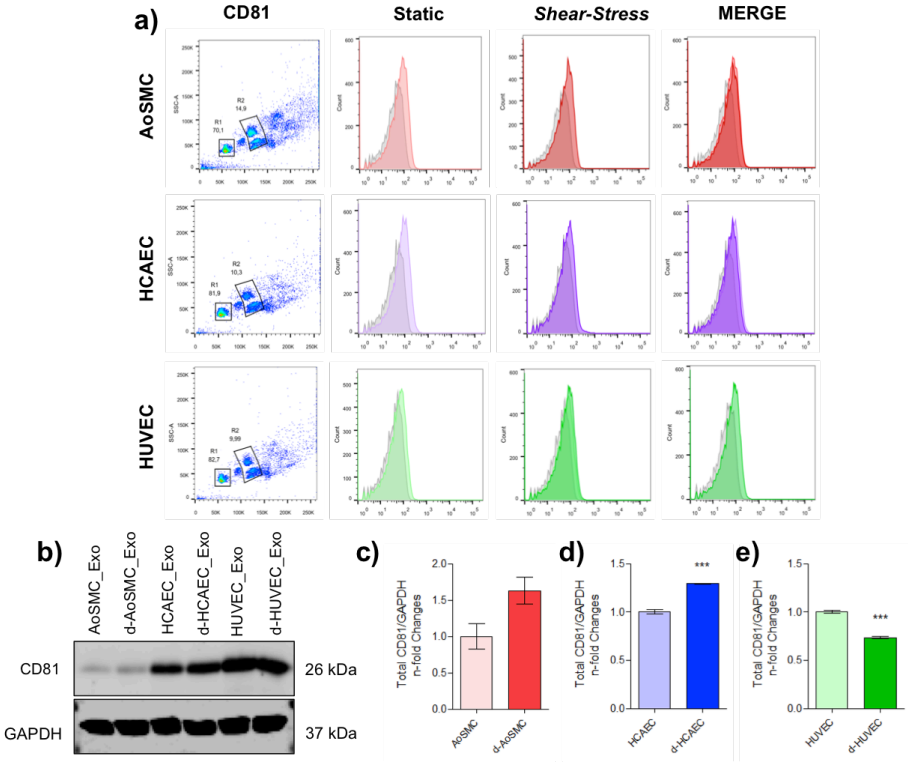

Figure 5. Characterization of CD81 in endothelial cells. After 3 days of culture the different cells were collected to evaluate the Tetraspanin-CD81. After the stage of attachment vesicle markers were evaluated by Flow Cytometry **(a)** and Western Blotting **(b - e)**. Expression assays were normalized with GAPDH reference gene. ***p<0.0002: Significant statistical difference when compared Static and *Shear-Stress*.

Our results show that there is no statistically significant difference between the different groups by FACS analysis, but Western Blotting revealed that Shear-Stress led to the increase of CD81 in AoSMC and HACEC regarding the released vesicles, while the opposite was found in HUVEC.

Profile of protein phosphorylation in exosomes:

To characterize the cargo of phosphorylated proteins that were possibly being carried by EVs, we initially used the western blotting approach, when a set of phosphor-proteins from different signaling pathways were evaluated. Also, we have paid attention to the phosphatases **(Fig. 6a)**, and we have seen that the content of phospho-SHP1, Alkaline Phosphatase (ALP) and PTP1B is decreased in AoSMC released vesicles subjected to *Shear-Stress*, but the effect causes opposite response in endothelial cell-released exosomes **(Fig. 6b–k)**.

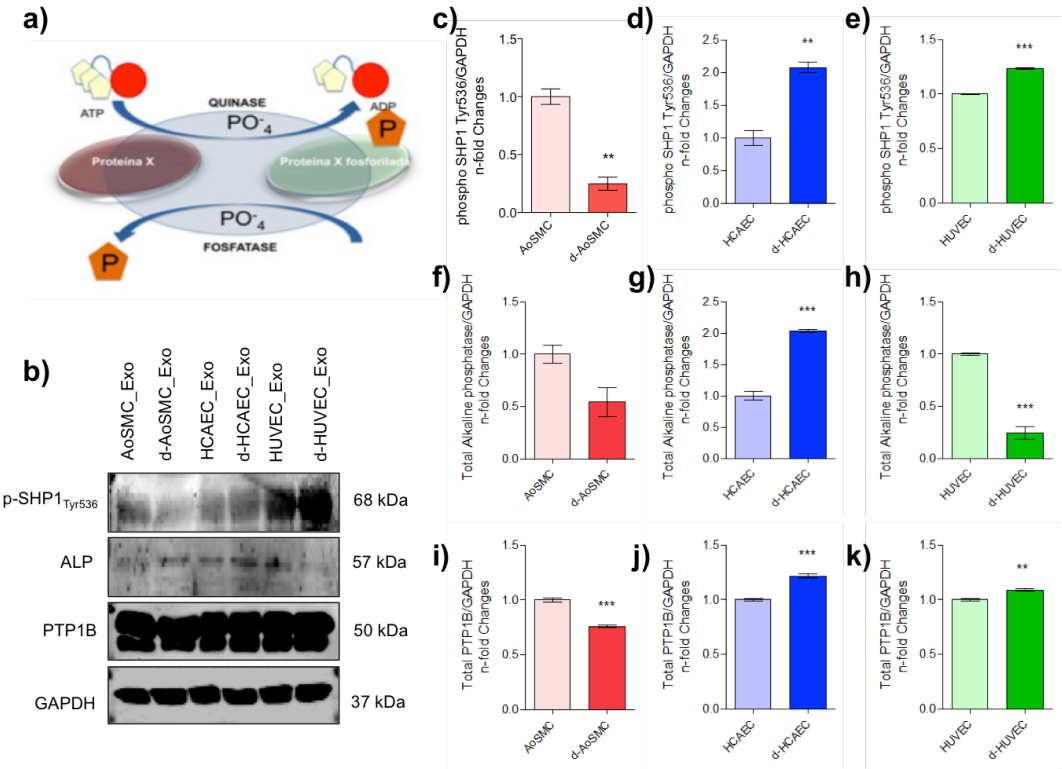

Figure 6. Phosphatase profile in exosomes released by endothelial cells. Phosphates act antagonistically to kinases **(a)**. After cells were exposed to experimental conditions,

the medium was collected and used to isolate exosomes. Samples were lysed with appropriate buffer and proteins revealed by Western Blotting: p-SHP1, ALP and PTP1B **(b - k)**. The expression results were normalizing by GAPDH. **p<0.1906; ***p<0.0002: Significant statistical difference when compared Static and *Shear-Stress.*

Since *Shear-Stress* might affect primary cell adhesion mechanisms, we decided to investigate whether proteins involved with this process could be exported via the extracellular vesicle **(Fig. 7a)** and this step of the development of this project was decisive to support new strategies forward. We have shown that *Shear-Stress* promotes increased Phospho-Integrin β3 ratio in HCEAC, while both FAK and Src phosphorylation were decreased. HUVEC behavior shows a decrease on both phospho-Integrin and phospho-Src when subjected to *Shear-Stress*. Importantly, these proteins are directly related to CD9, CD63 and CD81 which together regulate rearrangement of actin filaments through adhesion platforms **(Fig. 7b-k)**.

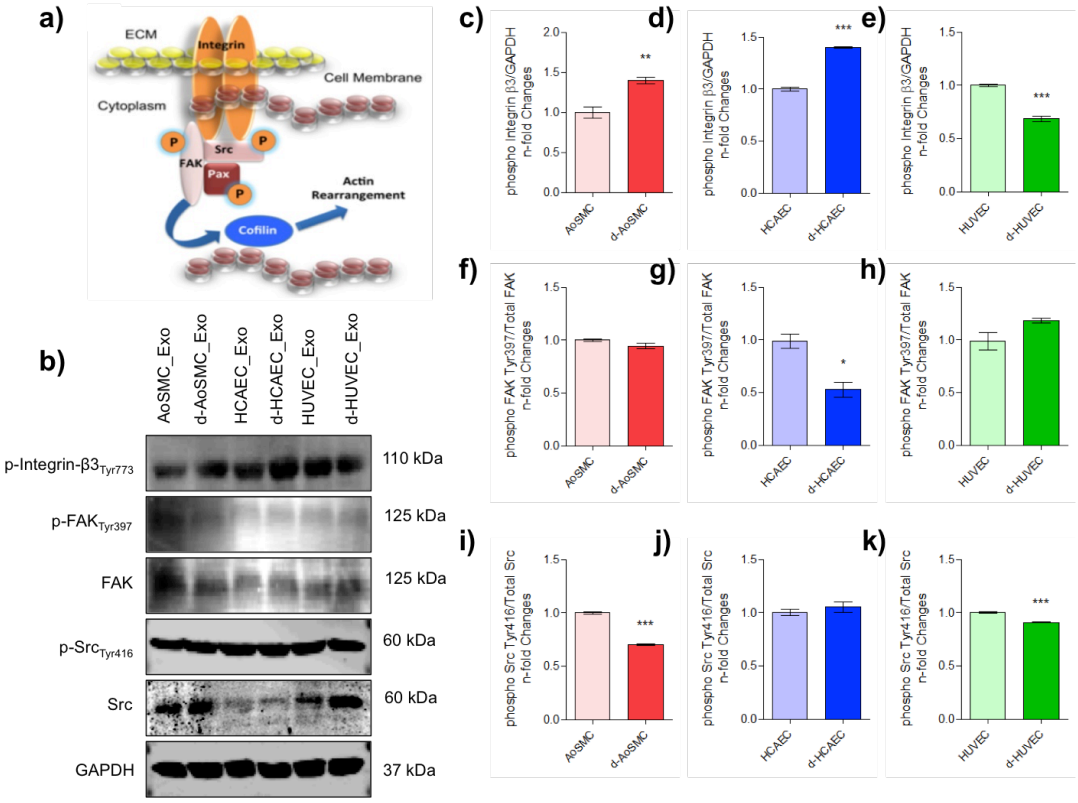

Figure 7. Characterization of adhesion proteins in exosomes released by primary cells. After the cells were *Shear-Stress* or in a static condition for 72 hours, the medium was collected and used to isolate exosomes. Samples were lysed with Laemilli buffer and proteins were revealed on SDS-PAGE gel. Proteins involved with cell adhesion pathway **(a)** were evaluated: p-Integrin β3, p-FAK, FAK, p-Src and Src **(b - k)**. The expression results were normalizing by GAPDH. *p<0.05; **p<0.1906; ***p<0.0002: Significant statistical difference when compared Static and *Shear-Stress.*

Another important set of proteins evaluated was the MAP-kinases. We have seen that the Phospho-ERK decreases in endothelial cell containing exosomes, in addition Phospho-JNK decreases significantly in AoSMC and increases six-fold changes in HUVEC **(Fig. 8a-j)**.

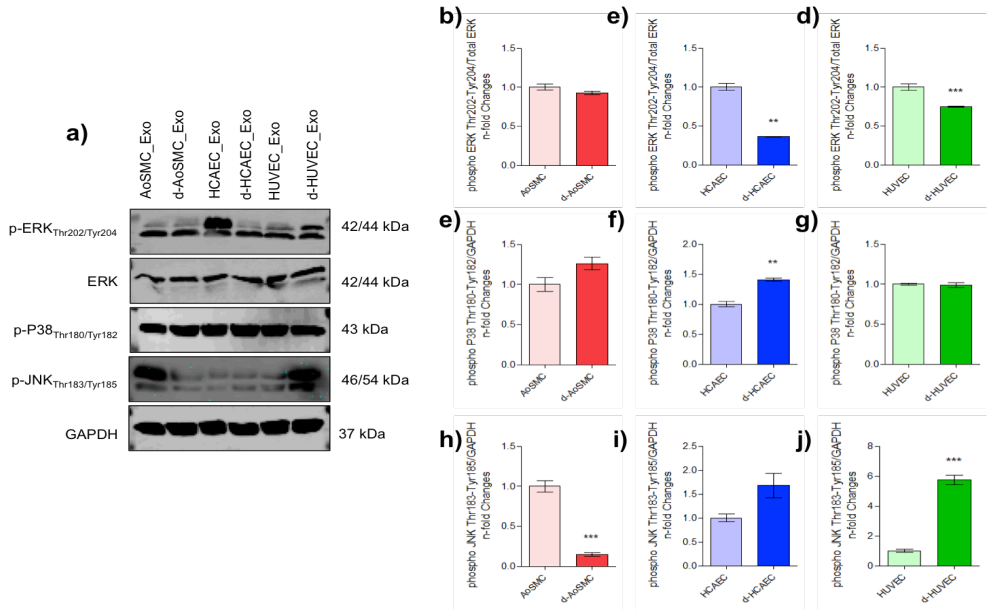

Figure 8. *Shear-Stress* modulates the content of MAP-Kinases within Endothelial cell released exosomes. Endothelial cell released exosomes were lysed in Laemilli buffer and the protein content used to run SDS-PAGE gel electrophoresis: p-ERK, ERK, p-P38, p-JNK **(a - j)**. The expression results were normalizing by GAPDH. **p<0.1906; ***p<0.0002: Significant statistical difference when compared Static and *Shear-Stress.*

Using the CIMminer online tool, we have used the values observed in densitometry to assess familiarity between the different EV's-related groups **(Fig. 9)**.

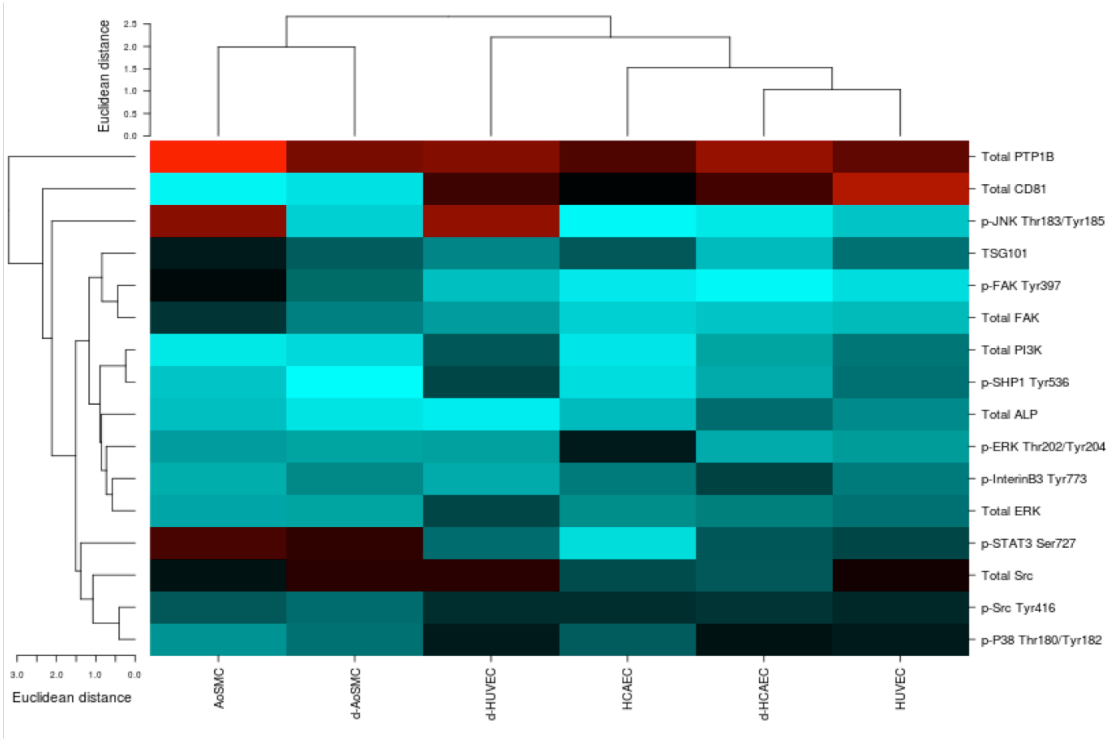

Figure 9. Cluster identification to represent results of protein content expression in endothelial cell exosomes.

The data shows that *Shear-Stress* did not change the phosphorylation profile in AoSMC, since AoSMC and d-AoSMC (subjected to Shear Stress) are arranged side by side within the graph. The phosphorylation profile in HCAEC was similar to d-HUVEC and HUVEC to the profile observed in d-HCAEC. However, the endothelial cell groups bring a familiarity. A hypothesis here from these findings is the arterial hemodynamic forces exerted by the bloodstream in the vessel's wall, so the pressure observed in Arterial cells is higher than that observed in venous cells.

Effect of Medium or Exosomes considering Undifferentiated Mesenchymal stem Cells

Importantly, we have widely used osteoblast in the experiments carried out in Brazil, it being necessary to address these findings on undifferentiated cells. This approach is very important once the osteoblast is already a compromised cell with bone biology and the osteoblast-osteocyte transition is already favorable. Now, therefore, we have decided to repeat our experiments using an Undifferentiated Human Mesenchymal Cell (MSC), obtained from Internal Medicine Department at Erasmus MC.

As described in Materials and Methods, our experiments were divided into 3 moments, as follows: 10 minutes, 18 hours and 28 days. In Brazil we hypothesized that the Osteoblast- Osteocyte transition was being mediated by Exosomes, so at that time

MSC were treated with only Exosomes isolated from primary cell conditioned culture medium and with Complete Culture Medium, following our own biological model. According to the results obtained in Brazil, AoSMCs are the most interesting cells to evaluate further the osteocyte transition. Thus, we have used the exosome-enriched medium from AoSMCs to treat Mesenchymal Stem Cells (MSC). Our findings show that after a short-manner strategy there is no significances on the phosphorylation of strategically proteins when compared with the positive osteogenic medium **(Fig. 10a,b,c)**.

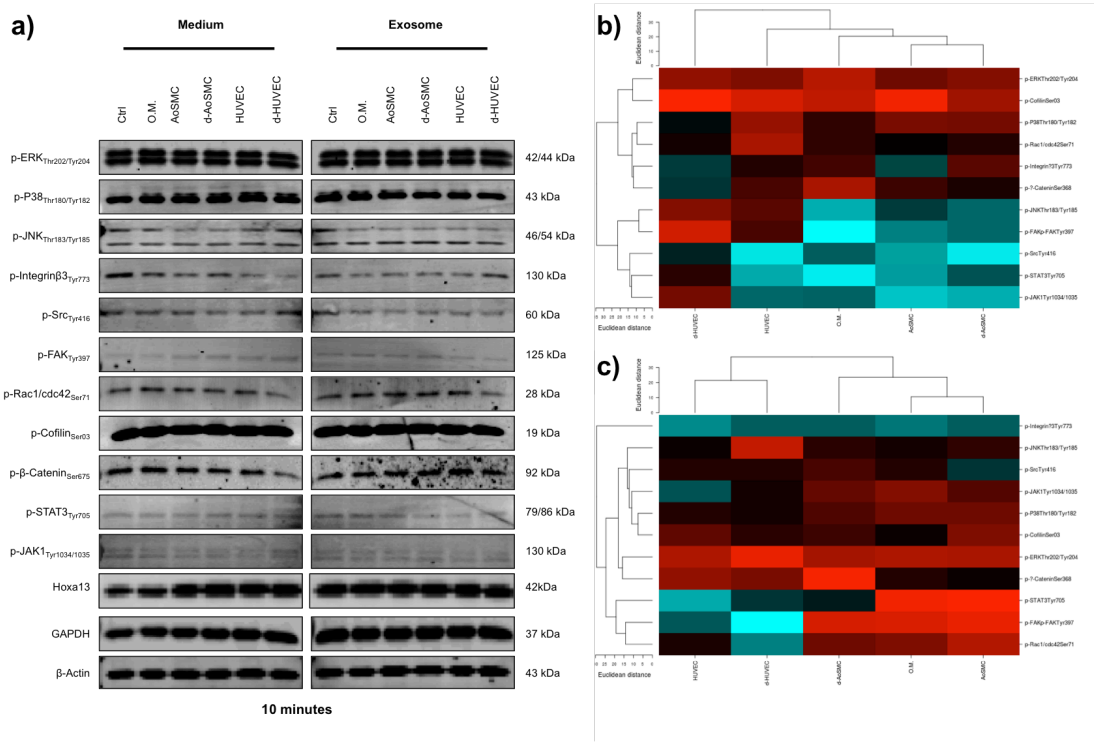

Figure 10. Effect on phosphorylation process in undifferentiated mesenchymal cells caused by endothelial cell products. After 10 minutes of treatment with Medium or Exosomes alone, cells were collected and lysed in Laemilli buffer and proteins evaluated by SDS-PAGE gel. Proteins from different signaling pathways were evaluated: p-ERK, p-P38, p-JNK, p-Integrin β3, p-Src, p-FAK, p-Rac, p-Cofilin, p-β-Catenin, p-STAT3 and p-JAK1, has still been rated Hox13. As references used GAPDH and B-Actin **(a)**. Bands were quantified and protein content expression values were compared by use of CMminer to identify familiarity between the groups: **b)** Treatment with culture medium, **c-)** Treatment with Exosomes.

The effect caused after 18 hours of exposure to different treatments showed that genes involved with calcium homeostasis such as TNAP, NPP1 and Fetuin-A1 were increased only in the O.M group and decreased in the other experimental groups when compared to the control cultures, regardless of treatment: Medium or Exosome **(Fig. 11a-j)**. This suggests that the positive control may modulate in the early periods of treatment

the calcium and phosphate metabolism.

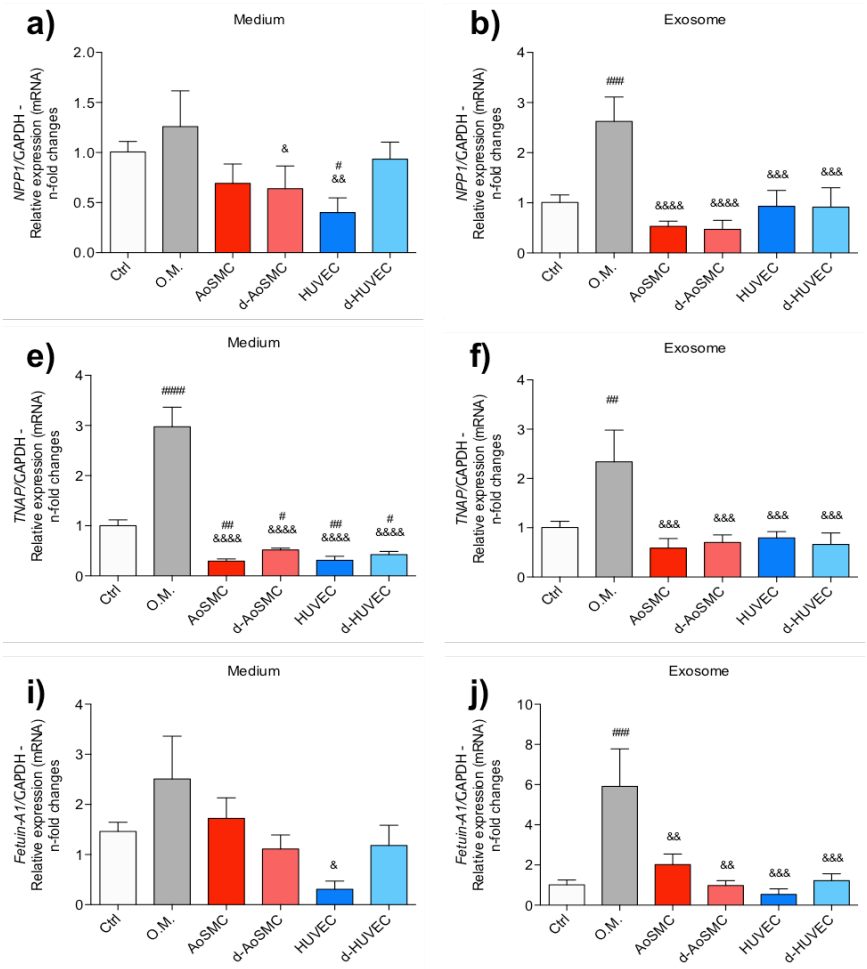

Figure 12: Primary cells modulate mineral homeostasis genes in MSC in the first hours of treatment. After 18 hours of treatment, Medium or Exosome, MSC were collected in TriZOL for RNA extraction and cDNA synthesis. The samples were evaluated for NPP1 **(a - b)**, TNAP **(c - d)** and Fetuin-A1 **(e - f)** expression. Expression values were normalized by GAPDH reference gene. #p<0.05; ##p<0.1906, ###p<0.0002: Significant statistical difference when compared to control. $^{\&}$p<0.05; $^{\&\&}$p<0.1906, $^{\&\&\&}$p<0.0002, $^{\&\&\&\&}$p<0.0001: Statistical difference when compared with the Osteogenic Medium.

Another important signaling pathway studied in this project was the Wnt/β-Catenin pathway and we evaluated the differential expression at mRNA level: where both DKK1 and sFRP2 genes were decreased, while β-Catenin showed there is no difference when compared to the control group, showing an increase only in the O.M. **(Fig. 12a - j)**.

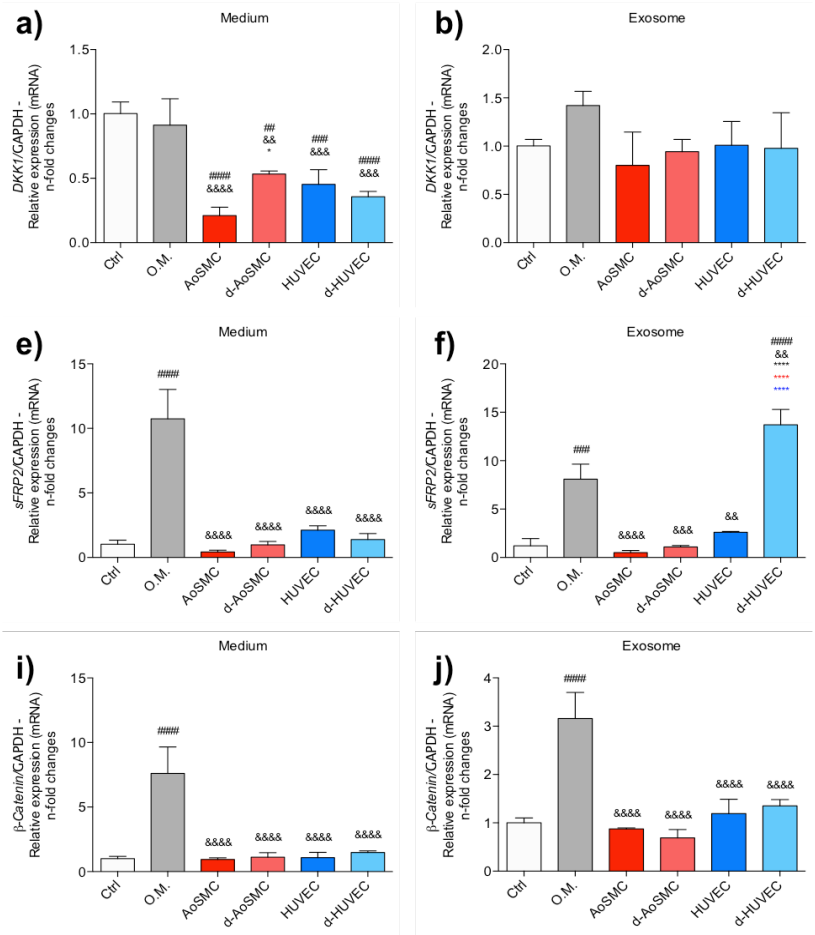

Figure 12. Endothelial cells modulate β-Catenin pathway protein expression in undifferentiated Mesenchymal cells. MSCs submitted to treatment with Medium or Exosomes from primary endothelial cells were collected to study the gene expression of DKK1 **(a - b)**, sFRP2 **(c - d)** and β-Catenin **(i - j)**. Expression values were normalized by GAPDH reference gene. ##p<0.1906, ###p<0.0002, ####p<0.0001: Significant statistical difference when compared to control. $^{\&\&}$p<0.1906, $^{\&\&\&}$p<0.0002, $^{\&\&\&\&}$p<0.0001: Statistical difference when compared with the Osteogenic Medium. *p<0.05, ****p<0.0001: Statistical difference when compared with the AoSMC treatment. ****p<0.0001: Statistical difference when compared with the d-AoSMC treatment. ****p<0.0001: Statistical difference when compared with the HUVEC treatment.

We also investigated the expression of osteocyte markers in the challenged MSCs: our data validates those obtained previously by osteoblast, once there is a significant increase of SOST in response to d-AoSMC-conditioned medium. Surprisingly, there was also a significant increase in SOST mRNA in the groups that received AoSMC and d-AoSMC Exosomes. In addition, FGF23 and DMP1 were also increased in the d-AoSMC - Exosomes group **(Fig. 13)**. In this early phase of differentiation, the increase in SOST may be due to feedback from the increased β-Catenin signaling, whereas FGF23 and DMP1 may be an immediate response to increased calcium and phosphate

processing in response to increased NPP1 and TNAP, which may be associated with ATP breakdown and inorganic phosphate (Pi) releasing during tissue mineralization.

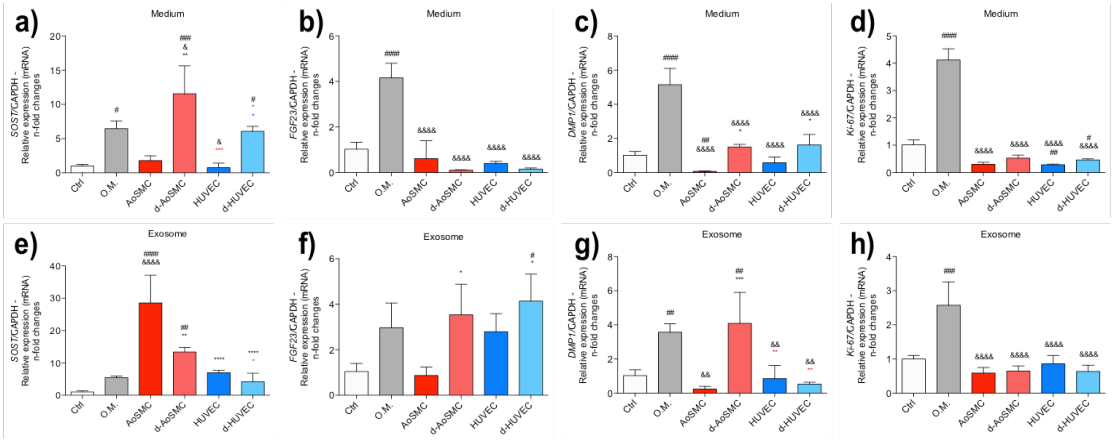

Figure 13. Exosomes modulate expression levels of osteocyte markers. MSCs submitted to treatment with Medium or Exosomes from primary endothelial cells were collected in TriZOL for RNA extraction and cDNA synthesis and gene expression: SOST, FGF23, DMP1 and Ki-67 **(a – h)**. Expression values were normalized by GAPDH reference gene. #p<0.05, ##p<0.1906, ###p<0.0002, ####p<0.0001: Significant statistical difference when compared to control. $^{\&}$p<0.05, $^{\&\&}$p<0.1906, $^{\&\&\&\&}$p<0.0001: Statistical difference when compared with the Osteogenic Medium. *p<0.05, **p<0.1906, ****p<0.0001: Statistical difference when compared with the AoSMC treatment. *p<0.05, **p<0.1906, ***p<0.0002: Statistical difference when compared with the d-AoSMC treatment. *p<0.05: Statistical difference when compared with the HUVEC treatment.

Finally, after 18 hours of treatment, we investigated important proteins related to the proliferation and differentiation of osteoblasts: Phospho-β-Catenin, PTP1B, ERK, Phospho-ERK, Phospho-JNK and Phospho-P38 **(Fig. 14)**.

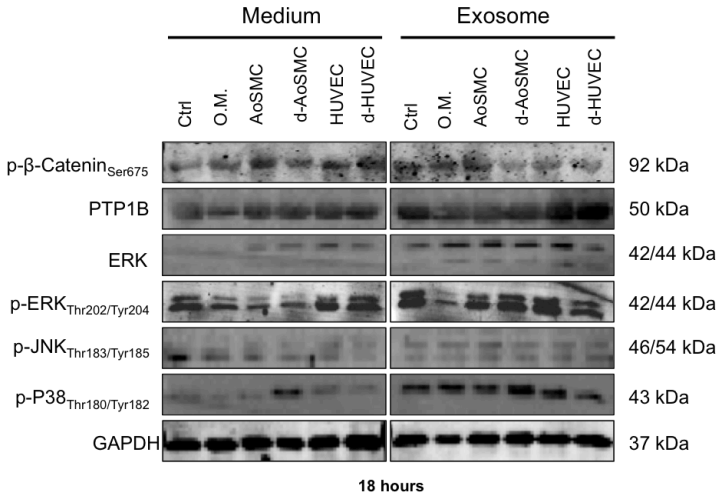

Figure 14. Paracrine effect of exosomes on proliferation and differentiation proteins evaluated in mesenchymal cells. Cells collected after treatments were lysed to

investigate protein content: p-B-Catenin, PTP1B, ERK, p-ERK, p-JNK, p-P38. The references used GAPDH.

Endothelium cell-paracrine effect on mesenchymal stem cells during osteogenic phenotype acquisition

To evaluate the whether the conditioned medium was affecting osteoblast phenotype of mesenchymal stem cells, we subjected MSCs with conditioned medium obtained from either AoSMCs or HUVECs up to 28 days, with medium changes every 3 days to maintain the biological properties of the experiment. As it is very known, an important effect on bone tissue mineralization is mineralization of the extracellular matrix carrying enzymes acting on the minerals available in the extracellular environment. In order to verify this process on our experimental design, we have monitored the differentiation process by looking to the calcium deposition using Xylenol Orange dye to observe mineral nucleation and the images show intense staining in the positive cultures, but it is not observed with the same intensity in the other treatments **(Fig. 15a** and **16a)**. In parallel, gene encoding proteins related with ATP breakdown, TNAP and NPP1, were increased in the MSC responding to the AoSMC-related conditioned medium; as well it was also observed in the Fetuin-A1 expression **(Fig. 15b-c, e)**. For groups receiving AoSMC, HUVEC and d-HUVEC conditioned media, a significant increase of ALP expression was observed **(Fig. 15d)**.

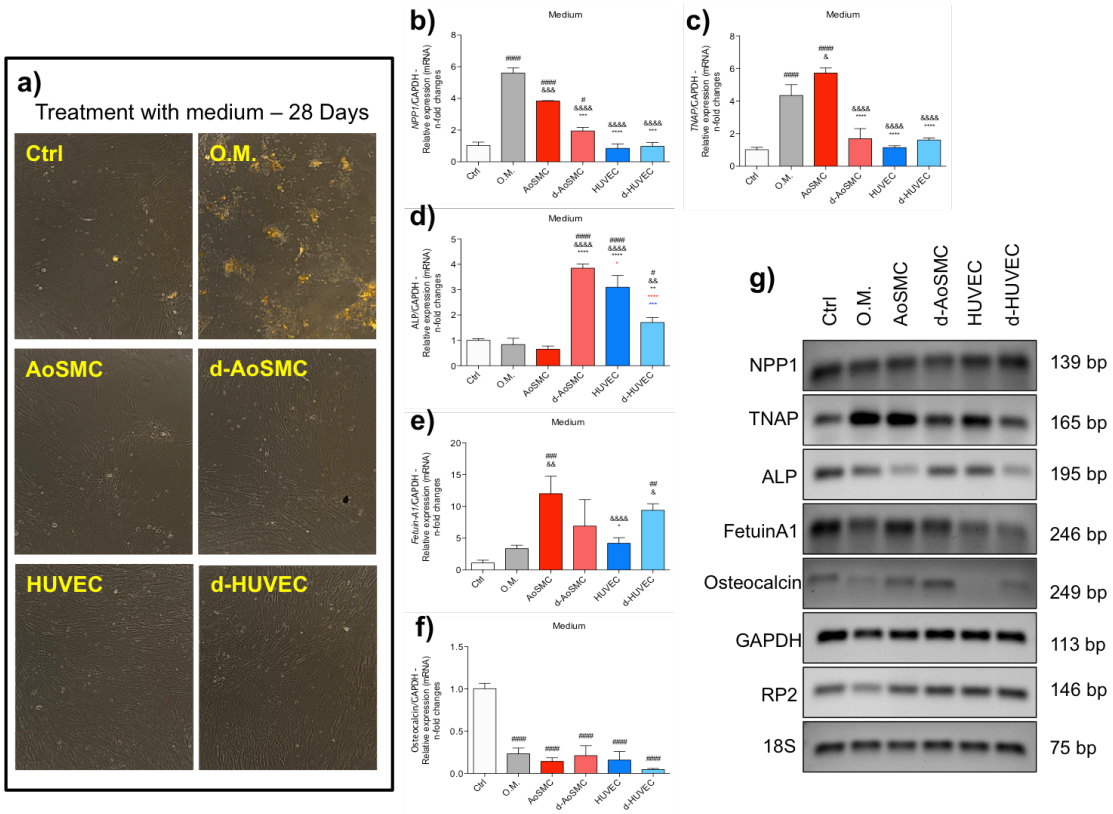

Figure 15. Effect of conditioned medium on phosphate calcium homeostasis on mesenchymal cell differentiation. After 28 days of treatment with primary cell conditioned medium, mesenchymal cells were stained with Xylenol Orange to assess cell-site calcium points **(a)**, were also collected in TriZOL to study gene expression of genes involved with Calcium Homeostasis. and Tissue phosphate: NPP1, TNAP, ALP, Fetuin-A1 and Osteocalcin **(b - f)**. After PCR-real time runs, the samples were run on agarose gel to reveal the bands **(g)**. Expression values were normalized by GAPDH reference gene. #p<0.05, ###p<0.0002, ####p<0.0001: Significant statistical difference when compared to control. $^{\&}$p<0.05, $^{\&\&}$p<0.1906, $^{\&\&\&}$p<0.0002, $^{\&\&\&\&}$p<0.0001: Statistical difference when compared with the Osteogenic Medium. *p<0.05, **p<0.1906, ***p<0.0002, ****p<0.0001: Statistical difference when compared with the AoSMC treatment. *p<0.05, ****p<0.0001: Statistical difference when compared with the d-AoSMC treatment. ***p<0.0002: Statistical difference when compared with the HUVEC treatment.

As evaluated in conditioned media treatments, cells were subjected to treatment only with exosomes, isolated from primary cell conditioned culture medium, and we observed increased expression of NPP1 and TNAP only in O.M groups. and d-HUVEC **(Fig. 16b-c)**, while Fetuin-A1 increased in groups receiving smooth muscle cell exosomes (Fig. 16e). Osteocalcin increased significantly only in response to d-HUVEC group, when compared to the other experimental groups **(Fig. 16f)**.

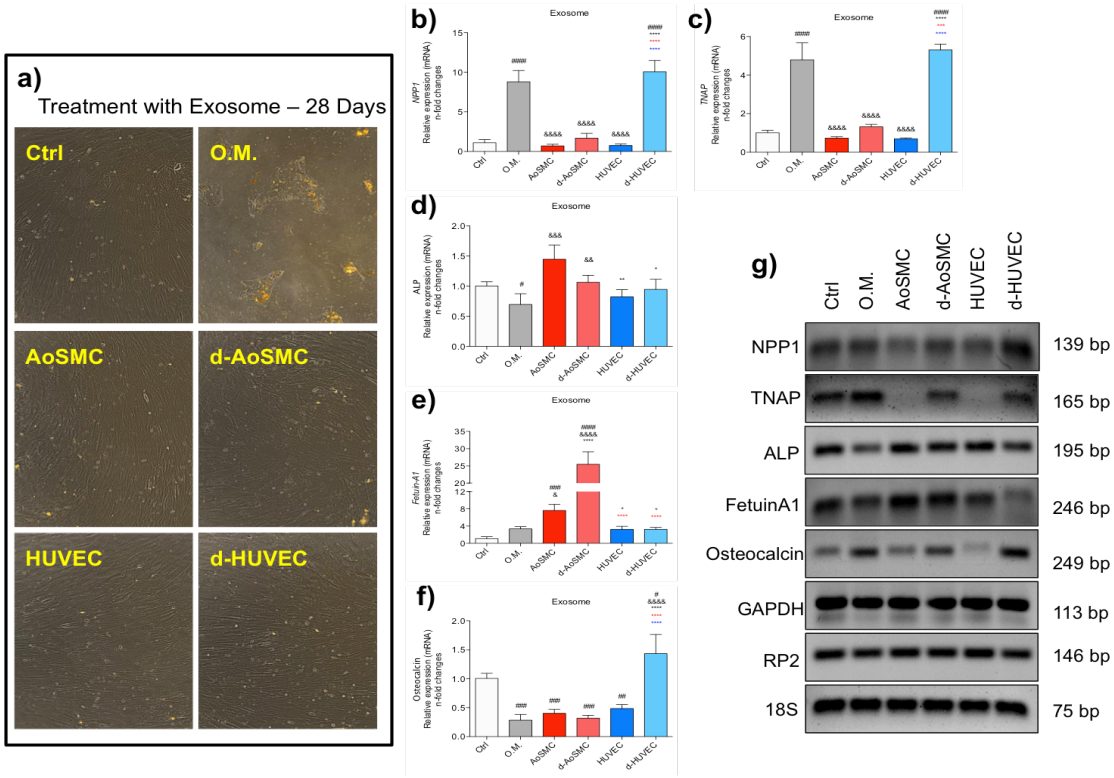

Figure 16. Effect of Exosome from Endothelial cells on phosphate calcium homeostasis on mesenchymal cell differentiation. After 28 days of treatment with Exosome from primary cell, MSC were stained with Xylenol Orange to assess cell-site calcium points **(a)**, were also collected in TriZOL to study gene expression of genes involved with Calcium Homeostasis. and Tissue phosphate: NPP1, TNAP, ALP, Fetuin-A1 and Osteocalcin **(b - f)**. After PCR-real time runs, the samples were run on agarose gel to reveal the bands **(g)**. Expression values were normalized by GAPDH reference gene. #p<0.05, ###p<0.0002, ####p<0.0001: Significant statistical difference when compared to control. $^{\&}$p<0.05, $^{\&\&}$p<0.1906, $^{\&\&\&}$p<0.0002, $^{\&\&\&\&}$p<0.0001: Statistical difference when compared with the Osteogenic Medium. *p<0.05, **p<0.1906, ***p<0.0002, ****p<0.0001: Statistical difference when compared with the AoSMC treatment. *p<0.05, ****p<0.0001: Statistical difference when compared with the d-AoSMC treatment. ***p<0.0002: Statistical difference when compared with the HUVEC treatment.

We investigated the Runx2 gene behavior also considering the same experimental design **(Fig. 17a)**. In turn, Runx2 is a transcription factor that can be activated via β-Catenin. Our findings show and increased expression of DKK1 and SOST in the d-AoSMC-conditioning medium group. In addition, SOST was significantly increased in HUVEC and d-HUVEC responses, but d-HUVEC have been shown to be high β-Catenin expression when compared to the other experimental groups **(Fig. 17b - f)**.

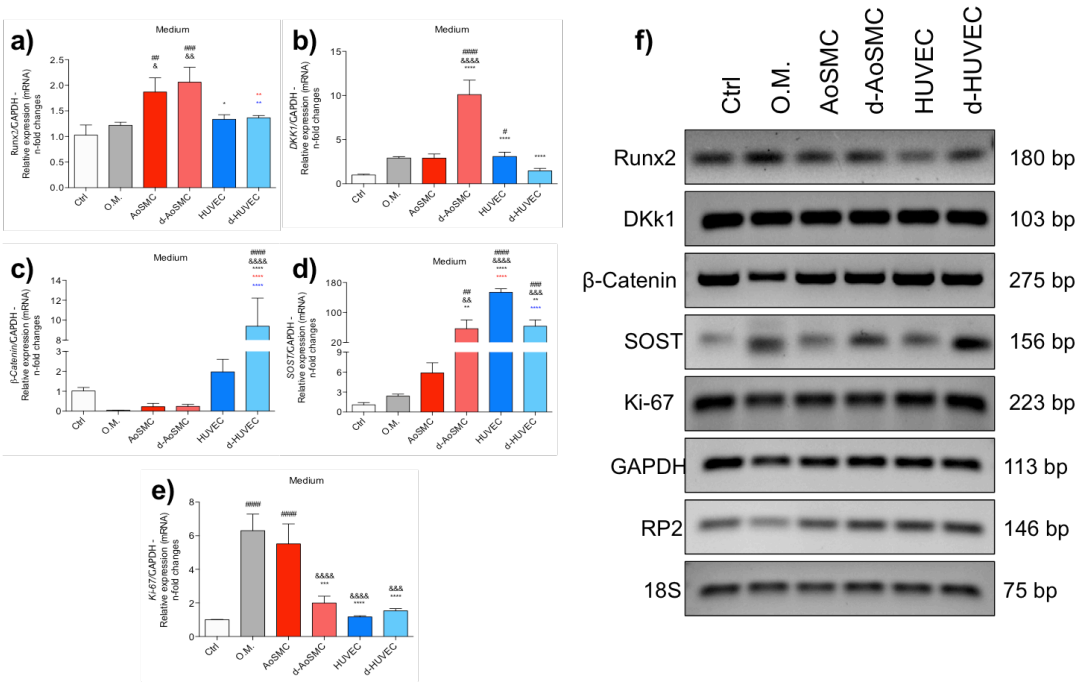

Figure 17. Gene expression profile of β-Catenin pathway components in undifferentiated mesenchymal cells. After 28 days of cell culture, cells that were treated with conditioned medium were collected in TriZOL. After cDNA collection and synthesis, Runx2 **(a)** and β-Catenin pathway genes were evaluated by Real Time PCR: DKK1, β-Catenin, SOST and Ki-67 **(b - f)**. Expression values were normalized by GAPDH reference gene. #p<0.05, ##p<0.1906, ###p<0.0002, ####p<0.0001: Significant statistical difference when compared to control. $^{\&}$p<0.05, $^{\&\&}$p<0.1906, $^{\&\&\&}$p<0.0002, $^{\&\&\&\&}$p<0.0001: Statistical difference when compared with the Osteogenic Medium. *p<0.05, ***p<0.0002, ****p<0.0001: Statistical difference when compared with the AoSMC treatment. **p<0.1906, ****p<0.0001: Statistical difference when compared with the d-AoSMC treatment. **p<0.1906, ****p<0.0001: Statistical difference when compared with the HUVEC treatment.

β-Catenin signaling pathway related members were evaluated in groups that received only primary cell-derived exosomes. An increase in SOST-related gene was observed only in the d-AoSMC and HUVEC groups **(Fig. 18e)**.

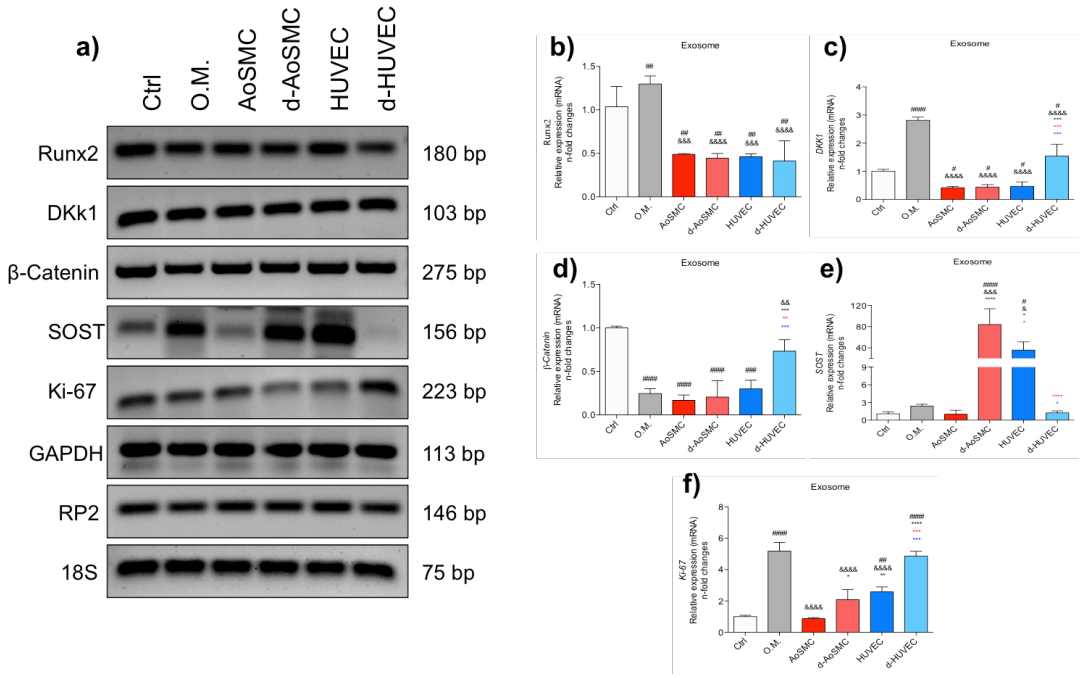

Figure 18. Gene expression profile of β-Catenin pathway components in undifferentiated mesenchymal cells treated with Exosome from Endothelial cells. After 28 days of cell culture, cells that were treated with Exosome were collected in TriZOL. After cDNA collection and synthesis, Runx2 **(b)** and β-Catenin pathway genes were evaluated by Real Time PCR: DKK1, β-Catenin, SOST and Ki-67 **(c - f)**. Expression values were normalized by GAPDH reference gene. #p<0.05, ##p<0.1906, ###p<0.0002, ####p<0.0001: Significant statistical difference when compared to control. $^{\&}$p<0.05, $^{\&\&}$p<0.1906, $^{\&\&\&}$p<0.0002, $^{\&\&\&\&}$p<0.0001: Statistical difference when compared with the Osteogenic Medium. *p<0.05, **p<0.1906, ***p<0.0002, ****p<0.0001: Statistical difference when compared with the AoSMC treatment. *p<0.05, **p<0.1906, ***p<0.002, ****p<0.0001: Statistical difference when compared with the d-AoSMC treatment. *p<0.05, ***p<0.0002: Statistical difference when compared with the HUVEC treatment.

In the terminal phase of osteoblasts differentiation is undergo to apoptosis or differentiating in osteocytes, once they are embedded into the synthesized matrix. Thus, we now evaluate genes that are specific markers of this cell type. The groups that received medium conditioned by smooth muscle cells showed high levels of expression in these cell markers. Genes involved with Calcium and Phosphate (DMP1, MEPE, PHEX and MMP14) were increased, in addition to GP-38, a gene involved with dendrite formation **(Fig. 19a-g)**.

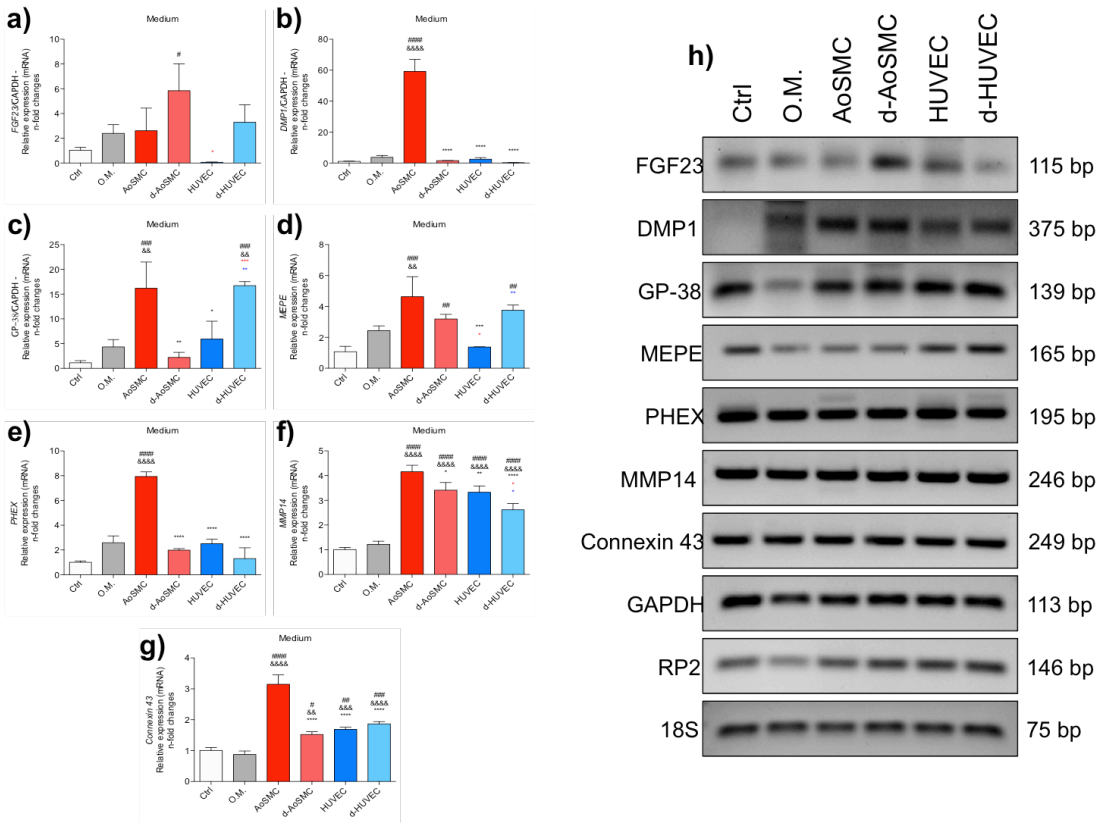

Figure 19. Osteocyte gene markers evaluated in Mesenchymal Cells treated with media conditioned by primary endothelial cells. After the experimental period and RNA collection for cDNA synthesis, specific osteocyte targets were evaluated by the real time PCR technique: FGF23, DMP1, GP-38, MEPE, PHEX, MMP14 and Connexin-43 **(a - g)**. At the end of the machine runs, samples were collected and run on agarose gel to reveal band intensity **(h)**. Expression values were normalized by GAPDH reference gene. #p<0.05, ##p<0.1906, ###p<0.0002, ####p<0.0001: Significant statistical difference when compared to control. $^{\&\&}$p<0.1906, $^{\&\&\&}$p<0.0002, $^{\&\&\&\&}$p<0.0001: Statistical difference when compared with the Osteogenic Medium. *p<0.05, **p<0.1906, ***p<0.0002, ****p<0.0001: Statistical difference when compared with the AoSMC treatment. *p<0.05, ***p<0.002: Statistical difference when compared with the d-AoSMC treatment. *p<0.05, **p<0.1906: Statistical difference when compared with the HUVEC treatment.

For the groups receiving Exosomes we observed a different expression profile than that observed with culture medium. FGF23 and GP-38 were expressed at higher levels in the group receiving HUVEC released exosomes that did not experience *Shear-Stress*, while DMP1 and MEPE were more expressed in the d-HUVEC group. MMP14 and Connexina-43 were more expressed in all groups except Osteogenic Medium when compared to the control group **(Fig. 20b-h)**.

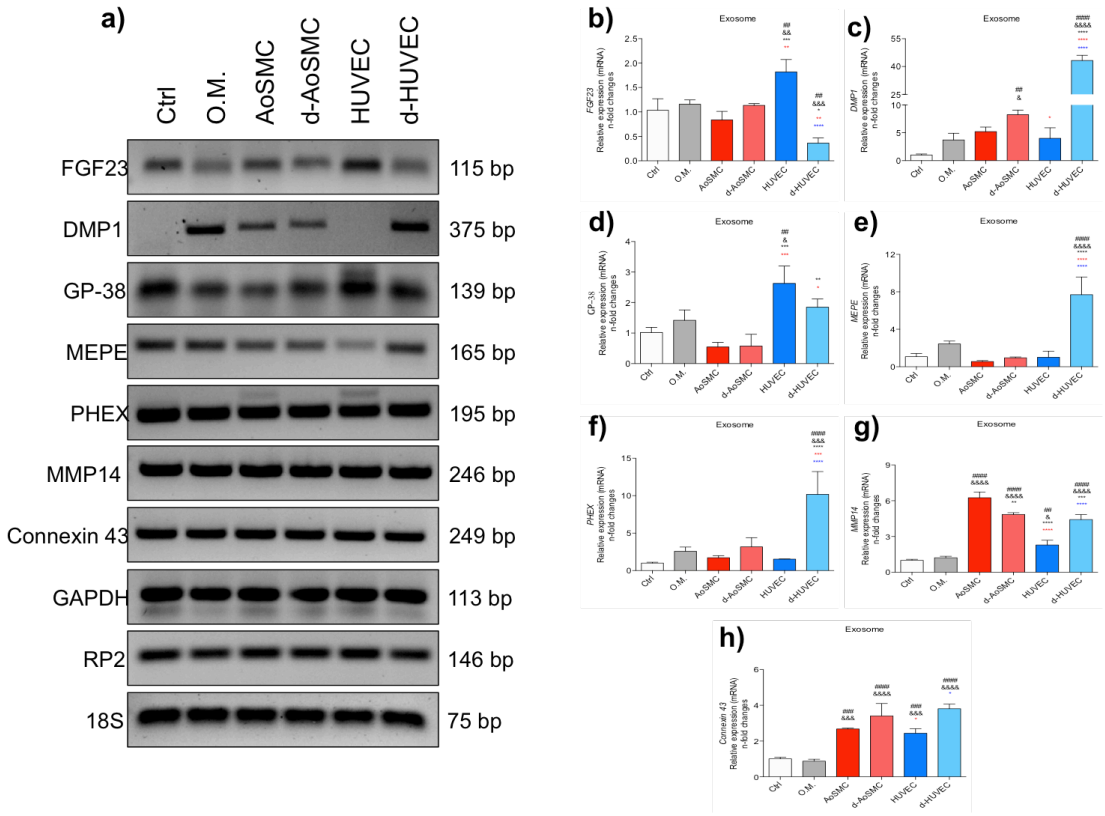

Figure 20. Osteocyte markers evaluated in exosome treated mesenchymal cells released by primary endothelial cells. After the experimental period and RNA collection for cDNA synthesis, specific osteocyte targets were evaluated by the real time PCR technique: FGF23, DMP1, GP-38, MEPE, PHEX, MMP14 and Connexin-43 **(a - g)**. At the end of the machine runs, samples were collected and run on agarose gel to reveal band intensity **(h)**. Expression values were normalized by GAPDH reference gene. ##p<0.1906, ###p<0.0002, ####p<0.0001: Significant statistical difference when compared to control. $^{\&}$p<0.05, $^{\&\&}$p<0.1906, $^{\&\&\&}$p<0.0002, $^{\&\&\&\&}$p<0.0001: Statistical difference when compared with the Osteogenic Medium. *p<0.05, **p<0.1906, ***p<0.0002, ****p<0.0001: Statistical difference when compared with the AoSMC treatment. *p<0.05, **p<0.1906, ***p<0.002, ****p<0.001: Statistical difference when compared with the d-AoSMC treatment. *p<0.05, ****p<0.001: Statistical difference when compared with the HUVEC treatment.

By using String tool (*in silico*), we can able to identify an interaction between genes evaluated as biomarkers of osteoblast-osteocyte transition (**Fig. 21**).

Primary cells modulate the expression of genes involved with epigenetic mechanisms in mesenchymal cells.

Effects on gene expression may be the result of modifications in DNA structure, undergoing by epigenetic issues. These mechanisms modulate DNA folding in Histones, which alters the exposure of gene expression promoting regions and may therefore

promote or inhibit the content of certain genes. In order to verify whether the proposed treatments (Medium or Exosomes) could alter the expression of genes involved with epigenetic control mechanisms, we investigated the expression of DNA Methyltransferase (DNMT) promoting enzymes and Demethylation promoting enzymes (Tet Methylcytosine Dioxygenase (TET)). Our results showed that primary cell conditioned media promoted a significant increase in DNMT3A expression in AoSMC and d-HUVEC cultures, and there was an increase in TET1 and TET2 expression in all groups receiving HUVEC or AoSMC Endothelial cell conditioned media. *Shear-Stress* or Static **(Fig. 22a-f)**.

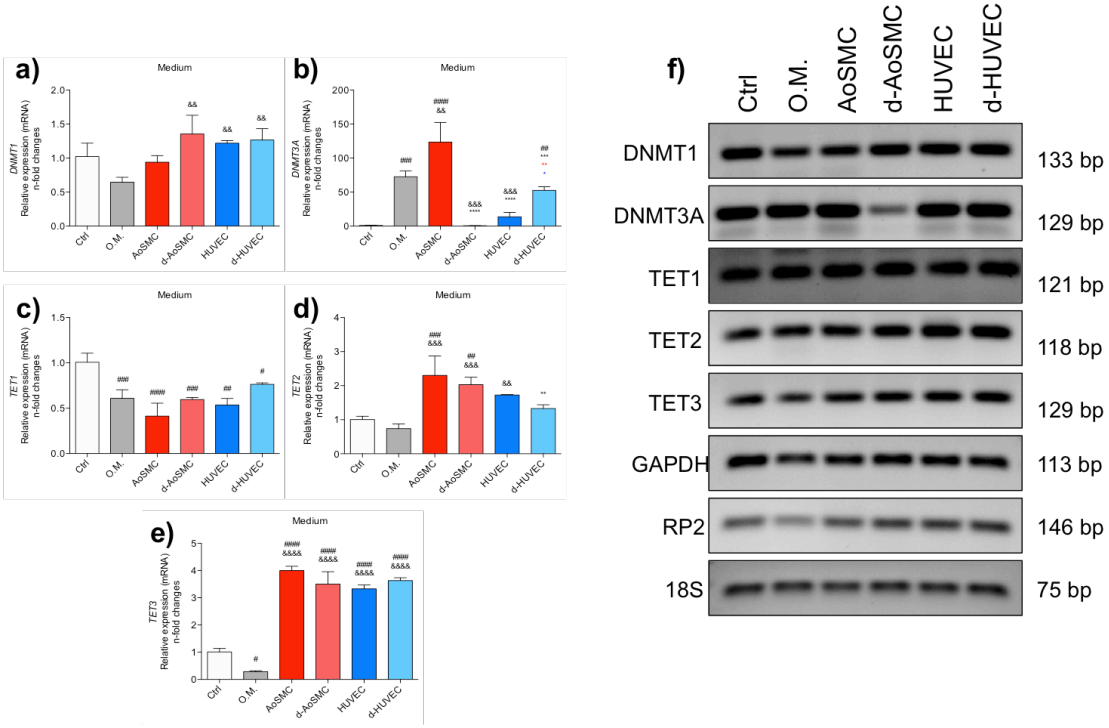

Figure 22. Effect of primary cell conditioned medium on the expression of mesenchymal cell DNMTs and TETs. After the experimental period, the cells receiving the conditioned medium were collected in TriZOL and the extracted RNA used for cDNA synthesis. Using the real - time PCR tool, genes involved with DNA methylation and demethylation **(a - e)** were evaluated, and after machine run the samples were collected and applied on agarose gel **(f)**. Expression values were normalized by GAPDH reference gene. #p<0.05, ##p<0.1906, ###p<0.0002, ####p<0.0001: Significant statistical difference when compared to control. $^{\&\&}$p<0.1906, $^{\&\&\&}$p<0.0002, $^{\&\&\&\&}$p<0.0001: Statistical difference when compared with the Osteogenic Medium. **p<0.1906, ***p<0.0002, ****p<0.0001: Statistical difference when compared with the AoSMC treatment. **p<0.1906: Statistical difference when compared with the d-AoSMC treatment. *p<0.05: Statistical difference when compared with the HUVEC treatment.

Compared to that observed with the culture medium, exosomes did not positively

modulate TET expression, but d-AoSMC and d-HUVEC promoted increased expression of DNMT3A **(Fig. 23a - f)**.

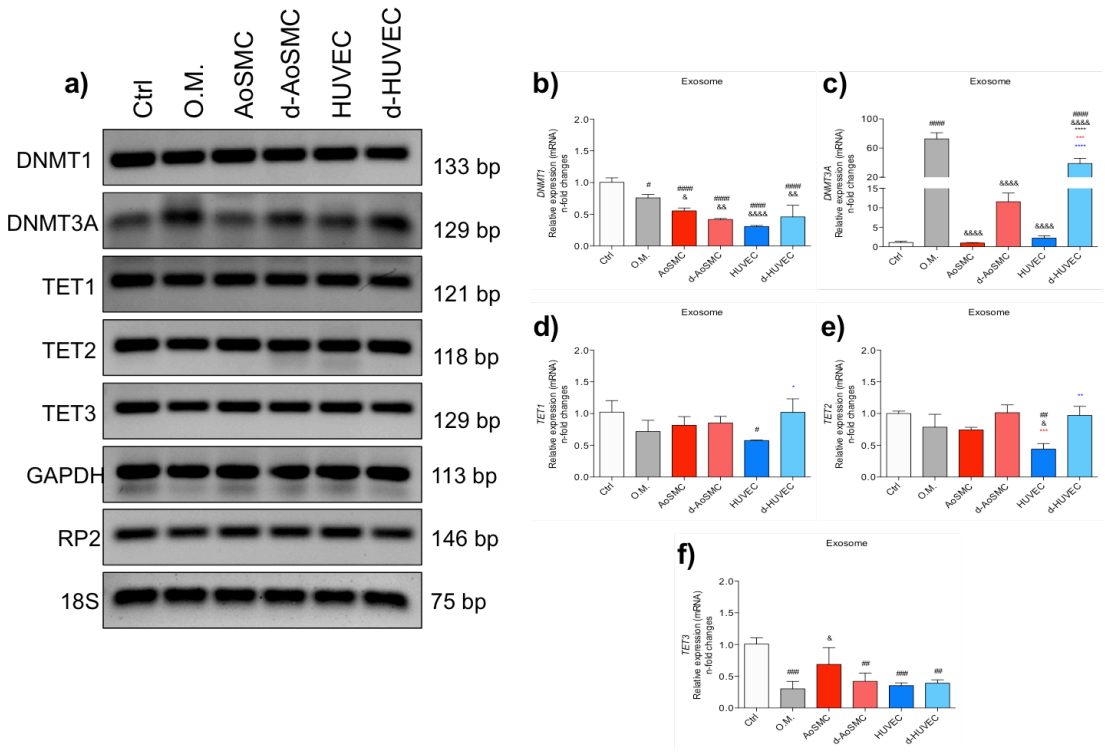

Figure 23. Effect of exosomes released by primary cells on the expression of mesenchymal cell DNMTs and TETs. After the experimental period, cells receiving the different Exosome treatments were collected in TriZOL and the extracted RNA used for cDNA synthesis. Using the real - time PCR tool, genes involved with DNA methylation and demethylation (b - f) were evaluated, and after machine run the samples were collected and applied on agarose gel (a). Expression values were normalized by GAPDH reference gene. #p<0.05, ##p<0.1906, ###p<0.0002, ####p<0.0001: Significant statistical difference when compared to control. $^{\&}$p<0.05, $^{\&\&}$p<0.1906, $^{\&\&\&\&}$p<0.0001: Statistical difference when compared with the Osteogenic Medium. ****p<0.0001: Statistical difference when compared with the AoSMC treatment. ***p<0.0002: Statistical difference when compared with the d-AoSMC treatment. *p<0.05, **p<0.1906, ****p<0.0001: Statistical difference when compared with the HUVEC treatment.

While the Methylation/Demethylation process takes place on the DNA strand, another important epigenetic mechanism promotes histone Acetylation/Deacetylation. They act in the same way by exposing the gene transcription regions of DNA. The data involving the expression of HDACs was quite interesting to us, as HDAC1, HDAC2 and Sirt1 expression was increased in all treatments receiving the primary cell-conditioned medium, while the fewer genes were down-regulated in the groups receiving Exosomes from the same cells that conditioned the medium **(Fig. 24a - j).**

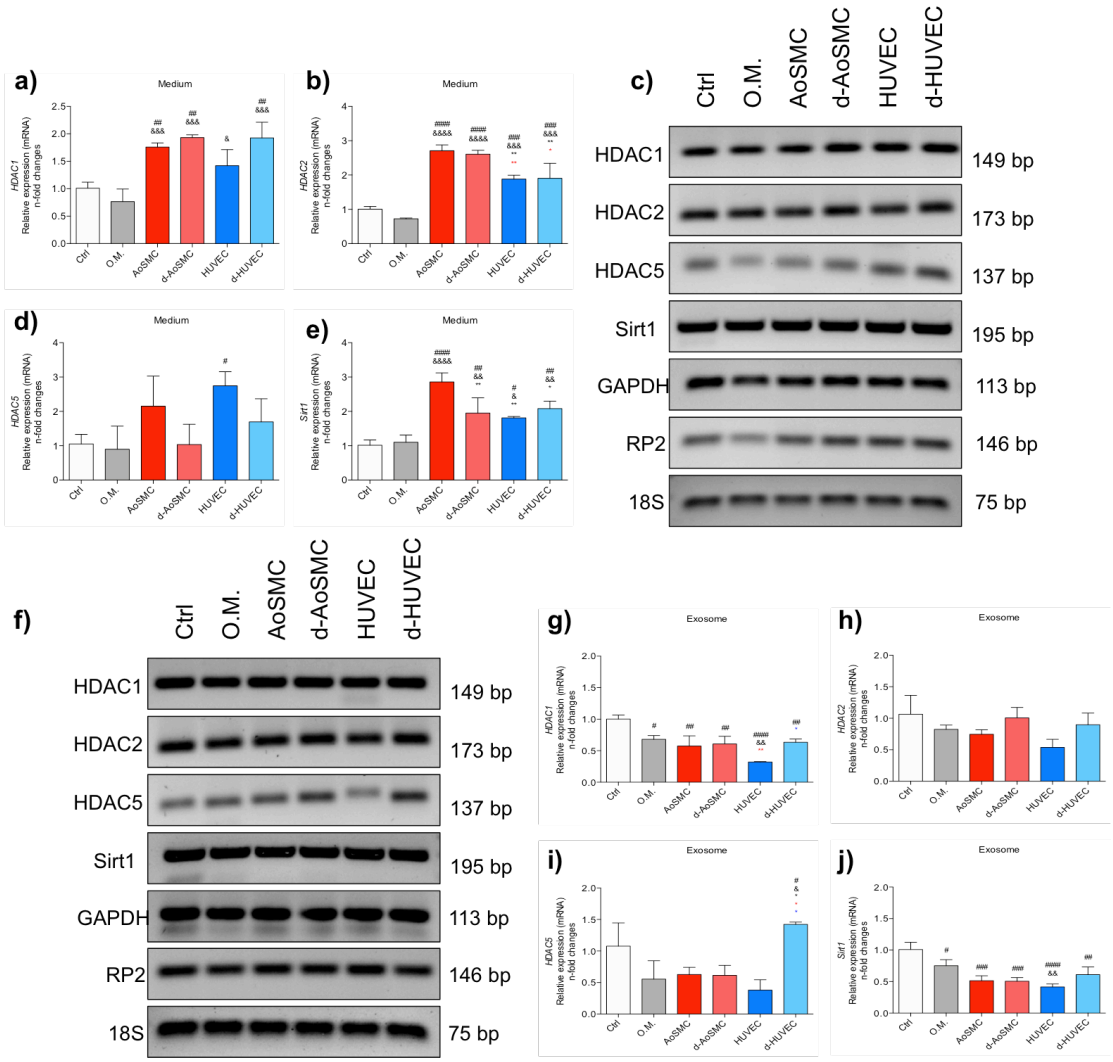

Figure 24. Cellular crosstalk between endothelial and mesenchymal cells in DNA acetylation gene expression. After the experimental period and RNA collection for cDNA synthesis, we use the real time PCR technique to evaluate the expression of HDAC1 **(a, g)**, HDAC2 **(b, h)**, HDAC5 **(d, i)** and Sirt1 **(e, j)**. The PCR results were collected after the end of the race and applied in agarose gel **(c, f)**. Expression values were normalized by GAPDH reference gene. #p<0.05, ##p<0.1906, ###p<0.0002, ####p<0.0001: Significant statistical difference when compared to control. $^{\&}$p<0.05, $^{\&\&}$p<0.1906, $^{\&\&\&}$p<0.0002, $^{\&\&\&\&}$p<0.0001: Statistical difference when compared with the Osteogenic Medium. *p<0.05, **p<0.1906: Statistical difference when compared with the AoSMC treatment. *p<0.05, **p<0.1906: Statistical difference when compared with the d-AoSMC treatment. *p<0.05: Statistical difference when compared with the HUVEC treatment.

Two other important genes evaluated in this study are those involved with cell metabolism, which seems requires the involvement of HOTTAIR and Hoxa8. Both genes showed increased expression in the groups responding to conditioned medium by smooth muscle cells **(Fig. 25 - b)**. While HOTTAIR decreased in d-AoSMC, HUVEC and d-

HUVEC **(Fig. 25c)** and Hoxa8 decreased in HUVEC and d-HUVEC, groups that received only exosomes. **(Fig. 25d)**.

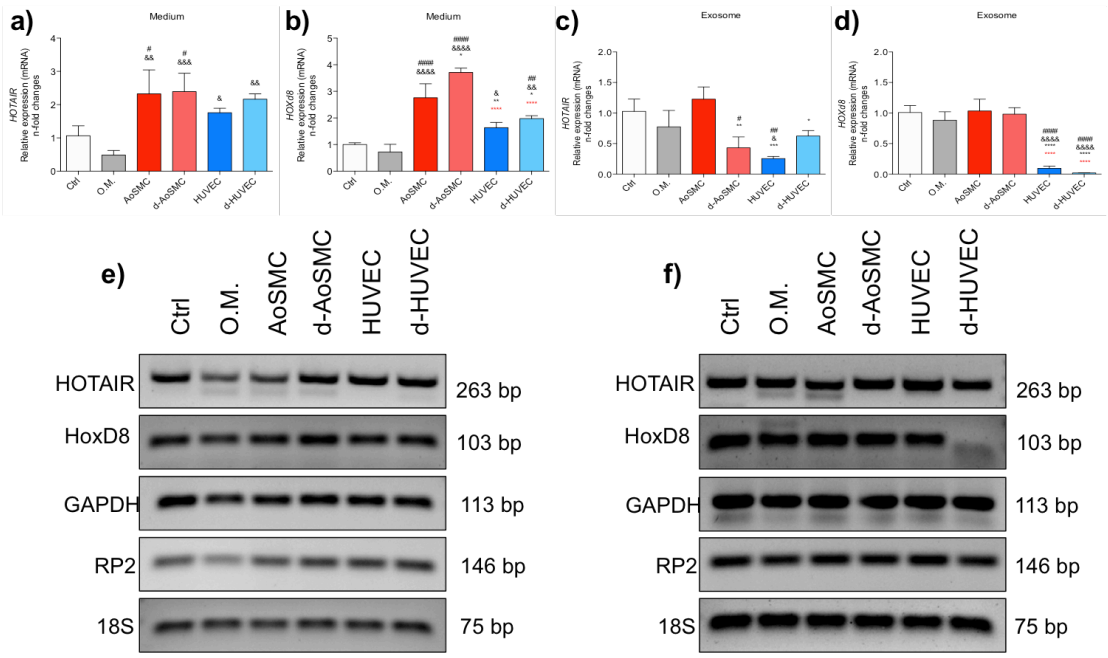

Figure 25. Effect on HOTTAIR and Hoxa8 in challenged mesenchymal stem cells. After 28 days of treatment with Medium or Exosome from primary cell, MSC were collected to study the gene expression of HOTTAIR **(a, c)** and Hoxa8 **(b, d)**. The amplified in real time PCR were collected and applied in agarose gel **(e, f)**. #p<0.05, ##p<0.1906, ####p<0.0001: Significant statistical difference when compared to control. $^{\&}$p<0.05, $^{\&\&}$p<0.1906, $^{\&\&\&}$p<0.0002, $^{\&\&\&\&}$p<0.0001: Statistical difference when compared with the Osteogenic Medium. *p<0.05, **p<0.1906, ***p<0.0002, ****p<0.0001: Statistical difference when compared with the AoSMC treatment. ****p<0.0001: Statistical difference when compared with the d-AoSMC treatment.

CONCLUSION

Together, these results validate the data found earlier by us, reinforcing the promotion of osteocyte acquisition by osteoblast responding to trophic molecules released by vascular smooth cells, and it is new within the field.

CAPÍTULO 7

DISCUSSÃO

Vasos sanguíneos são responsáveis por transportar diferentes componentes e promover a distribuição homogênea e necessária de nutrientes, gases e metabólitos celulares a todos os demais tecidos (Shalaby et al. 1995; Chen et al. 2016; Gamrekelashvili et al. 2016). Conduzidos através de veias e artérias, que se ramificam ao longo dos tecidos com variações no calibre do vaso, os componentes para homeostase celular circulam por ação da pressão cardíaca, o que gera uma tensão necessária para que a condução e distribuição aconteça, além de estimular a liberação de componentes pelas próprias células do tecido vascular (Matlung et al. 2009; Chatterjee and Fisher 2014; Chatterjee and Fisher 2014). Portanto a manutenção dos diferentes tecidos depende de refinados ajustes com o tecido endotelial.

Considerando o dinamismo do tecido ósseo, produção e degradação da matriz orgânica e mineral, e a necessidade de manutenção de nutrientes para que a regeneração óssea ocorra de maneira sinérgica, diversos estudos apontam a importância do acoplamento entre angiogênese e osteogênese (Ramasamy et al. 2014; Kusumbe et al. 2014; Kusumbe and Adams 2014; Ramasamy et al. 2016; Romeo et al. 2019). Alguns autores apontam para o acoplamento entre células de vasos e osteoblastos diante de uma injúria óssea, ou seja, a importância da formação de uma rede de capilares durante a cicatrização e regeneração do tecido perdido (Saran et al. 2014; Kazmers et al. 2015). Há dados, ainda, que apontam a necessidade de manutenção da microvascularização nos ossos e que o comprometimento desse processo diminui a osteogênese em indivíduos com grau inicial de osteoporose ou indivíduos idosos (Teti 2011; Fayyazbakhsh et al. 2017).

Ainda tratando da homeostase óssea, osteoblastos em fase final de diferenciação celular podem sofrer apoptose (≅40%) ou se diferenciarem em Osteócitos (≅60%) que compreendem cerca de 95% das células do tecido ósseo e através de mecanotransdução disparam sinais para as demais células do osso ou vasos e esse *crosstalk* ocorre através de

dendritos que se ramificam ao longo do tecido (Komori 2006; Dallas et al. 2013; Grabowski 2015). Nesse cenário, nós buscamos avaliar o impacto de células endoteliais (HCAEC e HUVEC) e de Células de Musculatura Lisa (Aorta) (AoSMC) na diferenciação e performance de osteoblastos, além de avaliar o impacto de fibroblastos nesse processo de diferenciação celular. Cabe nota que a interação destas células ocorre histologicamente no microambiente do osso.

Temos mostrado que fibroblastos atuam de maneira parácrina em pré-osteoblastos, modulando sua diferenciação de maneira independente a via de Sonic Hedgehog, ao mesmo tempo que secretam fatores importantes para remodelamento da Matriz Extracelular e ativação de genes marcadores de osteócitos como DMP1 e SOST (Ducy et al. 2000; da Costa Fernandes et al. 2017). Importante destacar que o efeito parácrino trouxe aumento da expressão de OPG, que atua de maneira antagônica a Rank-L na diferenciação de Osteoclastos (Winkler et al. 2003; Kobayashi et al. 2009; Zeng et al. 2017; Uda et al. 2017).

Nossos dados trazem ainda o efeito de células endoteliais na transição osteoblastos-Osteócitos. Mostramos que AoSMC atuam nesse fenômeno através de vesículas extracelulares, exossomos, e que cerream marcadores importantes para essa transição. Verificamos transcritos de SOST e miR-23a no carregamento dos exossomos produzidos e secretados em condições experimentais (Estático e Shear-Stress) e em osteoblastos que receberam os meios condicionados, esses marcadores inibem a diferenciação de osteoblastos (SOST inibe a via de β-Catenina inibindo sua translocação ao núcleo e levando a não transcrição de Runx2 (Semenov et al. 2005; Vimalraj et al. 2015; Zeng et al. 2017; Shao et al. 2018; Godfrey et al. 2018). Além disso, vimos aumento de FGF23 e DMP1 nos osteoblastos tratados, dois importantes reguladores de cálcio e fosfato no tecido ósseo que e que são marcadores de Osteócitos (Rios et al. 2005; Nicolella et al. 2006; Bonewald 2011; Mattinzoli et al. 2016; Pathak et al. 2016; Kuczera et al. 2016). Vale destacar que a transição de osteoblastos-osteócitos promove aumento da expressão de osteocalcina.

CAPÍTULO 8

CONSTATAÇÕES

Os resultados obtidos, com a execução do estudo, nos permitem constatar:

1. Fibroblastos produzem fatores tróficos que modulam o comportamento de pré-osteoblastos quanto a: Diferenciação e Remodelamento da Matriz Extracelular;
2. Células de musculatura lisa (AoSMC) atuam de maneira parácrina na transição Osteoblastos – Osteócitos através de vesículas extracelulares;
3. Marcadores gênicos de Osteócitos são produzidos por células Endoteliais e Musculares em diferentes níveis e transportados por vesículas extracelulares;
4. Nossas condições experimentais mostraram que as células do endotélio liberam vesículas caracterizadas como Exossomos em função do tamanhos (≅ 150nm);
5. A via de β-Catenina ocupa papel central da transição de Osteoblastos – Osteócitos através da ação de SOST;
6. Osteócitos obtidos experimentalmente são fontes de marcadores da diferenciação de Osteoclastos: RANKL e Osteoprotegerina (OPG);
7. Exossomos carream molécula de ATP que possui importante papel na minelização tecidual, uma vez que degradado forma Pi que pode ser acoplado a cálcio e formar hidroxiapatita em vesículas de mineralização.
8. Células endoteliais HUVEC modulam diferencialmente a transição de células mesenquimais a osteoblastos, quando comparadas às células AoSMC levando em consideração apenas vesículas ou meio de cultura completo.

CAPÍTULO 9

CONCLUSÃO

Levando em consideração nossas constatações, concluímos que células do tecido endotelial e fibroblastos contribuem com a homeostase do tecido ósseo, sobretudo guiando a transição osteoblasto-osteócito através de fatores tróficos e vesículas extracelulares.

CAPÍTULO 10

ATIVIDADES DESENVOLVIDAS NO PERÍODO

RESUMOS EM CONGRESSO:

[1] FERNANDES, Célio Junior da Costa; NASCIMENTO, Augusto Santana; ZAMBUZZI, Willian Fernando. Avaliação de efeitos heterótipos disparados por Fibroblastos na adesão celular e citotoxicidade de Osteoblastos. 2016.

[2] CARMO, M. D.; ROSSI, Mariana Correa; FERNANDES, Célio Junior da Costa; ZAMBUZZI, Willian Fernando. Meio condicionado a partir de ligas de Co-Cr afetam diferencialmente o comportamento de osteoblastos e fibroblastos. 2016.

[3] FERNANDES, Célio Junior da Costa; SILVA, R. A.; ZAMBUZZI, Willian Fernando. Avaliação de efeitos heterótipos disparados por Fibroblastos na adesão e diferenciação de Pré-osteoblastos. 2016.

[4] FELTRAN, G. S.; TAVORA, I. G.; FERNANDES, Célio Junior da Costa; SILVA, R. A.; ZAMBUZZI, Willian Fernando. ENVOLVIMENTO DA VIA DE SONIC HEDGEHOG (Shh) EM MECANISMOS DE MIGRAÇÃO DE CÉLULAS PROVENIENTES DE CARCINOMA ESCAMOSO BUCAL. 2016.

[5] SILVA, R. A.; FERNANDES, Célio Junior da Costa; FELTRAN, G. S.; ZAMBUZZI, Willian Fernando. INFLUENCIA FISIOLOGICA DO SHEAR STRESS NO COMPORTAMENTO DE CÉLULAS DE MUSCULATURA LISA. 2016.

[6] NASCIMENTO, Augusto Santana; FERREIRA, Marcel Rodrigues; FERNANDES, C. J. C.; ROSSI, Mariana Correa; CARANDINA, R. F.; ZAMBUZZI, Willian Fernando. Fosfoproteoma revela envolvimento crítico na sinalização de JAK-STAT na resistência química de células de câncer de mama. In: II Workshop de Biotecnologia, 2016, Botucatu. Anais II Workbiotec - Workshop de Biotecnologia, 2016.

[7] NASCIMENTO, Augusto Santana; FERREIRA, Marcel Rodrigues; FERNANDES, Célio Junior da Costa; CARANDINA, R. F.; ZAMBUZZI, Willian Fernando. Phosphoproteome reveals critical PKS and JAK-STAT signaling involvement on breast cancer cells chemical resistance. In: 45th Annual Meeting of the Brazilian Society for Biochemistry and Molecular biology (SBBq), 2016, Natal. SBBq, 2016.

[8] FERNANDES, Célio Junior da Costa; JORGE, LG; DANADAI, A. C.; NASCIMENTO, Augusto Santana; ZAMBUZZI, Willian Fernando. CHEMICAL MODULATORS OF PTKS ACTIVITY AS STRATEGY FOR OSTEOBLAST DIFFERENTIATION. In: 45th Annual Meeting of the Brazilian Society for Biochemistry and Molecular biology (SBBq), 2016, Natal. SBBq, 2016.

[9] MARUMOTO, A.; NASCIMENTO, Augusto Santana; FERNANDES, Célio Junior da Costa; CARANDINA, R. F.; MILANI, R.; FERREIRA, C V.; ZAMBUZZI, Willian Fernando. Osteoblast morphological chances is autocrine-Sonic Hedgehog-dependent in a bio-inspired three-dimensional in vitro model. In: 45th Annual Meeting of the Brazilian Society for Biochemistry and Molecular biology (SBBq), 2016, Natal. SBBq, 2016.

[10] ANDRADE, A. F. C.; FELTRAN, G. S.; FERNANDES, Célio Junior da Costa; SILVA, R. A.; ZAMBUZZI, Willian Fernando. Reprogramação osteogênica a partir do efeito sinérgico do hormônio T_3 e células endoteliais. In: XXIX Congresso de Inciação Científica da UNESP, 2017, Botucatu. XXIX CIC, 2017.

[11] MARTINS, B. R.; FERNANDES, Célio Junior da Costa; BEZERRA, Fábio; ZAMBUZZI, Willian Fernando. Revisitando a biocompatibilidade de liga de titânio sob um aspecto intracelular. In: XXIX Congresso de Inciação Científica da UNESP, 2017, Botucatu. XXIX CIC, 2017.

[12] Santaella F ; FERNANDES, Célio Junior da Costa; FELTRAN, G. S.; ZAMBUZZI, Willian Fernando. Ligas de Cobalto-Cromo modulam adesão através de vias de reorganização do citoesqueleto de pré-osteoblastos. In: XXIX Congresso de Inciação Científica da UNESP, 2017, Botucatu. XXIX CIC, 2017.

[13] Kang HR; FERNANDES, Célio Junior da Costa; CONSTANTINO, V.; KOH, I. H. J.; ZAMBUZZI, Willian Fernando. Nanopartículas de Hidróxido Duplo Lamelares (HDLs) promovem expressão dinâmica de marcadores gênicos na diferenciação osteogênica. In: XXIX Congresso de Inciação Científica da UNESP, 2017, Botucatu. XXIX CIC, 2017.

[14] ANDRADE, A. F. C.; FERNANDES, Célio Junior da Costa; FELTRAN, G. S.; SILVA, R. A.; ZAMBUZZI, Willian Fernando. SYNERGIC EFFECT OF THYROID HORMONE (T3) AND MECHANICALLY-STRESSED ENDOTHELIAL CELLS-RELEASED FACTORS ON IN VITRO HUMAN MESENCHYMAL STEM CELL MINERALIZATION. In: 46 Annual Meeting of Brazilian Society for Biochemistry and Molecular Biology, 2017, Águas de Lindóia. SBBq, 2017.

[15] CARMO, M. D.; FERNANDES, Célio Junior da Costa; BEZERRA, FJB; Santaella F; FELTRAN, G. S.; ROSSI, MC ; SILVA, R. A.; ZAMBUZZI, Willian Fernando. COBALT-CHROME DIFFERENTIALLY GOVERN PRE-OSTEOBLAST AND FIBROBLAST PERFORMANCE BY MODULATING SURVIVAL INTRACELLULAR PATHWAYS. In: 46 Annual Meeting of Brazilian Society for Biochemistry and Molecular Biology, 2017, Águas de Lindóia. SBBq, 2017.

[16] Kang HR; FERNANDES, Célio Junior da Costa; SILVA, R. A.; CONSTANTINO, V.; KOH, J. H. I.; ZAMBUZZI, WF. LAYERED DOUBLE HYDROXIDE MODULATES PRE-OSTEOBLAST AND FIBROBLAST PERFORMANCE. In: 46 Annual Meeting of Brazilian Society for Biochemistry and Molecular Biology, 2017, Águas de Lindóia. SBBq, 2017.

[17] TAVORA, I. G.; FELTRAN, G. S.; FERNANDES, Célio Junior da Costa; SILVA, R. A.; ZAMBUZZI, Willian Fernando. Shh signaling suppression up-modulates B1-integrin expression and compromises cell performance. In: 46 Annual Meeting of Brazilian Society for Biochemistry and Molecular Biology, 2017, Águas de Lindóia. SBBq, 2017.

[18] SILVA, R. A.; Pinto TS; FERNANDES, Célio Junior da Costa; FELTRAN, G. S.; ANDRADE, A. F. C.; GOMES AM; ZAMBUZZI, Willian Fernando. EPIGENETIC MACHINERY DISRUPTS GSK3ß/ß-CATENIN SIGNALING-BASED TIMP-1 EXPRESSION IN MECHANICALLY-STRESSED PRIMARY SMOOTH MUSCLE CELLS. In: 46 Annual Meeting of Brazilian Society for Biochemistry and Molecular Biology, 2017, Águas de Lindóia. SBBq, 2017.

[19] GOMES AM; SILVA, R. A.; da Costa Fernandes C jr; FELTRAN, G. S.; ANDRADE, A. F. C.; ZAMBUZZI, Willian Fernando. Comportamento molecular e Epigenéticos de células endoteliais submetidas ao Shear Stress. 2017.

[20] SILVA, R. A.; Pinto TS; da Costa Fernandes C jr; FELTRAN, G. S.; ANDRADE, A. F. C.; GOMES AM; ZAMBUZZI, Willian Fernando. Maquinaria epigenética interfere na expressão de TIMP1 modulada pela via GSK3β/β-Catenina em células de músculo liso primário mecanicamente estressadas. 2017.

[21] Kang HR; da Costa Fernandes C jr; CONSTANTINO, V.; KOH, J. H. I.; ZAMBUZZI, Willian Fernando. Nanopartícula inorgânicas de Hidróxido Duplos Lamelares (HDL?s) como modulador de desempenho de pré-osteoblastos e fibroblastos. 2017.

[22] ANDRADE, A. F. C.; da Costa Fernandes C jr; FELTRAN, G. S.; SILVA, R. A.; ZAMBUZZI, Willian Fernando. Efeitos sinérgicos do hormônio da tireoide (T3) e fatores tróficos liberados por células endoteliais sob Shear stress ? Efeitos na mineralização de células mesenquimais humanas in vitro. 2017.

[23] CARMO, M. D.; da Costa Fernandes C jr; BEZERRA, Fábio; Santaella F; FELTRAN, G. S.; ROSSI, Mariana Correa; SILVA, R. A.; ZAMBUZZI, Willian Fernando. O cobalto-cromo governa

diferencialmente o desempenho pre-osteoblástico e fibroblástico através da modulação das vias intracelulares de sobrevivência. 2017.

[24] ISHIKAWA, A. S. K.; EVANGELISTA, G.; FERNANDES, CÉLIO J. C.; DOYAMA, J. T.; SAEKI, M.; ZAMBUZZI, Willian Fernando; BOSCO, S.; OLIVEIRA, S.. Evaluation of the Dillapiol Effect in Fibroblast Viability. 2017.

[25] GOMES AM; SILVA, R. A.; FERNANDES, CÉLIO J. C.; FELTRAN, G. S.; ANDRADE, A. F. C.; ZAMBUZZI, Willian Fernando. Alterations in matrix remodeling and in the activity of metalloproteinases in endothelial cells submitted to shear stress. 2017.

[26] FERNANDES, CÉLIO J. C.; SILVA, R. A.; ZAMBUZZI, Willian Fernando. Paracrine effect of shear-stress-stimulated endothelial cells on osteoblasts differentiation. 2017.

[27] FERNANDES, CÉLIO J. C.; Santaella F; SILVA, R. A.; ZAMBUZZI, Willian Fernando. Cobalt-Chromium enriched medium requires a reprogramming inflammatory gene repertory. 2017.

[28] FERNANDES, CÉLIO J. C.; Santaella F; SILVA, R. A.; BEZERRA, Fábio; ZAMBUZZI, Willian Fernando. Cobalt and chromium enriched media modulates the expression of inflammatory cytokines in fibroblasts and alter the cell adhesion protein signaling profile. 2017.

[29] FELTRAN, G. S.; ANDRADE, A. F. C.; FERNANDES, CÉLIO J. C.; SILVA, R. A.; ZAMBUZZI, Willian Fernando. Generation and characterization of endothelium tissue spheroids. 2017.

[30] FERNANDES, CÉLIO J. C.; Kang HR; SILVA, R. A.; ZAMBUZZI, Willian Fernando. Fibroblasts contribute to the remodeling of the cytoskeleton by p-Rac1 in undifferentiated cells. 2017.

[31] Pinto TS; FERNANDES, CÉLIO J. C.; SILVA, R. A.; ZAMBUZZI, Willian Fernando. Shear Stress Modulates Cytoskeleton and Extracellular Matrix proteins in an in vitro Hypertension model. 2017.

[32] FERREIRA, Marcel Rodrigues; FERNANDES, CÉLIO J. C.; BEZERRA, Fábio; ZAMBUZZI, Willian Fernando. ZrO_2 enriched medium stimulates ECM-remodeling as a prerequisite to preosteoblast adhesion/proliferation by a possible interference on cell anchoring. 2017.

[33] ANDRADE, A. F. C.; SILVA, R. A.; FELTRAN, G. S.; FERNANDES, CJC; ZAMBUZZI, Willian Fernando. Sinergismo entre o hormônio tireoidiano (T_3) e os fatores tróficos liberados pelas células endoteliais na reprogramação gênica de células hMSC submetidas a osteogênese. In: 30 Congresso de Inicicação Científica da UNESP - Primeira Fase, 2018, Botucatu. 30 Congresso de Inicicação Científica da UNESP - Primeira Fase, 2018.

[34] ANDRADE, A. F. C.; SILVA, R. A.; FELTRAN, G. S.; FERNANDES, CJC; ZAMBUZZI, Willian Fernando. Sinergismo entre o hormônio tireoidiano (T_3) e os fatores tróficos liberados pelas células endoteliais na reprogramação gênica de células hMSC submetidas a osteogênese.. In: 30 Congresso de Inicicação Científica da UNESP - Segunda Fase, 2018, São Paulo. 30 Congresso de Inicicação Científica da UNESP - Segunda Fase, 2018.

[35] SILVA, R. A.; FERNANDES, CJC; FELTRAN, G. S.; GOMES AM ; ANDRADE, A. F. C.; C, A. D.; PEPPELENBOSCH, MAIKEL P.; ZAMBUZZI, W.F. Shear Stress Promotes Epigenetic Reprogramming of Timp1 gene guarantying Mmp2 activity in human primary smooth muscle cells. In: 47 Annual Meeting of Brazilian Society for Biochemistry and Molecular Biology, 2018, Joinville. 47 Annual Meeting of Brazilian Society for Biochemistry and Molecular Biology, 2018.

[36] FELTRAN, G. S.; ANDRADE, A. F. C.; FERNANDES, CJC; SILVA, R. A.; ZAMBUZZI, W.F. Generation and characterization of equivalent endothelium tissue for understanding the crosstalk between endothelial and smooth muscle cells. In: 47 Annual Meeting of Brazilian Society for Biochemistry and Molecular Biology, 2018, Joinville. 47 Annual Meeting of Brazilian Society for Biochemistry and Molecular Biology, 2018.

[37] Pinto TS; SILVA, R. A.; FERNANDES, CJC; GOMES AM; ZAMBUZZI, WILLIAN F. AN IN VITRO MODEL FOR STUDYING INTERMITTENT HYPERTENSION REVEALS AN INTRACELLULAR PICTURE CONCOMITANT TO ECM REMODELING IN ENDOTHELIAL CELLS. In: 47 Annual Meeting of Brazilian Society for Biochemistry and Molecular Biology, 2018, Joinville. 47 Annual Meeting of Brazilian Society for Biochemistry and Molecular Biology, 2018.

[38] ANDRADE, AMANDA F.C.; FELTRAN, G. S.; SILVA, R. A.; FERNANDES, CJC; ZAMBUZZI, W.F. THE ROLE OF THYROID HORMONE (T_3) AND MECHANICALLY-STRESSED ENDOTHELIAL CELL PARACRINE SIGNALING SYNERGISM IN GENE REPROGRAMMING DURING HMSC-STIMULATED OSTEOGENIC PHENOTYPE IN VITRO. In: 47 Annual Meeting of Brazilian Society for Biochemistry and Molecular Biology, 2018, Joinville. 47 Annual Meeting of Brazilian Society for Biochemistry and Molecular Biology, 2018.

[39] GOMES AM; SILVA, R. A.; FERNANDES, CJC; Pinto TS; ZAMBUZZI, W.F. CYTOSKELETON REARRANGEMENT AS A PREREQUISITE FOR MAINTAINING ESSENTIAL INTRACELLULAR PATHWAYS IN MECHANICALLY-STRESSED ENDOTHELIAL CELLS. In: 47 Annual Meeting of Brazilian Society for Biochemistry and Molecular Biology, 2018, Joinville. 47 Annual Meeting of Brazilian Society for Biochemistry and Molecular Biology, 2018.

[40] FERNANDES, CJC; SILVA, R. A.; FERREIRA, C V.; ZAMBUZZI, W.F. Dynamic Regulation of Osteocytogenesis by Aortic Smooth Muscle Cells-Derived Exosomes. In: 47 Annual Meeting of Brazilian Society for Biochemistry and Molecular Biology, 2018, Joinville. 47 Annual Meeting of Brazilian Society for Biochemistry and Molecular Biology, 2018.

[41] FERNANDES, CJC; SILVA, R. A.; ZAMBUZZI, Willian Fernando. SMOOTH MUSCLE CELLS-RELEASED EXOSOMES PROMOTE OSTEOBLAST-OSTEOCYTE TRANSITION VIA B-CATENINA. In: XIX Congress of the Brazilian Society for Cell Biology, 2018, São Paulo. XIX Congress of the Brazilian Society for Cell Biology, 2018.

[42] NUNES, PRISCILA REZECK; ROMAO, M.; MATIAS, M. L.; RIBEIRO, VANESSA ROCHA; FERNANDES, CÉLIO JÚNIOR DA C.; DE OLIVEIRA, LEANDRO; RODRIGUES, JOSE RICARDO; BORGES, V. T.; PERACOLI, J. C.; Peraçoli, M T S. Vitamin D decreases gene and protein expression of $NLRP_3$ inflammasome in placental explants cultured with hydrogen peroxide from women with preeclampsia. In: International Society for the Study of Hypertension in Pregnancy (ISSHP), 2018, Amsterdam. International Society for the Study of Hypertension in Pregnancy (ISSHP), 2018.

[43] SILVA, R. A.; Janmat V T; FERNANDES, CJC; FELTRAN, G. S.; ZAMBUZZI, W.F.; PEPPELENBOSCH, MAIKEL P. . Epigenetic control of HOXA gene family cluster in osteoblast differentiation. 2018.

[44] Pinto TS; SILVA, R. A.; FERNANDES, CJC; GOMES AM; ZAMBUZZI, Willian Fernando. AN IN VITRO MODEL FOR STUDYING INTERMITTENT HYPERTENSION REVEALS AN INTRACELLULAR PICTURE CONCOMITANT TO ECM REMODELING IN ENDOTHELIAL CELLS. 2018.

[45] FERNANDES, CJC; FERREIRA, Marcel Rodrigues; ZAMBUZZI, W.F. BIOINFORMATIC TOOLS DRAW BIOLOGICAL PANORAMA INVOLVED WITH OSTEOBLAST - OSTEOCYTE TRANSITION. 2018.

[46] MARTINS, B. R.; FERNANDES, CJC; Pinto TS; ZAMBUZZI, Willian Fernando. Meio enriquecido com titânio interfere em vias de sobrevivência e proliferação de células endoteliais. 2018.

[47] ALBANO, C. S.; GOMES AM; FELTRAN, G. S.; FERNANDES, CJC; TRINO, L. D.; ZAMBUZZI, Willian Fernando; LISBOA-FILHO, P. N. Titânio para aplicações Biomédicas: Análise do repertório molecular. 2018.

[48] Pinto TS; GOMES AM; FERNANDES, CJC; SILVA, R. A.; ZAMBUZZI, Willian Fernando. Shear Stress Em Um Modelo De Hipertensão In Vitro Desencadeia Respostas Em Vias De SobrevivêNcia. 2018.

[49] FELTRAN, G. S.; FERNANDES, CJC; SILVA, R. A.; ZAMBUZZI, Willian Fernando. Caracterização morfológica e molecular na obtenção de tecidos equivalentes de endotélio: uma metodologia alternativa ao estudo de suas interações. 2018.

[50] NUNES, PRISCILA REZECK; PERECOLI, M. T.; ROMAO, M.; MATIAS, M. L.; RIBEIRO, VANESSA ROCHA ; FERNANDES, CJC; Peraçoli, J C; RODRIGUES, JOSE RICARDO; DE OLIVEIRA,

LEANDRO. Association between adverse maternal clinical outcomes and imbalance of cytokines and angiogenic factors in preterm preeclampsia. 2018.

[51] NUNES, PRISCILA REZECK; PERECOLI, M. T.; ROMAO, M.; MATIAS, M. L.; RIBEIRO, VANESSA ROCHA; FERNANDES, CJC; Peraçoli, J C; RODRIGUES, JOSE RICARDO; DE OLIVEIRA, LEANDRO. Vitamin D decreases gene and protein expression of NLRP3 inflammasome in placental explants cultured with hydrogen peroxide from women with preeclampsia. 2018.

[52] Pinto TS; SILVA, R. A.; GOMES AM; FERNANDES, CJC; ZAMBUZZI, Willian Fernando. Epigenetic-Related Chromatin Compaction Is Required On Hypertensive-Stressed Endothelial Cell Phenotype. 2019.

[53] SILVA, R. A.; FERREIRA, Marcel Rodrigues; FELTRAN, G. S.; FERNANDES, CJC; ZAMBUZZI, Willian Fernando. Endothelial-based paracrine osteogenic signaling requires dynamic epigenetic marks. 2019.

[54] ALBANO, C. S.; GOMES AM; FELTRAN, G. S.; FERNANDES, CJC; TRINO, L. D.; ZAMBUZZI, Willian Fernando; LISBOA-FILHO, P. N. Comportamento de pré-osteoblastos frente às superfícies de titânio revestidas com alendronato e albumina. 2019.

[55] GOMES AM; ALBANO, C. S.; FERNANDES, CJC; ZAMBUZZI, Willian Fernando. Extracellular matrix remodeling behavior in fibroblast-responding to different titanium surfaces. 2019.

[56] ALBANO, C. S.; GOMES AM; FERNANDES, CJC; FELTRAN, G. S.; TRINO, L. D.; ZAMBUZZI, Willian Fernando; LISBOA-FILHO, P. N. Bioactive titanium surfaces tailored with alendronate and albumin. 2019.

[57] ALBANO, C. S.; GOMES AM; FELTRAN, G. S.; FERNANDES, CJC; TRINO, L. D.; ZAMBUZZI, Willian Fernando; LISBOA-FILHO, P. N. Avaliação do comportamento de pré-osteoblastos em contato indireto com superfícies de titânio biofuncionalizadas. 2019.

[58] CAMARGO, B. A.; FELTRAN, G. S.; FERNANDES, CJC; SILVA, R. A.; ZAMBUZZI, Willian Fernando. Biological effect triggered by Zirconia in endothelial cells during adhesion and synthesis / remodeling of extracellular matrix. 2019.

PRÊMIOS:

[1] Presented Talk in Current Topics Biochemistry: Epigenetic control HOXA gene family cluster in osteoblast differentiation, Current Topics in Biochemistry.

[2] Menção honrosa na apresentação - Evaluation of the Dillapiol Effect in Fibroblast Viability, III Workbiotech: Workshop da Pós Graduação em Biotecnologia e II Symposium on Cellular Dynamics.

[3] Menção honrosa na apresentação - Alterations in matrix remodeling and in the activity of metalloproteinases in endothelial cells submitted to shear stress, III Workbiotech: Workshop da Pós Graduação em Biotecnologia e II Symposium on Cellular Dynamics.

[4] Menção honrosa na apresentação - Cobalt and chromium enriched media modulates the expression of inflammatory cytokines in fibroblasts and alter the cell adhesion protein signaling profile, III Workbiotech: Workshop da Pós Graduação em Biotecnologia e II Symposium on Cellular Dynamics.

[5] 3 Lugar na Apresentação Painel, trabalho intitulado "Avaliação de efeitos heterótipos disparados por Fibroblastos na adesão celular e citotoxicidade de Osteoblastos", V Congresso de Biociências de Botucatu.

[6] Melhor pôster na Apresentação Painel, trabalho intitulado Osteoblast morphological chances is autocrine-Sonic Hedgehog-dependent in a bio-inspired three-dimensional in vitro model, Sociedade Brasileira de Bioquímica e Biologia Molecular - SBBq.

[7] 2 Lugar na Apresentação Painel, trabalho intitulado Meio condicionado a partir de ligas de Co-Cr afetam diferencialmente o comportamento de osteoblastos e fibroblastos, V Congresso de Biociências de Botucatu.

VÍDEOS E ENTREVISTAS:

[1] FAPESP Week London. 2019 (https://www.instagram.com/p/BtyaV_TgN9E/)

[2] Aluno do IB estuda ação de células arteriais na biologia óssea. 2019 (https://www.ibb.unesp.br/#!/noticia/1337/aluno-do-ib-estuda-acao-de-celulas-arteriais-na-biologia-ossea/)

[3] Unespianos pelo Mundo (https://www.youtube.com/watch?v=WSNYQj8hh8w)

ATIVIDADES COMPLEMENTARES:

[1] **2016 – 2016**: Técnicas de Cultura Celular. Núcleo de Aprimoramento Científico, NAC, Brasil.

[2] **2016 – 2016**: Biossegurança em Laboratórios. Universidade Estadual Paulista Júlio de Mesquita Filho, UNESP, Brasil.

[3] **2016 – 2016**: Fundamentos da PCR Quantitativa em Tempo Real (qPCR). ThermoFisher-SCIENTIFIC, TF-S, Brasil.

[4] **2016 – 2016**: Técnicas de Biologia Molecular. Núcleo de Aprimoramento Científico, NAC, Brasil.

[5] **2016 – 2016**: Extensão em Boas Práticas de Laboratório e Biossegurança. Universidade Estadual Paulista Júlio de Mesquita Filho, UNESP, Brasil.

[6] **2016 – 2016**: Técnicas Laboratoriais com DNA. Núcleo de Aprimoramento Científico, NAC, Brasil.

[7] **2016 – 2016**: Técnica de imuno-histoquímica pré-embedding: Imunogold e Imunoperoxidase. Universidade Estadual Paulista Júlio de Mesquita Filho, UNESP, Brasil.

[8] **2017 – 2017** :Extensão universitária em Ética. Veduca, Veduca, Brasil.

[9] **2017 – 2017**: Técnicas em Biologia Molecular I. Núcleo de Aprimoramento Científico, NAC, Brasil.

[10] **2017 – 2017**: Web of Bioprocess. Merck, MERCK S/A, Brasil.

[11] **2017 – 2017**: Técnicas em Biologia Molecular II. Núcleo de Aprimoramento Científico, NAC, Brasil.

[12] **2017 – 2017**: Manipulação Molecular em Softwares análises em softwares gratuitos. Núcleo de Aprimoramento Científico, NAC, Brasil.

[13] **2018 – 2018**: Programação fetal: Do ambiente uterino ao envelhecimento da prole. Sociedade Brasileira de Biologia Celular, SBBC, Brasil.

[14] **2018 – 2018**: Curso de Inglês para Sobrevivência. InglêsWinner, I.W., Brasil.

[15] **2018 – 2018**: Reparo e bioengenharia do Tecido Ósseo: das Ciências Básicas à Clínica. Sociedade Brasileira de Biologia Celular, SBBC, Brasil.

[16] **2018 – 2018**: Terapias Celulares em doenças cardiovasculares. Sociedade Brasileira de Biologia Celular, SBBC, Brasil.

[17] **2018 – 2018**: Célula artificial: microfabricação e microfluidica. Sociedade Brasileira de Biologia Celular, SBBC, Brasil.

[18] **2018 – 2018**: Cultura celular: sistemas 2D e 3D, cocultura e modelo de chimeras. Sociedade Brasileira de Biologia Celular, SBBC, Brasil.

[19] **2019 – 2019**: Docência no ensino superior: fundamentos e práticas pedagógicas. Universidade Estadual Paulista, UNESP, Brasil.

[20] **2020 – 2020**: Comunicação e Escrita Científica. ACS - Publications, ACS, Brasil.

[21] **2020 – 2020**: Extracellular Vesicles and Immunology. International Society for Extracellular Vesicles, ISEV, Estados Unidos.

[22] **2020 – 2020**: The most versatile microscope for Life Sciences - LSM 980. ZEISS, ZEISS, Brasil.

[23] **2020 – 2020**: Advanced Battery Characterization: Using Microscopy. ZEISS, ZEISS, Brasil.

[24] **2020 – 2020**: A New Level of Ease and Efficiency in your Lab. ZEISS, ZEISS, Brasil.

[25] **2020 – 2020**: Massive material removal and ultrafast site-specific sample preparation. ZEISS, ZEISS, Brasil.

[26] **2020 – 2020**: Ciclo Virtual de Seminários da SBMM. Sociedade Brasileira de Microscopia e Microanálise, SBMM, Brasil.

PATENTES:

[1] Fleuri, Luciana Francisco; Capoville, B. L.; Athanázio-Heliodoro, Julia Carolina; Zambuzzi, Willian F.; **Fernandes, Célio Júnior Da C.**; Silva, R. A. Patente: Privilégio de Inovação. Número do registro: BR1020190014873, título: "*MÉTODO DE OBTENÇÃO DE PRODUTOS DE HIDRÓLISE CATALISADAS POR LIPASES FÚNGICAS PRODUZIDAS EM RESÍDUOS INDUSTRIAIS E PRODUTOS RESULTANTES*", Instituição de registro: INPI - Instituto Nacional da Propriedade Industrial. Depósito: 24/01/2019.

ARTIGOS PUBLICADOS:

[1] Bezerra, Fábio; Ferreira, Marcel R.; Fontes, Giselle N.; **Jr Da Costa Fernandes, Célio**; Andia, Denise C.; Cruz, Nilson C.; Da Silva, Rodrigo A.; Zambuzzi, Willian F. Nano hydroxyapatite-blasted titanium surface affects pre-osteoblast morphology by modulating critical intracellular pathways. Biotechnology And Bioengineering, 2017.

[2] **Da Costa Fernandes, Celio J.**; Do Nascimento, Augusto Santana; Da Silva, Rodrigo A.; Zambuzzi, Willian F. Fibroblast contributes for osteoblastic phenotype in a MAPK-ERK and sonic hedgehog signaling-independent manner. Molecular And Cellular Biochemistry, 2017.

[3] Marumoto, Ariane; Milani, Renato; Da Silva, Rodrigo A.; **Da Costa Fernandes, Celio Junior**; Granjeiro, Jose Mauro; Ferreira, Carmen V.; Peppelenbosch, Maikel P.; Zambuzzi, Willian F. Phosphoproteome analysis reveals a critical role for hedgehog signalling in osteoblast morphological transitions. Bone, 2017.

[4] Rossi, Mc; Bezerra, Fjb; Silva, Ra; Crulhas, Bp; **Fernandes, Cjc**; Nascimento, As; Pedrosa, Va; Padilha, P; Zambuzzi, Wf. Titanium-released from dental implant enhances pre-osteoblast adhesion by ROS modulating crucial intracellular pathways. Journal Of Biomedical Materials Research Part A, 2017.

[5] **Fernandes, Célio J. C.**; Bezerra, Fabio; Do Carmo, Maiara Das D.; Feltran, Georgia; Rossi, Mariana C.; Da Silva, Rodrigo A.; Padilha, Pedro De M.; Zambuzzi, Willian F. CoCr enriched medium modulates integrin-based downstream signaling and requires a set of inflammatory genes reprograming in vitro. Journal Of Biomedical Materials Research Part A, 2017.

[6] Okino-Delgado, Clarissa Hamaio; Prado, Débora Zanoni Do; Facanali, Roselaine; Marques, Márcia Mayo Ortiz; Nascimento, Augusto Santana; **Fernandes, Célio Junior Da Costa**; Zambuzzi, William Fernando; Fleuri, Luciana Francisco. Bioremediation of cooking oil waste using lipases from wastes. PLoS One, 2017.

[7] Nascimento, Augusto S.; Peres, Luisa L.; Faria, Alessandra V. S.; Milani, Renato; Silva, Rodrigo A.; **Jr. Da Costa Fernandes, Celio**; Peppelenbosch, Maikel P.; Ferreira-Halder, Carmen V.; Zambuzzi, Willian F. Phosphoproteome profiling reveals critical role of JAK-STAT signaling in maintaining chemoresistance in breast cancer. Oncotarget, 2017.

[8] Kang, Ha Ram; **Da Costa Fernandes, Célio Junior**; Da Silva, Rodrigo Augusto; Constantino, Vera Regina Leopoldo; Koh, Ivan Hong Jun; Zambuzzi, Willian F. Mg-Al and Zn-Al Layered Double Hydroxides Promote Dynamic Expression of Marker Genes in Osteogenic Differentiation by Modulating Mitogen-Activated Protein Kinases. Advanced Healthcare Materials, 2017.

[9] **Fernandes, Célio J.C.**; Bezerra, Fábio; Ferreira, Marcel R.; Andrade, Amanda F.C.; Pinto, Thais Silva; Zambuzzi, Willian F. Nano hydroxyapatite-blasted titanium surface creates a biointerface

able to govern Src-dependent osteoblast metabolism as prerequisite to ECM remodeling. Colloids And Surfaces B-Biointerfaces, 2017.

[10] **Da Costa Fernandes, Celio J.**; Ferreira, Marcel Rodrigues; Bezerra, Fábio J. B.; Zambuzzi, Willian F. Zirconia stimulates ECM-remodeling as a prerequisite to pre-osteoblast adhesion/proliferation by possible interference with cellular anchorage. Journal Of Materials Science-Materials In Medicine, 2018.

[11] Correa, D.R.N.; Kuroda, P.A.B.; Lourenço, M.L.; **Fernandes, C.J.C.**; Buzalaf, M.A.R.; Zambuzzi, W.F.; Grandini, C.R. Development of Ti-15Zr-Mo alloys for applying as implantable biomedical devices. Journal Of Alloys And Compounds, 2018.

[12] Olimpio, Regiane M. C.; De Oliveira, Miriane; De Sibio, Maria T.; Moretto, Fernanda C. F.; Deprá, Igor C.; Mathias, Lucas S.; Gonçalves, Bianca M.; Rodrigues, Bruna M.; Tilli, Helena P.; Coscrato, Virgínia E.; Costa, Sarah M. B.; Mazeto, Gláucia M. F. S.; **Fernandes, Célio J. C.**; Zambuzzi, Willian F.; Saraiva, Patrícia P.; Maria, Durvanei A.; Nogueira, Célia R. Cell viability assessed in a reproducible model of human osteoblasts derived from human adipose-derived stem cells. PLoS One, 2018.

[13] Athanázio-Heliodoro, Julia Carolina; Okino-Delgado, Clarissa Hamaio; **Fernandes, Célio Júnior Da Costa**; Zanutto, Mirella Rossitto; Prado, Débora Zanoni Do; Da Silva, Rodrigo Augusto; Facanali, Roselaine; Zambuzzi, Willian Fernando; Marques, Márcia Ortiz Mayo; Fleuri, Luciana Francisco. Improvement of lipase obtaining system by orange waste-based solid-state fermentation: production, characterization and application. PREPARATIVE Biochemistry & Biotechnology, 2018.

[14] **Da Costa Fernandes, Celio J.**; Bezerra, Fábio J.B.; De Campos Souza, Bruno; Aparecida Campos, Mônica; Zambuzzi, Willian Fernando. Titanium-enriched medium drives low profile of ECM remodeling as a pre-requisite to pre-osteoblast viability and proliferative phenotype. Journal Of Trace Elements In Medicine And Biology, 2018.

[15] Da Silva, Rodrigo A.; De Camargo Andrade, Amanda Fantini; Da Silva Feltran, Geórgia; **Fernandes, Célio Júnior Da C.**; De Assis, Rahyza Inacio F.; Ferreira, Marcel Rodrigues; Andia, Denise C.; Zambuzzi, Willian F. The role of triiodothyronine hormone and mechanically-stressed endothelial cell paracrine signalling synergism in gene reprogramming during hBMSC-stimulated osteogenic phenotype in vitro. Molecular And Cellular Endocrinology, 2018.

[16] Nunes, Priscila Rezeck; Peracoli, Maria Terezinha Serrão; Romao-Veiga, Mariana; Matias, Mariana Leticia; Ribeiro, Vanessa Rocha; **Da Costa Fernandes, Celio Junior**; Peracoli, Jose Carlos; Rodrigues, Jose Ricardo; De Oliveira, Leandro. Hydrogen peroxide-mediated oxidative stress induces inflammasome activation in term human placental explants. Pregnancy Hypertension-An International Journal of Womens Cardiovascular Health, 2018.

[17] Francisco, Valesca Cristiane Benelli; Okino-Delgado, Clarissa Hamaio; Zanutto Elgui, Mirella R.; **Fernandes, Célio Junior Da Costa**; Facanali, Roselaine; Da Silva, Rodrigo Augusto; Zambuzzi, Willian Fernando; Marques, Márcia Ortiz Mayo; Fleuri, Luciana Francisco. Plant oil bioconversion into increase biological activity through lipases derived from wastes. INTERNATIONAL JOURNAL OF FOOD SCIENCE AND TECHNOLOGY, 2018.

[18] Nunes, Priscila Rezeck; Romao-Veiga, Mariana; Matias, Mariana Leticia; Ribeiro, Vanessa Rocha; **Da Costa Fernandes, Celio Jr.**; De Oliveira, Leandro Gustavo; Rodrigues, Jose Ricardo; Medeiros Borges, Vera T.; Peracoli, Jose Carlos; Serrao Peracoli, Maria T.. 172. Vitamin D decreases gene and protein expression of NLRP3 inflammasome in placental explants cultured with hydrogen peroxide from women with preeclampsia. Pregnancy Hypertension-An International Journal of Womens Cardiovascular Health, 2018.

[19] Pinto, Thaís Silva; **Fernandes, Célio Junior Da Costa**; Da Silva, Rodrigo Augusto; Gomes, Anderson Moreira; Vieira, José Cavalcante Souza; Padilha, Pedro De M.; Zambuzzi, Willian F..

c-Src kinase contributes on endothelial cells mechanotransduction in a heat shock protein 70-dependent turnover manner. JOURNAL OF CELLULAR PHYSIOLOGY, 2018.

[20] Da Silva, Rodrigo A.; **Fernandes, Célio Jr Da C.**; Feltran, Geórgia Da S.; Gomes, Anderson M.; De Camargo Andrade, Amanda Fantini; Andia, Denise C.; Peppelenbosch, Maikel P.; Zambuzzi, Willian F.. Laminar shear stress-provoked cytoskeletal changes are mediated by epigenetic reprogramming of in human primary smooth muscle cells. JOURNAL OF CELLULAR PHYSIOLOGY, 2019.

[21] Da Silva Feltran, Geórgia; **Da Costa Fernandes, Célio Junior**; Rodrigues Ferreira, Marcel; Kang, Ha Ram; De Carvalho Bovolato, Ana Lívia; De Assis Golim, Márjorie; Deffune, Elenice; Koh, Ivan Hong Jun; Constantino, Vera Regina Leopoldo; Zambuzzi, Willian F.. Sonic hedgehog drives layered double hydroxides-induced acute inflammatory landscape. COLLOIDS AND SURFACES B-BIOINTERFACES, 2019.

[22] Feltran, Georgia Da S.; Bezerra, Fábio; **Fernandes, Célio Júnior Da Costa**; Ferreira, Marcel Rodrigues; Zambuzzi, Willian F.. Differential inflammatory landscape stimulus during titanium surfaces-obtained osteogenic phenotype. JOURNAL OF BIOMEDICAL MATERIALS RESEARCH PART A, 2019.

[23] **Fernandes, Célio Jr. Da Costa**; Veiga, Mariana R.; Peracoli, Maria Terezinha Serrão; Zambuzzi, Willian F.. Modulatory effects of silibinin in cell behavior during osteogenic phenotype. JOURNAL OF CELLULAR BIOCHEMISTRY, 2019.

[24] Machado, Mariana Issler Pinheiro; Gomes, Anderson Moreira; Rodrigues, Marcel Ferreira; Pinto, Thais Silva; **Da Costa Fernandes, Célio Júnior**; Bezerra, Fábio J.; Zambuzzi, Willian Fernando. Cobalt-chromium-enriched medium ameliorates shear-stressed endothelial cell performance. JOURNAL OF TRACE ELEMENTS IN MEDICINE AND BIOLOGY, 2019.

[25] Da Silva, Rodrigo A.; Fuhler, Gwenny M.; Janmaat, Vincent T.; **Da C. Fernandes, Célio Júnior**; Da Silva Feltran, Geórgia; Oliveira, Flávia Amadeu; Matos, Adriana Arruda; Oliveira, Rodrigo Cardoso; Ferreira, Marcel Rodrigues; Zambuzzi, Willian F.; Peppelenbosch, Maikel P. HOXA cluster gene expression during osteoblast differentiation involves epigenetic control. BONE, 2019.

[26] **Jr. Da Costa Fernandes, Célio**; Pinto, Thaís Silva; Kang, Ha Ram; Magalhães Padilha, Pedro; Koh, Ivan Hong Jun; Constantino, Vera Regina Leopoldo; Zambuzzi, Willian F. Layered Double Hydroxides Are Promising Nanomaterials for Tissue Bioengineering Application. Advanced Biosystems, 2019.

[27] Zanoni Do Prado, Débora; Oliveira, Samara Louzada; Okino-Delgado, Clarissa Hamaio; Auer, Susann; Ludwig-Müller, Jutta; Ribeiro Da Silva, Magali; **Júnior Da Costa Fernandes, Célio**; Carbonari, Caio Antonio; Zambuzzi, William Fernando; Fleuri, Luciana Francisco. Aspergillus flavipes as a novel biostimulant for rooting-enhancement of Eucalyptus. JOURNAL OF CLEANER PRODUCTION, 2019.

[28] GOMES, ANDERSON M.; PINTO, THAIS S.; **COSTA FERNANDES, CÉLIO J.**; SILVA, RODRIGO A.; ZAMBUZZI, WILLIAN F. Wortmannin targeting phosphatidylinositol 3-kinase suppresses angiogenic factors in shear-stressed endothelial cells. JOURNAL OF CELLULAR PHYSIOLOGY, v. 19, p. 1-14, 2019.

[29] ALBANO, CAROLINA SIMÃO; GOMES, ANDERSON MOREIRA; DA SILVA FELTRAN, GEÓRGIA; **DA COSTA FERNANDES, CÉLIO JUNIOR**; TRINO, LUCIANA DANIELE; ZAMBUZZI, Willian Fernando; LISBOA-FILHO, PAULO NORONHA. Publisher Correction: Bisphosphonate-based surface biofunctionalization improves titanium biocompatibility. JOURNAL OF MATERIALS SCIENCE-MATERIALS IN MEDICINE, v. 31, p. 112, 2020.

[30] ALBANO, CAROLINA SIMÃO; GOMES, ANDERSON MOREIRA; DA SILVA FELTRAN, GEÓRGIA; **DA COSTA FERNANDES, CÉLIO JUNIOR**; TRINO, LUCIANA DANIELE; ZAMBUZZI, Willian Fernando; LISBOA-FILHO, PAULO NORONHA. Bisphosphonate-based

surface biofunctionalization improves titanium biocompatibility. JOURNAL OF MATERIALS SCIENCE-MATERIALS IN MEDICINE, v. 31, p. 1-13, 2020.

[31] ALBANO, CAROLINA SIMÃO; MOREIRA GOMES, ANDERSON; DA SILVA FELTRAN, GEÓRGIA; **DA COSTA FERNANDES, CÉLIO JUNIOR**; TRINO, LUCIANA DANIELE; ZAMBUZZI, Willian Fernando; LISBOA-FILHO, PAULO NORONHA. Biofunctionalization of titanium surfaces with alendronate and albumin modulates osteoblast performance. HELIYON, v. 6, p. e04455, 2020.

[32] ROCHA CAMARGO, TAVANI; RAMOS, PATRÍCIA; MONSERRAT, JOSÉ M.; PRENTICE, CARLOS; **J. C. FERNANDES, CÉLIO**; ZAMBUZZI, WILLIAN F.; VALENTI, WAGNER C. Biological activities of the protein hydrolysate obtained from two fishes common in the fisheries bycatch. FOOD CHEMISTRY, v. 1, p. 128361, 2020.

[33] LEVINK, IRIS J.; NESTERUK, KATERYNA; VISSER, D.I.; SIEUWERTS, A.M.; **FERNANDES, CÉLLO J.**; JANSEN, M.P.H.M.; PEPPELENBOSCH, MAIKEL; CAHEN, D.L.; FUHLER, GWENNY; BRUNO, MARCO J. Tu1609 METHODOLOGY OF PANCREATIC JUICE COLLECTION FROM THE DUODENUM FOR BIOMARKER DISCOVERY AND EARLY DETECTION OF PANCREATIC CANCER. GASTROENTEROLOGY, v. 158, p. S-1136, 2020.

[34] MARTINS, BRUNA RODRIGUES ; PINTO, THAIS SILVA ; DA COSTA FERNANDES, CÉLIO JUNIOR ; BEZERRA, Fábio ; ZAMBUZZI, Willian Fernando . PI3K/AKT signaling drives titanium-induced angiogenic stimulus. JOURNAL OF MATERIALS SCIENCE-MATERIALS IN MEDICINE, v. 32, p. 1-9, 2021.

[35] **COSTA FERNANDES, CÉLIO JR DA**; ZAMBUZZI, Willian Fernando. Fibroblast-secreted trophic factors contribute with ECM remodeling stimulus and upmodulate osteocyte gene markers in osteoblasts. BIOCHIMIE, v. 168, p. 92-99, 2020.

[36] DA SILVA, RODRIGO A.; DA S. FELTRAN, GEÓRGIA; **DA C. FERNANDES, CÉLIO JÚNIOR**; ZAMBUZZI, WILLIAN F. Osteogenic gene markers are epigenetically reprogrammed during contractile-to-calcifying vascular smooth muscle cell phenotype transition. CELLULAR SIGNALLING, v. 66, p. 109458, 2020.

[37] SARTORETTO, SUELEN C.; CALASANS-MAIA, MONICA D.; ALVES, ADRIANA T.N.N.; RESENDE, RODRIGO F.B.; **DA COSTA FERNANDES, CÉLIO JUNIOR**; DE MAGALHÃES PADILHA, PEDRO; ROSSI, ALEXANDRE M.; TETI, ANNA; GRANJEIRO, JOSÉ M.; ZAMBUZZI, WILLIAN F. The role of apoptosis associated speck-like protein containing a caspase-1 recruitment domain (ASC) in response to bone substitutes. Materials Science & Engineering C-Materials for Biological Applications, v. 112, p. 110965, 2020.

[38] Célio da Costa Fernandes Jr, Victor Manuel Ochoa Rodríguez, Andrea Soares-Costa, Joni Augusto Cirelli, Daniela Morilha Neo Justino, Bárbara Roma, Willian Fernando Zambuzzi, Gisele Faria. Cystatin-like protein of sweet orange (CsinCPI-2) modulates pre-osteoblast differentiation via β-Catenin involvement. J Mater Sci Mater Med. 2021 Mar 22; 32 (4): 33.

DEMAIS ATIVIDADES:

[1] **2019 -** Avaliador na 1ª fase do XXXI Congresso de Iniciação Científica da Unesp.

[2] **2020 -** Avaliador na 1ª fase do XXXII Congresso de Iniciação Científica da Unesp.

[3] **2020 -** Professor PAADES da disciplina de Bioquímica Geral para o Curso de Ciências Biológicas

[4] **2020 -** Professor PAADES da disciplina de Química e Bioquímica Animal para o Curso de Medicina Veterinária

[5] **2020 -** Professor PAADES da disciplina de Bioquímica para o Curso de Nutrição

[6] **2020 -** Palestra: Vesículas extracelulares: regeneração por transporte funcional de cargas. 33° Semana da Biologia – UNITAU.

CAPÍTULO 11

REFERÊNCIAS BIBLIOGRÁFICAS

Admyre C, Johansson SM, Qazi KR, Filen J-J, Lahesmaa R, Norman M, Neve EPA, Scheynius A, Gabrielsson S. 2007. Exosomes with immune modulatory features are present in human breast milk. *Journal of immunology (Baltimore, Md. : 1950)* **179**:1969–1978.

Akimoto S, Mitsumata M, Sasaguri T, Yoshida Y. 2000. Laminar shear stress inhibits vascular endothelial cell proliferation by inducing cyclin-dependent kinase inhibitor p21(Sdi1/Cip1/Waf1). *Circulation research* **86**:185–190.

Anderson HC. 1969. Vesicles associated with calcification in the matrix of epiphyseal cartilage. *The Journal of cell biology* **41**:59–72.

Anderson HC, Garimella R, Tague SE. 2005. The role of matrix vesicles in growth plate development and biomineralization. *Frontiers in bioscience : a journal and virtual library* **10**:822–837.

Aspenberg P. 2013. Special Review: Accelerating fracture repair in humans: a reading of old experiments and recent clinical trials. *BoneKEy reports* **2**:244.

Balaguru UM, Sundaresan L, Manivannan J, Majunathan R, Mani K, Swaminathan A, Venkatesan S, Kasiviswanathan D, Chatterjee S. 2016. Disturbed flow mediated modulation of shear forces on endothelial plane: A proposed model for studying endothelium around atherosclerotic plaques. *Scientific Reports* **6**:27304. http://dx.doi.org/10.1038/srep27304.

Balaj L, Lessard R, Dai L, Cho Y-J, Pomeroy SL, Breakefield XO, Skog J. 2011. Tumour microvesicles contain retrotransposon elements and amplified oncogene sequences. *Nature communications* **2**:180.

Bartek J, Bartkova J, Lukas J. 1996. The retinoblastoma protein pathway and the restriction point. *Current opinion in cell biology* **8**:805–814.

Basso M, Bonetto V. 2016. Extracellular Vesicles and a Novel Form of Communication in the Brain. *Frontiers in neuroscience* **10**:127.

Bazmara H, Soltani M, Sefidgar M, Bazargan M, Mousavi Naeenian M, Rahmim A. 2016. Blood flow and endothelial cell phenotype regulation during sprouting angiogenesis. *Medical & biological engineering & computing* **54**:547–558.

Bezerra F, Ferreira MR, Fontes GN, da Costa Fernandes CJ, Andia DC, Cruz NC, da Silva RA, Zambuzzi WF. 2017. Nano hydroxyapatite-blasted titanium surface affects pre-osteoblast morphology by modulating critical intracellular pathways. *Biotechnology and bioengineering*.

Biancone L, Bruno S, Deregibus MC, Tetta C, Camussi G. 2012. Therapeutic potential of mesenchymal stem cell-derived microvesicles. *Nephrology, dialysis, transplantation : official publication of the European Dialysis and Transplant Association - European Renal Association* **27**:3037–3042.

Bobrie A, Colombo M, Raposo G, Thery C. 2011. Exosome secretion: molecular mechanisms and roles in immune responses. *Traffic (Copenhagen, Denmark)* **12**:1659–1668.

Bonewald LF. 2011. The amazing osteocyte. *Journal of bone and mineral research : the official journal of the American Society for Bone and Mineral Research* **26**:229–238.

Brody I, Ronquist G, Gottfries A. 1983. Ultrastructural localization of the prostasome - an organelle in human seminal plasma. *Upsala journal of medical sciences* **88**:63–80.

Califano JP, Reinhart-King CA. 2010. Exogenous and endogenous force regulation of endothelial cell behavior. *Journal of biomechanics* **43**:79–86.

Carreira AC, Alves GG, Zambuzzi WF, Sogayar MC, Granjeiro JM. 2014. Bone Morphogenetic Proteins: structure, biological function and therapeutic applications. *Archives of biochemistry and biophysics* **561**:64–73.

CHARGAFF E, WEST R. 1946. The biological significance of the thromboplastic protein of blood. *The Journal of biological chemistry* **166**:189–197.

Chien S. 2008. Effects of disturbed flow on endothelial cells. *Annals of biomedical engineering* **36**:554–562.

Clancy JW, Sedgwick A, Rosse C, Muralidharan-Chari V, Raposo G, Method M, Chavrier P, D'Souza-Schorey C. 2015. Regulated delivery of molecular cargo to invasive tumour-derived microvesicles. *Nature communications* **6**:6919.

Cocucci E, Racchetti G, Meldolesi J. 2009. Shedding microvesicles: artefacts no more. *Trends in cell biology* **19**:43–51.

Colombo M, Raposo G, Thery C. 2014. Biogenesis, secretion, and intercellular interactions of exosomes and other extracellular vesicles. *Annual review of cell and developmental biology* **30**:255–289.

Cortez MA, Bueso-Ramos C, Ferdin J, Lopez-Berestein G, Sood AK, Calin GA. 2011. MicroRNAs in body fluids--the mix of hormones and biomarkers. *Nature reviews. Clinical oncology* **8**:467–477.

Cunningham KS, Gotlieb AI. 2004. The role of shear stress in the pathogenesis of atherosclerosis. *Lab Invest* **85**:9–23. http://dx.doi.org/10.1038/labinvest.3700215.

Dolo V, Ginestra A, Cassara D, Violini S, Lucania G, Torrisi MR, Nagase H, Canevari S, Pavan A, Vittorelli ML. 1998. Selective localization of matrix metalloproteinase 9, beta1 integrins, and human lymphocyte antigen class I molecules on membrane vesicles shed by 8701-BC breast carcinoma cells. *Cancer research* **58**:4468–4474.

Ducy P, Desbois C, Boyce B, Pinero G, Story B, Dunstan C, Smith E, Bonadio J, Goldstein S, Gundberg C, Bradley A, Karsenty G. 1996. Increased bone formation in osteocalcin-deficient mice. *Nature* **382**:448–452.

van der Eerden BCJ, Teti A, Zambuzzi WF. 2014. Bone, a dynamic and integrating tissue. *Archives of biochemistry and biophysics*. United States.

Eshkar-Oren I, Viukov S V, Salameh S, Krief S, Oh C, Akiyama H, Gerber H-P, Ferrara N, Zelzer E. 2009. The forming limb skeleton serves as a signaling center for limb vasculature patterning via regulation of Vegf. *Development (Cambridge, England)* **136**:1263–1272.

Fong GH, Rossant J, Gertsenstein M, Breitman ML. 1995. Role of the Flt-1 receptor tyrosine kinase in regulating the assembly of vascular endothelium. *Nature* **376**:66–70.

Fruhbeis C, Frohlich D, Kuo WP, Kramer-Albers E-M. 2013. Extracellular vesicles as mediators of neuron-glia communication. *Frontiers in cellular neuroscience* **7**:182.

Gao M, Gao W, Papadimitriou JM, Zhang C, Gao J, Zheng M. 2018. Exosomes-the enigmatic regulators of bone homeostasis. *Bone research* **6**:36.

Haga M, Yamashita A, Paszkowiak J, Sumpio BE, Dardik A. 2003. Oscillatory shear stress increases smooth muscle cell proliferation and Akt phosphorylation. *Journal of vascular surgery* **37**:1277–1284.

Hahn C, Schwartz MA. 2009. Mechanotransduction in vascular physiology and atherogenesis. *Nat Rev Mol Cell Biol* **10**:53–62. http://dx.doi.org/10.1038/nrm2596.

Hasegawa T, Tsuchiya E, Abe M, Amizuka N. 2016. [Cellular interplay of bone cells and vascular endothelial cells in bone]. *Clinical calcium* **26**:677–682.

Hill Gallant KM, Spiegel DM. 2017. Calcium Balance in Chronic Kidney Disease. *Current osteoporosis reports*.

Hristov M, Erl W, Linder S, Weber PC. 2004. Apoptotic bodies from endothelial cells enhance the number and initiate the differentiation of human endothelial progenitor cells in vitro. *Blood* **104**:2761–2766.

Jabalee J, Hillier S, Franz-Odendaal TA. 2013. An investigation of cellular dynamics during the development of intramembranous bones: the scleral ossicles. *Journal of Anatomy* **223**:311–320. http://www.ncbi.nlm.nih.gov/pmc/articles/PMC3791124/.

Kalra H, Drummen GPC, Mathivanan S. 2016. Focus on Extracellular Vesicles: Introducing the Next Small Big Thing. *International journal of molecular sciences* **17**:170.

Koppler B, Cohen C, Schlondorff D, Mack M. 2006. Differential mechanisms of microparticle transfer toB cells and monocytes: anti-inflammatory propertiesof microparticles. *European journal of immunology* **36**:648–660.

Kuczera P, Adamczak M, Wiecek A. 2016. Fibroblast Growth Factor-23-A Potential Uremic Toxin. *Toxins* **8**.

Lacaud G, Kouskoff V. 2017. Hemangioblast, hemogenic endothelium, and primitive versus definitive hematopoiesis. *Experimental hematology* **49**:19–24.

Laurie LE, Kokubo H, Nakamura M, Saga Y, Funato N. 2016. The Transcription Factor Hand1 Is Involved In Runx2-Ihh-Regulated Endochondral Ossification. Ed. Jung-Eun Kim. *PLoS ONE* **11**:e0150263. http://www.ncbi.nlm.nih.gov/pmc/articles/PMC4769249/.

Lawson C, Vicencio JM, Yellon DM, Davidson SM. 2016. Microvesicles and exosomes: new players in metabolic and cardiovascular disease. *The Journal of endocrinology* **228**:R57-71.

Lee B, Thirunavukkarasu K, Zhou L, Pastore L, Baldini A, Hecht J, Geoffroy V, Ducy P, Karsenty G. 1997. Missense mutations abolishing DNA binding of the osteoblast-specific transcription factor OSF2/CBFA1 in cleidocranial dysplasia. *Nature genetics* **16**:307–310.

Lima GAC, Lima PDA, Barros M da GCRM de, Vardiero LP, Melo EF de, Paranhos-Neto F de P, Madeira M, Farias MLF de. 2016. Calcium intake: good for the bones but bad for the heart? An analysis of clinical studies. *Archives of endocrinology and metabolism* **60**:252–263.

Lin K, Hsu PP, Chen BP, Yuan S, Usami S, Shyy JY, Li YS, Chien S. 2000. Molecular mechanism of endothelial growth arrest by laminar shear stress. *Proceedings of the National Academy of Sciences of the United States of America* **97**:9385–9389.

Ling ITC, Rochard L, Liao EC. 2017. Distinct requirements of wls, wnt9a, wnt5b and gpc4 in regulating chondrocyte maturation and timing of endochondral ossification. *Developmental biology* **421**:219–232. http://www.ncbi.nlm.nih.gov/pmc/articles/PMC5266562/.

Matlung HL, Bakker ENTP, VanBavel E. 2009. Shear stress, reactive oxygen species, and arterial structure and function. *Antioxidants & redox signaling* **11**:1699–1709.

Momen-Heravi F, Balaj L, Alian S, Mantel P-Y, Halleck AE, Trachtenberg AJ, Soria CE, Oquin S, Bonebreak CM, Saracoglu E, Skog J, Kuo WP. 2013. Current methods for the isolation of extracellular vesicles. *Biological chemistry* **394**:1253–1262.

Morel O, Toti F, Hugel B, Freyssinet J-M. 2004. Cellular microparticles: a disseminated storage pool of bioactive vascular effectors. *Current opinion in hematology* **11**:156–164.

Muralidharan-Chari V, Clancy J, Plou C, Romao M, Chavrier P, Raposo G, D'Souza-Schorey C. 2009. ARF6-regulated shedding of tumor cell-derived plasma membrane microvesicles. *Current biology : CB* **19**:1875–1885.

Nevins JR. 1998. Toward an understanding of the functional complexity of the E2F and retinoblastoma families. *Cell growth & differentiation : the molecular biology journal of the American Association for Cancer Research* **9**:585–593.

Nicolella DP, Moravits DE, Gale AM, Bonewald LF, Lankford J. 2006. Osteocyte lacunae tissue strain in cortical bone. *Journal of biomechanics* **39**:1735–1743.

Ochi H, Takeda S. 2014. [Bone metabolism and cardiovascular function update. Nerve system and mutual interaction between bone and blood vessel]. *Clinical calcium* **24**:77–83.

van Oers RFM, Wang H, Bacabac RG. 2015. Osteocyte shape and mechanical loading. *Current osteoporosis reports* **13**:61–66.

Von Offenberg Sweeney N, Cummins PM, Cotter EJ, Fitzpatrick PA, Birney YA, Redmond EM, Cahill PA. 2005. Cyclic strain-mediated regulation of vascular endothelial cell migration and tube formation. *Biochemical and biophysical research communications* **329**:573–582.

Palumbo C, Ferretti M, De Pol A. 2003. Apoptosis during intramembranous ossification. *Journal of Anatomy* **203**:589–598. http://www.ncbi.nlm.nih.gov/pmc/articles/PMC1571194/.

Passerini AG, Polacek DC, Shi C, Francesco NM, Manduchi E, Grant GR, Pritchard WF, Powell S, Chang GY, Stoeckert CJJ, Davies PF. 2004. Coexisting proinflammatory and antioxidative endothelial transcription profiles in a disturbed flow region of the adult porcine aorta. *Proceedings of the National Academy of Sciences of the United States of America* **101**:2482–2487.

dela Paz NG, Walshe TE, Leach LL, Saint-Geniez M, D'Amore PA. 2012. Role of shear-stress-induced VEGF expression in endothelial cell survival. *Journal of cell science* **125**:831–843.

Percival CJ, Richtsmeier JT. 2013. Angiogenesis and Intramembranous Osteogenesis. *Developmental dynamics : an official publication of the American Association of Anatomists* **242**:909–922. http://www.ncbi.nlm.nih.gov/pmc/articles/PMC3803110/.

Pisitkun T, Shen R-F, Knepper MA. 2004. Identification and proteomic profiling of exosomes in human urine. *Proceedings of the National Academy of Sciences* **101**:13368–13373. http://www.pubmedcentral.nih.gov/articlerender.fcgi?artid=516573&tool=pmcentrez&rendertype=abstract.

Plein A, Fantin A, Ruhrberg C. 2014. Neuropilin regulation of angiogenesis, arteriogenesis, and vascular permeability. *Microcirculation (New York, N.Y. : 1994)* **21**:315–323.

van der Pol E, Boing AN, Harrison P, Sturk A, Nieuwland R. 2012. Classification, functions, and clinical relevance of extracellular vesicles. *Pharmacological reviews* **64**:676–705.

Prideaux M, Findlay DM, Atkins GJ. 2016. Osteocytes: The master cells in bone remodelling. *Current opinion in pharmacology* **28**:24–30.

Regente M, Corti-Monzon G, Maldonado AM, Pinedo M, Jorrin J, de la Canal L. 2009. Vesicular fractions of sunflower apoplastic fluids are associated with potential exosome marker proteins. *FEBS letters* **583**:3363–3366.

Rizov M, Andreeva P, Dimova I. 2017. Molecular regulation and role of angiogenesis in reproduction. *Taiwanese journal of obstetrics & gynecology* **56**:127–132.

Rodriguez-Nunez I, Romero F, Saavedra MJ. 2016. [Exercise-induced shear stress: Physiological basis and clinical impact]. *Archivos de cardiologia de Mexico* **86**:244–254.

Sakurai A, Hasegawa T, Kudo A, Shen Z, Nagai T, Abe M, Yoshida T, Hongo H, Yamamoto T, Yamamoto T, Oda K, Freitas PHL de, Li M, Sano H, Amizuka N. 2017. Chronological immunolocalization of sclerostin and FGF23 in the mouse metaphyseal trabecular and cortical bone. *Biomedical research (Tokyo, Japan)* **38**:257–267.

Salari P, Keshtkar A, Shirani S, Mounesan L. 2017. Coronary Artery Calcium Score and Bone Metabolism: A Pilot Study in Postmenopausal Women. *Journal of bone metabolism* **24**:15–21.

Salsoso R, Farias M, Gutierrez J, Pardo F, Chiarello DI, Toledo F, Leiva A, Mate A, Vazquez CM, Sobrevia L. 2017. Adenosine and preeclampsia. *Molecular aspects of medicine*.

Schweitzer JK, D'Souza-Schorey C. 2004. Finishing the job: cytoskeletal and membrane events bring cytokinesis to an end. *Experimental cell research* **295**:1–8.

Shah KM, Orton P, Mani N, Wilkinson JM, Gartland A. 2016. Osteocyte physiology and response to fluid shear stress are impaired following exposure to cobalt and chromium: Implications for bone health following joint replacement. *Journal of orthopaedic research : official publication of the Orthopaedic Research Society*.

Shalaby F, Rossant J, Yamaguchi TP, Gertsenstein M, Wu XF, Breitman ML, Schuh AC. 1995. Failure of blood-island formation and vasculogenesis in Flk-1-deficient mice. *Nature* **376**:62–66.

Sho E, Sho M, Singh TM, Nanjo H, Komatsu M, Xu C, Masuda H, Zarins CK. 2002. Arterial enlargement in response to high flow requires early expression of matrix metalloproteinases to degrade extracellular matrix. *Experimental and molecular pathology* **73**:142–153.

Tatischeff I, Bomsel M, de Paillerets C, Durand H, Geny B, Segretain D, Turpin E, Alfsen A. 1998. Dictyostelium discoideum cells shed vesicles with associated DNA and vital stain Hoechst 33342. *Cellular and molecular life sciences : CMLS* **54**:476–487.

Tatischeff I, Lavialle F, Pigaglio-Deshayes S, Pechoux-Longin C, Chinsky L, Alfsen A. 2008. Dictyostelium extracellular vesicles containing hoechst 33342 transfer the dye into the nuclei of living cells: a fluorescence study. *Journal of fluorescence* **18**:319–328.

Uda Y, Azab E, Sun N, Shi C, Pajevic PD. 2017. Osteocyte Mechanobiology. *Current osteoporosis reports* **15**:318–325.

Urbich C, Dernbach E, Reissner A, Vasa M, Zeiher AM, Dimmeler S. 2002. Shear stress-induced endothelial cell migration involves integrin signaling via the fibronectin receptor subunits alpha(5) and beta(1). *Arteriosclerosis, thrombosis, and vascular biology* **22**:69–75.

Vechetti IJJ, Valentino T, Mobley CB, McCarthy JJ. 2021. The role of extracellular vesicles in skeletal muscle and systematic adaptation to exercise. *The Journal of physiology* **599**:845–861.

Wang M, Obi Y, Streja E, Rhee CM, Lau WL, Chen J, Hao C, Hamano T, Kovesdy CP, Kalantar-Zadeh K. 2017. Association of Parameters of Mineral Bone Disorder with Mortality in Patients on Hemodialysis according to Level of Residual Kidney Function. *Clinical journal of the American Society of Nephrology : CJASN*.

Winkler DG, Sutherland MK, Geoghegan JC, Yu C, Hayes T, Skonier JE, Shpektor D, Jonas M, Kovacevich BR, Staehling-Hampton K, Appleby M, Brunkow ME, Latham JA. 2003. Osteocyte control of bone formation via sclerostin, a novel BMP antagonist. *The EMBO journal* **22**:6267–6276.

Wolf P. 1967. The nature and significance of platelet products in human plasma. *British journal of haematology* **13**:269–288.

Xu L, Zhang Y, Yang K, Ren L, Wang Q. 2013. [Influence of copper-bearing stainless steel on adhesion, proliferation and apoptosis of vascular endothelial cell]. *Hua xi kou qiang yi xue za*

zhi = Huaxi kouqiang yixue zazhi = West China journal of stomatology **31**:17-20,25.

Yagami K, Suh J-Y, Enomoto-Iwamoto M, Koyama E, Abrams WR, Shapiro IM, Pacifici M, Iwamoto M. 1999. Matrix Gla Protein Is a Developmental Regulator of Chondrocyte Mineralization And, When Constitutively Expressed, Blocks Endochondral and Intramembranous Ossification in the Limb. *The Journal of Cell Biology* **147**:1097–1108. http://www.ncbi.nlm.nih.gov/pmc/articles/PMC2169349/.

Yang Y-Q, Tan Y-Y, Wong R, Wenden A, Zhang L-K, Rabie ABM. 2012. The role of vascular endothelial growth factor in ossification. *International Journal of Oral Science* **4**:64–68. http://www.ncbi.nlm.nih.gov/pmc/articles/PMC3412670/.

Zhao H, Zhou W, Yao Z, Wan Y, Cao J, Zhang L, Zhao J, Li H, Zhou R, Li B, Wei G, Zhang Z, French CA, Dekker JD, Yang Y, Fisher SE, lucker HO, Guo X. 2015. Foxp1/2/4 regulate endochondral ossification as a suppresser complex. *Developmental biology* **398**:242–254. http://www.ncbi.nlm.nih.gov/pmc/articles/PMC4342236/.

Zhou H, Yang M, Li M, Cui L. 2017. Radial artery sclerostin expression in chronic kidney disease stage 5 predialysis patients: a cross-sectional observational study. *International urology and nephrology*.